Politechnika Wrocławska

FIELD OF SCIENCE: Engineering and technology

DISCIPLINE OF SCIENCE: Environmental Engineering, Mining and Energy

DOCTORAL DISSERTATION

Characterization and modeling of the innovative cooling water mattress for heat stress mitigation in cattle

Jagoda Błotny

Supervisor:
DSc, PhD, Eng. Sabina Rosiek-Pawłowska

Keywords: cooling system, heat transfer, cattle's heat stress

WROCŁAW 2025

Financial Support

This research was carried out with the financial assistance of the Polish National Agency for Academic Exchange, Polish Returns 2018, with the project identification number 07PP/0001/19.

Abstract

Climate change has an important impact on the natural environment, by making climate warmer or more variable, which affects cattle breeding in many parts of the world. The heat extremes and prolongate heat wave periods caused by climate change can be especially dangerous for those animals, affecting their day-today life by the heat stress episodes. Dairy cattle are especially susceptible to such conditions, due to their high metabolic heat production caused by the lactation processes. High relative humidity and temperature of the air, which often characterize the cowshed environment in heat stress periods, make cattle' natural thermoregulation processes insufficient in heat dissipation, being a cause of numerous and potentially serious health, fertility and welfare problems. At the same time, those environmental conditions are difficult to optimize, concerning both, the animals' needs, as well as energy consumption of applied systems. Cooling cowsheds is very complex, expansive and not well established, especially taking into account the immense thermal losses from their structures. For that reason, an appropriate cooling mechanism as an effective heat abatement strategy applied to the cowshed becomes crucial for cattle breeding, especially considering the lowest possible environmental effect. That is why within this PhD thesis, an innovative cooling water mattress for cattle, based on conductive heat transfer between the lying animal and chilled water circulating inside the water mattress, was developed. Such an approach to cooling enables local heat removal during animals' resting period (for dairy cattle normally varying between 12-14h), especially when the applicability of other available cooling solutions is limited or less effective.

The geometry of the developed water mattress was selected within four different propositions, which were simulated as the Computational Fluid Dynamic models in the Ansys Fluent environment. Such a preliminary study enabled the selection of the most promising geometry in terms of the water distribution inside the water mattress, and heat transfer on its surface. Chosen geometry was then developed as the prototype test stand and experimentally tested in both, laboratory conditions, as well as real barn conditions, during two different experimental campaigns conducted in the summer periods of 2022 and 2023. The developed water mattress was supplied with the chilled water produced and distributed by the conventional chiller-based hydraulic system, supervised by the control and data acquisition system. It enabled the regulation of the operational parameters of the developed water mattress, intended to follow the individual needs of the animal.

Conducted experimental campaigns enabled observation of the developed water mattress' cooling effect on animals' bodies for different chilled water temperature setpoints, and changing environmental conditions, compared to the commercially available non-cooled water mattress. For this purpose, an infrared thermography was used to observe the local change in cows' skin temperature. The selection of the most suitable for the animal mattress' operational parameters, became an important aspect of this research, influenced by the natural thermoregulatory mechanisms of the cow. For that reason, the second experimental campaign was extended not

only by the second cooling water mattress applied to the test stand with the main goal to obtain the comparative results, but also a novel measurement strategy of the cows' physiological responses, informing about active thermoregulatory processes. Such data were also expected to be significant in early heat stress detection in cattle, being decisive, when an appropriate cooling strategy needs to be applied.

The conducted in this PhD thesis study proved the cooling effectiveness of the developed water mattress, indicating its potential as a novel cooling solution for cattle, especially for environmental conditions, in which the application of other available technologies is limited. Due to the frontier character of this study area, and considering the knowledge from different disciplines, at this moment there is a lack of available sensors, apparatus, and methodology, to bring into light, one specific parameter defining the threshold of the heat stress level. Nonetheless, such a parameter would be significant to better understand heat stress effects on health and well-being that occur when cows are exposed to thermally challenging environments. The future potential of the developed water mattress is especially oriented to its operational algorithm, adapting it to the individual needs of the animal for changing environmental conditions. Furthermore, it could be coupled with hybrid systems based on renewable energy sources, such as the photovoltaic system, geothermal system, or absorption chiller, based solely on the use of alternative energies that surpasses the performance of existing solutions, thereby advancing the state of the art and helping to mitigate global climate change.

Streszczenie

Występujące zmiany klimatyczne mają znaczący wpływ na środowisko naturalne, powodując zarówno ocieplenie klimatu jak i jego większą zmienność, co ma istotne znaczenie dla hodowli bydła w różnych częściach świata. Ekstremalne i długotrwałe fale upałów spowodowane takimi zmianami mogą być szczególnie niebezpieczne dla tych zwierząt, będąc przyczyną występującego u nich stresu cieplnego. Krowy mleczne są szczególnie podatne na wskazane warunki pogodowe ze względu na ich wysoką produkcję ciepła metabolicznego związanego z procesami laktacyjnymi. Jednocześnie wraz ze wzrostem temperatury oraz wilgotności względnej powietrza związanymi z warunkami środowiskowymi w oborze w okresach gorąca, możliwości termoregulacyjne tych zwierząt stają się coraz bardziej ograniczone. W rezultacie mogą one stać się niewystarczające do zachowaniu równowagi cieplnej zwierzęcia, będąc przyczyną stresu cieplnego i związanych z nim licznych problemów zdrowotnych, w tym reprodukcyjnych oraz poważnego zaburzenia dobrostanu zwierzęcia.

Budynki inwentarskie, takie jak obory, charakteryzują się natomiast dużymi stratami ciepła poprzez ich strukturę, co sprawia, że zachowanie właściwych dla zwierzęcia warunków środowiskowych, przy jednocześnie niskim nakładzie energetycznym, jest szczególnie złożone i trudne do osiągnięcia. Dlatego też dobór odpowiedniej metody chłodzenia tych budynków, która skutecznie niwelowałaby występowanie stresu cieplnego u zwierząt, przy jego jednoczesnym niewielkim wpływie na środowisko jest kluczowym zagadnieniem do rozwoju. Biorąc pod uwagę te czynniki, w przedstawionej rozprawie doktorskiej rozwinięty został innowacyjny materac chłodzący dla krów, którego działanie opiera na odbieraniu ciepła od zwierzęcia i przewodzeniu go do wody chłodzącej cyrkulującej wewnątrz materaca. Takie podejście do procesu chłodzenia pozwala na lokalny odbiór ciepła od zwierzęcia podczas jego spoczynku (dla bydła mlecznego czas spędzony w pozycji leżącej powinien normalnie wynosić 12-14 godzin na dobę). Aspekt ten jest szczególnie znaczący biorąc pod uwagę ograniczenia innych rozwiązań dostępnych na rynku i ich stosowalności w obszarze legowiska.

Przedstawiony w tej rozprawie doktorskiej, chłodzący materac wodny, został zaprojektowany przy wcześniejszym zamodelowaniu w środowisku Ansys Fluent jego czterech różnych geometrii, spośród których wybrana została ta, która charakteryzowała się największym potencjałem, biorąc pod uwagę rozpływ wody chłodzącej oraz strumień ciepła uzyskany na jego powierzchni. Geometria ta została następnie rozwinięta do prototypowego stanowiska badawczego, przetestowanego zarówno w warunkach laboratoryjnych jak i w wybranej oborze, podczas dwóch różnych kampanii eksperymentalnych przeprowadzonych w okresie letnim w 2022 i 2023 roku. W warunkach rzeczywistych materac zasilany był wodą chłodzącą produkowaną przez konwencjonalny agregat chłodniczy i rozprowadzaną w całym układzie hydraulicznym, objętym systemem kontroli i akwizycji danych. Układ ten umożliwił regulację parametrów pracy chłodzącego materaca wodnego, co miało również na celu dostosowanie ich do indywidualnych potrzeb zwierzęcia.

Przeprowadzone kampanie eksperymentalne umożliwiły zaobserwowanie efektu chłodzącego wspomnianego materaca bezpośrednio na ciałach zwierząt, przy zmieniających się warunkach środowiskowych i jednoczesnym rozróżnieniu uzyskanych wyników poprzez zmianę nastaw temperatury wody chłodzącej i odniesienie ich to niechłodzonego materaca. Podczas badań zastosowano termografię, jako narzędzie, które umożliwiło sprawdzenie lokalnej zmiany temperatury ciała zwierzęcia. Wybór najbardziej odpowiednich dla zwierzęcia parametrów pracy materaca chłodzącego okazał się szczególnie istotnym aspektem badań, ze względu na wpływ złożonych mechanizmów termoregulacyjnych zwierzęcia na odczuwalny przez zwierzę efekt chłodzący. Dlatego też, druga kampania eksperymentalna została rozszerzona o nową strategię opomiarowania fizjologicznych reakcji krowy, będących wskaźnikami informującymi i procesach wymiany ciepła z otoczeniem. Ponadto, stanowisko badawcze zostało rozszerzone o drugi materac wodny o tej samej geometrii, tak aby umożliwić sprawdzenie powtarzalności uzyskanych wyników. Uzyskane w kampanii dane, miały również mieć istotne znaczenie pod względem sprawdzenia użyteczności zaproponowanych sposobów opomiarowania do wczesnej detekcji stresu cieplnego u krów, wpływając tym samym na decyzję o podjęciu odpowiedniej strategii chłodzenia.

Przeprowadzone w obszarze tej rozprawy doktorskiej badania potwierdziły skuteczność chłodzenia bydła przy użyciu opisanego wcześniej materaca wodnego, wskazując na jego potencjał jako nowego rozwiązania chłodzącego w sektorze hodowlanym, szczególnie przy takich warunkach środowiskowych, w których działania innych dostępnych komercyjnie metod jest ograniczone. Biorąc pod uwagę interdyscyplinarność tego obszaru badań, na ten moment brakuje odpowiednich czujników i metod opomiarowania bydła, która umożliwiłaby wskazanie jednego parametru określającego poziom doświadczanego przez zwierzę stresu cieplnego. Parametr ten byłyby natomiast szczególnie istotny, chcąc właściwie zrozumieć złożone oddziaływanie procesów termoregulacyjnych zwierzęcia na jego równowagę termiczną i dobrostan oraz odpowiedź na procesy chłodzenia, podczas doświadczanego przez nie obciążenia cieplnego. Przyszły potencjał tego rozwiązania jest szczególnie zorientowany na dobór odpowiedniej sekwencji i parametrów jego pracy, dostosowując je do indywidualnych potrzeb zwierzęcia dla zmiennych warunków środowiskowych. Ponadto, biorąc pod uwagę układ zasilający materac w wodę chłodzącą, szczególnie istotnym kierunkiem jego rozwoju jest możliwość hybrydowej pracy, stosując rozwiązania oparte na odnawialnych źródłach energii, wykorzystując do tego systemy fotowoltaiczne. geotermalne, a także poprzez zastosowanie agregatu absorpcyjnego. Takie podejście pozwala na wykorzystanie alternatywnych źródeł energii, podnoszących wydajność chłodzenia względem konwencjonalnych rozwiązań, przyczyniając się tym samym do rozwoju tego obszaru naukowego oraz złagodzenia zmian klimatycznych.

Table of contents

Chapter 1

Introduction

This chapter describes the background of the conducted research in terms of global challenges of industrial development, such as climate change, water scarcity, increasing energy consumption, and food security problems. Life on earth is increasingly threatened by society's consumer needs and structures. For that reason, the sustainable approach becomes crucial for further development, and wellbeing. Sustainable means that actions taken to cover the needs preserve also the balance of the ecosystem, preventing the depletion of natural or physical resources. Green solutions oriented on water and energy savings, and conscious living, implemented not only in the industrial and agricultural sectors but also in the cultural and social environments, shape the future world, based on broadly understood respect for life and balance between nature, and technology, being an important element of sustainable living. This paragraph is divided into four main sections: first, the global challenges of industrial development will be extended, then it will focus on how they affect the breeding sector, and what solutions are already implemented, and finally, the developed in this PhD thesis solution will be introduced, as the innovative approach for heat stress reduction in dairy cattle.

1.1. Global challenges of industrial development

The rapid, and unconscious, in terms of the globally shared responsibility, increase in industrial world development within the last century, became the cause of unbalanced ecosystems on the globe. The ongoing climate change, extreme weather events, the water scarcity, are the planet's response to excessive exploitation of resources. Simultaneously, both, the increasing needs of the consumer world, as well as, climate change, and connected to it rise of the cooling demand, increased energy consumption, influencing food insecurity. Breaking that vicious circle by sustainable development, and conscious living, become of utmost importance to the earth and society. In the following sections, the mentioned challenges will be discussed more widely.

Climate change

Global industrial development in the last century increased significantly greenhouse gas emissions, such as carbon dioxide (CO_2) and methane (CH_4). In the state of balance, existing in nature, greenhouse gases ensure the proper level of temperature on the Earth, which is called the greenhouse effect. In this process, the mentioned gases transfer the shortwave radiation emitted by the Sun to the Earth and absorb the longwave radiation emitted by the warmed Earth. To maintain the stable temperature of the Earth, the amount of absorbed (emitted by the Sun, and by the greenhouse gases), and emitted energy need to be equivalent. However, the increased amount of greenhouse gases in the atmosphere disturbs the natural balance of the planet, by absorbing more energy and making more difficult its emission to cosmic space. In effect, that surplus energy is accumulated on the Earth (especially in the oceans), increasing its global temperature. In Figure 1.1, the deviation of a 2023 year's average surface temperature from the 1991-2020 mean is presented as a world map [1]. Countries characterized by extensive industrial development are characterized by the highest temperature increase, up to 1.5°C, and Poland is close to that value with a temperature of 1.37°C. Furthermore, in Figure 1.2 the global average land-sea temperature anomaly relative to the 1961-1990 average temperature baseline is presented. The rapid increase of the global temperature started in 1980, and continues to this day achieving in 2024 a value close to the threshold of 1.5°C. Therefore, the global shift to green solutions, based on reduced greenhouse gas emissions is crucial for further life on the Earth.

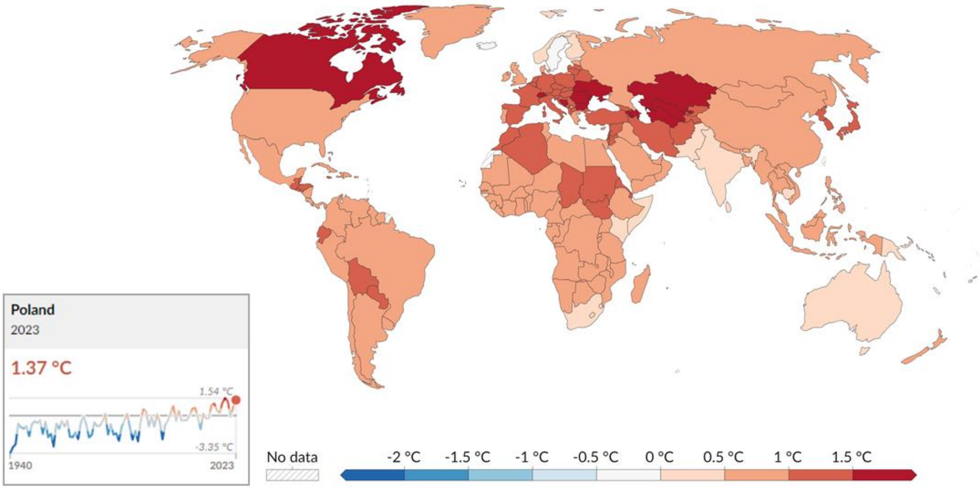

Figure 1.1. The deviation of a 2023 year's average surface temperature from the 1991-2020 mean (data source: Contains modified Copernicus Climate Change Service information, from Our World in Data, 2024 [1]).

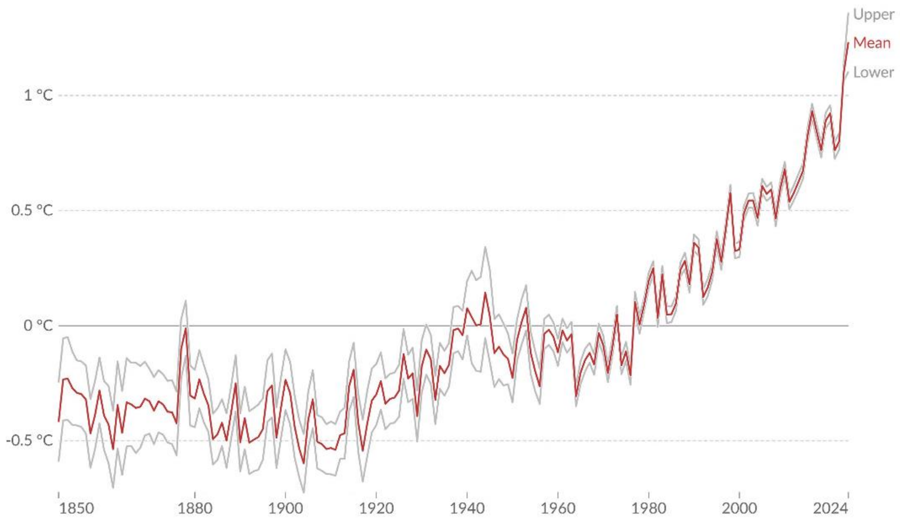

Figure 1.2. Global average land-sea temperature anomaly relative to the 1961-1990 average temperature baseline, the gray lines represent the upper and lower bounds of the 95% confidence interval (source: Met Office Hadley Centre, from Our World in Data, 2024 [1])

However, the increase in the global average temperature is not the only indicator of climate change. The weather anomalies become more frequent, and dangerous for all living beings on the Earth. The one that is an easy noticeable in day-to-day life, is the heat waves occurrence. Generally, the heat wave is a prolongate period of abnormally hot weather, when temperature increases above the threshold. The thresholds are differently defined, but according to [2], [3], it is a period of at least 3 days, when the exterior temperature exceeds 30°C. The cause of the heat wave is high atmospheric pressure that moves in and pushes warm air toward the ground. The compressed this way air warms up. Furthermore, the high-pressure system expands vertically, causing changes in the courses of other weather systems. Minimized wind and cloud cover effects with its prolongate character. The heating effect becomes intensified due to the warmed, moisture-less ground, which additionally accumulates the heat, which becomes trapped by the high-pressure system. In terms of climate change, the frequency, duration, magnitude, and extent are monitored. In Figure 1.3 trends of these parameters in years 1950-2021 are presented on the global map [4]. Significant increase in all parameters is observed within the world, especially in South America, Europe, North Africa, South Asia, and what is crucial in terms of glaciers melting, the South Pole. In Poland the heat wave extent and magnitude are the most important parameters in terms of their intensity within the last decades. It results with persisting high air temperatures over a large area of the country, affecting a large share of the national breeding sector, within one heat wave period.

Within recent years, the heat wave issue has become even more crucial for living beings [5] Between 2000-2019 it was estimated that approximately 489 000 deaths caused by heat stress occurred each year (45% of these in Asia, 36% in Europe) [6]. In the summer period of 2022 in Europe, 61 672 deaths have been estimated to occur due to heat stress [7]. However, the heat waves are even more dangerous for farm animals, such as cattle, and sheep [8]. Cattle natural boundaries of thermal comfort are shifted to lower temperatures, whose ranges can vary from the source, according to [9], [10] it is in a range of 5-25°C. Furthermore, numerous herds are naturally kept on the pastures, and if barns are applied, they are not equipped with air cooling systems, due to the complex building structures, and enormous heat losses. In effect, thousands of cattle deaths were reported in the USA in the summer periods of 2022-2023 [11], [12] highlighting the heat wave importance in the breeding sector.

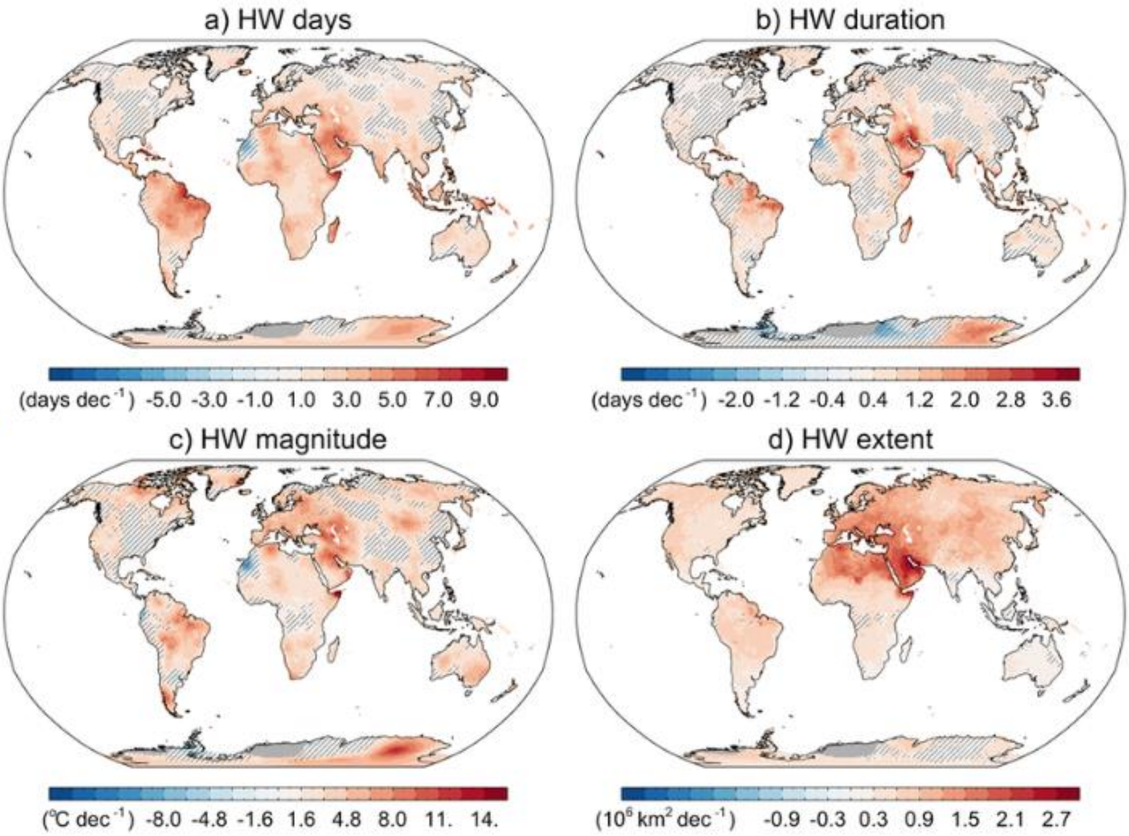

Figure 1.3. Trends over the 1950-2021 period, in warm-season heat wave (HW) characteristics: a) annual frequency (in days decade $^{-1}$); b) maximum duration in the year (in days decade $^{-1}$); c) magnitude (in °C decade $^{-1}$); d) annual maximum areal extent (in 10^6 km^2 decade $^{-1}$). Gray shading identifies regions of missing data [4]. Source: Berkely Earth data set.

Global energy consumption

Both, industrial development, as well as covering people's needs to maintain their wellbeing, are the reason for the increased global energy demand, and consumption. It concerns also the increased energy demand for air cooling, caused by climate change. Figure 1.4 presents the rising trend in energy consumption over 1990-2023, differentiated by regions, where Asia contributes the most to that increase. In 2023, the global energy consumption growth accelerated, reaching 2.2%, being much higher than its average 2010-2019 growth rate, which reached 1.5%/year [13].

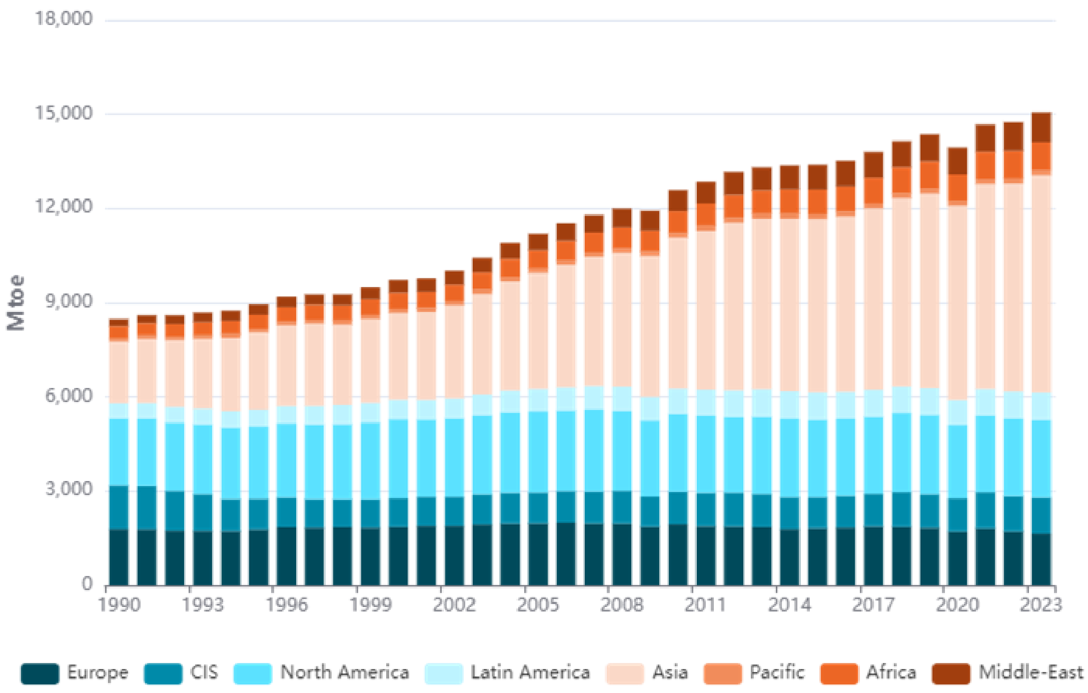

Figure 1.4. The trend in energy consumption over 1990-2023 (in Mtoe) [13].

The main problems with global energy consumption are connected with the extremely different situations among the countries. Highly developed countries produce too large amount of greenhouse gas emissions, contributing to the global temperature increase. On the other hand, there are still countries characterized by energy poverty. Poverty means a lack of access or limited access to heating energy, and electricity, influencing people's living conditions and health. In Figure 1.5 the CO_2 emissions per capita are presented with marked countries affected by energy poverty [14].

Therefore, the development in the energy sector needs to be based on clean, renewable energy sources, with high economic accessibility, which could reduce greenhouse gas emissions, and reduce energy poverty. Such balance is difficult to achieve, and at this moment, there is a lack of large-scale energy alternatives to fossil fuels that would be cheap, safe, and sustainable. However, global change can be made by taking small steps in individual sectors and changing awareness of the problems.

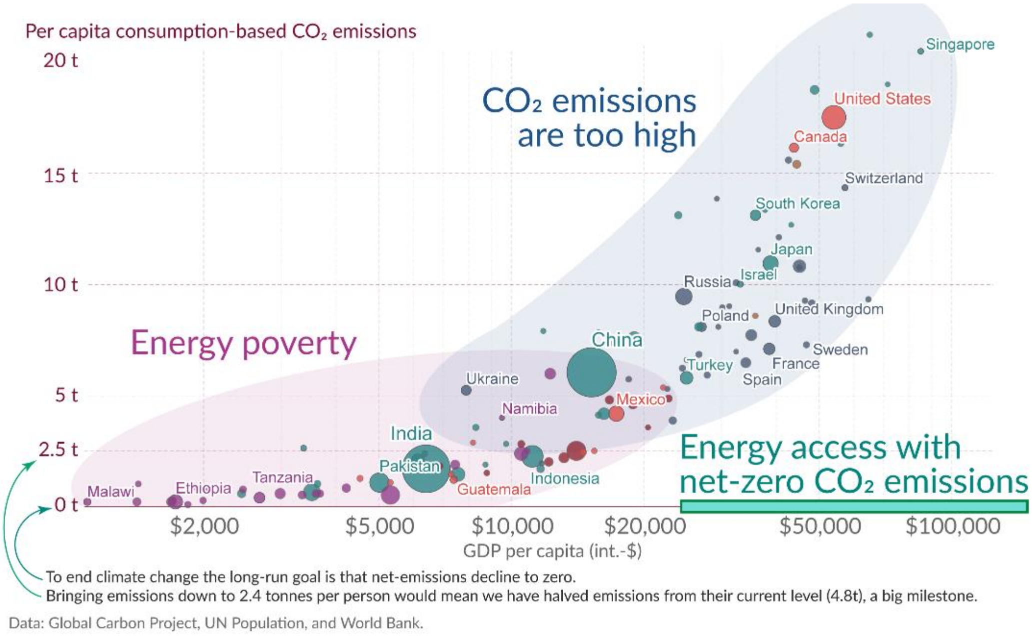

Figure 1.5. CO2 emission per capita vs GDP per capita (source: Global Carbon Budget (2024); Population based on various sources (2024) – with major processing by Our World in Data [14])

Although fossil fuels are still dominant in the energy mix with its rising trend, due to increased energy consumption, the shift to renewable energy sources is visible with its increased contribution to overall electricity production. Therefore the innovative solutions based on renewable energy sources, implemented in varied industrial sectors and domestic applications, could beneficially contribute to tackling energy problems.

Water scarcity

Another significant challenge is increasing water scarcity. The global water budget is under pressure, due to annual water withdrawals, defined as freshwater taken from the ground or surface water sources (permanently or temporarily) and transported to a place of use, achieving the 10% of internal renewable water resources from rivers and aquifers (amount to 44 000 km^3/year) [15]. The level of water stress, which occurs when water demand exceeds its available amount in a certain period and considered area, generated by all sectors is presented in Figure 1.6. Although, the average water scarcity on the globe reached 18%, substantial regional variations can be observed. Furthermore, the substantial contribution to water withdrawals is caused by the agricultural sector, which is presented in Figure 1.7. Comparing both maps, it is worth noticing that regions with a high water stress level, such as Central Asia, Middle East–Western Asia, and Northern Africa, or the USA, are also using a large amount of their water withdrawals for the agricultural sector. Therefore, the solutions based on water reuse and desalination should be already applicable in water-scarce areas (Middle East–Western Asia). However, such contribution level highlights the urgent need for sustainable, greener solutions, providing water savings in this sector.

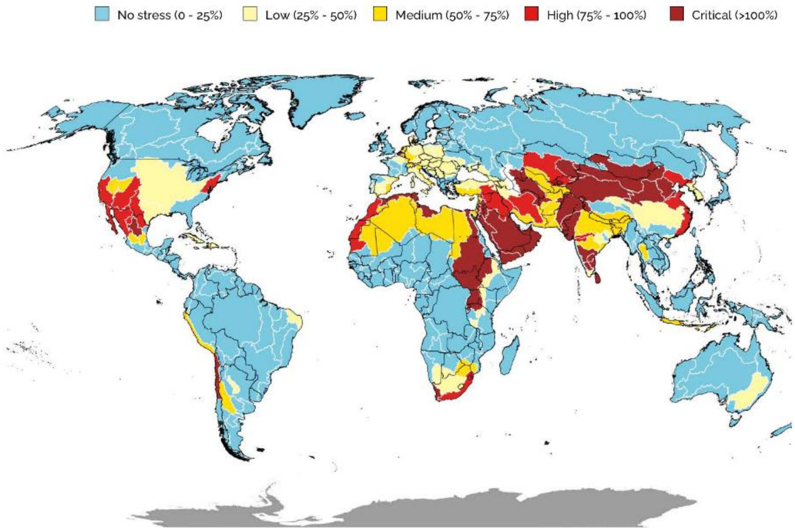

Figure 1.6. Level of water stress of all sectors by major basin, 2018 [15].

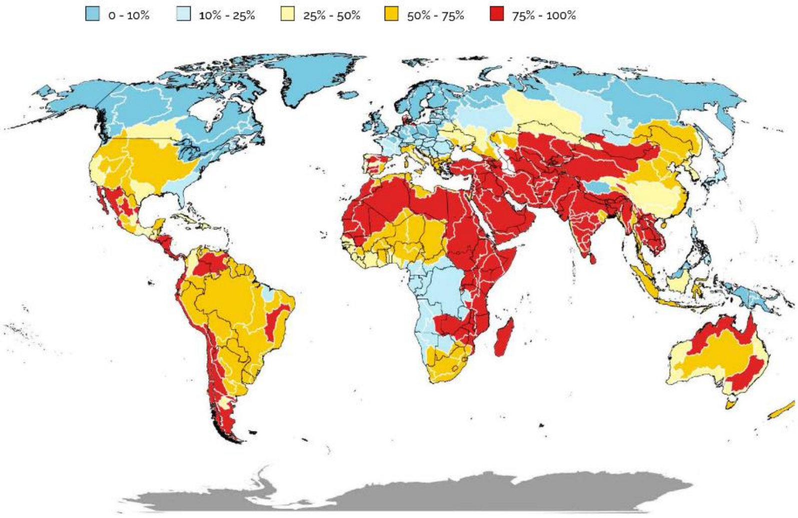

Figure 1.7. Level of water stress due to the agricultural sector by basin, 2018 [15].

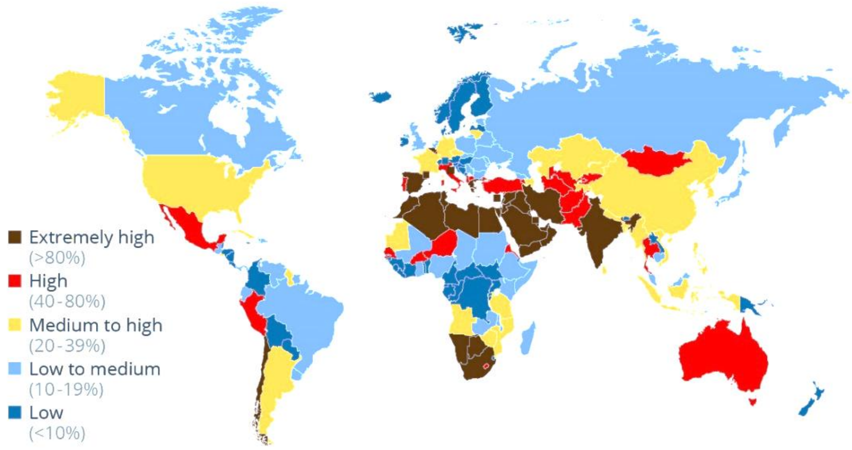

Figure 1.8. Projected ratio of human water demand to water availability (water stress level) in 2050, according to „business as usual" scenario=midle-of-the-road future where temperature increase by 2.8°C to 4.6°C by 2100 (data source: World Resources Institute [16], [17]).

Following, the global development and population increase, the future predictions indicate that water demand will increase significantly by 2050, according to World Resources Institute projections [16], [17]. Predictions presented in Figure 1.8, indicate that 51 of the 164 analyzed regions are expected to be affected by extremely high water stress, which corresponds to 31% of the population. Although for Poland water stress level is low at this moment, the predicted consumption rate will reach from 20% to 40% of available resources. It is also worth noticing a high consumption rate predicted for Australia, which is also one of the global leaders in the developing breeding sector, with a large cattle population. The presented scenario highlights the importance of the sustainable approach to global water distribution and consumption, being necessary for future living..

Food security

The definition of food security evolved within the development of globalization, from the basic meaning of the ability to ensure biological survival, to also the availability/affordability of food, its nutritional quality, and the sustainability of food systems (according to the UN and the Food and Agriculture Organization of the United Nations (FAO)). Since 2014, the number of people in hunger is gradually increasing. The reason for that is a continuously rising global population (from 2.6 mld in 1950 to 8.2 mld in 2024), which corresponds to the increased food demand, as well as excessive food production in highly developed countries, being the cause of food waste. FAO’s estimation indicates, that about 8.9% of the world's population is suffering from hunger. According to FAO statistics [18] not only Africa is affected by food insecurity, but also such regions as Australia, South America, and Brazil, or numerous European countries, characterized also by a large cattle population, and developed dairy sector. Unsustainable, in terms of global needs, food production, as well as climate changes threatening the crops and breeding, due to droughts, heat waves, and water scarcity problems, became the major contributors to global food insecurity. Therefore, the sustainable approach, and implementation of non-conventional, green solutions, alleviating the effects of these factors, will take a significant role in future food systems development.

Challenges for the breeding sector

The breeding sector has been under intensive development in recent years. Increased demand for food, with a special interest in dairy products, caused the growing number of cattle in the world. In

Table 1.1 top 10 world and European countries in terms of the number of dairy cattle in 2022 are presented [19]. India, Brazil, and the USA are the countries with a huge number of cattle. They are also characterized by the hot climate, and for that reason especially affected by climate change. Furthermore, in those countries, there is a relatively high level of heat wave occurrence, water scarcity, and food security problems. Such conditions make cattle breeding in those regions very challenging, especially in terms of global development trends. Furthermore, in countries such as India, which are affected by energy poverty, the development of the breeding sector needs to be based on solutions that could provide energy savings.

Hot weather conditions are difficult to tackle by cattle, due to their thermal comfort boundaries shifted to lower air temperatures, between 5°C and 25°C. Additionally, dairy cattle produce more metabolic heat necessary for milk production. For that reason, the European countries, characterized by lower summer temperatures, such as Germany, France, as well as Poland, which also lead in statistics, especially considering the density of cattle (number of heads per square kilometer), need to face the same challenges in the breeding sector.

Table 1.1. Top 10 world and European countries in terms of the number of dairy cattle in 2022.

No	World	No of cattle, An	Europe	No of cattle, An
1	India	55640213	Russian Federation	6268581
2	Pakistan	15764000	Germany	3809720
3	Brazil	15740153	France	3230860
4	China, mainland	12176453	Poland	2037280
5	United States of America	9377000	Italy	1865000
6	Ethiopia	9054213	United Kingdom of Great Britain and Northern Ireland	1850000
7	Bangladesh	8645000	Netherlands	1570000
8	Sudan	8326629	Ireland	1510310
9	United Republic of Tanzania	7859658	Ukraine	1483800
10	South Sudan	7382078	Belarus	1447300

The increase in air temperature and humidity affects animals' natural thermal balance. When a cow produces more heat than can dissipate to the environment, she becomes under heat stress increasing her body temperature. The increase even by 0.5°C causes negative consequences to the animal's health [20]. To tackle that issue, animal activates the thermoregulatory processes, which will be the focus of Chapter 7 of this PhD thesis. When the air temperature reaches the level of skin temperature (35°C), the main heat dissipation capability is through the evaporative processes. The prolongate heat stress conditions, being an effect of heat waves, make an animal unable to regenerate even during the night. Furthermore, the hormonal and behavioral changes start to occur [21]. Cow stands for a longer time to increase the convective heat losses [22]. Furthermore, she reduces the feed intake, and milk production [23] to reduce the metabolic heat production. In effect, numerous health problems, such as lameness, or acidosis affect the animal [24], being the cause of economic losses for the breeder, due to veterinary services and reduced milk production. In extreme conditions, heat stress becomes the cause of animal death [25], which was globally reported during recent summer periods. It makes this issue significant in terms of the worldwide food security problem.

Therefore, the effective cooling systems applied to the barns could reduce the heat stress problem. However, due to the structure of the livestock buildings, characterized by no or little insulation, and open air circulation, the application of traditional air condition systems would generate much more losses than benefits, especially in the point of need. For that reason, cattle's cooling systems available on the market are based on local cooling, by intensifying animals' heat dissipation through convective and evaporative heat losses. However, such systems are usually based on fan systems, and open water circuits applied to sprinklers or mist systems [26]. Such solutions are characterized by high electricity and water consumption, and limited application in terms of animal wellbeing. Considering, the global increase in energy demand, and water scarcity, the development of innovative solutions, which could tackle the heat stress issue became crucial for future breeding. The review of the available cooling systems for cattle will be described in detail in the next subsection.

1.2. Cooling technologies in the dairy sector

The basic method used for improving the thermal comfort of the animal is providing proper shading to reduce the heat gains through radiation. Such an approach is beneficial for cattle in terms of their physiology, behavior, and production [27], [28], [29]. However, it does not provide proper thermal conditions for the animal, since high temperature and humidity of air still limit the animals' natural ability for heat dissipation [30]. It is the only applicable passive method used for the outdoor environment. Indoor methods are focused on modifying the construction of livestock buildings and used materials, as well as enhancing natural ventilation methods [31]. However, passive methods alone are not sufficient for heat stress alleviation, especially concerning the ongoing climate change. For that reason, the development of active solutions become crucial in this field. This paragraph will be focused on active cooling systems installed inside the barn, and based on local heat removal from cattle. They can be divided by the heat dissipation mechanisms. Convective cooling is intensified by air supply systems, evaporative cooling by sprinkler systems, and conductive cooling uses different types of heat exchangers in bedding areas. In the following section available solutions will be discussed more precisely.

Convective cooling - air supply systems

Livestock buildings, due to their functionality need to be properly ventilated to maintain hygiene conditions. Both, the digestive and excretory processes are the source of harmful gases, such as methane (CH_4) and ammonia (NH_3) [32], and reduction of their concentration is crucial for animal wellbeing. For this purpose, natural or mechanical ventilation systems are used, in which fresh air is supplied by the special ducks located in the walls or open window systems, and used air is discharged through the chimney or other side of the barn. The natural ventilation process is based on thermal air movement, and the mechanical one on the pressure difference forced by the exhaust fan systems (chimney or wall fans). The combined systems [33] (c.f. Figure 1.9), in which the natural ventilation can be switched to the mechanical one, provide better management of the ventilation process and reduced electricity consumption. Although such systems regulate the air quality, the achieved within them air movement usually is not sufficient in terms of convective cooling.

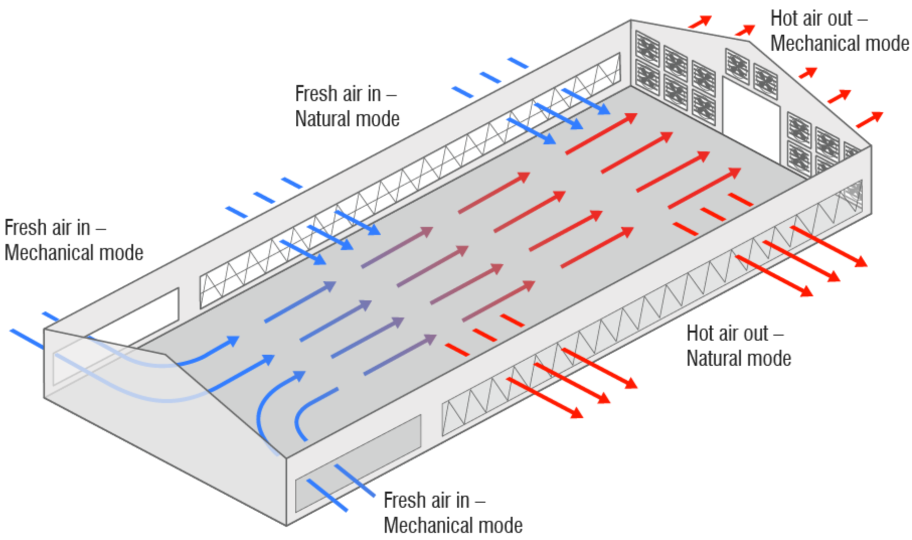

Figure 1.9. Combined natural and mechanical ventilation systems, applied to the barns (Figure source: [34]).

The air-forced convective cooling effect is achieved by directing the airflow toward the cows. It is one of the commonly used methods to maintain optimal environmental conditions and mitigate heat stress [35], [36]. The most common technology applicable in cowsheds is based on designed for this purpose sailing fan systems [37]. However, to cover each cow with the fan's operating range, a significant number of them must be implemented, which increases the installation costs and electricity consumption. Furthermore, the effectiveness of cooling is determined by the airflow and direction, which differs among the cows' locations [38]. The effectiveness of convective cooling is higher for lower air temperatures, suggesting its applicability to the nocturnal hours [39]. Figure 1.10 presents a scheme and a real photo of a commercially available fan-based solution.

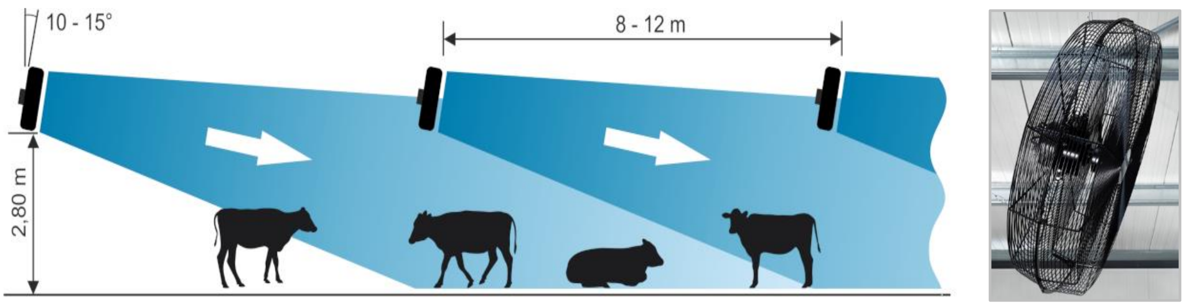

Figure 1.10. The scheme and the picture of a commercially available fan-based convective cooling system (Figures source: [40]).

The alternative solutions developed in recent years are focused on individual precision cooling systems for cows. The precision air supply system [41] consists of the main duct with several subsidiary distribution tubes, directed to the animal under a selected angle (c.f. Figure 1.11). The perforated air-ducting system [42], [43], [44], usually is based on ducts or tubes with small orifices along their length adjusted to the animals' location inside the barn. The commercially available solution, based on these approaches is a positive pressure vent tube system (c.f. Figure 1.11). It consists of the fresh air-supplied tubes, fitted to the length of the building, and suspended directly above the animals. Each tube is supplied with air by fun located at its one end, which is delivered directly to the area of animals' bodies through precisely fitted orifices. The positive-pressure precision ventilation system described in [45] is intended to provide jet flows inside the barn using the positive-pressure fans introducing the air to the collector chamber, which is then precisely distributed to animals [46].

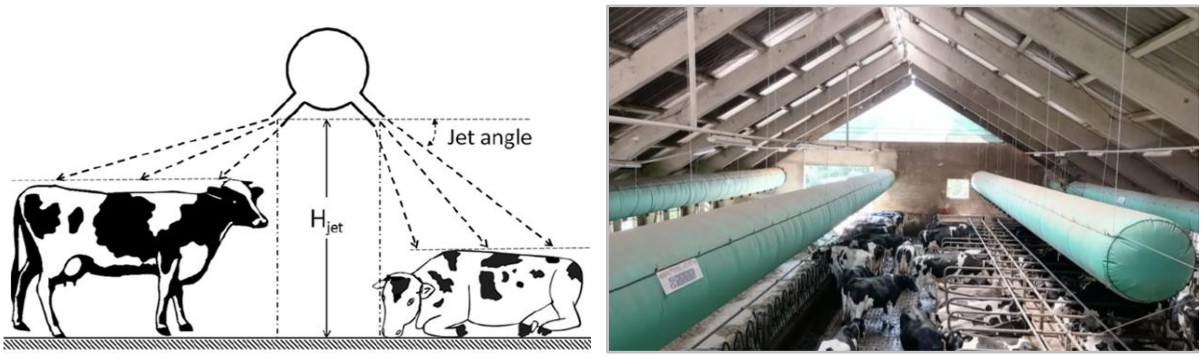

Figure 1.11. On the left-hand side, the scheme of a precision air supply system and on the right-hand side the picture of a commercially available positive pressure vent tube system used for convective cooling (Figures sources: [41], [47]).

Therefore, such solutions are better adapted to animals' needs, improving the cooling effectiveness, and reducing costs, and energy consumption by the limited number of fans. However, the cooling effectiveness of that solution is limited by the air temperature supplying the tube system, bringing it applicability only for moderately high ambient temperatures, when activated convective heat losses are still a sufficient thermal regulation method. Therefore, adding the evaporative cooling pads to reduce the air temperature needs to be considered for higher ambient temperatures [45].

Evaporative cooling - open water cycles

Convective cooling methods become insufficient in heat stress reduction for extremely hot environmental conditions especially when the ambient temperature reaches the temperature of the animal's skin. For that reason, usually, they are combined with the evaporative cooling methods as misting fans [48]. The most widely used evaporative method is a sprinkler system [35], which provides water directly on the animal's body, wetting their surface, where heat can be dissipated within the evaporation. Droplets' size is a crucial parameter in achieving cooling effectiveness within this method [49]. They need to be large enough to ensure the water penetration of the hair coat and wet cows' skin. Small droplets are used in mist systems, whose main goal is to reduce the temperature of the air around the cow. However, it leads to increasing air humidity, and for that reason, their application is limited to the dry climate [50]. Both systems increase the water demand in the livestock sector, due to their operation in open water cycles. Furthermore, due to the hygiene conditions, they can not be used in the bedding areas [51], which limits their applicability in the cow's daily cycle. Usually, they are used in the feeding lines (c.f. Figure 1.12), and before the milking. A recent study [52] considered the supplemental cooling method. based on providing the cooled air and mist, that an animal could inhale, and thus be cooled down while lying down in free-stalls. To reduce the water demand, consideration of the external environment and cows' activities need to be taken into account in control algorithms [53]. Further development of that solution focused on applying the proper control system, which turns on the system only when the air temperature exceeds the threshold and works in time intervals, or when animal movement is detected (in the corridor area) [54]. Lastly, evaporative systems can be used only, when the air humidity is low enough, due to their contribution to its increase, and in effect limited heat dissipation capabilities. Moreover, the studied psychological response of the cattle, proved that this method is not the animals' preferable one [49].

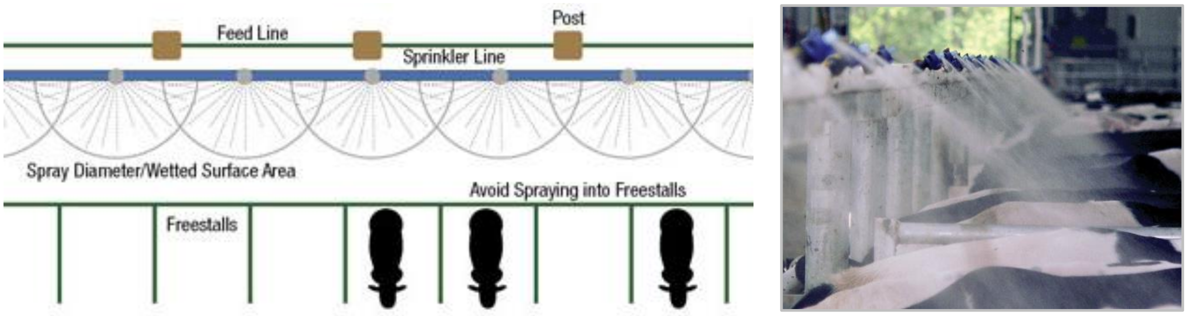

Figure 1.12. The scheme and the picture of the sprinklers system applied in the feed line (Figures sources: [55], [54]).

The innovative pad cooling solution, developed commercially, provides air cooling in the evaporation process [56], before its application to the barn through the tube systems. Although it can reduce the air temperature, it is still limited by the relative humidity of the air.

Conductive cooling – heat exchangers

Limitations of the previously described solutions directed further development of the cooling technologies to the conductive heat dissipation. Dairy cattle kept in freestall barns need to rest in the lying position from 12h to 14h per day [57]. Furthermore, the lying position limits the convective cooling, due to reduced skin surface washed by the airflow. For that reason, the solution that would enable heat removal in the bedding area became a potential alternative to the well-known solutions. However, the conduction efficiency depends mostly on the contact surface between the cow and the bedding, which amounts to only 20% of the cow's entire body [58]. This aspect cannot be changed and is therefore one of the constraints limiting this solution. The first developed and experimentally verified solutions were based on a heat exchanger with circulating water buried under the bedding. Due to the mechanical limitations, and the animals' comfort, it has to be covered with a thick layer of litter (sand or straw). The type and depth of the litter were studied by Radoń et al. [59], who developed a CFD (Computational Fluid Dynamic) model in which they took into consideration the transient heat exchange between the cow's body and the bedding (a mattress with rubber granules). His research showed that sand bedding had a higher heat flux than straw and a mattress with rubber granulates. Ortiz et al. [60] studied the heat exchanger operation, considering a different layer thickness of the litter. Zhao et al. [61] considered conductive cooling using 3 water pipes buried under the sand as a heat exchanger, for which there was a positive effect on the heat transfer between the sand and the simulated cow. Mondaca et al. [62], in a similar solution, proved the relationship between the heat exchanger's efficiency and the thickness of the bedding present between the heat exchanger and the animal. The model they created was capable of predicting the amount of heat transferred from the cow by conduction, which was in the range of 100 - 200 W/m^2, previously reported also by Bastian et al. in [58]. A different type of heat exchanger, utilizing a waterbed, was proposed and simulated by Rojano [63], with similar values of the achieved heat fluxes. This idea was later developed by Perano et al. [64]. It was based on a commercially available water mattress for dairy cattle, modified by cutting diagonally opposite corners to ensure the circulation of ice water inside the mattress. The surface of the mattress was covered with a thin layer of bedding, providing greater thermal conductivity compared to heat exchangers buried under the sand. Further study indicated also a high influence of the litter thickness especially considering the insulative properties of the rubber [65]. The CFD model from the experimental results was developed by Gebremedhin et al. [66]. Since the last experiments conducted in that area, two conductive cooling technologies have become commercially available, and only one being cooling solution developed for waterbeds, characterized by additional pipes for the water coolant immersed in its design [67].

The interesting proposition is also the evaporative chiller conduction cooling, in which conductive cooling through water-supplied mats is combined with the evaporative chiller used to cool down the air, directed toward the cow [68]. Therefore, such systems could replace the commonly used combination of soakers or sprinkler systems and fans. Both combinations are presented in Figure 1.13.

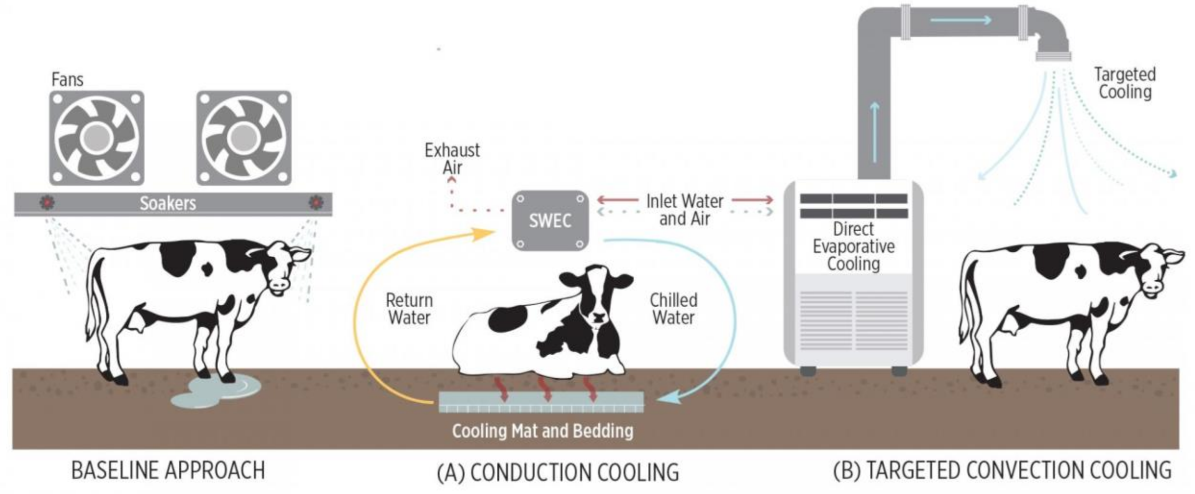

Figure 1.13. Proposed the evaporative chiller conduction cooling as the alternative to soakers and fans combination (Figure source: [68]).

Although conductive cooling is reported as a promising method for future application, the water mattress design, especially determining the water distribution system became its crucial aspect in terms of cooling efficiency. Nonetheless, little research has been done in this area. Based on the state of the literature review, there is only one study [63], which considered the heat exchanger's design, with no focus on the waterbed-based solutions. Therefore, this PhD thesis is an answer tentative approach to this knowledge gap and progressive challenges of industrial development, described previously.

1.3. Motivation and Contributions

The introduction outlined the importance of climate change and its impact on the breeding sector, especially in terms of the heat stress phenomenon in cattle, being a significant problem for numerous countries in the world. Within the last decade, the interest in the heat stress of cattle increased rapidly in the scientific community, highlighting the importance of that interdisciplinary field. The scale of this problem encompasses animals' welfare and serious health consequences, limited by the efficiency of cooling methods applicable to the cowsheds caused by the great thermal losses through their structure, as well as limitations of specific cooling solutions and their overall impact on the environment.

As presented above, many of the developed solutions for heat stress mitigation in cattle are based on convective and evaporative heat dissipation based on forced airflow and various sprinkler systems, commonly combining their operation. These solutions are commercially accessible and often used in the cowsheds. However, their operation is connected with high electricity and water consumption. Furthermore, their applicability is limited by the hygiene conditions in the bedding area, as well as the increased relative humidity of the air, which restricts the heat losses from the animal. The main objective of this study was to develop an innovative cooling mattress for cattle, allowing alleviation of the effect of the heat stress phenomenon, covering the research gap recently reported by numerous authors in this interdisciplinary field.

Therefore this PhD thesis provides a novel cooling solution for cattle, based on the cooling water mattress used as the bedding, trying to tackle the aformentioned limitations of the conventional cooling technologies in the breeding sector. The developed solution is based on conductive heat transfer from the animal to the water mattress surface, and thus to the circulating chilled water. In the research community, there are still only a few studies focused on this subject. To the author's knowledge, based on the literature review, only four universities in the entire world, and all of them from the USA: Cornell University, The University of Arizona, The University of Wisconsin-Madison, and The University of California-Davis were so far, till recently involved in studies about the conductive cooling of dairy cows applying some sort of heat exchanger, which were described in the previous subsection of this PhD thesis. The main drawbacks highlighted by those studies focused on limited heat transfer from the animal, and a thick layer of insulative sand covering the heat exchangers to achieve proper comfort of the animal. Worldwide, till recently only one research group studied the water mattress application for this purpose. However, the influence of the water mattress geometry on the heat transfer was not considered, as well as the adaptation of the operational parameters of the water mattress to the individual needs of the animals in terms of their thermoregulatory mechanism, which is especially characterized by a high potential for such a solution. Such an approach was applied within this PhD thesis bringing a new perspective on this subject.

For this purpose, four different geometries of the cooling water mattress were proposed, and simulated in the Ansys Fluent environment, then compared in terms of the chilled water distribution, surface heat fluxes, technological challenges, and animal welfare. To the author's knowledge, such an approach was not attempted before in this interdisciplinary field, contributing with new concepts for the cooling water mattress design, and theoretical limitations of its different geometries, being important for the future development of such a solution.

Selected geometry was developed to the prototype test stand and experimentally tested in both, laboratory and real barn conditions. The water mattress was equipped with temperature sensors in its interior, which enabled the continuous observation of the chilled water temperature distribution. Furthermore, chilled water supplying the water mattress was produced and distributed by dedicated hydraulic installation, being under supervisory control and data acquisition system, enabling regulation of the operational parameters of the water mattress and its up-to-date observation. Two, 30 and 29 days long experimental campaigns conducted in real barn conditions enabled the practical assessment of the developed solution working under different chilled water temperature setpoints in changing environmental conditions. Such a system enables applying the adaptive approach to animals' cooling, following the individual needs of the cow, being a novel concept for such an application, contributing to its possible further development and future application in precisive farming.

To assess the direct cooling effect on the animal's body during the experiments, an IR thermography was used, being a susceptible tool for skin temperature observation, and correlated with it thermoregulatory mechanism of the animal. To the author's knowledge, such observations in terms of conductive cooling methods for cattle and possible limitations in heat transfer, caused by the natural thermal responses of the animal for the selected chilled water temperature setpoints, were not considered before. It provided a new perspective on the practical limitations of such a solution, highlighting the importance of the chilled water temperature suitably selected for animal needs in different environmental conditions.

Furthermore, to continuously monitor animals' physiological responses to cooling in terms of the experienced heat stress level, a novel approach in monitoring strategy was applied. The heart rate sensor and skin and body temperature sensor were applied during the second experimental campaign in 2023. Their application was limited, due to their novel character in the real barn environment, restricting their accuracy assessment. However, the observations made during the experiments indicated their potential for further development and future application in precisive breeding, which could be especially useful in early heat stress detection.

It is hoped that the results presented in this PhD thesis will contribute to the research community, providing both, theoretical and experimental study of the novel cooling solution for cattle.

JCR- list journal scientific articles and conferences:

J. Błotny, S. Rosiek. Heat transfer efficiency as the determinant of the water mattress design: a sustainable cooling solution for the dairy sector. **Energy**. 2022, 245, 1-14. https://doi.org/10.1016/j.energy.2022.123243. IF:9.0, LM:200.

J. Błotny, A. Szczepanowska-Białek, R.Kupczyński, A. Budny-Walczak, S. Rosiek. Cooling effectiveness of the sustainable cooling solution for cattle: Case study in Poland. **Applied Sciences.** 2024, 14(21), 1-19. https://doi.org/10.3390/app14219678. IF:2.5, LM:100.

J. Błotny, S. Rosiek-Pawłowska. Wpływ geometrii materaca wodnego dla bydła mlecznego na efektywność wymiany ciepła na drodze przewodzenia: Projekt RadMAT. II Edition of XII Conference "Młodzi w Energetyce", 2020, Wrocław, Poland.

J. Błotny, A. Szczepanowska, S. Rosiek. Radiative water mattress - conductive cooling solution as the dairy cattle's heat stress mitigation strategy for global milk security. PSN: Conference Climate Change: Science & Society, 2022, Wrocław, Poland.

A. Szczepanowska, J. Błotny, S. Rosiek, The innovative water mattress for the dairy cattle as a component of the renewable-based cooling system for the livestock buildings: RadMAT Project, EuroSun 2022 - International Conference on Solar Energy for Buildings and Industry, 2022, Kassel, Germany.

Chapter 2

Research hypothesis and outline of the conducted study

This chapter will present the research thesis that is under consideration within this PhD thesis, as well as the research questions raised during that process. The second subsection will be focused on the outline of the conducted study.

2.1. Research hypothesis and questions

The main goal of this PhD thesis was to develop an innovative cooling solution for the dairy sector, which could reduce the effect of heat stress in cattle. The novelty of the developed solution is based on applying a specially modified water mattress working in a closed chilled water circuit, providing conductive cooling to the animal. The research hypothesis that was experimentally proved within this study is as follows:

The modified flow-based water mattress for cattle is an effective cooling method allowing the reduction of cow's heat stress.

The interdisciplinarity of that topic area combines thermal science with technical and economic challenges, as well as the animal's welfare. The novelty of the developed solution and applied within the study methods brought several challenging research questions. The main ones were as follows:

- What geometry of the cooling water mattress improves the heat transfer between chilled water and animal, compared to known conductive cooling solutions, while ensuring animal comfort?
- What setpoints of the water mattress' operating parameters ensure the appropriate level of animal cooling?
- How does the developed water mattress influence the animal's physiological and behavioral reactions in terms of its thermal comfort?

Answering those questions determined the next stages of the conducted study, which are described in the following subsection of this chapter.

2.2. Outline of the conducted study

In order, to outline the framework of the study, as well as adopted research methods, the following stages of the study will be concisely described within this subsection.

First, the geometry of the water mattress was selected from among four different propositions, carefully considered in terms of the chilled water flow, heat transfer, feasibility of the concept, and animal welfare. Each of them was 3-D modeled, then, adopted to the Ansys meshing module. Computational Fluid Dynamic (CFD) simulations conducted in Ansys Fluent Environment provided information about potential heat fluxes achieved within these geometries, on which the selection process was based. Detailed information about this stage of the study is described in Chapter 3 of this PhD thesis.

Next, the prototype water mattress was built and iteratively improved in terms of its design to achieve its smooth operation with the chilled water production and distribution system. A detailed description of the entire cooling system is presented in Chapter 4 of this PhD thesis.

Such a test stand was applied to laboratory experiments. Their main goal was to monitor the cooling process within the developed water mattress in simplified boundary conditions, which were assumed for the simulation. The obtained results were then compared with those from the simulation. Furthermore, the observations made for different chilled water temperature setpoints used for cooling narrowed the range of this parameter used in further experimental campaigns. This stage is described in detail in Chapter 5 of this PhD thesis.

The following step was implementing the developed water mattress to real barn conditions in order to check its operation in a target environment and observe its cooling effect on cattle for different cooling water temperature setpoints. For that approach, the IR thermography was used. The experimental campaign was conducted during the summer period of 2022 and lasted one month, within several experimental series. A detailed methodology of this study and its results are described in Chapter 6 of this PhD thesis. Within the next year, the experimental set-up was extended by building the second water mattress, with the main goal of verifying the repeatability of the results. Furthermore, a new monitoring strategy of the animal's physiological reactions to cooling was developed and applied. For that purpose, several sensors for skin temperature, rumen temperature, and heart rate measurements were applied during the second experimental campaign conducted during the summer period of 2023. Details concerning the methodology and results can be also found in Chapter 6 of this PhD thesis.

Additionally, the cooling solution was compared with the referenced environment in terms of cattle thermal balance, distinguishing between conductive, convective, radiative, and evaporative heat losses. For that purpose, the equations used in the zootechnical sector were used. Results with the analysis of animal thermoregulatory processes are described in Chapter 7 of this PhD thesis. General conclusions are gathered and presented with proposed future works expanding this research area in Chapter 8, being the final one of this PhD thesis

Chapter 3

Model-based cooling water mattress design development

This chapter presents the designing and modeling process of the cooling water mattress, being the main subject of this PhD thesis. The first step of the proposed study was focused on the development of the water mattress geometry, which would be applicable in terms of the heat transfer between cooling water and the animal, the well-being of the animal, and the feasibility of that solution. To meet these three conceptual lines, four geometries, based on a modification of the commercially available water mattresses were proposed. Each geometry was developed as 3-D model using Autodesk Inventor Professional 2020 software. The conducted analysis considered three different commercially available mattresses: Dual Cow Chamber (DCC) Waterbed, Single Chamber version of this model, both from one company, and AquaStar model from another company. Each proposed geometry was then applied to the Ansys meshing tool and developed as a computational fluid dynamic model simulated in Ansys Fluent software. The presented chapter is based on the author's publication, namely: *Heat transfer efficiency as the determinant of the water mattress design: a sustainable cooling solution for the dairy sector,* Błotny J., S. Rosiek, (2022), Energy and thus uses direct text citations. Each proposed geometry and its model will be described in detail, then followed by the discussion and selection of the final geometry for further development in real conditions.

3.1. Proposed geometries of the cooling water mattress

All presented below models assumed an inlet on the upper part of the mattress and an outlet in the bottom part. It was conditioned by the 4° slope of the concrete stall surface in most of the cowsheds, however it wasn't considered in numerical simulations.

The first proposed design (Model **a**) creates a meandric channel inside the mattress; this extends the liquid flow path and makes the water flow more turbulent. Potentially, it would ensure more effective heat transfer. A solution like this was designed for a single-chamber water mattress modification, adding four external panels fixed at a 80° slope from the vertical line (c.f. Figure 3.1). The slope oriented to the bottom of the mattress would also improve hygiene conditions of the bedding, by liquid discharge to the sewer. The pressurized chambers created in this design can also improve the cushioning capabilities of the water mattress.

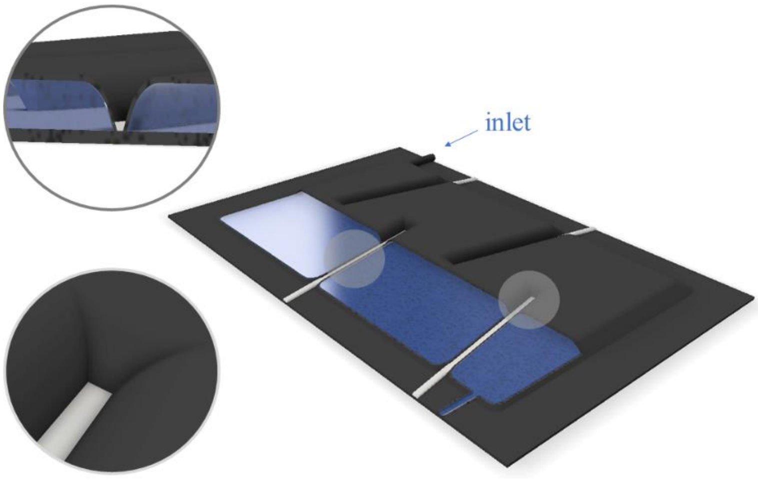

Figure 3.1. Water mattress with meandric channel (model **a**).

The second geometry was intended for a dual-chamber water mattress (the commercially available DCC Waterbed), and was an extension of the modification proposed by Perano at al. [64]. The innovative aspect of this design centered on the water distribution system. This comprises a distributor and a collector, each with a 25 mm diameter (c.f. Figure 3.2) and two rows of 22 orifices, with 12 mm and 15 mm diameters, respectively. The connection between the chambers limits the primary cushioning properties of the water mattress, but the smaller volume achieved by separating the chambers and the small diameter of the restricted channels (22 mm) might also create a sufficient effect.

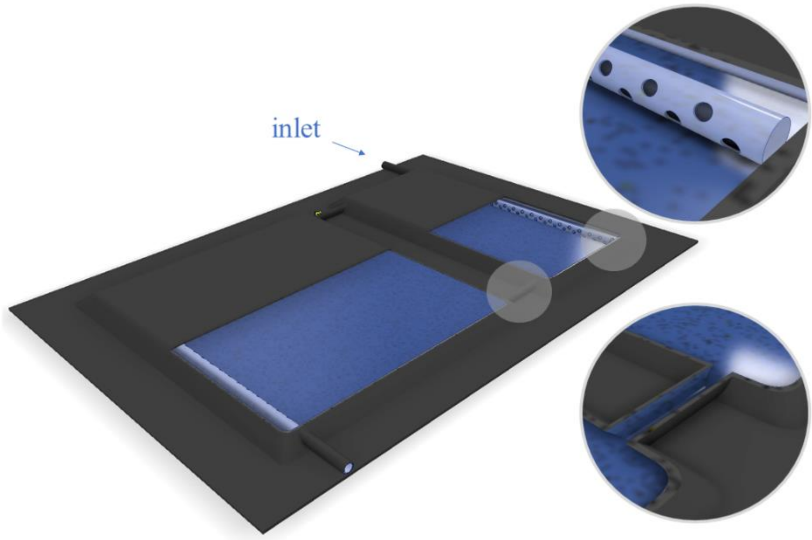

Figure 3.2. DCC Waterbed with water distribution system (model **b**).

The third design applied the same water distribution system (described above) to the single chamber water mattress: the commercially available AquaStar model from the Bioret-Agri company (cf. Figure 3.3). The selected model is equipped with additional latex foam, wrapped in foil. In the assembly procedure, the rubber mattress is rolled onto the bottom edge, fixed with panels, and placed on the foam, ensuring additional cushioning.

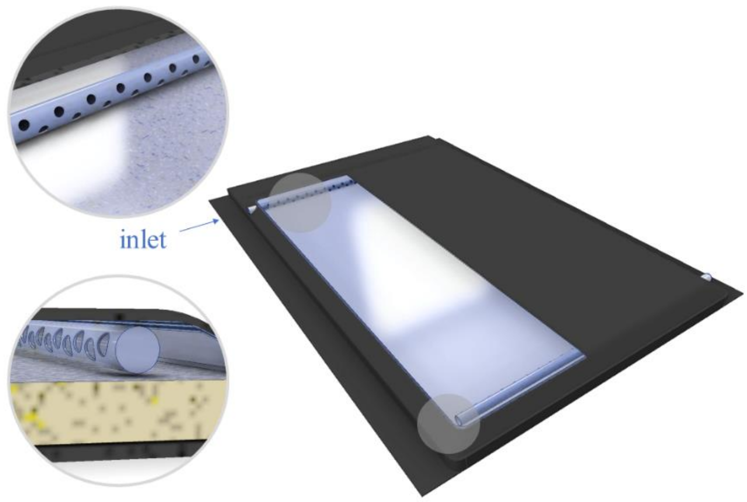

Figure 3.3. AquaStar water mattress with water distribution system (model **c**).

In the last design, a grooved rubber surface on the bottom of the mattress was proposed (cf. Figure 3.4). The structure ensures the water flow through the mattress, even when it is laden with the animal lying on top of it. The animal's comfort is maintained by the water chamber beneath the channel. A uniform water flow is achieved by adding a 50 mm-diameter water distributor with 10 orifices (each with a 10 mm diameter). The collector was replaced by a single 50 mm-diameter outer orifice.

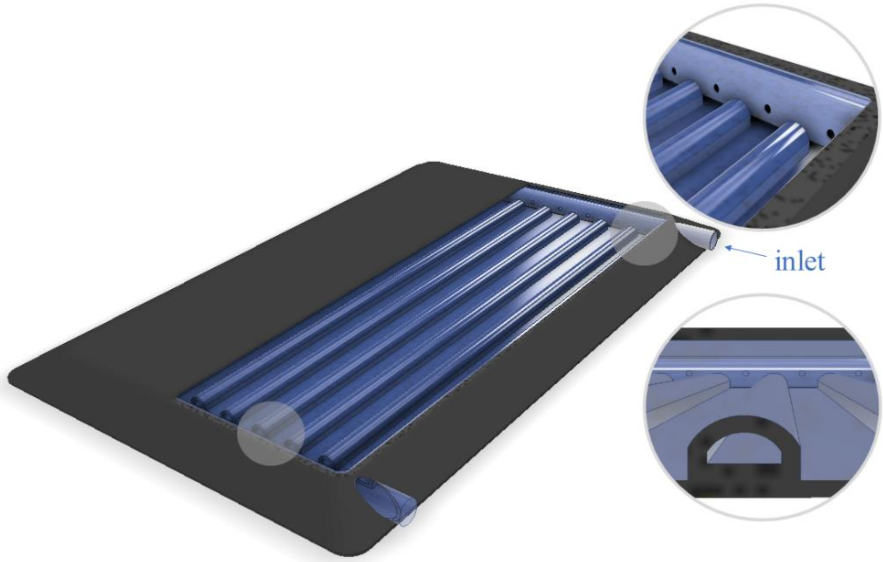

Figure 3.4. Water mattress with grooved rubber bottom and water distribution system (model **d**).

The water distribution system proposed in Model **d** is based on an perforated aluminium distributor. This system provides a more uniform flow inside the mattress, although it is more complex due to the higher demand on the coolant flow and the pressure in the system. The diameters of the distributor and the orifices were selected based on the pressure drop calculation, considering the technical guidelines for designing perforated pipes. The minimum diameter of the orifice should be at least d_0=13 mm to avoid plugging, although a smaller value would be acceptable in clean installations where there is a low risk of sediment build-up. The maximum orifice diameter is equal to 0.2 times that of the distributor's inner diameter. To provide sufficient pipe strength, the minimum distance (edge to edge) between adjacent orifices should be approximately equal to the hole diameter. Accordingly, the inner diameter chosen for the distributor is D_i=50 mm and the orifice diameter is 10 mm, which is possible given the cleanness of the installation and the distributor's 940 mm length. Such parameters provide an inlet mass flow equal to 0.85 kg/s and a velocity inside the distributor of 0.43 m/s.

The pressure drop required was calculated as being a ten-times greater than higher value between the kinetic energy (E_k) calculated using Equation (3.1) and the pressure change caused by friction and momentum recovery calculated using Equation (3.2).

$$E_k = 810 \cdot \alpha \cdot \rho \cdot \dot{V}^2 \cdot {D_i}^{-4} \tag{3.1}$$

$$\Delta P_p = 4000 \cdot f \cdot \rho \cdot L \cdot J_{as} \cdot (\alpha \cdot D_i - 1)^{-1} \cdot E_k \tag{3.2}$$

where f is the fanning friction factor, L is the distributor length, and J_{as} is a head loss factor.

The kinetic energy E_k expressed as kPa per volume was derived from the basic kinetic energy formula, where the mass was extended to the product of density ρ and the volume, while the velocity was extended to the ratio of the stream flow $\dot{V}$ (in l/s) and the flow's cross section, defined by the channel's inner diameter, D_i (in mm), in agreement with the continuity equation. The correction factor, α, takes into account the flow friction, correlated with the Reynolds number.

The minimum value of the pressure drop should be equal to 1.75 kPa to ensure uniform water distribution; this value was assumed for subsequent calculations. The number of orifices was determined by calculating the total area required for the pipe distributor orifices and the Reynolds number at the 2500 level, which already determines the distributor diameter.

3.2. Computational Fluid Dynamics models

In the following section, detailed information about the developed CFD models of the previously described cooling water mattress's geometries will be presented, as well as boundary conditions, which were applied for the conducted simulations.

3.2.1. Mesh development

The geometries presented above were created as 3D models using Inventor software, distinguishing the assumed domains and then applying them to the Ansys Fluent Meshing module. Models **a**, **b**, **c**, and **d** contain a water fluid domain and solid domains, which include the water distribution system and the rubber elements of the mattress. Given the irregularity in the shape of the geometries and the wide range of element sizes, the meshes were built separately for each model using meshing under the tetrahedrons as the discretization procedure. The energy transfer between the elements was achieved using the coupled wall boundary condition. Additionally, the mesh sizes have been defined by the element sizes, the maximal size of the elements defined using the same value as the element sizes and the defeature size.

The values vary between models due to their different complexity, as presented for the fluid domains in Table 3.1. Models with simpler geometries are characterized by higher maximal element sizes. Views of the meshes created for Models **a**, **b**, **c**, and **d**, are presented in Figures 3.5 - 3.8, showing the fluid domain and zooming in on the inlet area, including the solid domains that have been used.

Table 3.1. Mesh fluid-domain statistics for the geometry models considered

Model	Number of nodes	Number of elements	Max. size of elements	Defeature size
a	93753	454935	10 mm	5 µm
b	249946	1269685	6 mm	15 µm
c	256913	1310369	10 mm	50 µm
d	727127	3679359	8 mm	250 µm

The meshes have been checked in terms of the quality of the elements, with high results of between 0.70 - 1.00 mostly being achieved. The skewness of the elements is generally distributed between 0 and 0.50 with the highest concentration around 0.25, which is also an acceptable result. The aspect ratio is stabilized at a level of 2 with the highest value reaching 18, which is in line with the recommendations. Level of potential error is considered to be acceptable at this stage of the study, considering the mesh quality analysis, the computing time consumption, and the preliminary character of the conducted analysis.

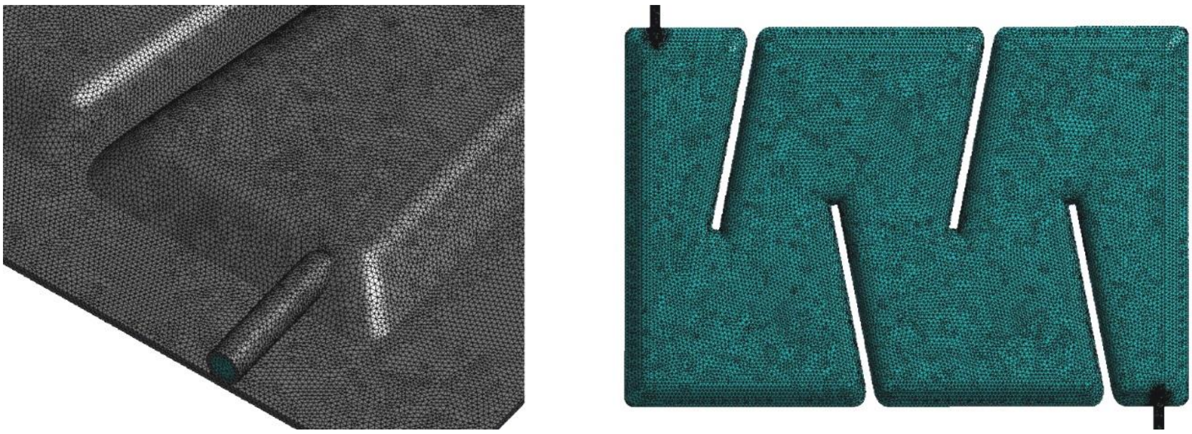

Figure 3.5. Mesh generated for all the Model **a** domains, zooming in on the inlet area (left-hand side) and the mesh generated only for the fluid domain of the same model (right-hand side).

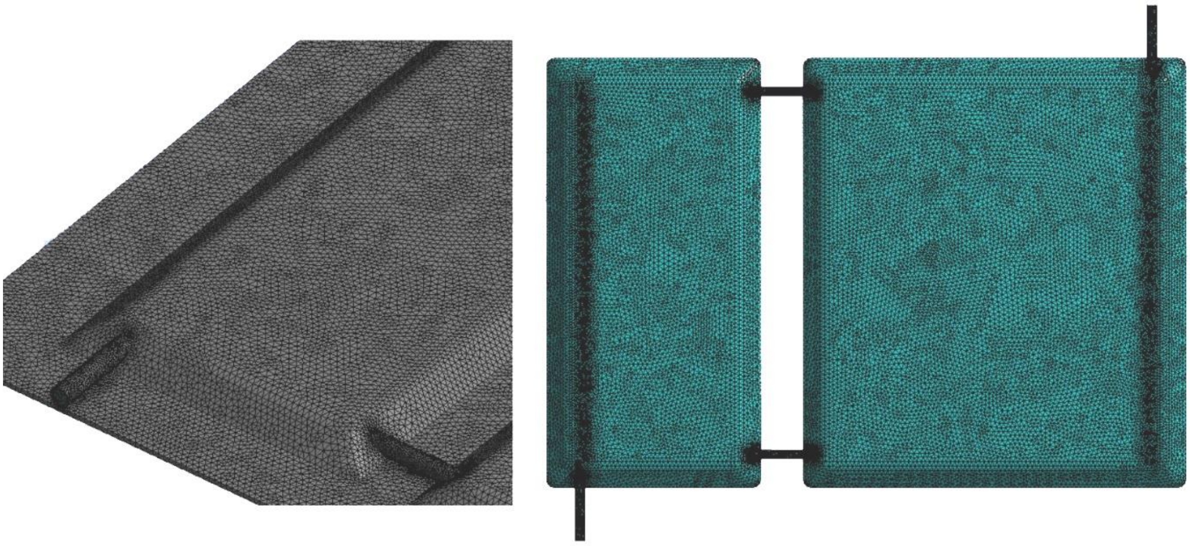

Figure 3.6. Mesh generated for all the Model **b** domains, zooming in on the inlet area (left-hand side) and the mesh generated only for the fluid domain of the same model (right-hand side).

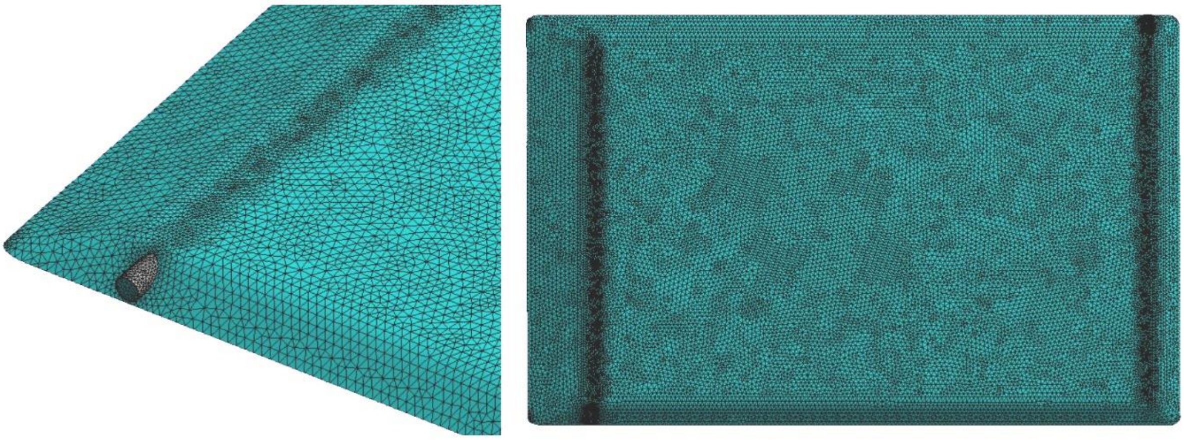

Figure 3.7. Mesh generated for Model **c**, zooming in on the inlet area (left-hand side) and the mesh generated only for the fluid domain of the same model (right-hand side).

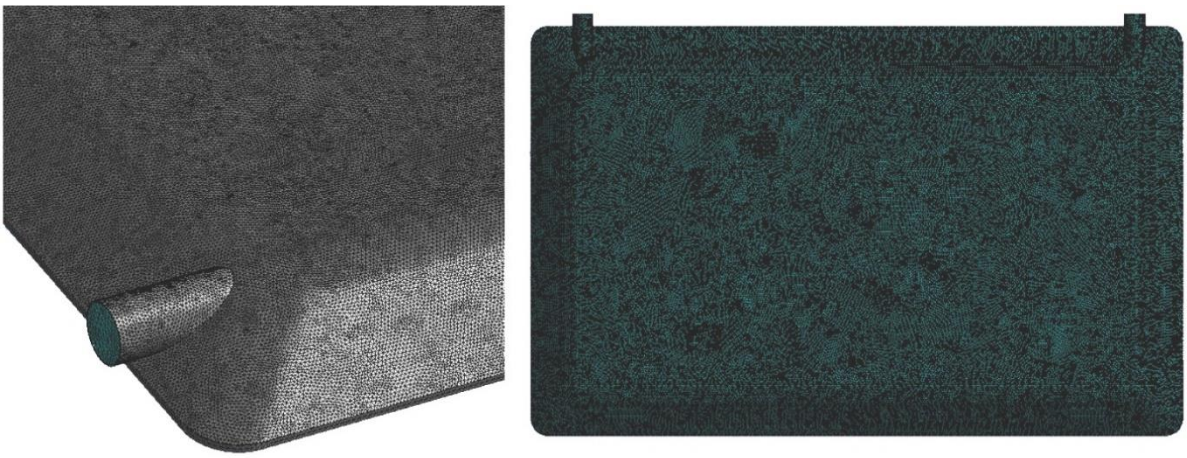

Figure 3.8. Mesh generated for Model **d**, zooming in on the inlet area (left-hand side) and the mesh generated only for the fluid domain of the same model (right-hand side).

The solver description and the boundary condition applied to the models will be developed in the following subsections of this chapter.

3.2.2. Assumptions and boundary conditions

The developed models, **a**, **b**, **c** and **d,** focus on a water mattress design that takes advantage of conductive heat transfer. Convection and radiation were not considered in this study. Such an assumption allowed one to analyze the influence of the water distribution system on local temperature changes and heat flux fluctuations. This information was crucial for optimizing the water mattress design. All simulations assumed the same environmental parameters, which were a ground temperature of 17°C and an ambient temperature of 27°C. The water coolant temperature assumed for all models was 4.5°C. The heat transfer coefficient for the air, considering natural convection, was estimated as the relationship between the Nusselt number, the thermal conductivity of the air and the characteristic factor of the rectangular surface, giving a value of 4 W/m^{2}K. This procedure requires calculating the Grashof and Prandtl numbers, and their product as the Rayleigh number.

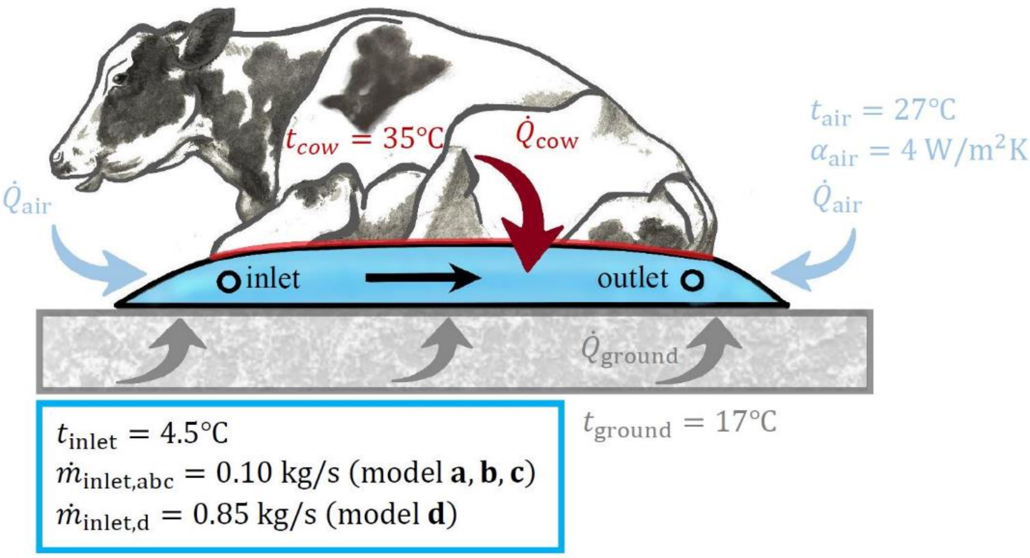

Figure 3.9. Simplified scheme explaining the simulation's boundary conditions.

The model considered the working fluid to be cold water, the distributor and collector to be made from aluminium and the mattress to be rubber. The properties of the added materials are summarized in Table 3.2.

Table 3.2. Summary of the assumed materials in the simulations performed.

Material	**Density** kg/m^3	**Specific heat** J/kgK	**Thermal conductivity** W/mK	**Viscosity** Ns/m^2
Water	998.2	4182	0.60	0.001003
Rubber	1100	800	0.10	-
Aluminium	2719	871	202.4	-

All the models were simplified with the assumption that the top surface of the mattress is in contact with the cow's body (whose temperature is 35°C). Furthermore, the mattress deformation under the cow's weight and the slope of the bedding area were not considered in the simulations. Nonetheless, these aspects were important for the water mattress design process. The described previously factors were included as the boundary conditions used for these simulations, which are presented in Table 3.3. The mass flows in Models **a, b,** and **c** were assumed to be 0.1 kg/s, which is optimal in terms of the electricity consumed to pump the coolant, the small distributor diameter, and the fluid domain volume. The construction of the Model **d** distributor requires a higher mass flow calculated using the procedure presented in Section 3.2. The described assumptions, which determine the boundary conditions that have been set, are presented as a simplified scheme (c.f. Figure 1.1) representing all the proposed models. The pressure of the coolant supplying the installation should be slightly higher than atmospheric pressure to cover linear and local pressure losses, including in the filled water mattress, which is assumed to be the last element before the tank. Pressure losses in the water mattress are also difficult to predict. It allows Models **a, b, c,** and **d** to be simplified by assuming an outlet gauge pressure equal to 0 Pa.

Table 3.3. Boundary conditions assumed for all the water mattress models.

Model	Inlet	Outlet	Top	Bottom	Walls	Coupled wall interfaces
a	Mass flow $\dot{m}$=0.1 kg/s t=4.5°C	Pressure p=0 Pa	Wall t=35°C	Wall t=17°C	Wall t =27°C α =4 W/m^{2}K	Water-rubber
b	Mass flow $\dot{m}$=0.1 kg/s t=4.5°C	Pressure p=0 Pa	Wall t=35°C	Wall t=17°C	Wall t =27°C α =4 W/m^{2}K	Water-rubber Water-collectors
c	Mass flow $\dot{m}$=0.1 kg/s t=4.5°C	Pressure p=0 Pa	Wall t=35°C	Wall t=17°C	Wall t =27°C α =4 W/m^{2}K	Water-collectors
d	Mass flow $\dot{m}$=0.85 kg/s t=4.5°C	Pressure p=0 Pa	Wall t=35°C	Wall t=17°C	Wall t =27°C α =4 W/m^{2}K	Water-rubber Water-collector Collector-rubber

3.2.3. Model formulation

All the simulations were performed in the Ansys Fluent environment with double precision under the steady-state condition. The water was modelled as an incompressible fluid. The turbulence in the fluid area was simulated using the k−ε realizable turbulence model employing enhanced wall treatment. The boundary conditions were set as described in Section 3.4. The SIMPLE algorithm with the second-order scheme was used for the pressure velocity coupling. Water flow was characterized by two governing equations, namely the continuity (3.3) and momentum equations (3.4). Heat transfer between the water coolant and the surrounding environment was determined using the energy equation (3.5) as the governing equation. The second-order upwind scheme was used as the discretization method. A precise description of the equations applied are presented in the next paragraph. A least-square cell-based scheme was used to calculate the gradients. The under-relaxation factor was set as the default. The calculations were performed in parallel mode on a personal workstation using 4 (Model **b**) or 7 Intel(R) Core (TM) i7-8665U CPU 1.90GHz 2.11 GHz processors.

Continuity equation

The general form of the continuity equation, valid for both compressible and incompressible flows [69], can be expressed as follows:

$$\frac{\partial \rho}{\partial t} + \nabla \cdot (\rho \cdot \vec{u}) = S_m \tag{3.3}$$

where, ρ is the water density, $\vec{u}$ is the velocity vector and S_m represents the source term of the mass. For incompressible flow with heat transfer, the term associated with the change in density, correlated with the fluid velocity, is equal to 0, although there is still change in density due to the influence of heat transfer.

Momentum equation

The momentum equation for turbulent flow is described by the Naiver-Stokes equation as follows:

$$\rho \left[\frac{\partial \vec{u}}{\partial t} + \vec{u} \cdot \nabla \vec{u} \right] = -\nabla p + \mu \nabla^2 \vec{u} \tag{3.4}$$

Energy equation

The general energy equation (3.5) was used for the heat transfer simulation [69], where k_{eff} is the effective conductivity, defined according to the turbulence model used in the calculations, and $\vec{J_j}$ is the diffusion flux of species j. The terms on the left-hand side of the equation represent the pressure work and kinetic energy, which for compressible flow are always accounted for during the modeling.

$$\frac{\partial}{\partial t}(\rho E) + \nabla \cdot (\vec{u}(\rho E + p)) = \nabla \cdot (k_{eff} \nabla T - \sum_j h_j \vec{J_j} + (\bar{\bar{\tau}}_{eff} \cdot \vec{u})) + S_h \tag{3.5}$$

The terms on the right-hand side of the equation (3.5) represent the energy transfer due to conduction, species diffusion, and viscous dissipation, respectively. In the case considered, the pressure-based solver has been used whereas the thermal energy created by the viscous shear in the flow has not been included in the calculations. Term $S_h$includes the heat of chemical reaction, and any other volumetric heat sources defined in the model. There is no volumetric source of energy in the created model, so this term is equal to 0. However, in the subsequent model, this element is going to describe the heat generated by the cow, which is simplified here to the wall boundary condition on the mattress.

In Equation 3.5, the total energy, E, can be defined by Equation 3.6.

$$E = h - \frac{p}{\rho} + \frac{v^2}{2} \tag{3.6}$$

where, for incompressible flows, sensible enthalpy is defined by Equation 3.7.

$$h = \sum_j Y_j h_j + \frac{p}{\rho} \tag{3.7}$$

In Equation 3.7, Y_j is the mass fraction of species j, and h_j is the sensible enthalpy of the species.

Transport equations

Closure of the governing equations requires additional formulas. For this purpose, the selected model uses transport equations for the turbulence kinetic energy (3.8) and its dissipation rate (3.9).

$$\frac{\partial}{\partial t}(\rho k) + \frac{\partial}{\partial x_j}(\rho k u_j) = \frac{\partial}{\partial x_j}\left[\left(\mu + \frac{\mu_t}{Pr_k}\right)\frac{\partial k}{\partial x_j}\right] + G_k + G_b - \rho\varepsilon - Y_M + S_k \tag{3.8}$$

where G_k is the turbulence kinetic energy generated due to the mean velocity gradients, G_b is the turbulence kinetic energy generated due to buoyancy, Y_M is the contribution of the fluctuating dilatation in the compressible turbulence to the overall dissipation rate, and Pr_k is the Prandtl number for k and S_k representing the source term [69].

$$\frac{\partial}{\partial t}(\rho\varepsilon) + \frac{\partial}{\partial x_j}(\rho\varepsilon u_j) = \frac{\partial}{\partial x_j}\left[\left(\mu + \frac{\mu_t}{Pr_\varepsilon}\right)\frac{\partial \varepsilon}{\partial x_j}\right] + C_1 S_\varepsilon - \rho C_2 \frac{\varepsilon^2}{k + \sqrt{\nu\varepsilon}} + C_{1\varepsilon}\frac{\varepsilon}{k} C_{3\varepsilon} G_b + S_\varepsilon \tag{3.9}$$

where:

$$C_1 = \max\left[0{,}43, \frac{\eta}{\eta + 5}\right];\ \eta = S\frac{k}{\varepsilon};\ S = \sqrt{2S_{ij}S_{ij}} \tag{3.10}$$

C_z and $C_{1\varepsilon}$ are the constants and Pr_ε is the Prandtl number for ε and S_ε, representing the source term.

The eddy viscosity in the model is calculated using Equation 3.11:

$$\mu_t = \rho C_\mu \frac{k^2}{\varepsilon} \tag{3.11}$$

The second-order upwind for momentum and energy was used. The fluid dynamic field was calculated with the pressure-velocity coupling algorithm following the SIMPLE (Semi-Implicit Method for Pressure Linked Equations) scheme. Flow through the mattress was assumed to be turbulent and calculated using the k-ε realizable model with enhanced treatment around the walls. The gravity on the Z axis was also set in the **a, b, c,** and **d** models. It is predicted that different flow types will occur throughout the fluid domain, caused by the geometry and nature of the mattress, especially when the fluid domain also includes the flow through the distributor. Additional pressure caused by the animal's movement would likewise be responsible for local turbulence in the flow.

3.3. Results of the simulations

The main purpose of the simulations performed was to observe the geometries of the water mattresses and how they relate to heat transfer efficiency in order to inform the preliminary selection of the developed cooling technology. An error of satisfaction of the conservation laws was achieved. Convergence of the energy conservation law was achieved for residuals in the order of 10^{-6}.

The proposed water distribution systems were evaluated in terms of the streamlines and velocity vectors generated in the models' cross sections. Insight into the turbulence of the flow, the velocity level and the water flow pattern, together with thermal parameters such as the water temperature in a cross section ($T_{\mathrm{w,cross}}$), the inlet-outlet temperature gradient ($\Delta T_{\mathrm{w,in-out}}$), the heat transfer ($\dot{Q}_{\mathrm{top}}$) and heat gains ($\dot{Q}_{\mathrm{bottom}}$), all indicate the thermal efficiency of the proposed solutions. Specific analyses of the **a**, **b**, **c**, and **d** models are presented in the following paragraphs.

Table 3.4. Average thermal efficiency indicators for the proposed models.

Model	$\boldsymbol{T_{\mathrm{w,cross}}}$ °C	$\boldsymbol{\Delta T_{\mathrm{w,in-out}}}$ °C	$\boldsymbol{\dot{Q}_{\mathrm{top}}}$ $\mathrm{W/m^2}$	$\boldsymbol{\dot{Q}_{\mathrm{bottom}}}$ $\mathrm{W/m^2}$
a	7.52	2.00	519	49.3
b	10.03	3.49	536	43.1
c	11.53	3.10	509	118.9
d	5.14	0.66	715	134.3

The meandric structure of Model **a** determines the sinusoidal shape of the water flow (c.f. Figure 3.10). As expected, the best thermal efficiency occurs in the upper part of the mattress because of the higher temperature gradient in that area. Within the flow, the water temperature increases slightly, reaching an average outlet temperature of 7.99°C (c.f.Figure 3.11). Every turn in the flow path (c.f. Figure 3.10) generates low energy swirls, which reduce the heat flux from 650 W/m^2 in the main stream down to 350 W/m^2 (c.f. Figure 3.13). These promising results are challenged by the potential risk of leaks or leg injuries to the cow due to the fixing methods and external elements.

The water distribution system proposed in Model **b** results in a dramatic decrease in velocity (from 0.30 to 0.003 m/s), with insufficient powering of the right channel (c.f. Figure 3.13). This phenomenon, in combination with stream deflection at the distributor orifices, determines turbulence occurrence. Adding the collector to the design makes uniform collection of the returning water difficult to achieve. Consequently, the thermal properties of the mattress chambers differ between one and the other by a 10°C temperature increase (c.f. Figure 3.14) and a 300 W/m^2 decrease in flux (c.f. Figure 3.15) compared to the upper chamber. The thermally beneficial conditions in the upper chamber overstate the average heat flux values available on the top of the mattress (c.f. Table 3.1). Given that the bottom chamber has the largest contact surface with the animal, such a correlation is not profitable.

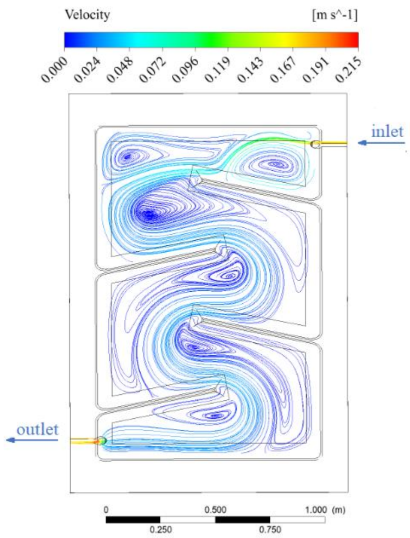

Figure 3.10. Surface streamlines generated in the cross section of Model **a**.

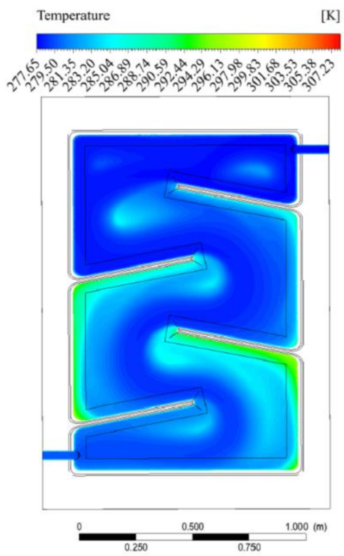

Figure 3.11. Temperature contour in the cross section of Model **a**.

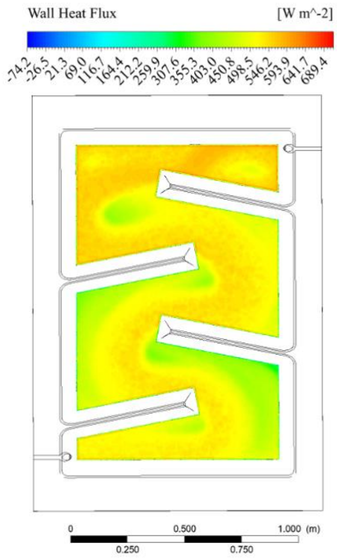

Figure 3.12. Heat flux on the top surface of Model **a**.

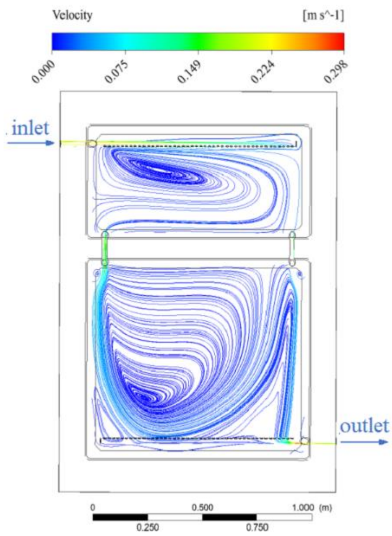

Figure 3.13. Surface streamlines generated in the cross section of Model **b**.

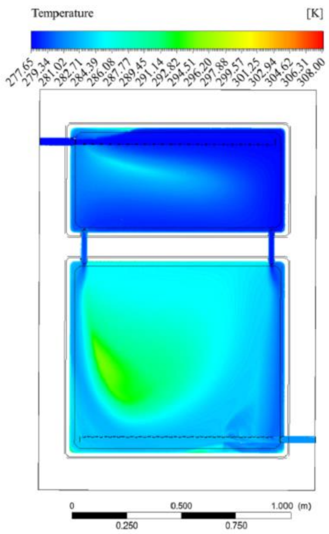

Figure 3.14. Temperature contour in the cross section of Model **b**.

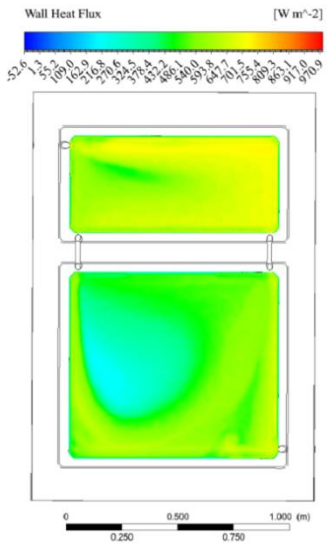

Figure 3.15. Heat flux on the top surface of Model **b**.

The same water distribution system applied to the single chamber water mattress (Model **c**) changes the water flow pattern and extends the upper swirl into the central one (c.f. Figure 3.16). Although higher collecting capabilities are observed, the left side of the mattress is not sufficiently powered by the coolant, as represented in the temperature profile in Figure 3.17.

This divides the water mattress into two thermal zones – the left one has an average heat flux value of 400 W/m^2 whereas the right one has an average heat flux value of 728 W/m^2 (c.f. Figure 3.18), making this solution inappropriate for the animal's needs. Additionally, the heat gains are double those of Models **a** and **b**, thus increasing the average temperature and reducing the thermal efficiency of the design.

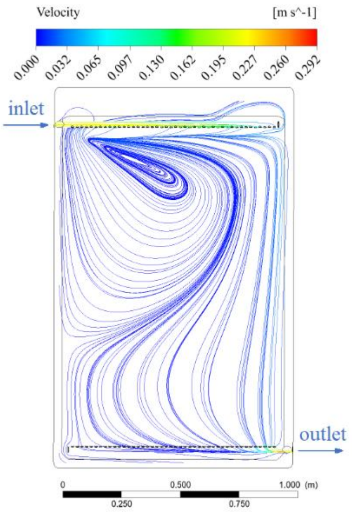

Figure 3.16. Surface streamlines generated in the cross section of Model **c**.

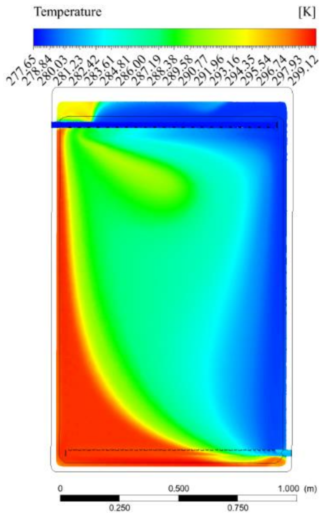

Figure 3.17. Temperature contour in the cross section of Model **c**.

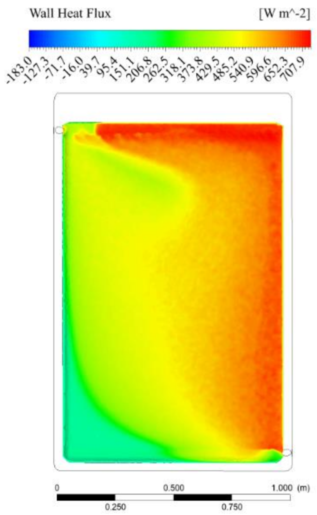

Figure 3.18. Heat flux on the top surface of Model **c**.

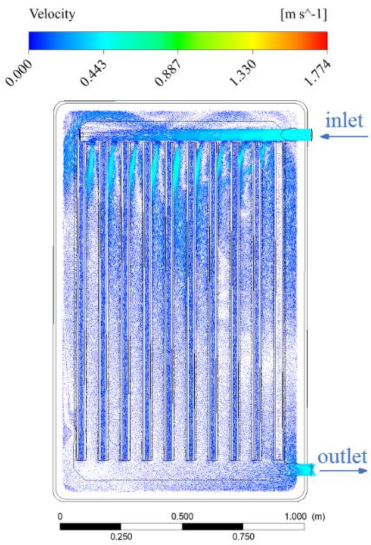

Figure 3.19. Velocity vectors for the cross section through the channels in Model **d**.

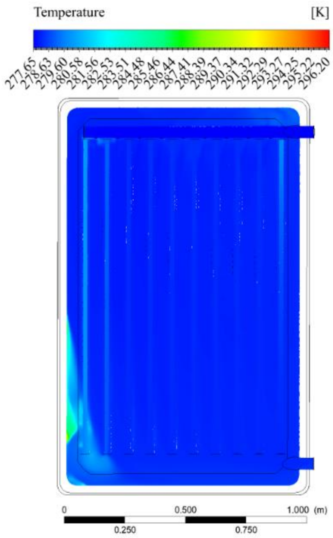

Figure 3.20 Temperature contour for the cross section through the channels in Model **d**.

Figure 3.21. Heat flux contour on the top of the mattress in Model **d**.

The dual geometry of Model **d** creates two distinct sections: the channel structure and the water chamber beneath it, characterized by different flow dynamics. Having the specially-designed distributor, the channels straighten the water flow and power all the orifices at a relatively high velocity, which ranges from 1.77 m/s to 0.44 m/s (c.f. Figure 3.19). The water chamber has a more stable flow character with lower velocities and negligible turbulence near the orifices. The temperature contour in cross section through the channels is uniform with a small heat zone in the left corner caused by insufficient water distribution (c.f. Figure 3.20). A small temperature difference - 0.66°C between the inlet and the outlet - confirms this relationship. As a result, the heat flux profile is uniform, with an average value of 715 W/m^2 (c.f. Figure 3.21); this is the highest value of all the presented models.

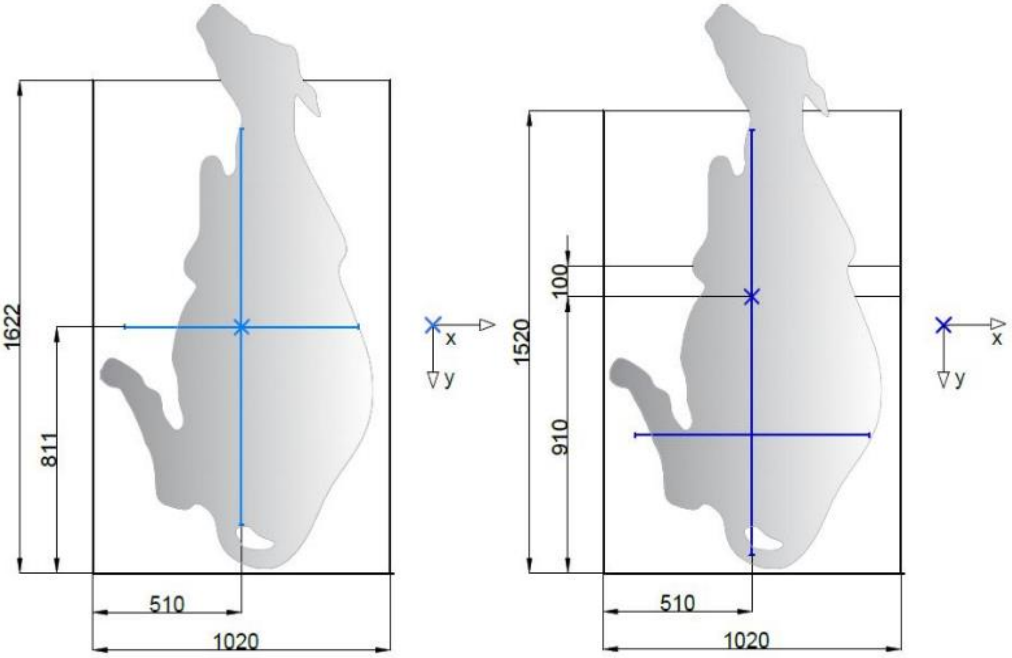

Figure 3.22. Contours of the mattresses with the shape of the cow lying on them, with the marked lines showing the sources of the collected data: on the left (in light blue) – Models **a**, **c**, and **d**; on the right (dark blue) – Model **b**.

A thermal comparison between the models was carried out by collecting a 1000 data samples from two lines: over the length (L) and width (W) of the mattress, as presented in Figure 3.22. The coordinate system for Model **b** starts with the bottom chamber, which is the surface in contact with the animal. Hence, the width line is set in the middle of that chamber. Figure 3.23 a and b present the heat flux distribution throughout the mattress for Models **a**, **b**, **c**, and **d**, expressed as the ratio of the y or x coordinates to the total length and width of the mattress. Model **a** is characterized by a lower contact surface with the animal, due to the external panels, which introduces discontinuity over the length of mattress (cf. Figure 3.23 a). Deviations ranging from 100 - 200 W/m^2 occur between the adjacent peaks of the chart. Nonetheless, the heat flux distribution over the width is more stable, at around 550 W/m^2, with a decrease on the left side of the mattress (c.f. Figure 3.23 b). The characteristics of Model **b** (cf. Figure 3.23 a and b) highlight the heat flux drop of up to 330 W/m^2 in the turbulence area visible in Figure 3.4, a similar tendency can be observed in the upper part of Model **c**. A heat flux above 700 W/m^2 (the highest result obtained) occurs in Model **d**; this is characterized by a stabilized profile over the length and width of the mattress, making it preferable in terms of thermal efficiency.

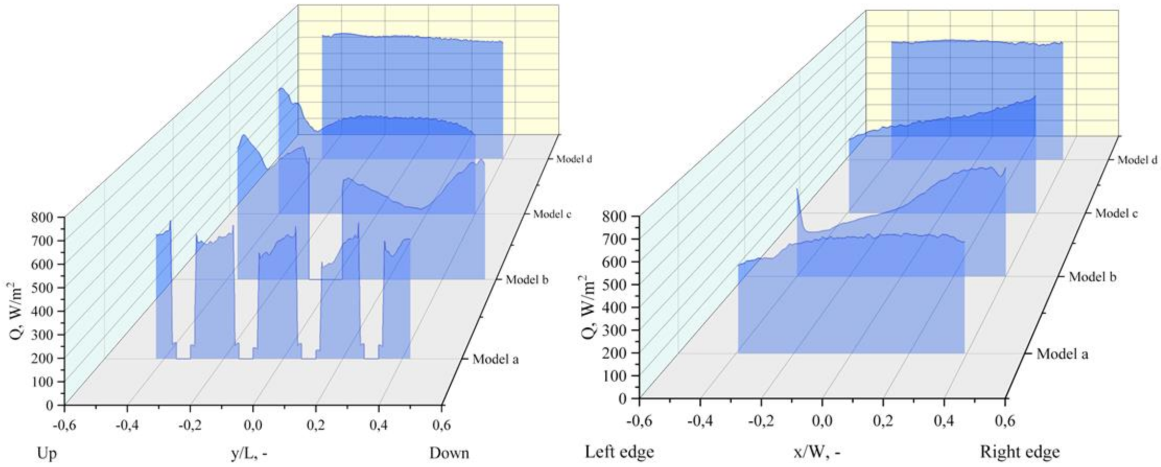

Figure 3.23. Heat flux distribution over: a - the length of the mattress expressed as y, and the total length (L) of the mattress ratio for all models; and b - over the width of the mattress expressed as x, and the total width (W) of the mattress ratio for all models.

3.4. Geometry selection

The following section presents the discussion of the previously presented cooling water mattress' geometries in terms of their technological, thermal, as well as animals' welfare oriented, advantages and disadvantages, in order to select the final geometry for further development into the prototype test stand. Each proposed design was carefully analyzed not only in terms of the obtained in the simulations cooling effect (heat flux on the mattress' surface) but also the technological aspects, which could influence the feasibility of future test-stand development. It took into consideration the sensitive elements of the construction, which could cause tightness or endurance problems with the mattress. Furthermore, the target application of the developed solution, intended for a real barn environment indicated the animals' welfare aspects, such as proper cushioning of the animal's body, stability of the bedding surface, as well as hygiene conditions. The summarized comparison of the proposed designs in terms of all of these aspects is presented in Table 3.5.

Table 3.5. Comparison of the proposed models in terms of the technological, thermal and welfare (dis)advantages (+ advantages, - disadvantages).

Model	Technological (dis)advantages	Welfare (dis)advantages	Thermal (dis)advantages
a	- possible leakage at the rubber-panel connection + modification does not require opening the vulcanized mattress + shaped channel directs the flow and reduces the risk of flow blockage	+ liquids naturally run off the mattress in the direction of the cowshed's corridor - possible leg injury caused by the panels	+ high potential heat flow from the resting cow - high heat flux fluctuation over the mattress - reduced contact surface with the animal
b	- possible difficulties modifying the mattress due to limited access to the mattress's interior - difficulty implementing a large-scale application - possible flow blockage	- flow connection between the chambers negates the primary function of the DCC Waterbed, which is to provide greater support to the front limbs	- heat accumulation in the larger mattress chamber + intensive cooling in the upper water chamber
c	- possible flow blockage - small distributor and collector, which makes coolant distribution uneven	+ latex foam layer would give additional support to the cow's knees	- high coolant temperature in the area in contact with the cow's body - high heat gains from the ground
d	+ modification concepts offer the possibility of locating sensors inside the mattress + the created channels ensure flow through the laden mattress	- / + channels inside the mattress might be uncomfortable for the cow; however, the water chamber above the channels should compensate for this effect	+ a more even temperature contour of the coolant + a high and uniform potential heat flow from the cow - formation of a heat zone in left bottom corner - high heat gains from the ground

As the result of the conducted discussion presented in Table 3.5 the design with the channel structure inside the cooling water mattress and water distribution system (model **d**) was selected for further development into the prototype test stand. It was characterized not only by the highest heat flux, and the most uniform temperature distribution on its surface indicated by the simulation results, but also character of the water distribution, shaped by the channel structure in its interior. Thanks to it, the water flow should be maintained, even under the cow's body weight, being a cause of local mattress deformations in the real barn application. Furthermore, this design was characterized by its usefulness for the prototype application, in which the chilled water temperature in its interior could be monitored. The prototype test stand based on selected geometry is presented in detail in Chapter 4 of this PhD thesis.

3.5. Conclusions from the water mattress design development

This chapter of the presented PhD thesis presented the simulations' results of the developed CFD models for four different water mattress designs, working in the cooling mode, to provide cool surfaces for dairy cattle to lie on. The models simulated the flow pattern through the mattress, the temperature distribution, and the conductive heat flow on the top surface of the mattress, assuming its entire surface in the direct contact with the cow's skin (at a temperature of 35 °C). The predicted heat fluxes for the proposed models (a, b, c and d) obtained values of 518, 536, 509 and 715 W/m^2, respectively. The rationality of the obtained results and the similar heat flow ranges compared to research studies found in the literature indicated the preliminary validity of the models in terms of their usefulness in the mattress' geometry selection. The thermal character of the conducted study, connected with a consideration of the technological challenges, as well as animal welfare aspects of such solution enabled the selection of the cooling water mattress design, based on channel structure in the mattress' interior and water distribution system (model d), which was further developed as a part of the test stand used in this PhD thesis. Its detailed description will be the main focus of Chapter 4 of this PhD thesis. For further interpretation of the obtained results, the laboratory experiments were also conducted, during which model results were also compared with collected data and real work observations, which will be described in Chapter 5 of this PhD thesis

Chapter 4

Innovative cooling system description

The following chapter provides a detailed description of the developed cooling system for cattle based on the innovative water mattress, which geometry was previously selected throughout CFD simulation. The chapter consists of 3 subsections, first the water mattress design will be presented, focused on the designing and building process of the real-scale prototype, then the applied monitoring system is an integral part of the design will be developed, and lastly, the chilled water production and distribution system will be presented. It is worth mentioning that the mattress designing and building were iterative processes during which all technical challenges were confronted with the proper operation of the entire system and animal wellbeing. The novelty of that solution made it also entirely new in terms of feasibility studies, where each designing step was verified in terms of its applicability in the developed solution. Therefore in this chapter all aforementioned challenges will be also discussed.

4.1. Cooling water mattress design

Designing and building processes were focused on three main directions:

a) uniform water distribution achieved by channel structure and water-supplying distributor,
b) durable and leakproof construction with maintained animal comfort,
c) detachable construction with open access to the mattress's interior, for a research purpose only.

Furthermore, the monitoring strategy of the innovative water mattress was extensively analyzed, and it will be described in detail in the next section of this PhD thesis.

The basis of the designed cooling water mattress was a commercially available rubber mattress destined to be filled with water and used as the waterbed, but with no water circulation, in the cowsheds. Such a mattress is characterized by elasticity to reduce tension in the cow's body, at the same time its durability is enhanced thanks to the reinforced rubber from which it is made, and finally characterized by a 10-year guarantee given by the producer. It was used as the coating surface of the designed within this PhD thesis cooling water mattress. The bottom surface of the mattress was an integral part of the channel structure of the selected geometry. Commercial production of such components is based on specially prepared forms, which can be directly used on the production line. However high costs of such a form excluded it from a lab-scale prototype building process. Instead, the conventional 5 mm thick layer of rubber was vulcanized with rubber semicircle-shaped fenders (43 mm wide, 25 mm high). The choice was justified by the shock-absorbing properties of the fenders with maintained susceptibility to deformation under animal weight ensuring the comfort of usage. Furthermore, the semicircle shape of the fender reduces the insulative contact surface with coating rubber in case of deflection under the cow’s weight.

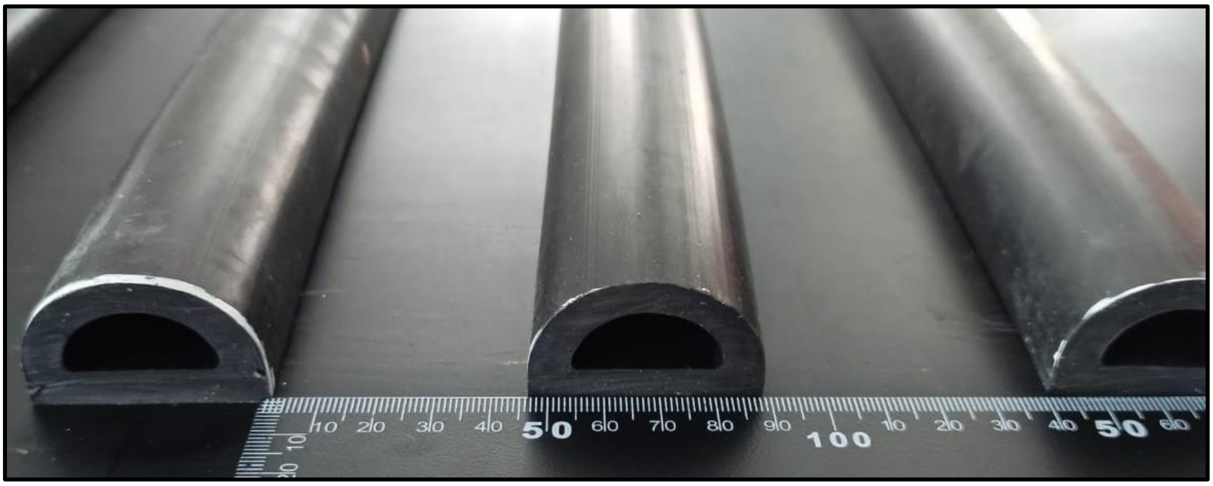

Figure 4.1 Channel structure inside the water mattress shaped by 10 fenders distanced by 46mm from each other.

Ten 1 m long fenders were spaced at around 46 mm distance (c.f. Figure 4.1) from each other, shaping the main channels of the cooling water flow. Distance was determined by the number of channels and width of the cow’s hoof to ensure safe standing and moving of the animal on the mattress surface, without the risk of dislocation of a limb.

To achieve uniform water distribution inside each channel, cooling water was supplied by 50 mm diameter distributor with 9 orifices with 10 mm diameter. Each orifice was positioned in the center of the channel (c.f. Figure 4.2). The distributor was made of stainless steel pipe. The collector which collects water from the channels was a short stainless pipe with the same diameter as a distributor.

Figure 4.2. View on the water distributor: on the left-hand side – in the preparation process, on the right-hand side: distributor fixed inside the water mattress witht the improvements applied after the preliminary experiments.

The main technical challenge of that solution was to stabilize the distributor inside the water mattress, to unable its dislocation, and to achieve leakproof derivation to the supplying system. For that reason, special supporting components were designed in Inventor software and 3-D printed using PLA filament.

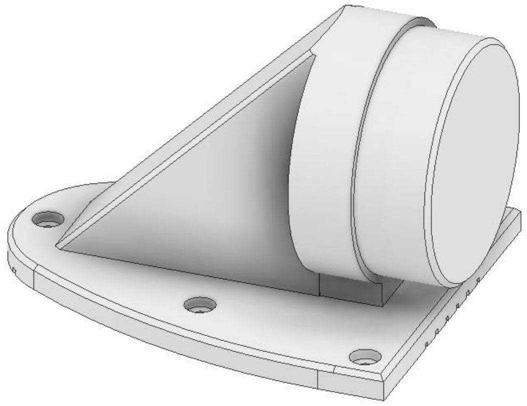
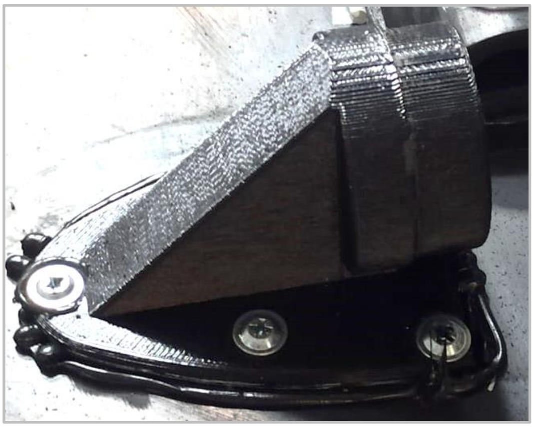

Figure 4.3. Improved within the second design supporting element for the distributor located inside the water mattress, on the left-hand side 3-D model, and on the right-hand side 3D printed element fixed inside the mattress.

The first one was located inside of the water mattress, closing the water distributor (c.f. Figure 4.3), improved in the second water mattress, in which also the additional supporting element was added in the form of the trough (c.f. Figure 4.4).

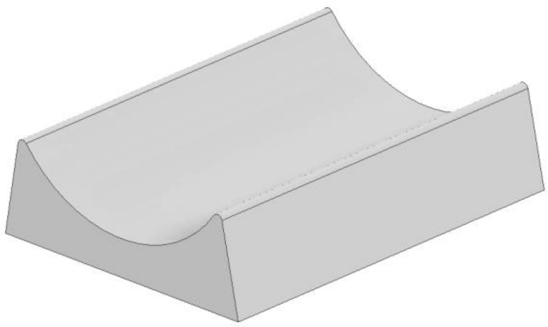
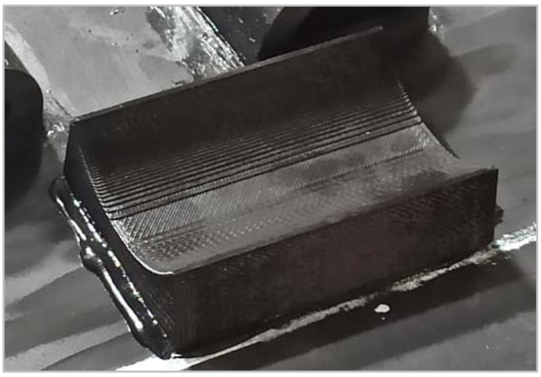

Figure 4.4 Added as the design improvement, supporting element for the water distributor located inside the water mattress, under the pipe, on the left-hand side 3D model, and on the right-hand side 3D printed element fixed in the water mattress.

Another one was outside the water mattress in the form of a sealed clamp connected with the rubber collar vulcanized to the rubber coating. A similar solution was used for a collector's connection, which is presented in Figure 4.5. The channel-shaped bottom rubber and the coating rubber were placed on the wooden chipboard for necessary stiffness to make the proper connection between them, consisting closed design of the water mattress. The main technical challenge was to achieve simultaneously leakproof with proper durability of the connection and its demountable character in case of necessary improvements in the mattress interior. It was achieved with silicone and the aluminum panel shaped for the labyrinth seal and screw connection.

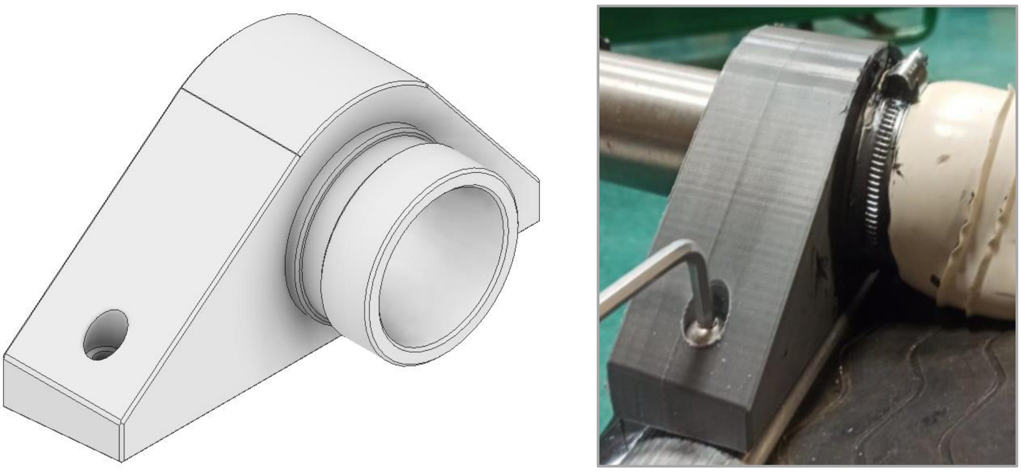

Figure 4.5 From the left-hand side: 3-D printed element supporting the collector in cooling water mattress built in 2023, and its connection between the rubber collar and distributor in the real prototype.

Due to the large size, the weight of the cooling water mattress, and its planned operation shifted from a laboratory to the cowshed, the water mattress was placed on the steel frame with wheels, which ensured the logistic elasticity of the water mattress handling module. Its final design is presented in Figure 4.6.

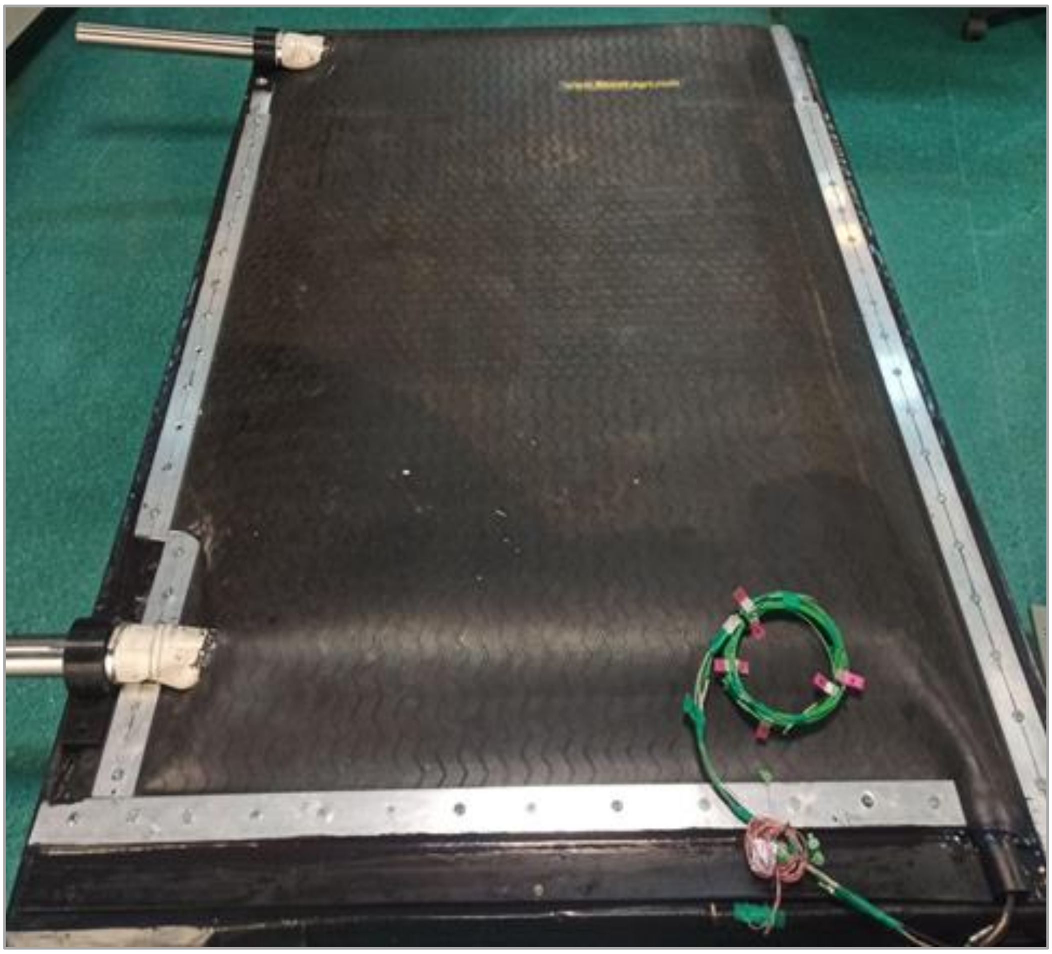

Figure 4.6. Assembly of the first developed cooling water mattress.

4.2. Monitoring system applied to the water mattress

One of the advantages of the selected geometry was the possibility of applying a monitoring system to the water mattress interior. Measurement of the temperature among channels enabled verification of the water distribution in the proposed design and to compare it among others with the results achieved throughout the simulation. It was also important from the research point of view, since the real experimental conditions the movements of the animal could be the reason for local flow disturbance, affecting the water mattress' cooling effectiveness. To monitor water distribution within the developed distributor-collector set-up, the first, middle, and last channels, counting from the inlet side were originally equipped with fiber optic temperature sensors (c.f. Figure 4.7 a). Four sensors, distanced 25 cm from each other, were located on two bundles and 5 sensors were on the bundle, which was placed in the first channel. The selection of that type of sensor was justified by its high accuracy and small size, which does not influence significantly the flow inside the channel. However, due to the novel application of those sensors, which was connected with the measurement risk, eight K-type (NiCr-Ni), thermocouples (with mineral insulation) with 2 m long and 1 mm wide probes from RS Company were also placed in two channels surrounding the middle one. This area was selected as the one with the major contact with the animal's body, which could be seen in water temperature difference. However, the susceptibility to damage and the measurement distortions of fiber optic temperature sensors were observed in the cowshed conditions in the experimental campaign of 2022. For that reason in the second cooling water mattress built in 2023, these sensors were replaced with thermocouples reducing also the number of measurement points (c.f. Figure 4.7 b).

Sensor selections were justified with its operation in low temperatures (the lowest temperature needed in the experiment was 4.5°C), durability, and elasticity of the probes, as well as the possibility of continuous operation in full immersion of water. Each probe was bent to the middle area of the channel and placed at the same height as the fiber optic temperature sensors. In the same way, the additional thermocouple was placed in the bottom left corner of the water mattress to verify if a hot zone, visible in the simulation results will be also observed in real conditions. Data from thermocouples were collected using KD-7 data logger with a 1-minute sampling time. Detailed sensors' location for both cooling water mattresses is presented in Figure 4.7.

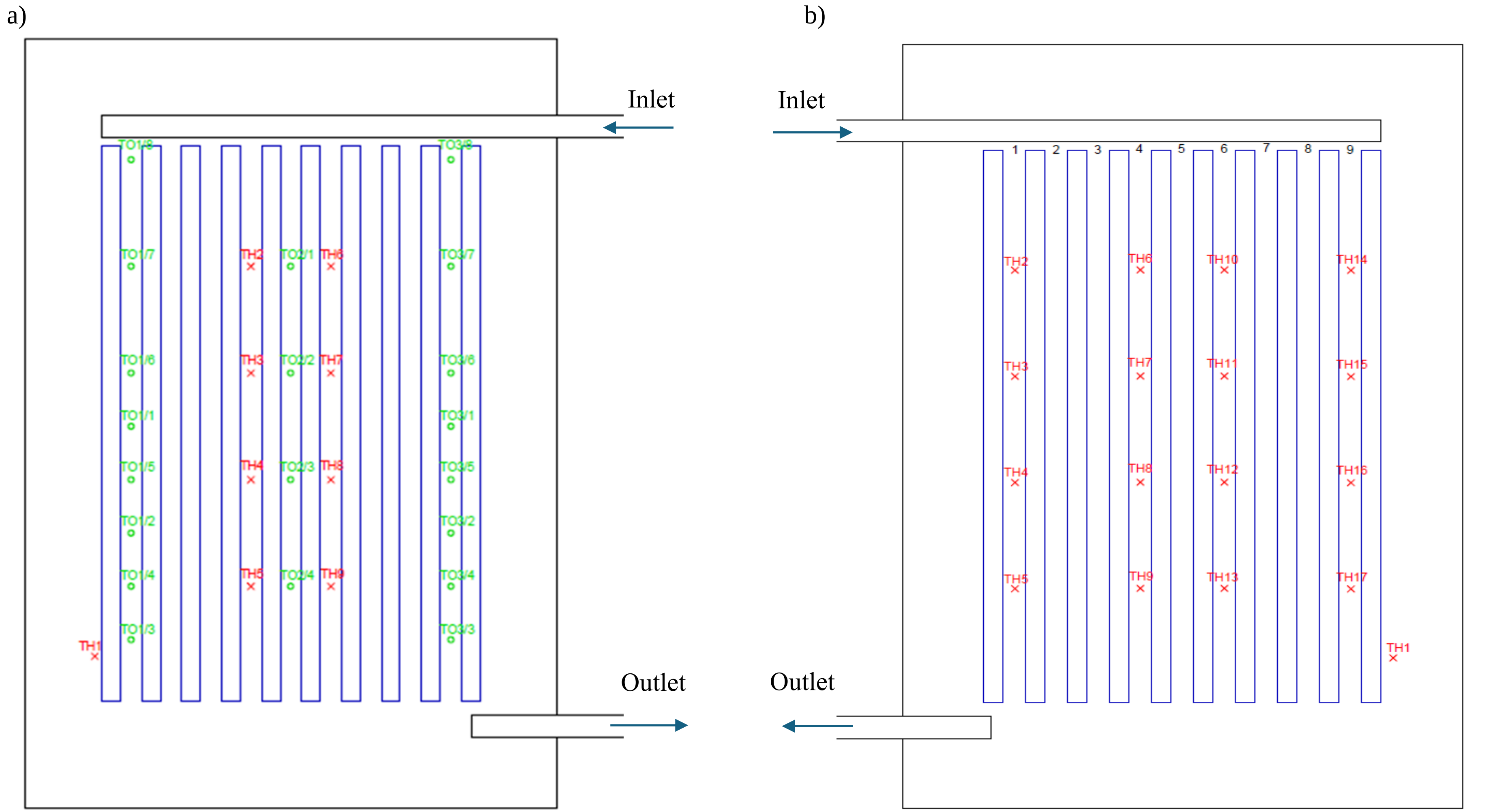

Figure 4.7. Scheme of temperature sensors located: a) in the first cooling water mattress (used in the experiments in 2021-2022) interior (TH - thermocouple, TO - fiber optic temperature sensor) b) in the second water mattress (used additionally in the experiments in 2023).

Figure 4.8. Graphic illustration of the sensors' arrangement: thermocouples and fiber optic temperature sensors (monitoring points are marked with yellow color) for the first water mattress.

The monitoring strategy included also the thought placement of the heat flux sensors on the top surface of the water mattress. Their application would give direct information about heat received from the animal to the cooling system, which could be compared with simulation results. For the experiments, the Omega HFS-5 sensor was selected, based on T-type thermocouples. The selection process took also into consideration the elasticity of the sensor, which was placed on the rubber surface. The strategy of sensor location was focused on applying them in the areas of direct contact with high heat production rates, such as the liver, heart, and udder of the animal. Possible sensors' distribution with marked animal organs and resting positions of the animal that was considered within this PhD thesis is presented in Figure 4.8. However, due to the limited number of available sensors and difficulties with their application to the rubber, grooved, elastic surface, finally, for lab-scale experiments only one sensor was used and its location will be described in Chapter 5 of this PhD thesis.

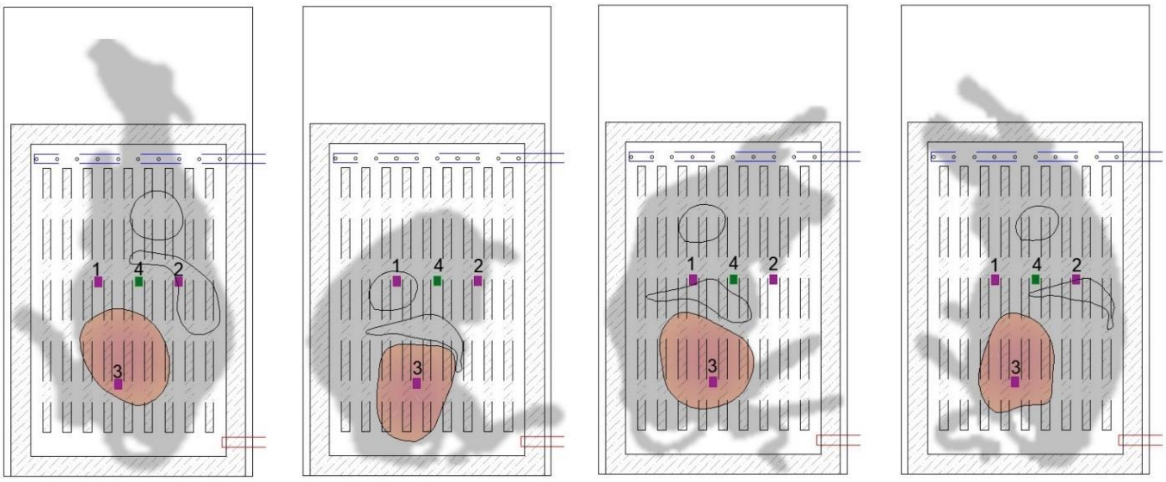

Figure 4.9. Considered heat flux sensor arrangement on the water mattress surface (sensors 1, 2, 3, sensor 4 are located on the bottom of the mattress), which takes into consideration animal organs characterized by high heat production rate (from the top: heart, liver and udder), and different positions on the designed mattress.

An additional heat flux sensor was applied under the bottom layer of rubber, to monitor heat gains from the ground. For this purpose special paste with high thermal conductivity was applied. Lastly, another T-type thermocouple (TTE500 model) from TermoAparatura Company was used as the reference surface temperature measurement for the thermal imaging of the cooling water mattress. Furthermore, the water temperature increase among the developed water mattress was measured using temperature sensors located at the chilled water supply and return distribution pipe (Vortex SV7204-SVR34XXX50KG/US-100, accuracy rating ±1°C, and ifm TA2115, accuracy rating ±0.1%, respectively).

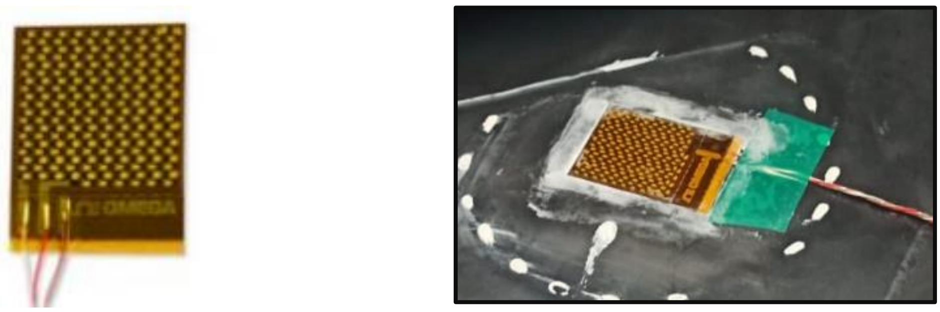

Figure 4.10. Omega HFS-5 heat flux sensor (source: [70]) and its location on the chipboard under the bottom layer of mattress' rubber to measure heat gains from the ground.

4.3. Chilled water production and supplying system

The cooling water temperature inside the water mattress can be maintained at the selected setpoint by the chilled water production and distribution system. The operation of the entire system was monitored by the supervisory control and data acquisition (SCADA) system, which enabled data collection with 1 min sampling time. The cooling system consists mainly of a chiller with 5 kW cooling capacity (Frimec MGC-V5W/D2N1), 200 l cold water storage tank, and four water circulation pumps with variable speed drivers (Ecocirc XL 32-80) and heat exchanger (Alfa Lava CB30) which separates two water circuits. The heat exchanger was added after multiple experimental tests in the laboratory conditions, which led to the conclusion that the chilled water tank and the water mattress need to be hydraulically separated to preserve proper flow through the mattress. The system was designed for the target operation with two water mattresses.

Flow was regulated from the level of circulation pumps and automatically by the electrovalve programmed in the SCADA system. Flow was measured with Vortex SV7204-SVR34XXX50KG/US-100 (accuracy rating ±2%) flow rate sensor. Cold water produced by the chiller was accumulated in the water storage tank, from which it was distributed to both water mattresses. On both, supplying and returning lines, the shut-off valves were mounted, enabling the fast detachment of the mattress from the system. Furthermore, between supplying and collecting hydraulic lines, the bypass was installed to enable chilled water production, without water flow through the mattress. Additionally, an electric three-way valve enabled supplying and returning water blending for temperature regulation. A view of the system is presented in Figure 4.11 and a simplified scheme of the installation is presented in Figure 4.12.

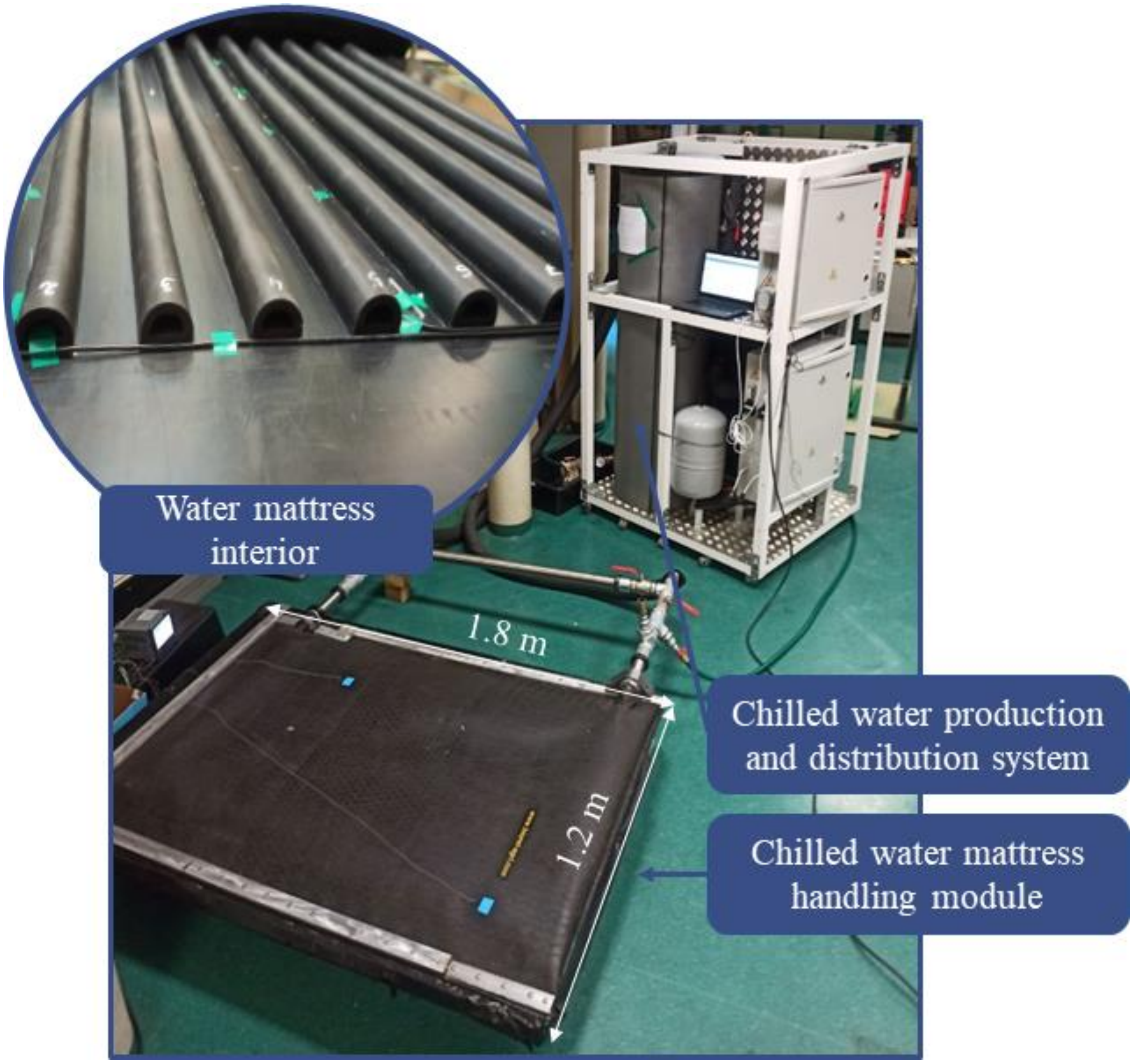

Figure 4.11. Picture of the developed within this PhD thesis cooling water mattress (on the left-hand side) with its supplying system (on the right-hand side).

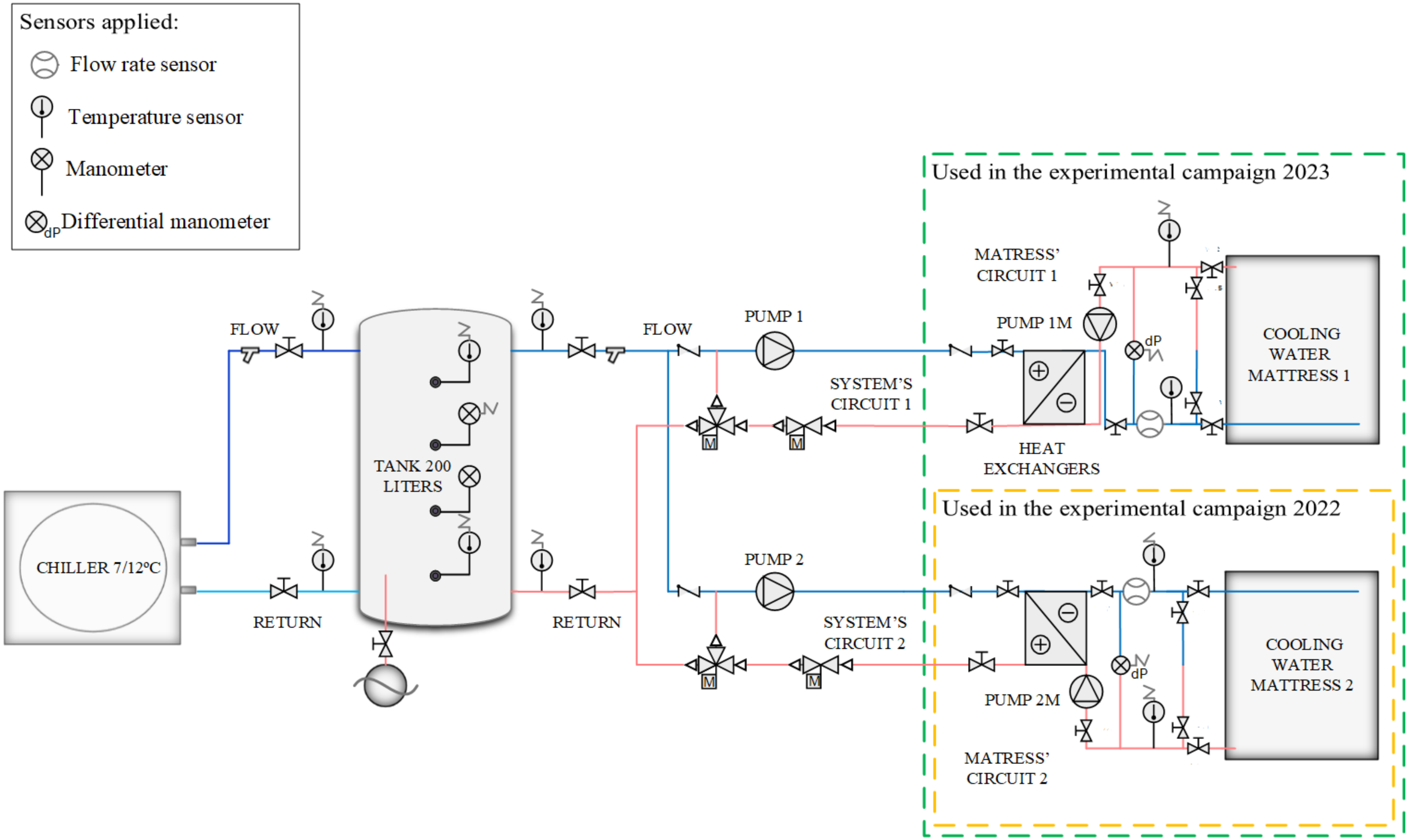

Figure 4.12. Scheme of the hydraulic installation of the cooling water production and distribution system supplying the developed water mattresses, in laboratory conditions and experimental campaign of 2022 working with one water mattress, and in experimental campaign of 2023 with both mattresses (marked with dashed line frames in orange and green colors respectively).

4.4. Accuracy of the data collection

This section presents the main considerations about the character of the conducted within this PhD thesis measurements in terms of their uncertainty analysis and the accuracy of the applied sensors. A detailed methodology of the conducted laboratory experiments as well as real barn experiments with the applied measurement strategy will be described in Chapter 5 and Chapter 6 of this PhD thesis, respectively. However, this section summarizes also information about the data collection.

Due to the character of the conducted study, which was mostly focused on observation and acquisition of the parameters over time, when environmental conditions were changing, the main measurements were carried out continuously. The cooling water mattress monitoring included its interior temperature, as well as surface temperature using thermocouples, and heat fluxes on its bottom and upper surfaces. Data collection of these parameters was carried out using a KD-7 data logger with a 1-min sampling period. Furthermore, inlet and outlet temperatures from the water mattress, as well as ambient temperature and humidity of the air (both, indoor and outdoor) were monitored and gathered through the SCADA system with a 2-min sampling period. Single measurements were realized using such instruments as the infrared thermometer for the mattress surface temperature measurement, a thermal image camera, as well as the anemometer, and katathermometer. Moreover, continuous measurements were realized for the cows' physiological reactions, such as rumen temperature, skin temperature, core body temperature, and heart rate. Data collection for those measurements was realized through the dedicated applications. All of the mentioned measurements had a direct character, except the cooling rate, calculated through the measurements of the katathermometer, as well as core body temperature, being a resultant of skin temperature measurements and other parameters, which relation applied to the algorithm has not been made available by the sensor's producer. Also, the heat flux value was based on the temperature measurement, being an indirect measurement, however, the output signal provided its processed value. Detailed information about used sensors and measurement instruments can be found in Table 4.1.

The uncertainty informs about the compartment, in which the measured value can vary, due to the limitations of the measurement process and used instruments. Concerning the uncertainty, for direct measurements, two types are normally distinguished: type A and type B, and as they result, the total uncertainty. Type A is connected with the measurement process, and can be calculated based on the standard deviation, when many independent measurements can be carried out with the same external conditions. Due to the character of the conducted in this PhD thesis experiments, in which observation over time with changing environmental conditions is their main focus, this type of uncertainty was not applicable in the analysis. On the other hand the B type uncertainty concerns the calibration of the instruments and their accuracy and is applied to each single measurement. Table 4.1 contains summarized information about all sensors and instruments used within all experiments carried out during this PhD thesis, their accuracy, range, and calculated B type uncertainty.

The laboratory experiments were conducted in a stable environment and with the controlled weight and heat load of the water mattress, for that reason the standard uncertainty can be applied. However, real barn conditions are much more complex and unpredictable, due to challenging environmental conditions, such as high temperature and humidity of the air, and a high concentration of harmful gases and solid particles. Furthermore, interaction with the animal becomes also important for the sensors monitoring animals' physiological reactions. For that reason, results obtained within skin and core body temperature as well as heart rate were not considered in the uncertainty analysis.

Table 4.1. Summarized information about sensors and measurement instruments applied during this PhD thesis, their accuracy, range (according to their data sheets), and calculated for them the B type uncertainty.

Measured parameter	Measurement instrument	Accuracy rating class	Range	B type uncertainty
Mattress interior temperature	K-type thermocouple (RS Pro) with 1mm probe	(first class) 0.4%	-40÷1100°C	2.63°C
Reference mattress surface temperature	T-type thermocouple TTE500	(first class) 0.4%	-40÷200°C	0.55°C
Mattress' surface heat flux	Omega HFS -5 heat flux sensor	5%	±150 kW/m^2	4.33 kW/m^2
Inlet water temperature (and flow)	Vortex SV7204-SVR34XXX50KG/ US-100	±1°C	-10÷90°C	0.58°C
Outlet water temperature	ifm TA2115	±0.1%	-50÷150°C	0.12°C
Indoor ambient temperature	NTC AKO015561 temperature sensor	1°C	-20÷125°C	0.58°C
Indoor relative humidity of the air	SONEE16F6A21	±3%	0÷100%	1.73%
Velocity of the air	Testo 440 anemometer (6351032 probe)	±(0.03 + 4% m.v)	0÷20 m/s	0.48 m/s
Surface temperature of the water mattress	Visiofocus 06620	±1°C	-7÷45°C	0.58°C
Cow and mattress temperature (IR)	TESTO 890 thermal image camera	±2% of m.v.	0÷350 °C	4.04°C
Rumen temperature	smaXtec reticulorumen bolus sensors	0.05°C	20÷60°C	0.03°C
Skin and core body temperature	CORE body temperature sensor greenTEG AG	0.21 °C	no manufacturer's data	-
Heart rate	CardioSport TP5 Heart Rate Monitor	no manufacturer's data	30÷240 bpm	-

The THI value calculated through Equation 6.1 was determined indirectly as a result of the measured indoor temperature and relative humidity of the air. For this measurement, the indirect uncertainty could be designated. However, the continuous measurement of the temperature and relative humidity of the air, being the components of the applied equation, as well as, the observational character of the THI value in the conducted study, makes the uncertainty assessment the lower importance in results interpretation.

Chapter 5

Laboratory experiments: Influence of changing the mattress' operational parameters on the heat transfer

The following chapter contains a detailed description of the laboratory experiments. Its structure is divided into three main paragraphs concerning the outline, the methodology, and the results of the conducted study. The last paragraph will focus on the comparison of the obtained experimental data with the results of the cooling water mattress simulation. The main aim of the laboratory experiments was to verify the cooling water mattress operation under different chilled water temperature setpoints, in simplified conditions assumed for previously conducted simulation, described in Chapter 4 of this PhD thesis. Such analysis enabled the selection of the cooling water mattress' operational parameters used in real barn conditions during experimental campaigns. The main simplification of the developed model focused on the mattress' constant temperature of 35°C, being the temperature of cow's skin. Whereas, in real conditions, animal continuously generates metabolic heat, whose level varies, and skin temperature is rather a gradient, dependent on the tissue properties and local vascular system. For that reason, prepared laboratory conditions were intended to verify the amount of transferred through the mattress heat, when its constant surface temperature was maintained for changing chilled water temperature setpoints. The obtained results were intended to provide information about both, the cooling effectiveness of the developed solution, as well as applicability of the developed model for predicting potential heat transfer in different operational parameters.

5.1. Outline of the experiments

The experimental campaign was conducted in the main laboratory hall in the D2 building of Wroclaw University of Science and Technology and lasted 5 days (28.07-02.08.2022). Each experimental day investigated mattress operation under one out of five chilled water temperature setpoints in the system's circuit 2 (c.f. Figure 4.12): 4°C, 6°C, 9°C, 12°C, and 15°C. At this stage of the system's modifications, the chilled water temperature sensors, being under the SCADA system control, were located in the aformentioned circuit. For that reason, the setpoints were selected assuming the 1°C temperature increase on the heat exchanger, obtaining target temperatures in the mattress' circuit 2. The experimental day with the temperature of 4˚C was focused on mattress operation in boundary settings of real conditions.

For this purpose, the lowest temperature of 4˚C and the highest pump's rotational speed of 3500 rpm, were selected. During the rest of the experimental days, the water flow rate was set on 3 levels, determined by the pump's rotational speed of: 3500 rpm, 2500 rpm, and 1500 rpm. The plan of the conducted study within experimental days is presented in Table 5.1. The following parameters were monitored:

- environmental conditions (ambient temperature, and humidity of the air),
- inlet and outlet temperature from the water mattress,
- chilled water temperature inside the water mattress, measured with thermocouples at 9 locations (c.f. Figure 4.7 and Figure 4.8),
- the water mattress surface temperature using the referenced thermocouple and thermal imaging,
- heat flux on the top and bottom surfaces of the water mattress.

A detailed sequence of conducted measurements will be discussed in the next paragraph focusing on the methodology applied during the experiments.

Table 5.1. Main schedule of the conducted laboratory experimental campaign in 2022.

	Day 0	**Day 1**	**Day 2**	**Day 3**	**Day 4**
T_{water}, ºC	4	6	9	12	15
	3500	3500	3500	3500	3500
Rotational speed, rpm		2500	2500	2500	2500
		1500	1500	1500	1500

To achieve the conditions assumed in the previously conducted simulation, which is operation of the water mattress with maintained surface temperature of 35°C on its surface, the electrically heated graphite mat (with 140 W/m^2 power output for the 40°C temperature) with a thermoregulator was used. Its structure enables fitting to the water mattress's irregular surface.

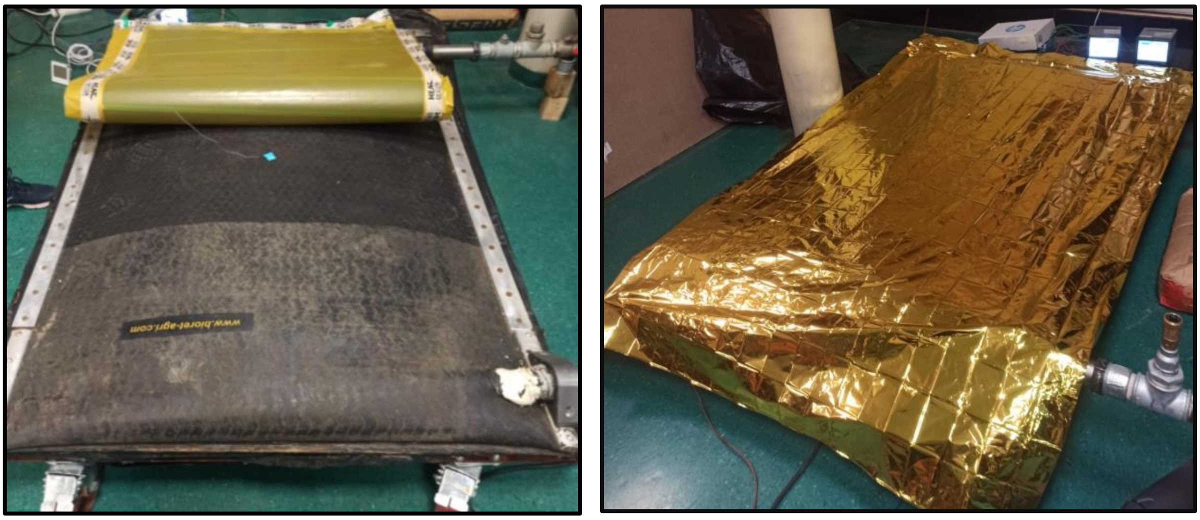

Figure 5.1. On the left-hand side the developed cooling water mattress with a heating mat, on the right-hand side, both covered with the thermal blanket.

However, due to its susceptibility to the water, it was covered with protecting foil. The heating mat placed on the developed water mattress is presented in Figure 5.1. Furthermore, to reduce heat losses to the environment during the heating period, the mat was covered with a material sheet and thermal blanket (c.f. Figure 5.1).

5.2. Methodology

The following paragraph is focused on the methodology applied during the laboratory experiments. Firstly, the sequence of the conducted measurements will be described. Subsequently, the measurements will be grouped into three groups, the one covered by the SCADA system measurements group, the temperature and heat flux measurements, and last, but not least, the thermal imaging.

5.2.1. Measurement sequence

The main goal of the conducted experiments was to observe the cooling water mattress operation, working under different chilled water temperature setpoints, as well as the pump's rotational speed in simplified laboratory conditions. The obtained results enabled also selection of the operational settings of the water mattress during experimental campaigns in real barn conditions. The measurement sequence was the same for each experimental day. First, the initial temperature of 20°C inside the water mattress was achieved (the average value from the thermocouple's readings). When this condition was fulfilled, the chilled water production system with assigned to considered experimental day chilled water temperature and the pump's rotational speed (starting from 3500 rpm) was launched and worked until the temperature inside the mattress reached the selected setpoint. This stage was the so-called water mattress precooling. During that process, thermal images of the mattress surface were taken every 5 minutes. Such a procedure was applied to monitor the mattress precooling process, and the time necessary to achieve a selected chilled water temperature setpoint starting from the same temperature level. Next, the heating mat at the temperature setpoint of 35°C, together with the thermal blanket and the sheet of cotton material were placed on the mattress surface. The chilled water production and distribution system operated under these conditions until the temperature inside the mattress achieved the level maintained before heating but for at least 1h. Such a condition was justified by the chiller's operational mode, in which it is switched on when the chiller's return water temperature exceeds the 10°C setpoint. This stage was a so-called water mattress heating. Because it was a longer than precooling process, thermal images were taken every 10 minutes. This process required a quick removement of the heating mat to see temperature distribution directly on the mattress surface. Next, the rotational speed was changed to the lower value, which was being verified, and the system worked for about 5-10 minutes without the load, after which thermal imaging was repeated twice: including sandbag and without it. Finally, the heating mat with its accessories was turned on once again and measurements were conducted following the aformentioned methodology, which was ended by the series for the pump's rotational speed of 1500 rpm. Such a daily sequence of measurements was finalized by the chilled water distribution system's turn-off.

The main goal of the thermal imaging applied during this experiment was to identify the possible air cushion inside the water mattress, which was justified by previously conducted preliminary trials.

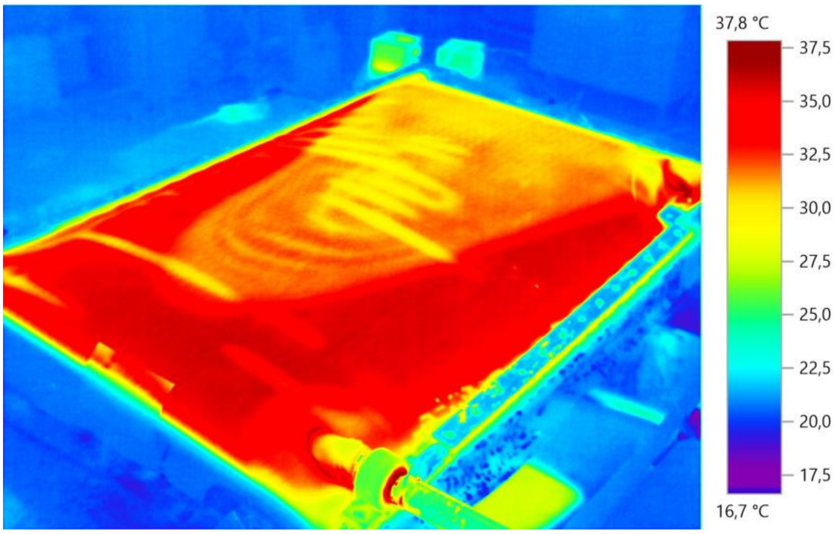

Figure 5.2. Thermal image from the initial trial of the developed water mattress operation, in which hot water was used.

In Figure 5.2, the thermal image from the first trial is presented, which was conducted with hot water at the initial stage of mattress improvements. It highlighted the major problem with the air accumulation inside the water mattress, which resulted in appyling the venting procedures in further actions.

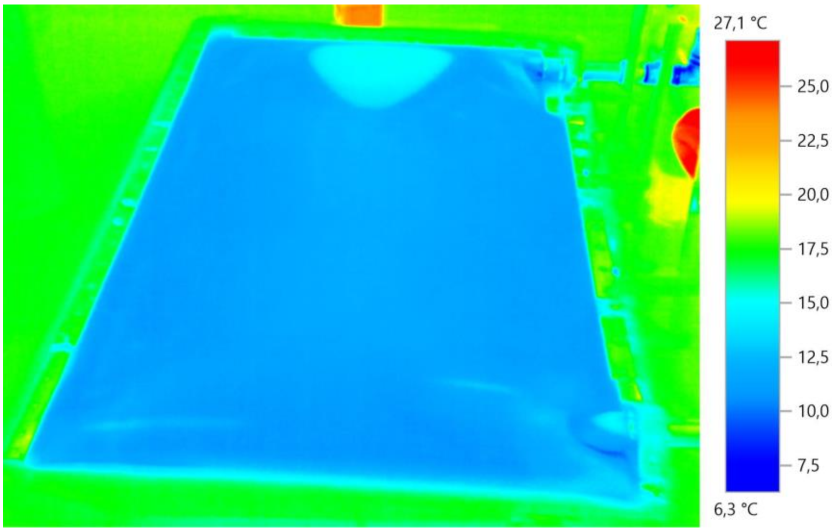

Figure 5.3. Thermal image from the second trial of the developed water mattress operation after applying venting procedures, in which chilled water was used.

After that, the next trial conducted for the chilled water, resulted in a much smaller air cushion (c.f. Figure 5.3), however, its full removal was still difficult to achieve, which indicated the need for thermal image observation during the experiments. Moreover, thermal imaging during the experiment was applied in the sequence system (with 5 and 10 min sampling periods, for a cooling down, and heating with the mat processes, respectively), to observe whether the temperature changes within both, the cooling and heating processes, were detected.

5.2.2. Measurements gathered by the chilled water production and distribution SCADA system

The SCADA system of the chilled water production and distribution system, measured continuously, with a 2-min sampling time, the inlet and outlet temperatures from the cooling water mattress and water flow in both water circuits. Furthermore, the ambient temperature and relative humidity of the air inside the laboratory hall were measured by the meteorological station, which is an integral part of the chilled water production and distribution system.

5.2.3. Temperature and heat flux measurement

Operation of the developed cooling water mattress was observed using the mattress monitoring system, which was based on K-type thermocouples mounted inside the water mattress. Since the aforementioned thermocouples are an integral part of the water mattress, they were selected and described in Chapter 4 of this PhD thesis. To monitor heat transfer through the mattress Omega HFS 5 sensor was selected, which was previously described in the aforementioned chapter

$$q'' = \frac{\Delta V_q}{S_{@T°\mathrm{C}}} \tag{5.1}$$

The sensor utilizes a differential-temperature thermopile design to measure the heat flux through its surface. The output of a sensor's measurement is a DC voltage ΔV_q , which is linearly proportional to the heat flux [70]. Its value was calculated following Equation 5.1, in which the sensitivity of the sensor $S_{@T°\mathrm{C}}$ was applied according to manufactuer's manual [70].

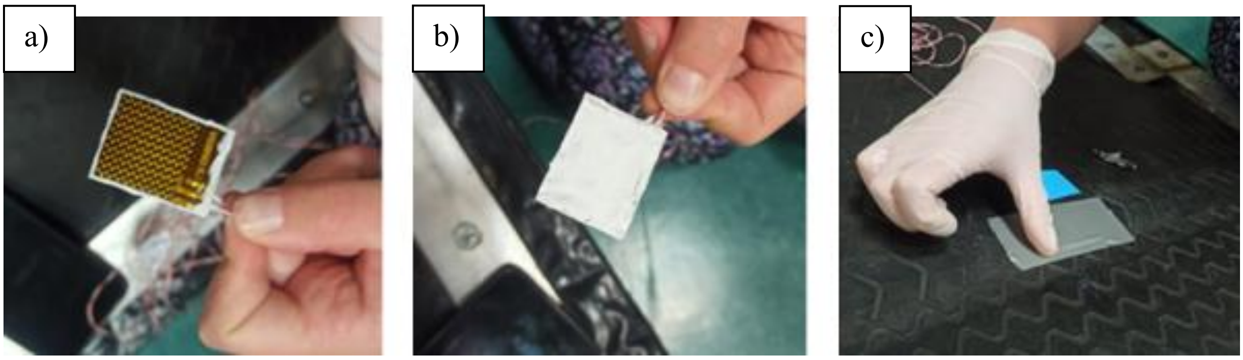

Figure 5.4. The heat flux sensor mounting procedure on the water mattress surface: a) covering the frame of the sensor with thermally conductive glue, b) covering rest of the sensor's surface with thermally conductive paste, c) additional fixing sensor to the mattress surface using forced tape.

The selected sensor was mounted to the mattress' surface between grooves of the coating rubber using thermally conductive glue on the sensor's frame (c.f. Figure 5.4 a), thermally conductive paste on its measuring surface (c.f. Figure 5.4 b), and it was secured from moving using the forced tape (c.f Figure 5.4 c). Furthermore, the surface T-type thermocouple (TT500 from TermoAparatura Company) was mounted to monitor the mattress surface temperature as the reference measurement for thermal imaging.

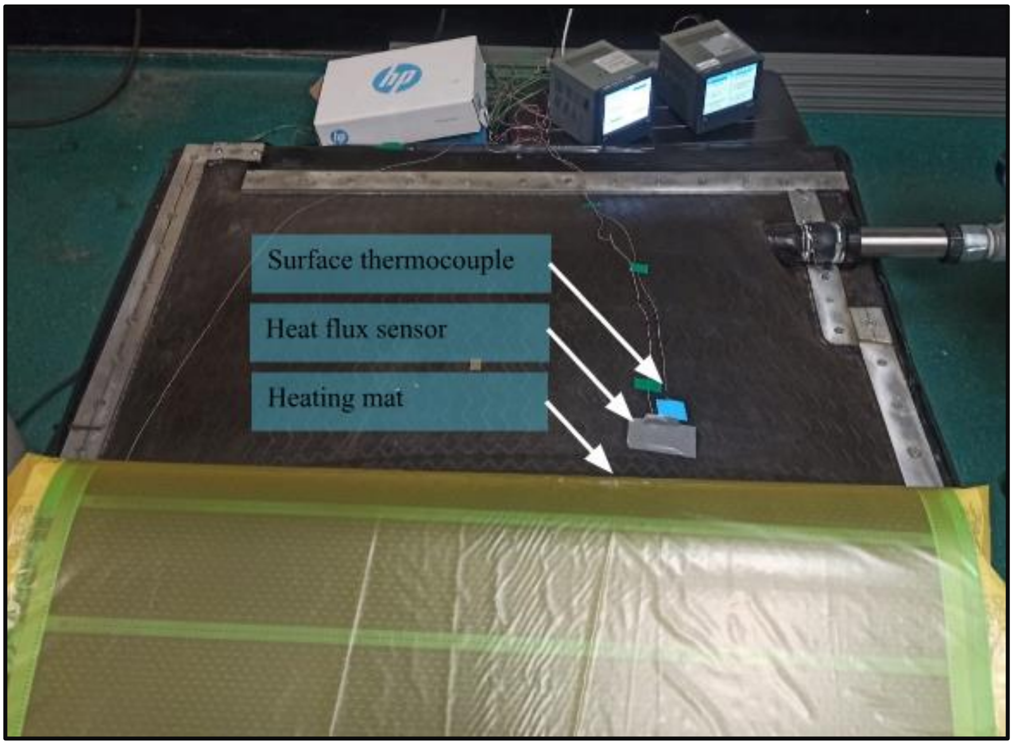

Figure 5.5 Location of the surface thermocouple and heat flux sensor on the developed mattress surface, covered with a heating mat during the experiments in the laboratory.

Both sensors are presented in Figure 5.5. All data were recorded using a KD-7 data logger with 1 min sampling time. To achieve proper contact between the sensor's and the heating mat's surfaces, it was also loaded with a 25 kg sandbag.

5.2.4. Thermal imaging

Thermal distribution on the water mattress surface was measured using thermal image camera Testo t890-2The. A thermogram was taken every 10 minutes during the heating period of the experiment and every 5 minutes during the cooling period. A thermal image camera was stably placed on a tripod in the designated for the whole experimental campaign place (c.f. Figure 5.6). Obtained thermograms were analyzed in IRSoft software.

Figure 5.6. Experimental set-up with marked on the right upper corner thermal image camera.

The thermal emissivity of the rubber was determined before the experiments, according to the following steps. Firstly the water mattress was filled with warm tap water, to achieve the temperature difference between the surface and environment greater than 20°C for accurate measurement. Two reference TTE500 (Cu - CuNi) thermocouples were placed on the mattress surface near the water distributor, where the water circulation was ensured. Emissivity had been changing on the thermal image camera until the temperature recorded in the location of the used thermocouple was equal to the one measured by this sensor. Following this procedure, the emissivity $\varepsilon = 0.94$ was selected, which is the same emissivity of hard rubber cited in the literature [71].

5.3. Results and conclusions

This paragraph contains the main results achieved during the laboratory experiments. All gathered data will be presented and discussed following the sequence of the experimental days. The analysis will be focused on the thermal response of the cooling water mattress for both, cooling, and heating periods, under changing operational setpoint of the temperature and water flow.

5.3.1. Developed water mattress operation under laboratory boundary conditions

The experimental campaign started with the verification of the chilled water mattress operation under boundary conditions applied during the simulation. However, the final prototype was limited by the water mattress distribution system's operational parameters. For that reason, both, the temperature setpoint of 4°C and mass flow of 0.85 kg/s, assumed in the simulation were not possible to achieve. In this experiment, the water mattress' boundary operating conditions possible to be achieved in the real test stand, which are the minimum chilled water temperature, and maximum water flow, were applied according to the previously described in Subsection 5.2 of this PhD thesis. In Figure 5.7 the average water temperature inside two monitored channels of the water mattress, and the mattress' surface temperature measured in the area of the heat flux sensor and on the left bottom corner of the mattress, are presented. Temperatures are juxtaposed with the heat flux measured on the bottom and top of the mattress. It can be observed that the chilled water temperature for both channels achieved the same values, which indicates uniform water flow through the mattress. Although the temperature setpoint in the SCADA system was 4°C, the final obtained temperature was 6°C. Surface temperature, on the other hand, maintained similar for both locations during the cooling period, and started to differ by 4°C during the heating period, obtaining a lower value in the heat flux sensors area. The reason for that relation is probably due to the load pressure of the sandbag, which could affect the graphite distribution inside the heating mat, and limit the heating effect of the air gaps between the mat, and the mattress' surface. The temperature inside the mattress increased by 4°C during the hour of heating, until the chiller switched on again. That increase corresponds to almost constant heat flux measured at the mattress' surface with the value of 200 W/m^2. However, it needs to be highlighted that the heat gains from the mattress' bottom reached significant in terms of the mattress thermal balance value of 100 W/m^2, which decreased to the value of 50 W/m^2 when water temperature increased. In the laboratory conditions heat exchange was based on convective heat transfer with air. In real barn conditions, the mattress is intended to lay down on a concrete surface with a lower temperature, where occurs conductive heat transfer with the ground, which would probably reduce the heat gains. However, the obtained results indicated the importance of mattress insulation from its bottom surface.

The significant observation in terms of the bedding's hygiene conditions for the cattle was the moisture condensation on the mattress surface presented in Figure 5.8. For that reason, an alternative litter with moisture-absorbing properties was considered for future application, under such operational parameters.

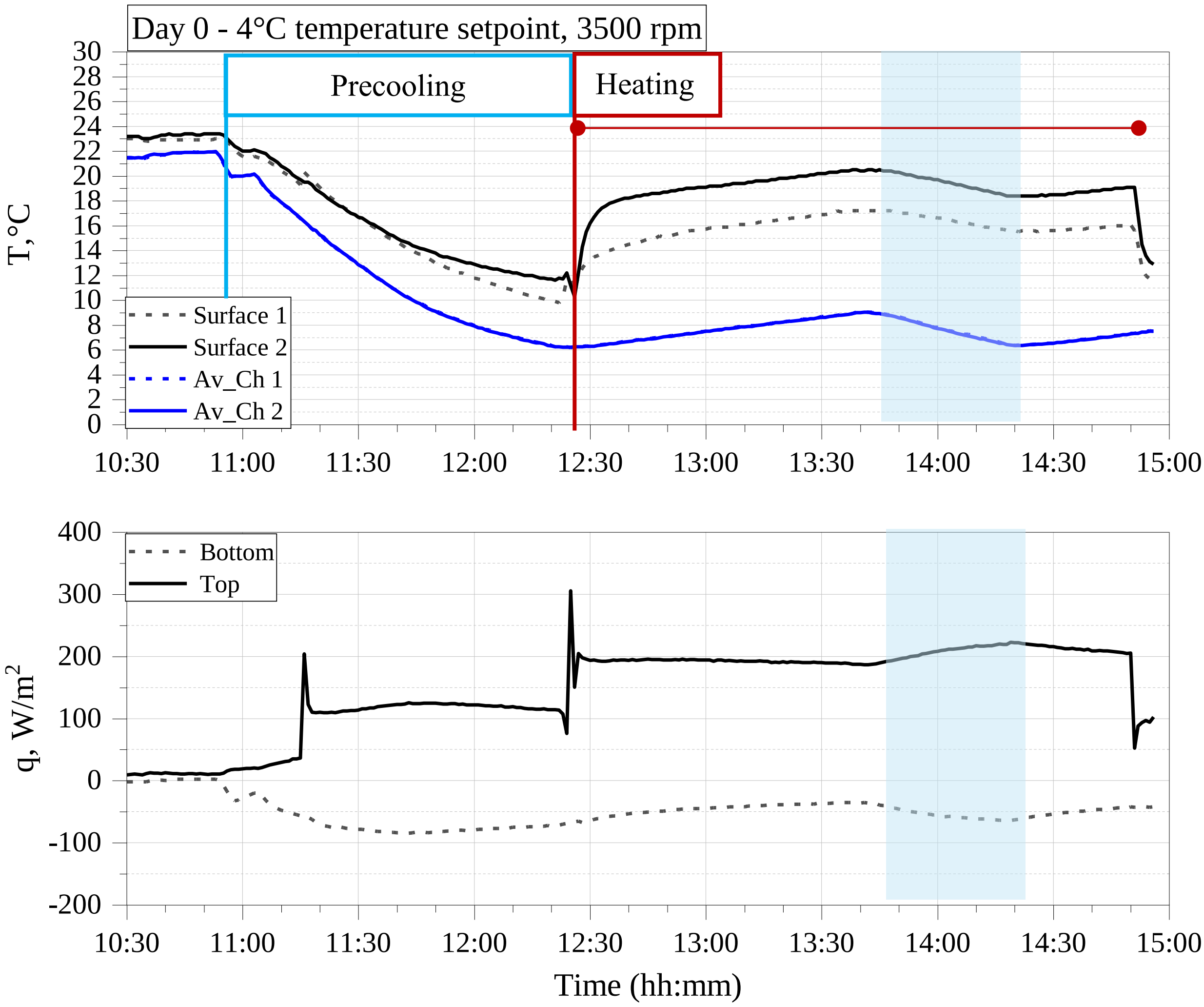

Figure 5.7. The top chart presents the temperature measured at the water mattress surface, in the area of the heat flux sensor (Surface 1), and in the left bottom corner of the mattress (Surface 2) juxtaposed with the average temperature of the cooling water in two monitored channels (Av_Ch1 and Av_Ch2), the bottom chart presents heat flux measured a the bottom and on the top of the water mattress.

Figure 5.8. Water mattress with visible moisture condensation on its surface.

Thermal imaging was conducted for three stages of the experiment: during the cooling down period, then for a heating period with the graphite mat, and after removing the heating mat. Thermal images as well as the temperature distribution charts from those stages are presented in Figure 5.9 – Figure 5.13.

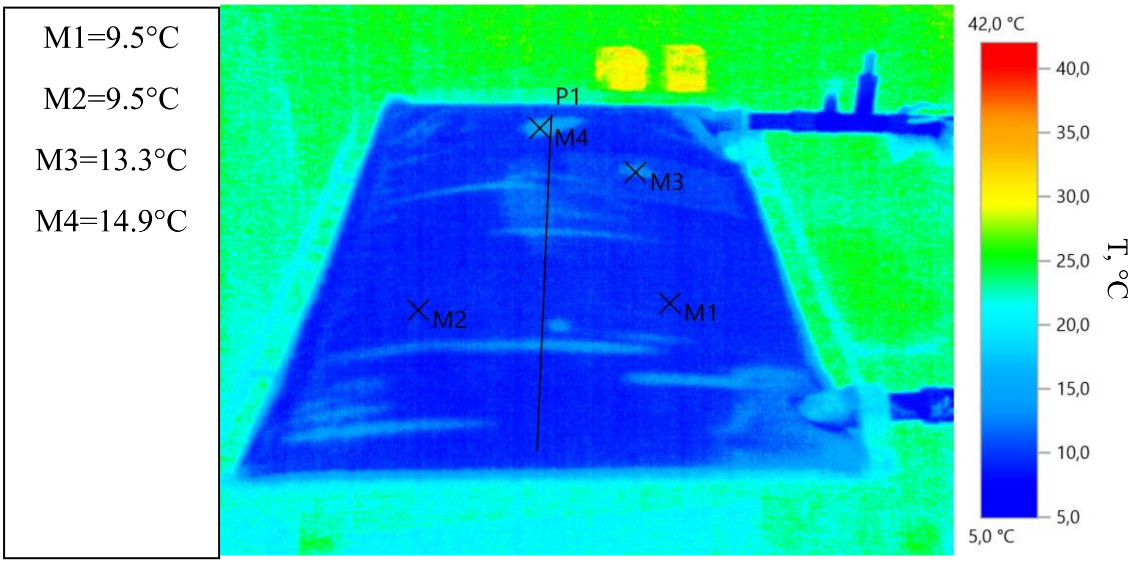

Figure 5.9. The thermal image of the water mattress cooled down to the setpoint, just before covering it with the heating mat.

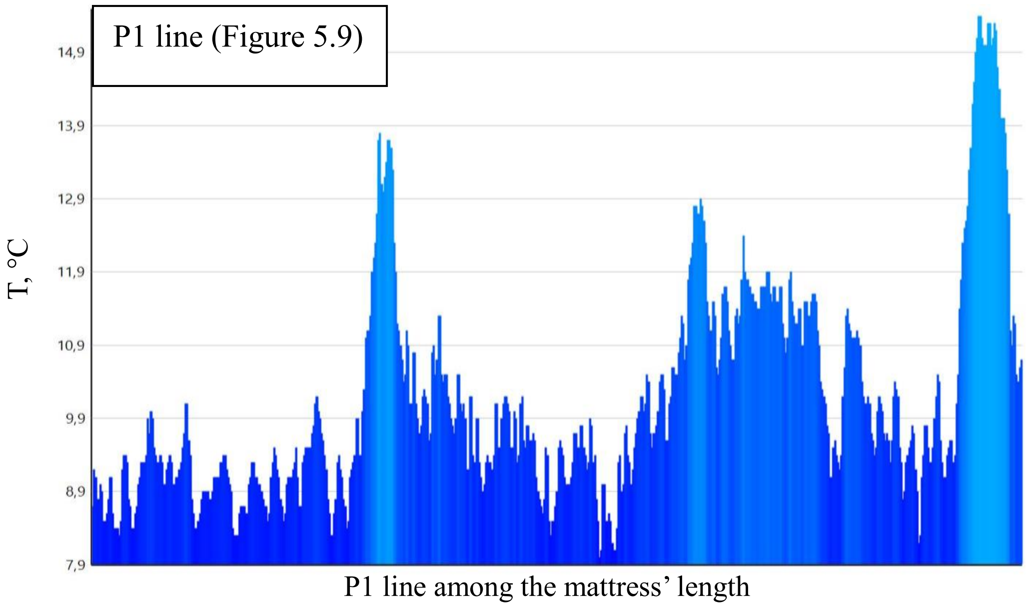

Figure 5.10. Temperature distribution among the water mattress cooled down to the setpoint just before covering it with the heating mat.

One of the observations is a lower temperature in the area, where the sandbag was loading the heat flux sensor, which indicates the uneven liquid graphite distribution(c.f. Figure 5.11). Furthermore, the irregular contact of the heating mat with the water mattress surface was observed, visible as the uneven temperature distribution (c.f. Figure 5.11)

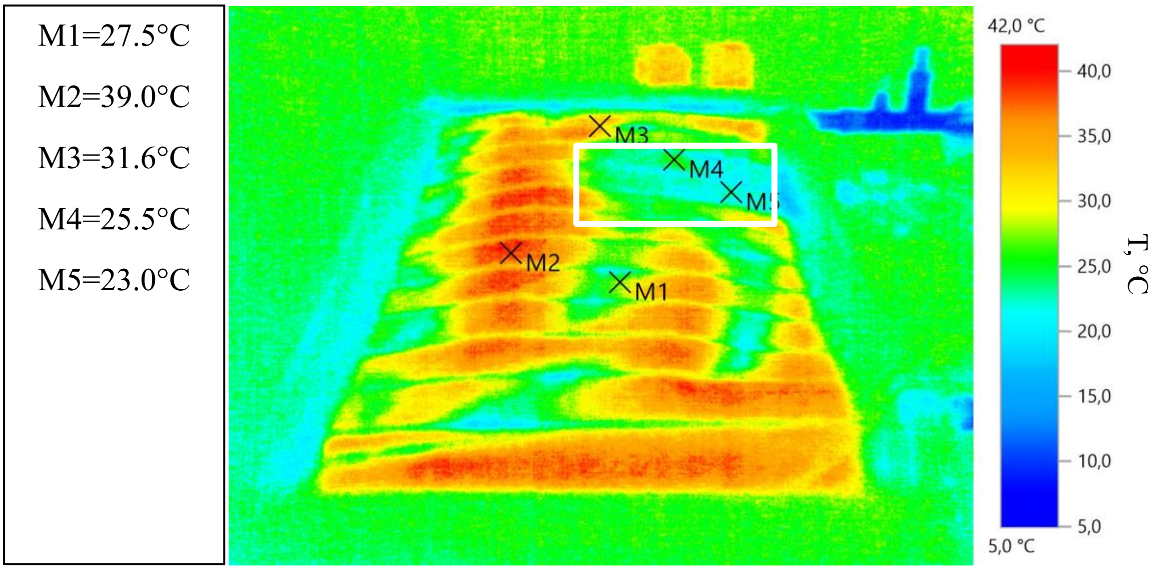

Figure 5.11. The thermal image of the water mattress at the end of the heating period, just after removing the sandbag from the heat flux sensor (location marked in white frame).

The main observation was the existence of the air pillow in the top part of the water mattress, in its significant influence on the surface temperature in this region. It was especially visible after the heating period, when the temperature of the air cushion was higher than the water temperature (c.f. Figure 5.12 and Figure 5.13).

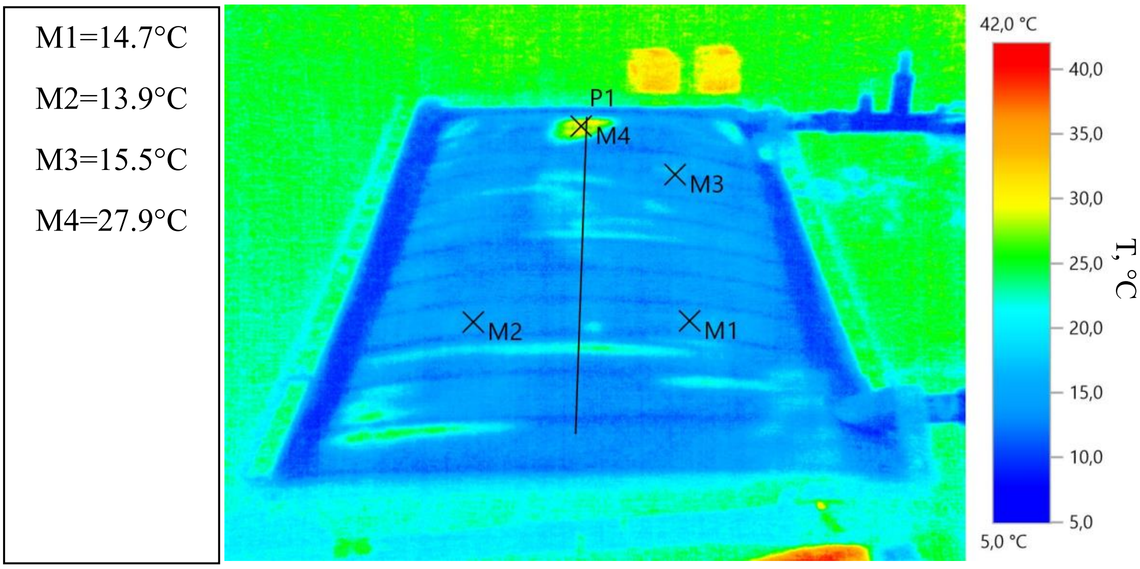

Figure 5.12. The thermal image of the water mattress just after removing the heating mat.

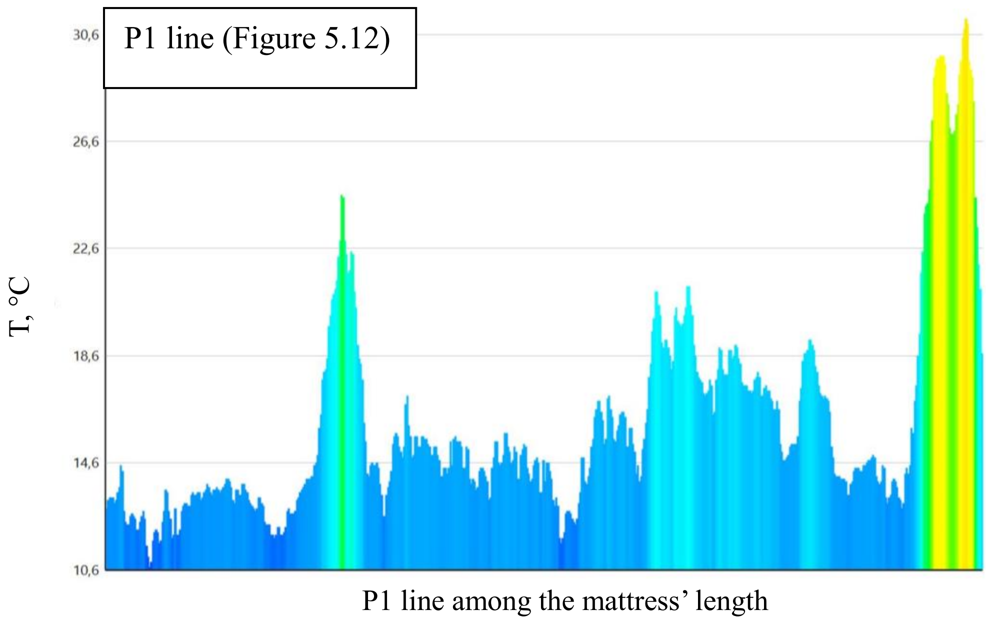

Figure 5.13. Temperature distribution among the water mattress just after covering it with the heating mat.

5.3.2. Water mattress operation under changing operational parameters

During the four experimental days, since the 1st day, it was investigated how changing the water mattress operational parameters, such as chilled water temperature, and water flow regulated on three levels by the pump's rotational speed, will influence the heat transfer on its surface. Furthermore, the operation of the water mattress and its supplying system under different chilled water settings were observed. The main goal of these experimental days was to select chilled water temperature setpoints used later in experimental campaigns in real barn conditions. Figure 5.14 and Figure 5.15 present the obtained results for four temperature setpoints, namely 6°C, 9°C, 12°C, and 15°C. It was observed that for the 6°C setpoint, the same as for 4°C (c.f. Figure 5.7), the temperature difference with the value obtained in the mattress achieved 2°C. Whereas, for the higher setpoints it achieved only 1°C (which was also a primary assumption), being more optimal from the operational point of view of the mattress and its supplying system. A similar conclusion can be made based on observation of the decreasing character of the difference between chilled water temperature and mattress surface, for increasing temperature setpoints. Furthermore, for a 6°C setpoint, the same as for a 4°C (c.f. Figure 5.7), during the heating with a mat period, the chiller switched on to maintain the chilled water temperature, which was visible as temperature peaks in Figure 5.7 and Figure 5.14. Its influence is less visible for operation under higher temperature setpoints. Simultaneously, the surface heat fluxes achieved for each water temperature setpoint were around 200 W/m^2, varying within this value in the range of ±50 W/m^2. The expected influence of the changed pump's rotational speed was observed only for 12°C and 15°C, increasing the heat flux value, when chilled water flow was reduced. The highest heat flux value of 240 W/m^2 was achieved for the 12°C temperature setpoint and 1500 rpm. For 15°C, the difference between 2500 and 1500 rpm was negligible. Therefore, concerning water flow through the water mattress' supplying distributor inside the water mattress, the 2500 rpm setpoint would be more optimal for higher water temperatures. For that reason, this value was selected for the experimental campaign in 2022, as well as higher chilled water temperature setpoints.

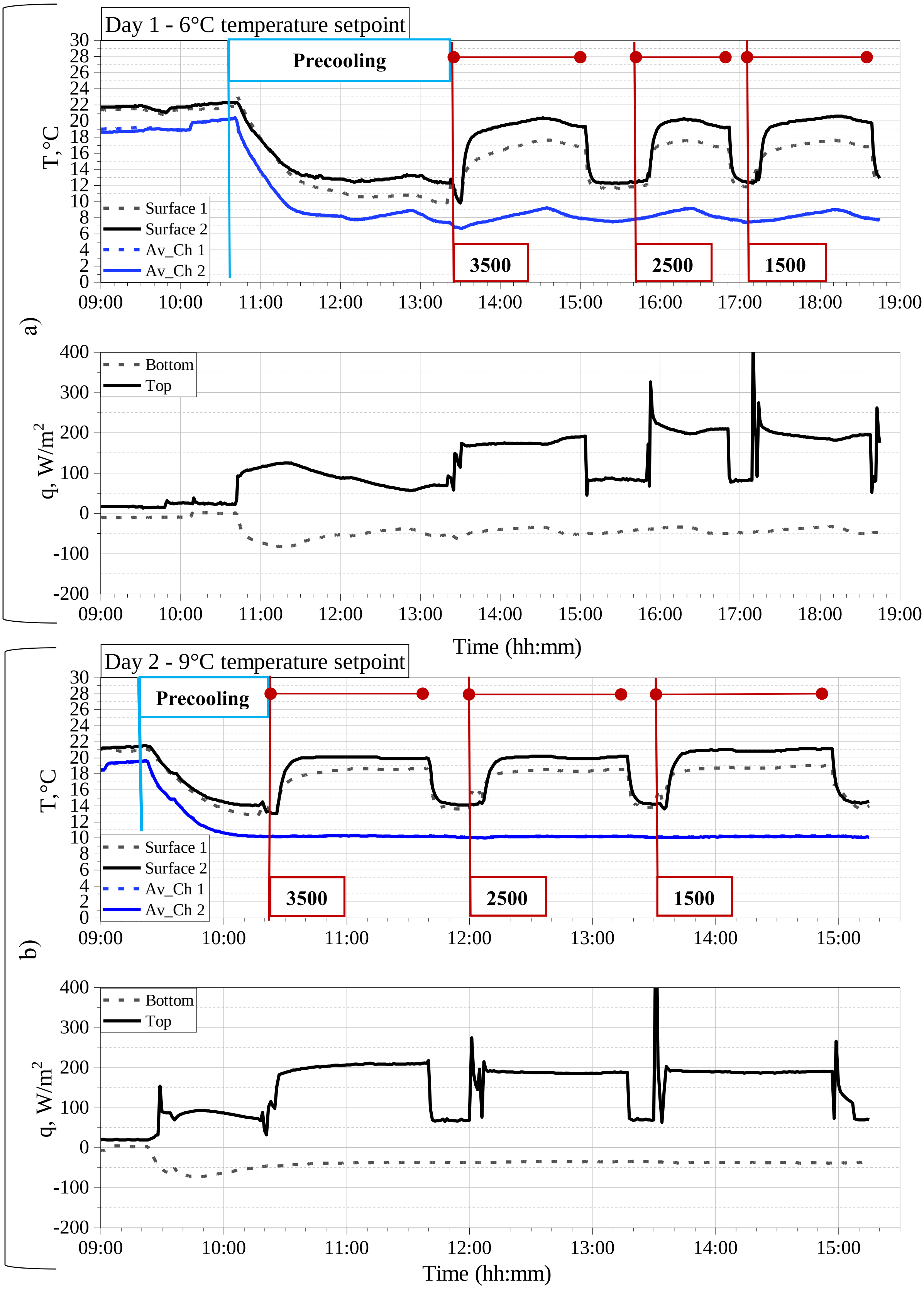

Figure 5.14. Mattress surface temperature, measured in the area of the heat flux sensor (Surface 1) and the left bottom corner (Surface 2), and average water temperature inside two channels (Av_Ch1 and Av_Ch2), juxtaposed with the surface heat fluxes obtained during 1st and 2nd day of the laboratory experiments.

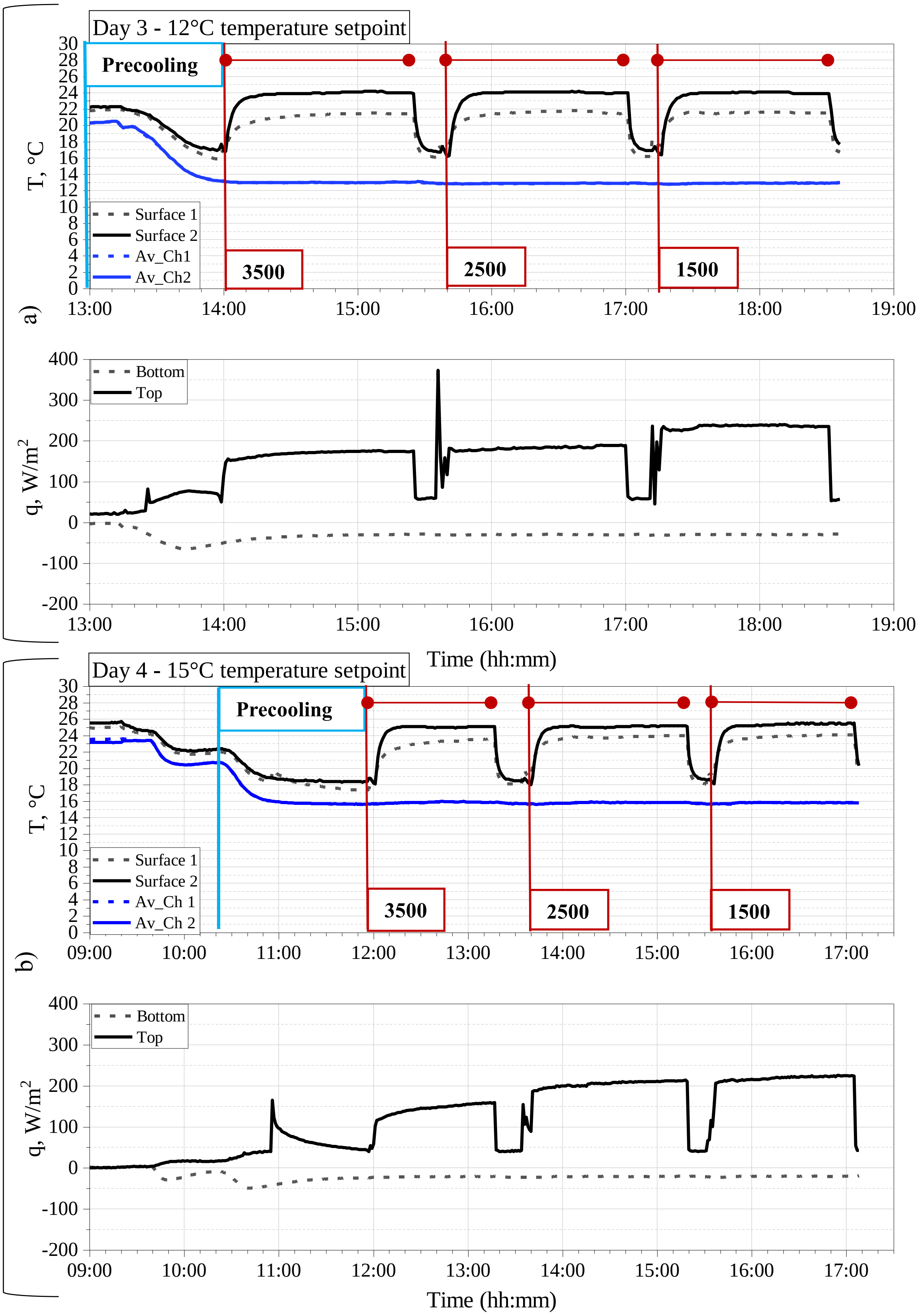

Figure 5.15. Mattress surface temperature, measured in the area of the heat flux sensor (Surface 1) and the left bottom corner (Surface 2), and average water temperature inside two channels (Av_Ch1 and Av_Ch2), juxtaposed with the surface heat fluxes obtained during 3rd and 4th day of the laboratory experiments.

5.3.3. Main conclusions from the laboratory experiments

Conducted laboratory experiments enabled the verification of the developed water mattress operation under real conditions, considering the hydraulic and physical chilled water production and distribution operation constraints, which limited the operational parameters of the water mattress. In the result, new values of assumed chilled water inlet boundary conditions were determined and further applied to the previously built CFD model, described in Chapter 3 of this PhD thesis, and simulated. Finally achieved parameters were the chilled water temperature of 6°C, and the water flow monitored on the pump 2.6 m^3/h (mass flow of 0.72 kg/s). All collected during the experiments data were important for further comparison with the results obtained in the aformentioned simulation, enabling evaluation of the developed water mattress working in real conditions, which will be described in detail in the next section.

The main goal of the second part of the experiments was to study the influence of changing operational parameters of the developed water mattress on the surface heat fluxes. It was observed, that higher water temperature setpoints of 9°C, 12°C, and 15°C were more optimal in terms of the thermal operation of the water mattress. It distinguished higher temperatures as preferable for operation in the real barn experimental campaigns. The highest heat flux was achieved for the setpoint of the chilled water of 12°C and the pump's rotational speed of 1500 rpm. However, the small differences in heat flux values between 1500 and 2500 rpm was rather small for higher chilled water temperatures, where the 2500 rpm, was more optimal in terms of the operation, considering the calculations of the supplying distributor presented in Chapter 3 of this PhD thesis. For that reason, the pump's rotational speed of 2500 rpm was selected as the one used during the real barn experimental campaign in 2022.

5.4. Water mattress model evaluation in laboratory conditions

In this section results of the CFD simulation of the developed water mattress working under conditions from the laboratory experiments will be described and compared with the collected data. The model of the developed cooling water mattress, described in detail in Chapter 3 of this PhD thesis, was modified in terms of the inlet and wall boundary conditions, adopting values achieved during laboratory experiments. Following these changes, inlet temperature and mass flow were set to 6°C (279.15 K) and 0.72 kg/s, respectively (c.f. Table 5.2, Laboratory 0). The temperature for the walls, including the ground wall was set to the ambient temperature in the laboratory, measured by the meteorological station of the developed system, which was 23.5°C (296.65 K). All other assumptions were the same as previously described in Chapter 3 of this PhD thesis. Calculations were proceeded achieving the convergence of the energy conservation law for residuals in the order of 10^{-6}.

5.4.1. Results of the simulation conducted for laboratory conditions

Analysis of the results includes the velocity vectors and temperature of the chilled water in the cross section through the channel structure, as well as heat flux achieved on the top surface of the mattress. Their graphical representations generated in Ansys CFD-Post Software are presented in Figure 5.16. Comparing them with the results from the previous simulation described in Chapter 3 of this PhD thesis, it can be observed that the chilled water velocity vector's profile in the channel structure remained similar (c.f. Figure 3.19). The water temperature profile is also similar but maintained at the higher level of about 6°C assumed for these calculations. The heat flux on the top surface achieved an average value of 678 W/m^2, which is only slightly lower than in the previously obtained simulations' results.

Nevertheless, considering a discrepancy of the obtained in the simulation heat flux value with the one measured in the laboratory two additional aspects were additionally taken into consideration for further results interpretation. For that purpose, two more simulations have been conducted, in which the chilled water temperature setpoint and mass flow were modified, respectively. Simulations enabled also the developed water mattress' model verification in terms of its sensitivity to those changes.

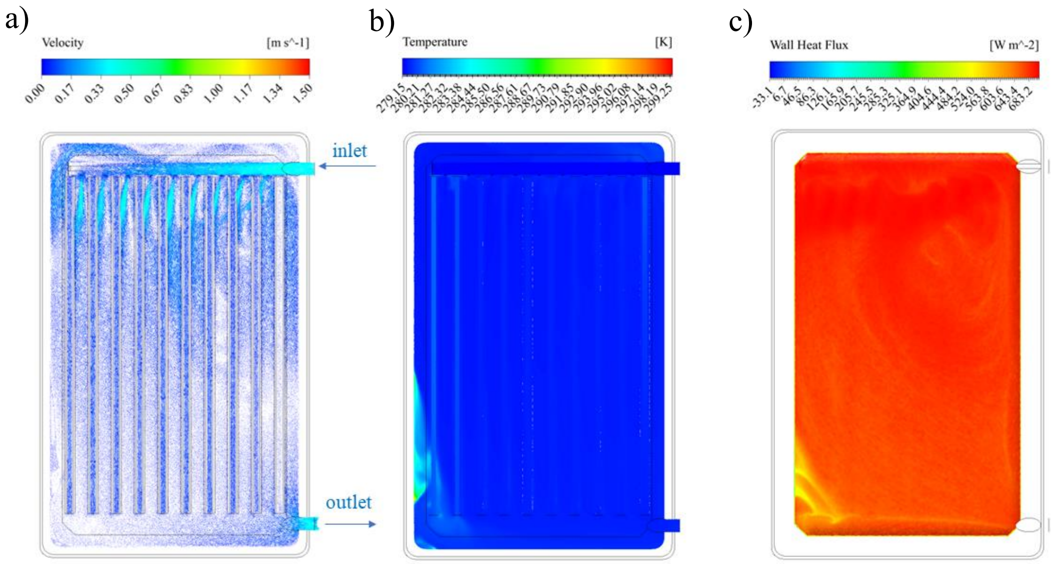

Figure 5.16. Results of the CFD simulation for the developed water mattress working in conditions from laboratory experiments: a) the velocity vectors, b) the temperature in the cross section through the channel structure, c) the heat flux on the top of the mattress.

The first concern was related to the possible measurement error of K-type thermocouples with 1st class of accuracy, used for temperature estimation, being in the range of ±1.5°. To verify its possible influence on the results, one more simulation has been conducted, in which the water temperature was assumed to be 7.5°C (280.65 K) (c.f. Table 5.2 Laboratory 1). The second concern was the possible discrepancy in the chilled water flow monitored on the pump (which also fluctuated while the pump was running) and the one occurring at the cooling water mattress inlet. The continuous measurement of the flow rate was not possible during the laboratory experiments, due to hydraulic modifications and the flow rate sensor location in the system's circuit 2, instead of its target location in the water mattress' circuit 2. For that reason, the flow rate value for a pump's rotational speed of 3500 rpm was read from data collected in real barn experiments, where it achieved the maximum value of 2.0 m^3/h. To verify the possible influence of change in chilled water flow, one more simulation was performed, in which the mass flow at the inlet was assumed to be 0.55 kg/s (corresponding to the 2.0 m^3/h flow rate value) (c.f. Table 5.2 Laboratory 2).

In Table 5.2 the average values of temperatures and heat fluxes, counted from the considered surfaces have been juxtaposed for conducted simulations. It can be noticed that the change in the temperature and mass flow influenced the heat flux on the top surface of the water mattress by only 35 W/m^2.The mass flow seems to have an almost negligible effect on the obtained results, suggesting the water mattress' low susceptibility to that parameter in terms of the heat flux values. However, considering the narrow range of the temperature change (1.5°C) between simulations, it can be assumed that for higher chilled water temperature setpoint that effect could be much more significant. To evaluate it, one more simulation with a 16° inlet water temperature was conducted (c.f. Table 5.2, Laboratory 3). Indeed for this assumption, the obtained heat flux value was significantly lower, achieving the difference of 230 W/m^2 in comparison to previous results. Whereas the measured during experiments values did not change significantly between 6°C and 15°C chilled water temperature setpoints (c.f. Figure 5.14b and Figure 5.15 b, respectively). Such observation indicated that the methodology applied for the heat flux measurement in laboratory conditions needs to be taken under special consideration, regarding the factors, which could influence the obtained results, which will be presented in the following paragraph.

Table 5.2.Average temperature and heat flux values from the considered surfaces obtained in conducted simulations and real measurements.

Considered model boundary conditions		$T_{\mathrm{w,cross}}$ °C	$\dot{Q}_{\mathrm{top}}$ W/m^2	$\dot{Q}_{\mathrm{bottom}}$ W/m^2
Preliminary assumption	(4.5°C, 0.85 kg/s)	5.1	715	134
Laboratory 0	(6.0°C, 0.72 kg/s)	6.5	678	194
Laboratory 1	(7.5°C, 0.72 kg/s)	8.0	643	177
Laboratory 2	(6.0°C, 0.55 kg/s)	6.7	671	191
Laboratory 3	(16°C, 0.55 kg/s)	16.4	441	81

First of all, the prototype water mattress working in the laboratory was characterized by the slightly semispherical surface, due to the rubber elasticity working under pressure. It was the reason of the air accumulation in its top parts. Although the venting process was conducted it was difficult to estimate if all air was moved out from the mattress. Thus, there is a possibility, that the heat flux sensor covered a region with reduced heat flow between a heating mat and water. Furthermore, used in the experiments heating mat, due to its foil covering, did not adhere to the water mattress surface, creating air zones between these two layers. For that reason in the measurement area, the heat flux sensor was loaded with the sandbag. Although it excluded the air zone problem, the pressure could influence the measurement, such a disruption was especially visible in heat flux peaks at the moment, when the sandbag was put down. Moreover, the liquid graphite filling of the heating mat could create a thinner layer within the measurement area resulting in a lower surface temperature than the setpoint of 35°C. Concerning those aspects, the obtained in measurements heat flux values are difficult for the true assessment in terms of their accuracy. Therefore, the methodology with different heating systems and an increased number of sensors could improve the interpretation of the aformentioned aspects. However, the complexity and costliness of such measurements for the considered water mattress' surface limit the affordability of such a procedure within this PhD thesis, especially considering the fact that the functional prototype of the developed water mattress required several intermediate steps. First, the modeling of the mattress' outline and its configuration, then the development of the laboratory full-scale prototype, which was followed by the rebuilding (reconstruction) of the functional prototype (being an iterative process), and finally experimental testing in real barn conditions. It is worth to underline that this approach allowed to answer to all research questions raised within this PhD thesis, which considered the interdisciplinary character of this research topic.

The measurement on the bottom surface of the water mattress also could be influenced by several aspects that need to be taken into account in the interpretation. In real conditions water mattress was fixed to the chipboard, being an additional insulator from the environment, which was not considered in the simulation. Furthermore, the air temperature at the bottom of the mattress could be lower than the one measured by the meteorological station. Taking into account the stable operation of the water mattress and even water distribution proved by the water temperature measurement through the channels, the influence of the constraints connected with heat flux measurement seems to have a dominant impact on a results discrepancy.

5.4.2. Conclusions from the model and laboratory results comparison

The conducted study based on the CFD simulations enabled the evaluation of the prototype water mattress operation under the experimental boundary conditions. Limitations of the real system applied to the mattress influenced the potential heat flux received from the animal, reducing it by at least 35 W/m^2 to 72 W/m^2, depending on the assumed temperature. The comparison of the simulation results with the one measured in the laboratory was intended to evaluate the applicability of the created previously and described in Chapter 3 of this PhD thesis, model for a heat flux prediction for different operational settings of the water mattress. The model was created to facilitate the preliminary study in terms of the water mattress geometry selection. For that reason, its functionality for such a purpose needed a more precise study. However, challenges described in the previous section of this thesis, connected with the heat flux measurements had a significant impact on the obtained results, making the comparison difficult for interpretation and precise error calculation. Therefore, applying a different heating system, which would adhere mattress' surface, as well as increasing the number of the heat flux sensors applied in different locations, to avoid an influence of the air inside the water mattress, could enhance the precision of the obtained results. However, it would require large financial outlays, and an innovative concept for heating, that could be applied in such conditions.

Although such a function of the model would be an added value in terms of the planned experimental campaign in the barn, it does not provide a complete view on the heat transfer in real conditions. For that purpose, the time-dependent study should be conducted, in which the amount of the received from the animal heat could be monitored, taking into account, both, the system's thermal inertia and the animals' thermoregulatory mechanisms. Such a monitoring set - up and procedure is a challenge, considering measurement conditions. Its application was tried within the barn experiments, however the heat flux sensors did not resist the process. More information about this measurement can be found in Chapter 6 of this PhD thesis.

Considering the complexity of this research issue, which is truly interdisciplinary in its nature, to obtain precise data, future models' creation needs a more experimentally based approach.

Chapter 6

Experimental campaigns in the real barn conditions

The main aim of the developed in this PhD thesis, cooling water mattress was to verify its operation and cooling effectiveness in a real barn with cattle under heat stress conditions. It allowed testing of the developed prototype in its target environment, demonstrating its possible future implementation on the industrial level. Cowsheds are characterized by very harsh environments due to the high humidity and temperature of the air, presence of the harmful gases, and dust pollution. Furthermore, the developed water mattress was directly confronted with animal weight load and its movement on the mattress, the presence of the manner and urine, as well as the layer of traditional bedding such as straw. All mentioned factors influence significantly water mattress operation, as well as the thermal and hygiene comfort of the animal. For that reason, an experimental case study was crucial for the proper evaluation of a developed solution. In this chapter two experimental campaigns conducted in the summer periods of 2022 and 2023 will be described in detail.

6.1. Description of the experimental campaigns

This paragraph provides detailed information about the structure of the conducted experimental campaigns in 2022 and 2023, and the applied planning approach. It is divided into two subsections, where each experimental campaign is separately described considering their leading research questions. Both experimental campaigns were conducted in the cowshed in the Research and Didactic Station in Swojczyce which is a part of the University of Environmental and Life Sciences in Wrocław in summer periods 2022 and 2023. The selected location was the result of cooperation with zootechnical experts from the aforementioned University. During both experimental campaigns animals had constant access to drinking water and feed and were under the regular care of zootechnical staff from the Didactic Station. In consultation with the chairman of the ethics committee, the ethical review and approval were waived for this study, due to routinely measured indicators of dairy cows and not executing procedures. However, the studies were evaluated following current European legislation (directive 2010/63/UE) (the European Parliament and of the Council, 2010) and were considered outside the scope of application.

6.1.1. Experimental campaign 2022: cooling effectiveness verification of the water mattress

The first experimental campaign was conducted between 12th September and 11th October of 2022, lasting 30 days. The main aim of that campaign was to investigate the operation of the developed water mattress under real barn conditions and to verify its cooling effectiveness in terms of the animal's body response to conductive cooling. For this purpose, the developed cooling water mattress supplied by the chilled water distribution system (c.f. Figure 6.1), was juxtaposed with two reference beddings, the first one was a conventional non-cooled water mattress working as the water pillow, and the second one was a traditional straw bedding. The cowshed in which animals were housed was naturally ventilated with no automatic regulation of environmental parameters.

Figure 6.1.The experimental test stand with the chilled water production and distribution system (on the right-hand side), as well as two reference beddings: convectional water mattress and straw (looking from the left-hand side).

Experiments were carried out with three milk breed Friesian dry cows, approximately 5-6 years old. Each of them was lying on different bedding: Zuzia on the cooling mattress, and Fruzia and Józia on respective reference beddings (c.f. Figure 6.2). The entire test stand was mounted before the experiments, during which animals were first observed in terms of their reaction to the new type of bedding as well as the presence of the research group members. The acclimatization period lasted for about 3 days, during which the cooling was switched off. Such a period was indicated by the Guide for the Care and Use of Laboratory Animals [72] as the minimum recommended, before minor procedures, which was considered sufficient since no invasive procedure was applied.

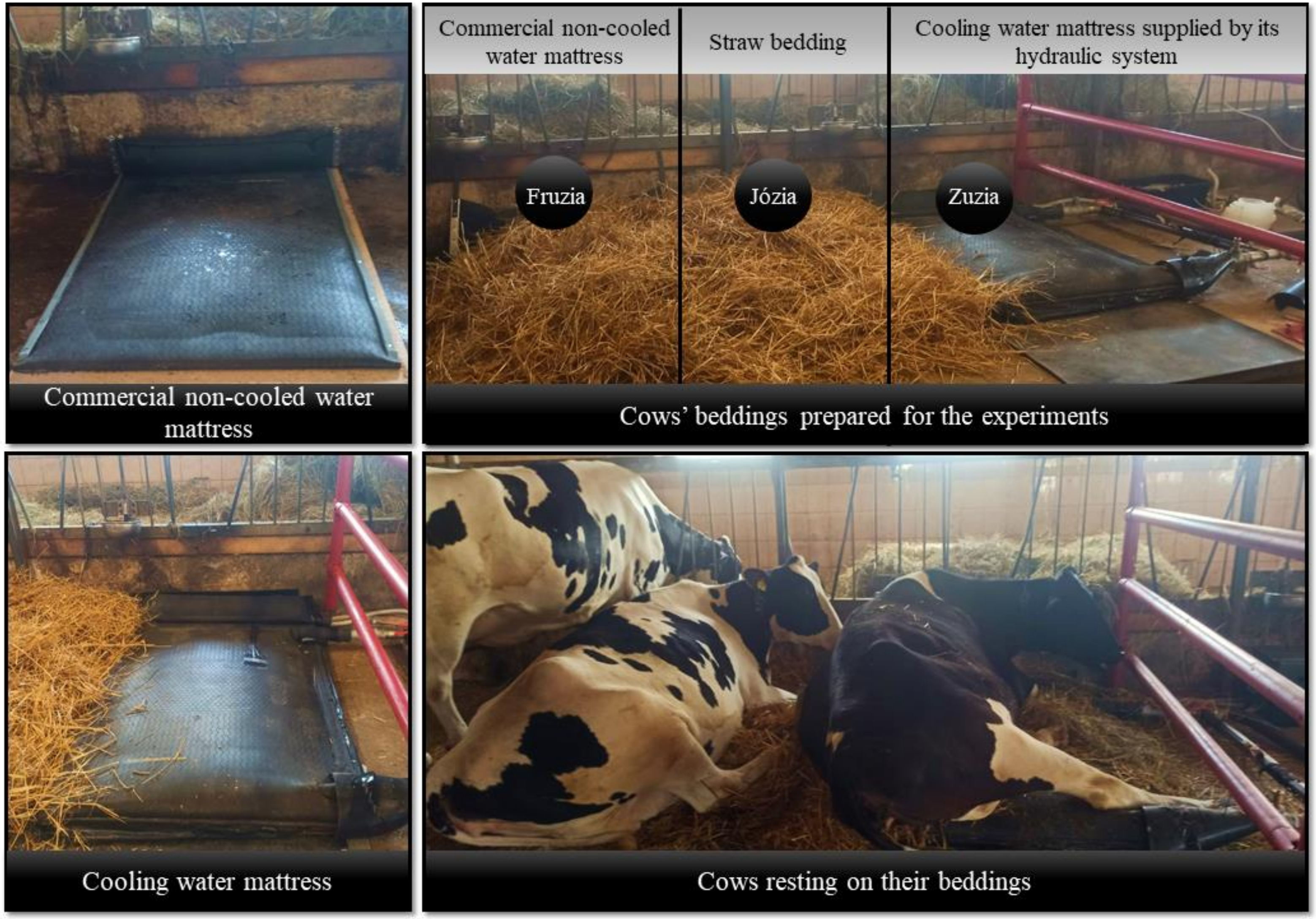

Figure 6.2 Three types of beddings that were under investigation during the experiments: the innovative cooling water mattress (with cooled cow Zuzia), the commercial water mattress (with Fruzia), and the conventional straw bedding (with Józia), where the last two are the referenced ones.

The experimental campaign was divided into 9 experimental series, during which operational parameters of the developed water mattress, such as supplying water temperature setpoint and water flow regulated through pump revolutions were changed. A detailed schedule of the experiments is presented in Table 6.1. Series 1, 2, 3, and 4 were 3 days long to ensure the animal's adaptation to the new conditions, and focused on the study of the influence of the chilled water mattress supplying temperature, changing between 16°C, 10°C, 13°C, and 19°C, respectively. Chilled water temperatures were assigned to the selected periods based on environmental parameters, applying the lowest temperature to the hottest days, and the highest temperature to the coldest days. Series 4, 5, and 6 were also 3 days long, during which the supplying water temperature was set at 19°C, and the flow rate was set to 2500 rpm, 3500 rpm, and 1500 rpm respectively. It allowed also a 9-day-long observation of the influence of one temperature setpoint, which gave the animal a longer time to adapt. Nocturnal chilled water temperature was set to 20°C as the result of the zootechnical consultation with the researchers from the Wrocław University of Environmental and Life Sciences. Such an increase in temperature was justified by reduced nocturnal ambient temperature. Weekends were characterized by no inference of the humane presence caused by the measurement, therefore, the diurnal and nocturnal temperature was set to 16°C, and only pump revolutions were changed remotely. Diurnal and nocturnal temperature setpoints were changed at 8:00 and 22:00, respectively. Such a time frame was selected due to the animals' feeding and management time in the morning hours, as well as thermal conditions in the barn during the evening hours. The hottest day at the beginning of the experiments – 19.08.2022 was focused on the direct investigation of the cooling effect on cows' skin using thermal imaging, in similar environmental conditions throughout the day. Lastly, three separate days were studied with a 16°C chilled water temperature setpoint and different pump revolutions, to extend the observation made for these conditions.

Table 6.1. Schedule of the experiments conducted in the summer period of 2022, between the 12th of August and the 11th of September (30 days of the experiments).

Date (2022)	**Series**	**No of days**	**T_{day}, °C**	**T_{night}, °C**	**Pump revolutions, rpm**	**Mode**
12.08	0	1	16	20	2500	Continuous
13-15.08	1	3	16	20	2500	Continuous
16-18.08	2	3	10	16	2500	Continuous
23-25.08	3	3	13	20	2500	Continuous
29-31.08	4	3	19	20	2500	Continuous
01-04.09	5	4	19	20	3500	Continuous
05-08.09	6	4	19	20	1500	Continuous
20-21.08 27-28.08 09-10.09	Weekend	2 2 2	16	16	2500 1500 3500	Continuous
22.08 26.08	rpm variable	1 1	16	20	3500 1500	Continuous

6.1.2. Experimental campaign 2023: influence of the developed water mattress in terms of cow's heat stress alleviation

The second experimental campaign was conducted in the summer period of 2023, between 11th August and 7th September 2023, lasting 29 days. The main goal of this campaign was to check the repeatability of the results through an extended experimental set-up, for which a second cooling water mattress was built and installed in a selected barn. Furthermore, the main interest of this campaign was to investigate the animals' heat stress indicators and the influence of a developed cooling water mattress on the studied animal, by a specially developed measurement strategy for observation of the physiological reactions of the animal, as the thermal indicators. The expected conclusion from this experimental campaign was also a selection of the most optimal chilled water temperature setpoint for operation in terms of animal comfort. Last, but not least, a new mode of developed water mattress operation, so-called "cyclical", was checked, where the water flow through the mattress was cyclically turned off for 2h, after achieving the previously selected chilled water temperature setpoint. Such operation gave deeper insights into the thermal exchange between the animal and water mattress surface, and this the chilled water, due to extended time for heat accumulation. Furthermore, such an operation could be beneficial in terms of electricity consumption of the entire chilled water production and distribution system.

Due to an expanded experimental set-up, in this campaign, two cows were lying on the developed cooling water mattress, and two other cows were lying on the commercially available non-cooled water mattresses as the reference beddings (c.f. Figure 6.3 a) All of them were covered with a layer of straw to improve hygiene conditions and help in adaptation to new types of bedding. Experiments were carried out in the same cowshed as in the previous year, with the same three Friesian dairy cows (c.f. Figure 6.3 b), and one (Tereska) newly adapted to the experiments (c.f. Figure 6.3 c). Fruzia and Zuzia (the same cows as in the previous campaign) were the cooled-down animals. All studied animals were assigned to one bedding type during the entire experimental campaign. All test stand components were installed in the barn before the experiments, following the same methodology previously described for 2022 experimental campaign, during which the meteorological data were gathered. Furthermore, all sensors (heart rate, core body and skin temperature, and Inertia sensor) mounted on the elastic belts to animals' bodies to monitor their physiological reactions, described in detail in Subsection 6.2.4 of this PhD thesis were applied before the experiments. It enabled previous acclimatization of the animals to the elastic belts and was intended to collect the reference data for no changes in bedding type applied.

The first research agenda considered experiments in the dairy farm and the correlation of the results of cooling with the milk yield of the animals, however, such cooperation was not possible due to logistical, financial, and technical limitations for the prototype solution. Nevertheless, future studies in this area would significantly enrich conclusions about the developed solution.

Figure 6.3. Water mattresses installed in the barn: a) the preparation stage, b) with an additional layer of straw on the top: counting from the left-hand side newly built cooling water mattress, non-cooled water mattress, and previously built cooling water mattress, c) fourth cow (Tereska) lying on the non-cooled water mattress.

As in the previous year, the second experimental campaign was divided into 9 series, however, the first 6 were grouped into 3 in terms of the diurnal supplying water temperature setpoint, with changing mode of operation. There were three levels of investigated temperatures 13°C, 16°C, and 19°C, where the nocturnal temperature was 20°C (in zootechnical consultation with the researchers from the Wrocław University of Environmental and Life Sciences). Continuous cooling was established for a 4-day-long period and followed by a 3-day-long period of cyclical cooling, since weekend days were organized with no humane presence in the barn, in the middle of the series with continuous mode. The flow rate for all of this series was regulated via the SCADA system as the percent of the pump's power as the result of changes made in a control algorithm. It resulted in a different pump's rotational speed of 3300 rpm in comparison to the previous campaign. The main goal of these experiments was to establish the most suitable, considering the environmental conditions, supplying chilled water temperature, and to verify if the water mattress' chilled water production and distribution system's cyclical operation maintains the cooling effect on the animal body when the flow was turned off. Series 4.1, 4.2, and 4.3 were assigned to one group because their main aim was to compare the results achieved for the maintained supplying water temperature setpoint and different flow rates at levels of 2750 rpm and 2200 rpm. A detailed schedule of the experimental campaign can be found in Table 6.2.

Table 6.2. Schedule of the experiments conducted in the summer period of 2023, between the 11th of August and the 8th of September (28 days of the experiments).

Date (2023)	**Series**	**No of days**	**T_{day}, °C**	**T_{night}, °C**	**Pump revolutions, % of power**	**Pump revolutions, rpm**	**Mode**
11-14.08	1.1	4	16	20	80%	3300	Continuous
15-17.08	1.2	3	16	16	80%	3300	Cyclical
18-21.08	2.1	4	13	20	80%	3300	Continuous
22-24.08	2.2	3	13	20	80%	3300	Cyclical
25-28.08	3.1	4	19	20	80%	3300	Continuous
29-31.08	3.2	3	19	20	80%	3300	Cyclical
01-03.09	4.1	3	19	20	60% 40% 60%	2750 2200 2750	Continuous
04-05.09	4.2	2	16 16	20 16	60%	2750	Continuous
06-07.09	4.3	2	13	20	60% 40%	2750 2200	Continuous

6.2. Methodology

The nature of the conducted experiments made them very diversified in terms of the applied methodology and measurement strategy, traversing boundaries between scientific disciplines, where energy, engineering, and zootechnical sectors are merged into the innovative cooling solution. For that reason, the developed methodology applies approaches from those scientific disciplines and gives a new measurement strategy plan, especially in terms of the physiological reactions of animals.

The first experimental campaign gave experience in data collection and measurement strategy for a continuously changing environment, in a cowshed. For that reason, the methodology applied in the second experimental campaign was enhanced, where it was needed, and extended in terms of the new goal of conducted campaign. In the following paragraphs, the methodology will be divided into four measurement groups and such way described: environmental parameters, cooling water mattress operation, IR thermography for direct observation of the cooling effect, and physiological reactions of the animals. Detailed information is provided in the following paragraphs.

6.2.1. Environmental data

Environmental parameters are necessary to provide information about the heat transfer conditions between animals and the surrounding environment. In the zootechnical sector, the temperature and humidity (THI) index is widely used to determine the heat stress level among animals. In literature several formulas were applied, however, the most widely used for moderate climates is the National Research Council formula (National Research Council. A guide to environmental research on animals, 1971) [73], given by Equation 6.1.

$$THI = (1.8 \cdot Tdb + 32) - (0.55 - 0.0055 \cdot RH) \cdot (1.8 \cdot Tdb - 26) \tag{6.1}$$

where:

Tdb – dry bulb temperature (°C);

RH – relative humidity (%).

Temperature and humidity of the air

To estimate the THI index, temperature (with NTC AKO015561 sensor - accuracy rating ± 1 °C) and relative humidity (with SONEE16F6A21 sensor - accuracy rating ± 3 %) were continuously recorded every 2 min, using a meteorological station controlled with Supervisory and Control Data Acquisition System. These data were collected for both outdoor and indoor environments (c.f. Figure 6.4 a and b, respectively) during both experimental campaigns. The outdoor data were gathered mainly to observe the general trend of these parameters in the direct area of the barn with an emphasis on heat wave phenomenon observations. Furthermore, the gathered data were also contrasted with data from the meteorological station located in the Observatory of Agro- and Hydrometeorology "Wrocław-Swojec", which is under the supervision of Wrocław University of Environmental and Life Sciences.

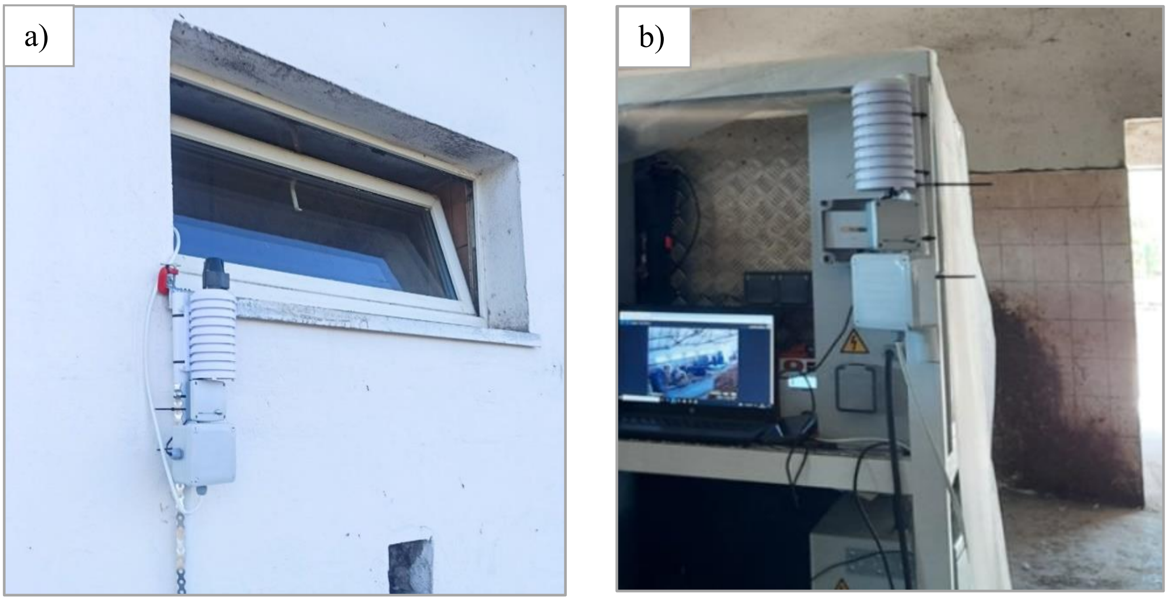

Figure 6.4. The meteorological station used during both experimental campaigns in the barn: a) for outdoor environment, b) for indoor environment, monitoring.

Velocity of the air

Furthermore, to designate the convective heat losses from the animals, the velocity of the air was measured manually using TESTO 440 thermo-anemometer (accuracy rating ±(0.03 + 4% m.v)). The measurement process is presented in Figure 6.5. The methodology differed between experimental campaigns. In the first one, it was a single measurement conducted in 5 locations: 2 in the barn’s corridor area between animals, and 3 on the height of animals' heads, repeated two times during measurement day, which is the first and last day of each experimental series. In the second experimental campaign, to achieve a more uniform result it was realized as an average value from 7 measurement points (measurement every 10 s for 1 min, starting from 1 s) in the same sequence.

Figure 6.5. Hand measurement of the air velocity: on the left-hand side measurement procedure in one of the three locations (windows), on the right hand side the TESTO 4040 thermo-anemometer that was used during the experiments.

Cooling rate

In the second experimental campaign, the methodology was enriched by the measurement of a cooling rate, that is a parameter describing biological cooling with consideration of environmental parameters, such as ambient temperature, the humidity of the air, the velocity of the air, and radiation. The measurement was realized using 2 katathermometers characterized by the constant F=405 mcal/cm^2 and F=167 J/dm^2, respectively. For that instrument, the directly measured parameter is the time of temperature drop of the liquid (alcohol inside the instrument) from 38°C to 35°C. According to the zootechnical norms, the measuring procedure considers three steps:

1) Heating the liquid inside the instrument until the liquid fills the upper vessel, which was realized by placing the katathermometer inside the cup with hot water (between 60°C and 80°C).
2) Drying the surface of the instrument in case of DRY measurement or wrapping with a wet wipe in case of WET measurement.

3) Placing the katathermometer in the target measurement location and waiting until the liquid's temperature reaches 38°C, in that moment the time measurement begins and lasts until the temperature achieves 35°C.

The achieved value was then recalculated using Equation 6.2 [74]:

$$H = \frac{F}{t} \tag{6.2}$$

where:

H - cooling rate, [W/dm^2]
F – constant of the katathermometer, [J/dm^2]
t – measured time. [s]

Measurements were always conducted with dry and wet kathatermoemter in the same locations as the velocity of the air (c.f. Figure 6.6). Such a series of measurements were repeated at least two times during measurement day, around 9:00 and 14:00. According [75] to optimal conditions for dairy cattle in their barns are characterized by a cooling rate between 2.7 and 3.6.

Figure 6.6. Measurement with the katathermometer: on the left-hand side one of the measurement carried out in the corridor, on the right-hand side measurements carried out near the windows and animals' heads.

6.2.2. Cooling water mattress operational data

Another line of conducted measurements was oriented on the cooling water mattress operation monitored through the cooling water temperature setpoint.

Cooling water temperature distribution

K-type thermocouples (first class, accuracy rating 0.4%) located inside the water mattress were intended to register the temperature distribution among the mattress' channel structure and collect them in the memory card of the KD-7 data logger, with a 1-minute sampling time. However, the wires of all thermocouples required extension for use in real barn conditions. In the first experimental campaign, used extensions proved to distort the measurement. Due to the nature of the experiments, which can be conducted only in hot weather conditions, and the prolonged time of waiting for the right compensation wires, gathered data were not appropriate for detailed analysis. Furthermore, it needs to be highlighted that any change in the experimental set-up disrupts all experimental periods, due to the necessity of the animals' removement from their bedding area and interruption in their natural routines of the day.

For that reason proper compensation wires were installed and tested before the second experimental campaign, enabling 24h per day data collection with 1-min sampling time, using a KD-7 data logger.

Inlet and outlet temperature from the water mattress

Inlet and outlet cooling water temperatures were measured using Vortex SV7204-SVR34XXX50KG/US-100 (accuracy rating ±1 °C) and ifm TA2115 (accuracy rating ±0.1%) sensors, respectively, which were installed on the hydraulic lines of the cooling water temperature distribution system. Data were collected continuously (24h per day) through the SCADA system with a 2-minute sampling time.

Surface temperature of the water mattress

Operation of the water mattress was also monitored through the measurement of its surface temperature, due to the insulative properties of the 5 mm thick, rainforced rubber. Such information provides data about the direct cooling effect on animals' bodies when lying down, compared to the conventional water mattress. Measurement was conducted manually by Visiofocus 06620 thermometer (accuracy rating ±1 °C). In the first experimental campaign, it was carried out in three locations: bottom, middle, and top, and it took place approximately every 1 hour (between 9:00 and 18:00). In the second experimental campaign the methodology was different, due to the difficulty accessing the mattresses in their top area. For that reason, measurement was carried out 2 times during measurement day, in 7 random locations in the bottom area of the mattresses, and then averaged. Furthermore, in the second experimental campaign, each measurement was followed by taking the thermogram of the mattress using the TESTO 890 thermal image camera (accuracy rating ±2°C; 2% of m.v.) for comparison of the obtained results. Further thermal image analysis considered the estimation of the average surface temperature as the average value from the 7 points selected in the IRSoft software.

Heat transfer between the water mattress and the environment

To verify the heat transfer between the animal and the cooling water mattress Omega HFS5 heat flux sensor (accuracy rating 5% of m.v.) described previously in Chapter 4 of this PhD thesis was applied. The one already mounted on the bottom surface of the mattress was monitoring heat gains from the ground. However, in the second experimental campaign, each water mattress (cooling and non-cooled ones) was also equipped with one heat flux sensor mounted on its top surface (c.f. Figure 6.7). Due to its susceptibility to mechanical damage and harsh operational conditions, several protecting elements were applied. The wires were pulled through a chemically resistant casing, then through the mechanically resistant casing made of metal fibers. The sensor's surface was fixed to the 1 mm thick copper plate, with 2.5 cm x 5 cm dimensions. Unfortunately, during the experiments, the sensors did not resist the extreme operation conditions mainly caused by the continuous movement of the cow. Finally, only one moment was recorded, when heat flux from the cow to the commercial water mattress was measured.

Figure 6.7. Heat flux sensor mounted on the top surface of the water mattress in the second experimental campaign.

6.2.3. IR thermography

The direct cooling effect of the developed water mattress on the animal's body was monitored through IR thermography. For this purpose Testo 890 thermal imaging camera (accuracy rating ±2 % of m.v.) was used. The recording was focused on several body areas: the thigh and abdomen, that was in direct contact with the water mattress.

Thermography of the abdomen and thigh region

In the first experimental campaign, thermal imaging was conducted on the first and last day of the experimental series, 5-minute videos of all 3 cows were recorded with the mentioned camera once the cows got up from bedding. The videos were recorded after the studied cow had rested for about one hour. An equal time interval was not possible to achieve, because it depends on the cow's individual predisposition and behavioural patterns. The thermographic videos were processed using IRSoft software. Data collection from those videos required applying a uniform methodology consisting of several steps, presented in Figure 6.8. First, the thermograms were extracted from the analysed video with a sampling time of 20 s. Additional thermograms were also extracted if there was a need for additional data from the considered shot (stage I in Figure 6.8). Then each thermogram was analysed in terms of the view on the cow's thigh and abdomen. The values of ambient air temperature and relative humidity measured on-site at the time of thermography were taken into account and entered into the IRSOFT software. Each mentioned area was marked with the same diameter assigned to this previously selected region on all thermograms to designate the average temperature, hot spot, and cold spot. The circle marked in black on the thermogram (stage II in Figure 6.8) determines the average temperature value from the points located in the middle. On the other hand, in the red area, only one point characterized by the highest temperature was checked, and likewise in the blue area, the software searched only for the coldest spot (stage II in Figure 6.8). Areas with minimum and maximum temperatures were marked to indicate whether they showed the same trend as the average values. The selected emissivity of 0.79 was chosen based on the publication of McGowan [76], who conducted studies to determine emissivity for several mammal species, including the Friesian cow. They indicated that the most commonly used emissivity at the level of 0.95-0.98 for most animals is greatly overestimated. Finally, all calculated using IRSoft software values were further transferred, analysed, and visualized (stage III in Figure 6.8).

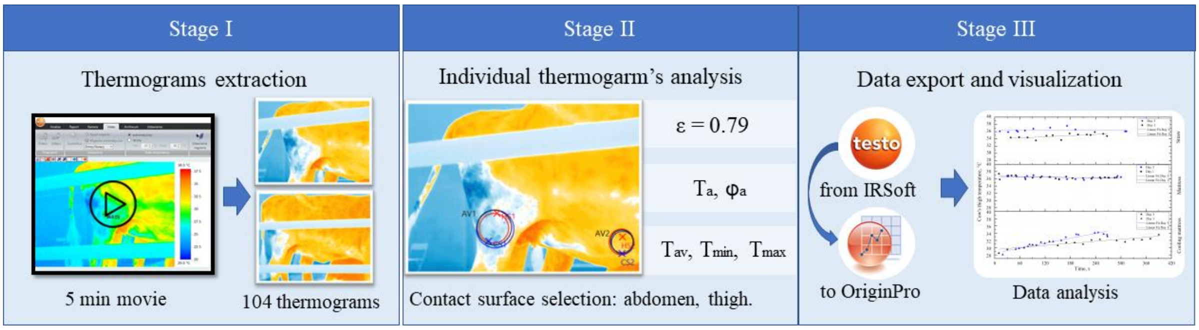

Figure 6.8. The methodology applied for IR thermography of abdomen and thigh regions.

In the second experimental campaign instead of videos, the sequence of 20 thermograms, with 30s sampling time was used. Further analysis of the thermograms was the same as previously described.

6.2.4. Cows physiological reaction data

Finally, the developed solution had to be evaluated in terms of its heat stress alleviation effect. For that reason, applied methodology considered also the physiological reaction of the animal. Nevertheless, the thermal regulation mechanism of the cattle is very complex and takes into account several cooling mechanisms: direct evaporation from the sweat, and saliva, and in the latent way, through the increased respiration rate, then regulation through the vascular system, and metabolic changes by reduced feed intake and milk production. A final indicator of an animal's thermal balance is core body temperature, which informs, that all thermoregulatory systems of an animal's body do not provide protection from thermal load. A detailed description of the thermal regulation will be described in Chapter 7 of this PhD thesis. In the first experimental campaign, only the core body temperature was measured, as the indicator of heat stress. However, this parameter is not so susceptible to the diurnal changes in thermal regulation, and direct cooling effect of the provided solution. For that reason, for the second experimental campaign, an extended measurement strategy was developed, focused on the measurement of additional parameters, such as skin temperature, heart rate, and respiration rate. The developed methodology is an original attempt to monitor the thermoregulatory systems of the animal and its heat exchange with the environment. In the following paragraph methodology applied for measurement of all mentioned indicators will be described in detail.

Core body temperature and skin temperature

There are several methods for measuring the core body temperature of the cow in the zootechnical sector: rumen, vaginal, and rectal methods. Rumen temperature is measured with boluses applied through the cow's digestive tract, the vaginal temperature with a specially designed sensor equipped with protrusions to be fixed in the genital tract, and rectal temperature with manual instruments. The first two methods are rather invasive in application, manual measurement on the other hand makes impossible continuous data collection. The cows that participated in the experiments had already applied smaXtec recticulo-rumen boluses (accuracy rating ± 0.05 °C), which enables the detection of feverish conditions, drinking behaviour, and estrus detection via heat index parameter, every 10 minutes. The last two parameters are the result of the algorithm applied by the company, based on temperature drop and animal motion detection. Such data collection was conducted for both experimental campaigns. However, rumen temperature is additionally burdened with the influence of drinking and digestive processes, which can result in a difference of up to 0.5°C than core body temperature [77]. For that reason in the second experimental campaign additionally, the rectal temperature was measured as the reference data. Measurement was conducted two times a day between 9:30 and 10:30, and between 14:30 and 15:30 on the first and last day of the experimental series, using a mercury thermometer (accuracy rating 0.1°C) dedicated to zootechnical use. Furthermore, the drawbacks of the previously mentioned methods were the reason for proposing a new system for core body temperature monitoring in the second experimental campaign. The proposed method was based on a CORE Body Temperature Sensor, dedicated to sport use to monitor the thermal reaction of the human body during activities. Originally it is worn on the chest belt in direct contact with the skin. The specially applied algorithm recalculates the skin temperature to the core body temperature based on the provided weight and type of activity. Data are collected with a 5-minute sampling time on the dedicated app, functioning also in the cloud. Such a sensor was mounted on the cow-tailored elastic belt, mounted in the forelegs area, where contact with the cow's body was the highest, and the extent of the cow's tongue was the lowest (c.f. Figure 6.9).. The main limitation of such a solution is an assigned algorithm dedicated to humans. However, the trend can be compared with rumen temperature, and future development of the algorithm into this application would have high potential in the breeding sector.

Heart rate

In the second experimental campaign, another indicator of the physiological reaction of the animal to cooling was measured. This parameter was the heart rate, which informs about the response from the circulatory system, and its increase indicates that the blood is pumped through the veins with higher pressure, and can be accompanied by shallow breathing. According to [78] one of the severe heat stress symptoms is panting, followed by the stage of quick and shallow breathing, indicating the potential interrelation of these two parameters in heat stress recognition.

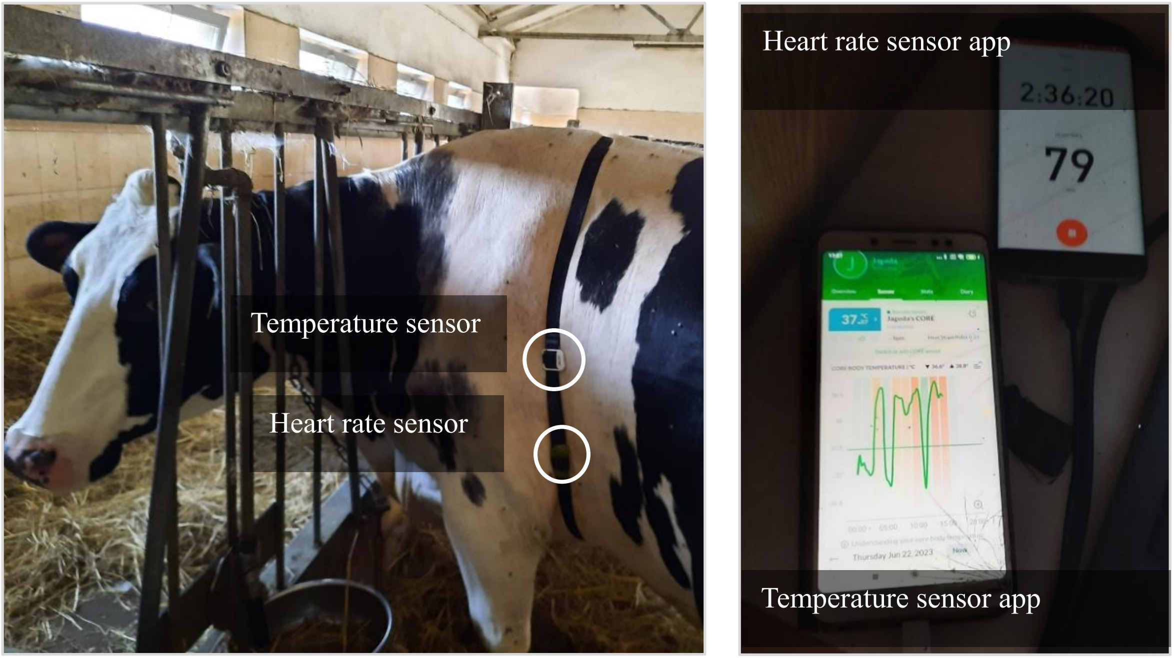

Figure 6.9. Measurement of the heart rate and the core and skin temperature: on the left-hand side location of the sensors mounted on the elastic belt in the cow's body, on the right-hand side view on the applications (apps) compatible with the sensors.

Due to the lack of commercially available solution for cattle, during the experiments, a novel approach was developed, where another human-designated CardioSport heart rate sensor, was applied. Its working principle is based on electrodes, which capture the electro signals from the pulse. The belt with electrodes was connected with the cow-tailored elastic belt and located in the region of the cow’s aorta, which is slightly above the left foreleg (c.f. Figure 6.9). Electrodes were regularly wetted during the experiments, to enable signal transfer. The sensor’s application was consulted with zootechnical experts from Wrocław University of Environmental and Life Sciences. Data were collected via the STRAVA phone application (app) with a 1 s sampling period.

Respiration rate

Data collection during the second experimental campaign was also extended by applying a new approach for continuous monitoring of the respiration rate. This parameter according to the literature was measured only by eye observation, which is a highly limiting method. The developed approach was based on a gyroscope Inertia ProvMove Mini Sensor, which measures the movement deviations in three dimensions (X, Y, Z axes). The sensor was mounted on the second elastic belt on the right flank of the animal's body, in the place that would be a target eye observation during the measurement (c.f. Figure 6.10). Data collection was conducted through the Inertia Studio software, which enabled data downloading from the sensors. However, the susceptibility of the sensor to any movement made the data difficult for precise measurement and thus interpretation.

Figure 6.10 Measurement of the flank movement sensor, which potentially could be processed to the respiration rate, on the left-hand side location of the sensor on the animal's body, on the right-hand side the necessary instruments connected with Inertia Studio software.

Behavioral monitoring

An additional indicator of cows' welfare was behavioral observation, focused on standing and lying time. The importance of this indicator is oriented on the direct response of the animal to the new bedding, and its cooling effect. Cows' reaction to the heat stress is connected with increased standing time, due to the convective heat losses to the environment in this position. Theoretically, increased lying time for animals with the cooling mattresses being their beddings, would inform about preferable by the cow cooling effect. Continuous monitoring was conducted during both experimental campaigns, using two cameras (c.f. Figure 6.11). The first one was the IMX477 camera for the first campaign and for the second campaign OdSeven Camera HD IR-CUT OV5647, working also in nocturnal mode, both coupled with Raspberry Pi - ArduCam B0241. The second camera was the TP-Link TAPO C200 camera recording 24h per day, oriented to the regions of animals' heads, to observe other behavioral patterns, such as licking, and chain shaking, and also the feed intake..

Figure 6.11 Diurnal (on the left-hand side) and nocturnal (on the right-hand side) recording from the TAPO camera in the second experimental campaign (2023).

These observations were not included within this PhD thesis, due to their zootechnical character, but they allowed general observation of the animals' reaction to the new bedding and interpretation of physiological measurements in terms of the conditions in the barn. Nonetheless, the behavioral character of data was also under analysis in cooperation with Wroclaw University of Environmental and Life Sciences.

6.3. Results

In this chapter results from both, the 2022 and 2023 experimental campaigns will be presented. The chapter is divided into two subsections, which focus on providing data necessary to answer the main research questions, previously presented in Chapter 2 of this PhD thesis. The aformentioned questions focus on water mattress operating conditions, which could provide an appropriate cooling level for the animal, as well as, the physiological reaction of the animals to cooling within the developed water mattress. Nevertheless, conducted experimental campaigns have provided an extensive database and the correlation of such diversified data is very complex, therefore, it needs to be highlighted that even with the main conclusions provided below, it is still a source of data for further studies.

6.3.1. Experimental campaign 2022: proved water mattress' cooling effectiveness

This subsection presents the main results obtained during the first experimental campaign in real barn conditions. The main goal of this campaign was to prove the cooling effectiveness of the developed solution in cattle's heat stress conditions. For that reason, this section will be divided into three main areas of analysis: environmental data, which provides information about the thermal load, caused by the weather conditions, then the cooling effect of the developed water mattress, and the response from the animal's body to cooling, directly presented in thermograms.

Environmental conditions of conducted experiments

The first experimental campaign was conducted in the summer period 2022. Monitored environmental data, such as relative humidity and air temperature, enabled THI designation, and considered together, were the main indicators of thermal conditions. In Figure 6.12 can be observed that especially August was characterized by high air temperatures with two heat waves (15^{th} -19^{th} and 25^{th} -27^{th}), defined as 3 days consecutive with temperatures higher than 30°C, according to [2], [3], [79]. Only a few rainy days between the 21^{st} and 24^{th} of August, which would provide relief in thermal conditions, were observed. Even September days were characterized by high ambient temperatures at the level of 25°C, which is the most often reported threshold of cow's thermal comfort [80], highlighting the high need for cooling in the breeding sector in Polish summer conditions.

Furthermore, calculated THI indicates heat stress conditions, assigned with a 72 threshold according to the literature [81] within the mentioned heat wave periods (c.f. Figure 6.12). However, according to the literature, the mentioned threshold can be lower, starting from 68 [82], which is the level achieved in most experimental days. It is also worth mentioning, that for the 8^{th} – 10^{th} of September days, the ambient temperature did not exceed 30°C to define them as a heat wave, but due to a high humidity level, those days were considered as the ones with heat stress conditions.

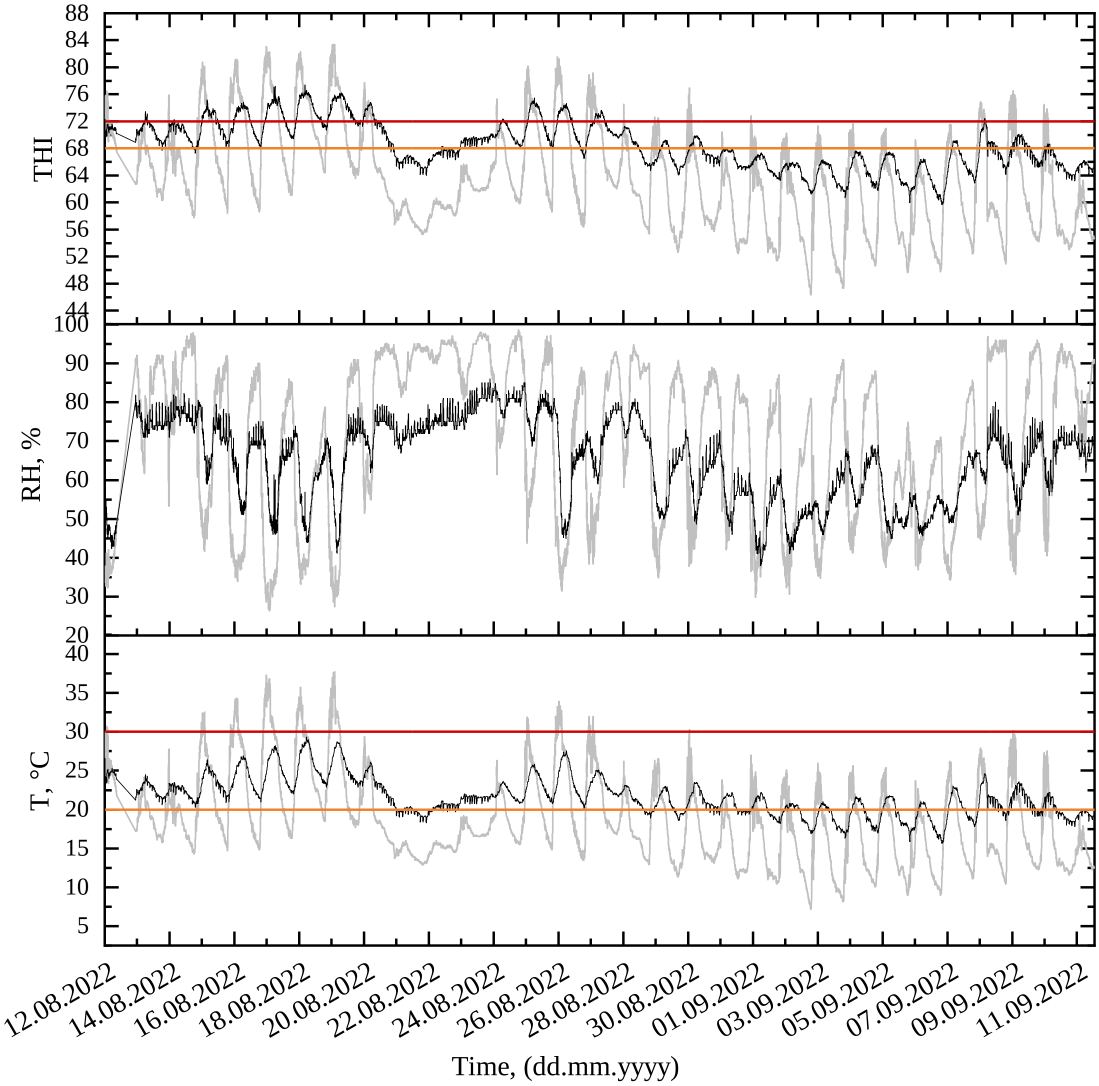

Figure 6.12. Indoor (black line) and outdoor (gray line) environmental conditions, such as THI with marked heat stress threshold of 72 (red line), and 68 (orange line), relative humidity, and air temperature, with a marked threshold level of 30°C considered for heat 3day long heat waves, and 20°C (orange line) as threshold of thermal comfort, during first experimental campaign from 12.08.2022 at 11:00 to 12.09.2022 at 00:00.

Water mattress cooling effect in real barn conditions

Monitored inlet and outlet temperature of the cooling water from the developed mattress proved its continuous cooling effect. In Figure 6.13, can be observed that the previously selected temperature setpoints of 10°C, 13°C, 16°C, and 19°C were properly maintained within the experimental series. Moreover, the stable level of temperature increase at the outlet indicated the uniform water distribution, without any flow blockage, that could be caused by the cow's weight. Detailed information about this parameter was provided by the thermocouples measurements, which were properly gathered in the second experimental campaign and described in Subsection 6.3.3 of this PhD thesis.

Furthermore, a narrow range of the increase indicates the high thermal inertia of the water mattress, caused by a large water capacity of 125L and a 5 mm-thick layer of insulative rubber. Such property could be beneficial for the cyclical operation of the developed water mattress, where the circulation pump is periodically switched off until the chosen temperature increase setpoint is achieved, bringing potential savings in electricity consumption. For that reason, this new operation sequence was further developed in the second experimental campaign and described in detail in Subsection 6.3.3 of this PhD thesis. It is also worth noticing that the analyzed temperature increase was the highest at 16°C (c.f. Figure 6.13), which suggests its optimal character in terms of the thermal exchange between the mattress and the animal. Nevertheless, it needs to be further investigated and will be a possible direction for future works.

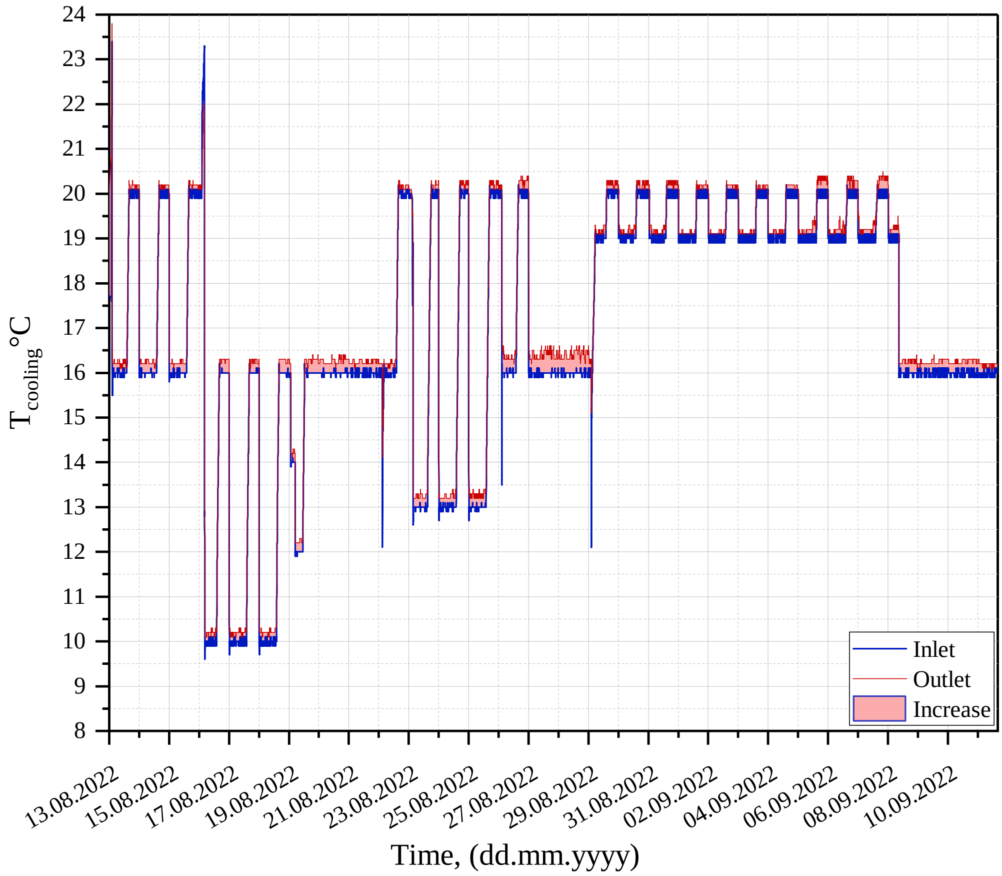

Figure 6.13. Chilled water temperature at the inlet and outlet to the water mattress during the first experiment campaign with marked temperature increase.

The surface temperature of the developed water mattress measured within 4 experimental series, when 10°C, 13°C, 16°C, and 19°C chilled water temperature setpoints were selected, is presented in Figure 6.14 with fitting analysis in Table 6.3. Bar graphs represent the temperature difference between cooling and conventional mattresses, indicating the magnitude of the developed water mattress's cooling effect. Although the chilled water mattress' temperature setpoint was achieved, the mattress' surface temperature differed significantly from the previously selected setpoint achieving temperature difference in the order of about 7°C, 5°C, 4°C, and 2°C, respectively. Such relations indicate the influence of the insulative properties of the rubber or the influence of environmental conditions and the film of liquids on the mattress' surface (condensation or urine). Nevertheless, the cooling effectiveness of the developed water mattress was proved for each studied temperature setpoint of the chilled water, which resulted in the temperature difference from the reference non-cooled mattress at of the order of 11°C, 10°C, 8°C, and 5°C, respectively (c.f. Figure 6.14).

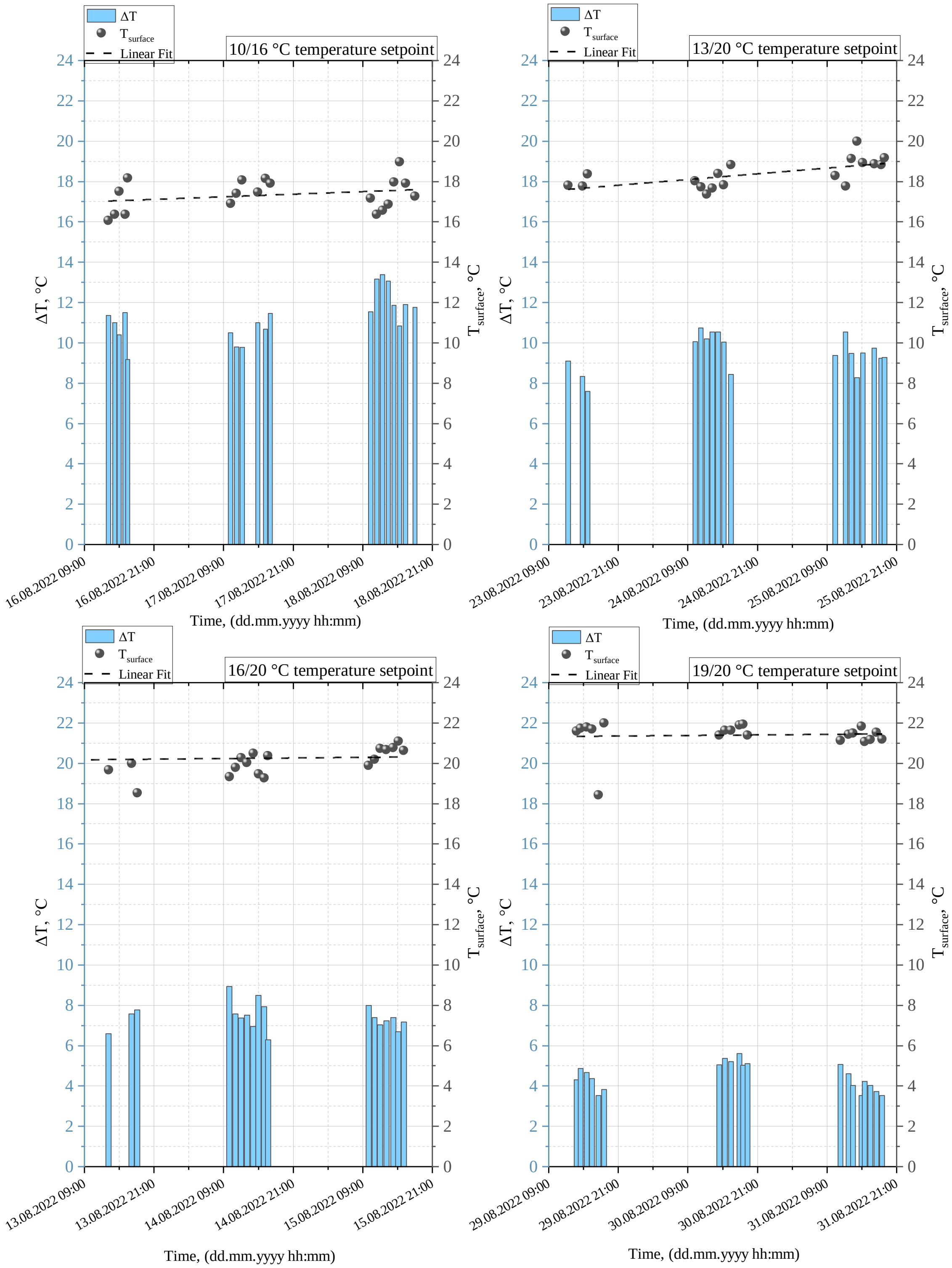

Figure 6.14. The cooling water mattress' surface temperature during 4 experimental series, where 10°C, 13°C, 16°C, and 19 °C of chilled water temperature setpoints were under research. The bar graphs represent the temperature difference between cooling and reference non-cooled mattresses.

Table 6.3. Fitting analysis for the results presented in Figure 6.14.

Fitting	**y=a+b·x**		
Setpoint:	a	b	R^2
10°C	-629974.5	0.26	0.07
13°C	-1391956.9	0.57	0.40
16°C	-146586.0	0.06	0.00
19°C	-134012.5	0.05	0.00

Animal's response to conductive cooling – IR thermography

The cooling effect of the developed mattress on an animal's body was investigated within IR thermography. Figure 6.15 a and b (with fitting analysis in Table 6.4) present the temperature for the abdomen and thigh area from the first and last day of the experimental series with the lowest diurnal chilled water temperature setpoint of 10°C and nocturnal setpoint of 16°C, juxtaposed with two cows lying on the reference non-cooled beddings – the commercial water mattress and a straw. Charts present data collected within the first 200 s or 300 s from getting up from their beddings after about 1h of continuous lying. The difference in considered period is caused by getting up of another cow during the measurement, and only one thermal image camera. It can be observed that for the cooled cow (Zuzia) skin temperature in the abdomen region was about 2°C and 4°C lower (c.f. Figure 6.15 a) on the first and last day, respectively, than the referenced cows, for which temperatures achieved similar levels. For that region of the cow's body, the achieved characteristics were rather stable. On the contrary, for the thigh region, characteristics for the first day of the experiment for two cows - the cooled one and the one lying on the straw had an upward trend, with a higher growth rate in the case of the cooled cow (c.f. Figure 6.15 b). It is worth mentioning that in both cases temperature increased to the value of the abdomen region. It indicates that after getting up, the blood circulatory system in the thigh area is being reactivated to its normal functioning in considered environmental conditions, changed either due to the tension or, returning to the preferable thermal balance of the body.

Furthermore, it can be easily noticed that during the last day of the experimental series measured skin temperature was lower for each cow, although this day was characterized by a higher temperature of the air and increased THI level, than the first day (c.f. Figure 6.8). Such a relation may indicate that cows activated other thermoregulatory mechanisms, such as evaporation rather than convective heat losses (connected with regulation within the blood circulatory system), to reduce the thermal load. Such an observation seems to be important for future analysis when the most suitable cooling method in terms of the environmental conditions, could be applied in mixed systems. More importantly, it indicates that the 10°C chilled water temperature setpoint could be too low for extremely high temperatures of the air when animals' body adapts to it within different mechanisms than through the circulatory system. Too low mattress' chilled water supply temperature may be the reason for restricted surface blood circulation, thus reducing the cooling capabilities of a conductive cooling solution.

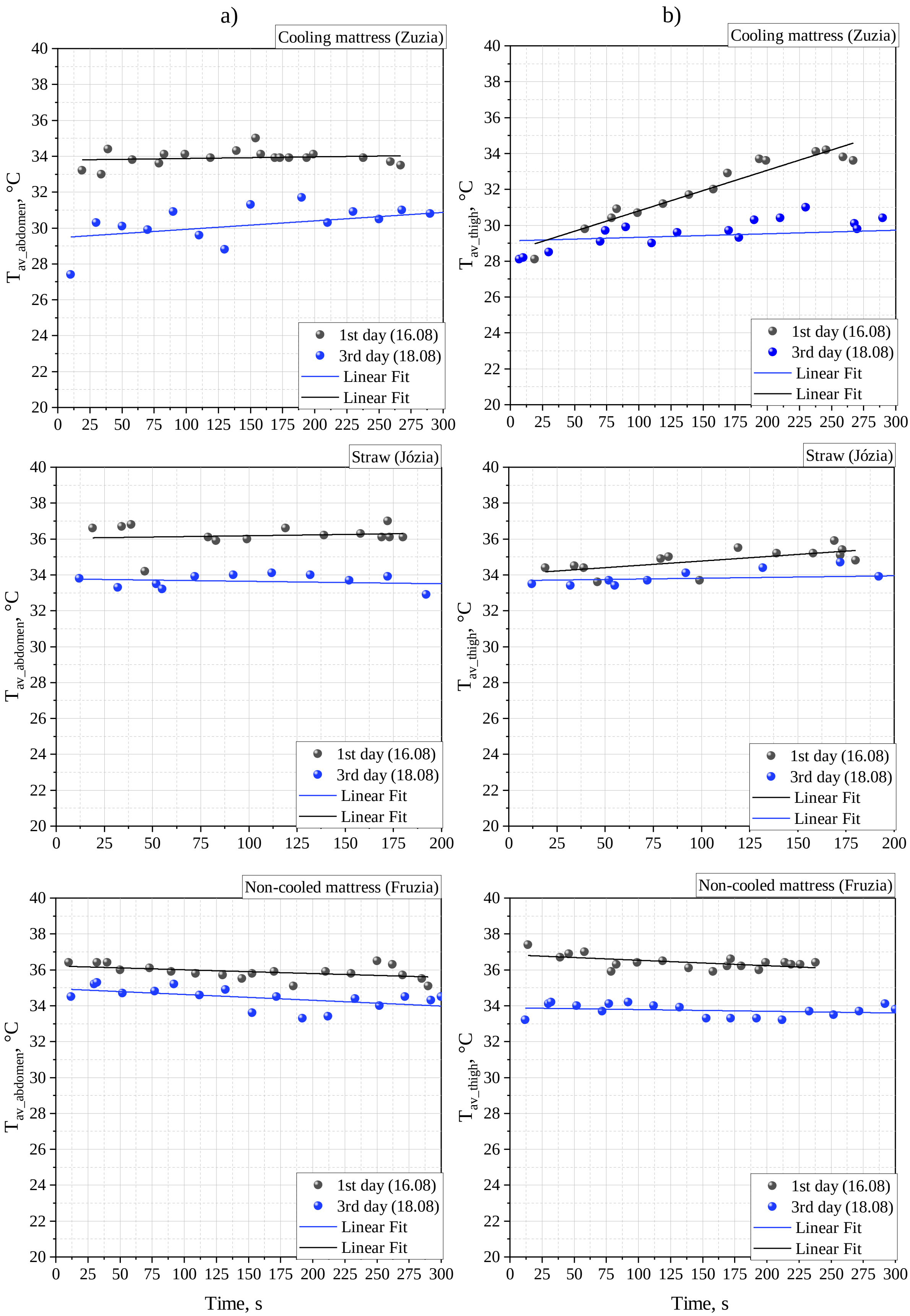

Figure 6.15. Results of the conducted IR thermography of: a) the abdomen, b) the thigh regions of each examined cow, for the first and last day of the experimental series of 2022 with 16°C (diurnal) and 20°C (nocturnal) chilled water temperature setpoint.

Table 6.4. Fitting analysis for the results presented in Figure 6.15.

Graph		**a) abdomen area**			**b) thigh area**		
Fitting		y=a+b·x			y=a+b·x		
Day and bedding type:		a	b	R^2	a	b	R^2
1st day	Cooling mattress	33.8	9.0 E^{-4}	0.02	28.5	2.3 E^{-2}	0.93
	Straw	36.0	1.4 E^{-3}	0.02	34.0	7.4 E^{-3}	0.43
	Non-cooled mattress	36.2	-2.1 E^{-3}	0.22	36.8	3.0 E^{-3}	0.32
3rd day	Cooling mattress	29.5	4.7 E^{-3}	0.32	29.1	2.0 E^{-3}	0.04
	Straw	33.8	-1.4 E^{-3}	0.11	33.7	1.4 E^{-3}	0.08
	Non-cooled mattress	34.9	-3.2 E^{-3}	0.27	33.9	-9.5 E^{-4}	0.06

For that reason one experimental day (19.09.2022), characterized by high environmental conditions (c.f. Figure 6.8), was dedicated to observations of the cooling effect on the animal's body within 45-60 minutes after getting up from the bedding, conducted for 12°C, 14°C, and 16°C chilled water temperature setpoints. Results for the abdomen and thigh areas are presented in Figure 6.16 with fitting parameters in Table 6.5. It can be observed that in the abdomen region, for the lowest cooling water temperature of 12°C, skin temperature increases rapidly within 15 min from 22°C to 36°C, similar tendency is visible for the thigh region, where temperature increases from 27°C to 36°C in both cases it becomes rather stable at this value. A similar tendency can be observed for the 14°C chilled water temperature setpoint, however characteristic differs for the abdomen area, where the lowest temperature was 34°C, which was probably caused by adopted by the cow position, where the cooled region was not so visible in thermograms. Nevertheless, both characteristics indicate a quick return to normal cow's skin temperature of 35-36°C, which suggests that although the tissues were cooled down by the mattress, the surface blood circulatory system was extremely reduced, and after getting up it was quickly returned to adopt an animal for convective heat losses to the environment. It means, that these chilled water temperature setpoints seem to be too low for high air ambient temperatures. Different mechanisms can be observed for the 16°C chilled water temperature, where the increase of the skin temperature extends for 30 min until stabilization at a lower temperature level of 32°C for the abdomen and 31°C for the thigh regions. Such a trend indicates that a 16°C chilled water temperature setpoint provides better thermal comfort for the animal, adapting more smoothly to its natural thermoregulatory systems. It also correlates with the observation in Figure 6.13 of a higher temperature increase in the chilled water temperature at the mattress outlet for 16°C.

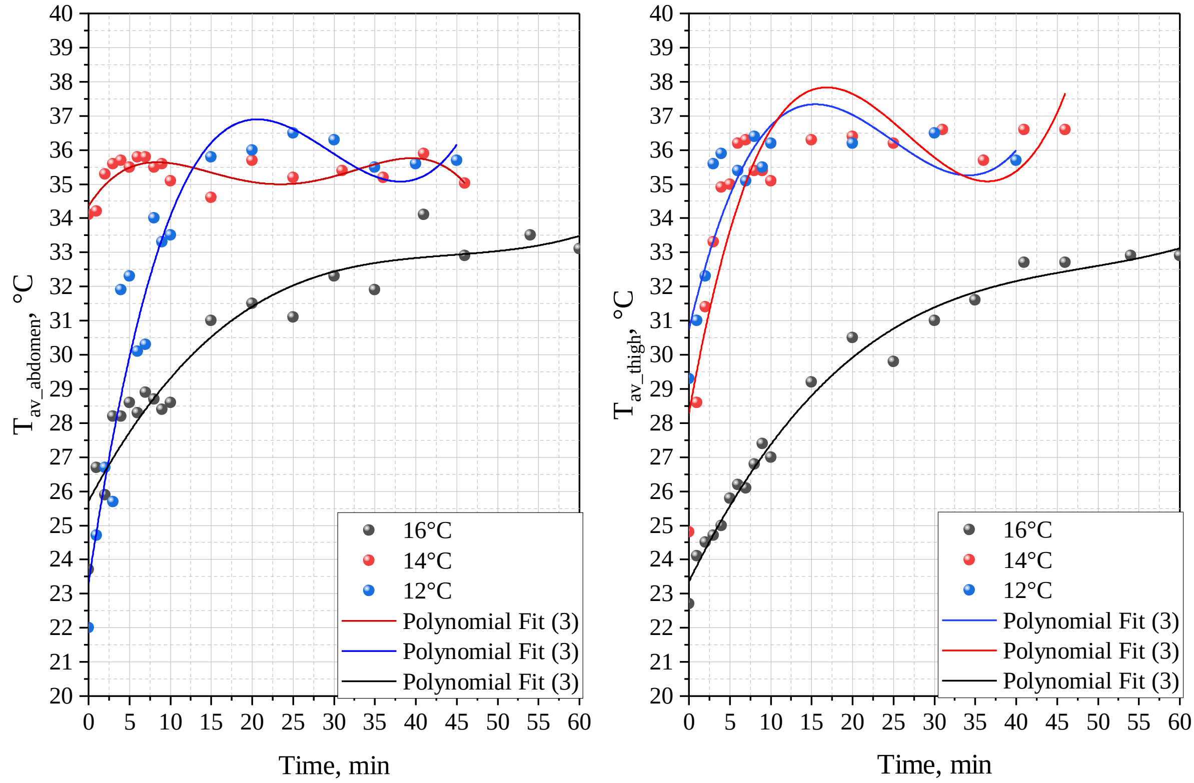

Figure 6.16. Skin temperature of the abdomen and thigh region of the cooled cow (Zuzia) within 45-60 min after she got up from the cooling water mattress for three chilled water temperature setpoints: 12°C, 14°C, and 16°C, for the experimental day 19.08.2022.

Table 6.5. Fitting analysis for the results presented in Figure 6.16.

Graph	**Abdomen area**					**Thigh area**				
Fitting	$Y=A+B1\cdot x+B2\cdot x^2+B3\cdot x^3$					$Y=A+B1\cdot x+B2\cdot x^2+B3\cdot x^3$				
Setpoint:	A	B1	B2	B3	R^2	A	B1	B2	B3	R^2
12°C	23.3	1.61	-0.06	$6.8E^{-4}$	0.92	30.7	1.01	-0.05	$6.4E^{-4}$	0.77
14°C	34.8	0.12	-0.01	$7.4E^{-5}$	0.18	28.3	1.34	-0.06	$7.3E^{-4}$	0.78
16°C	25.7	0.45	-0.01	$7.3E^{-5}$	0.91	23.4	0.49	-0.01	$6.4E^{-5}$	0.98

To observe the cooling effect of a 16°C mattress' chilled water supply temperature setpoint extended to a three-day-long experimental series. The IR thermography carried out for the last day of the series with a diurnal chilled water temperature setpoint of 16°C and 20°C as a nocturnal setpoint is presented in Figure 6.17 with fitting analysis in Table 6.6. It can be noticed that an increase in skin temperature measured in both, the abdomen and thigh region, for the cooled cow (Zuzia) is in a small range of 2°C within the considered period. At the end of the analyzed measurement period, skin temperature reached 30°C for the abdomen and 28°C for the thigh region, being significantly lower than for the referenced non-cooled cows, for which it reached 34°C (commercial non-cooled water mattress) and 36°C (straw), considering the abdomen region and about 33°C for the thigh region for both cows. It proved the previously observed good thermal adaptation of the animal to the investigated chilled water temperature setpoint. Furthermore, the surprising trend for reference cows can be noticed, where the skin temperature decreases within the considered period. Although, for the cow lying on straw, the decrease is rather narrow than for the cow lying on a commercial non-cooled water mattress, where the temperature difference was of the order of 4°C. Such a relation suggests, that the resting position of animals reduced their capabilities for heat dissipation, which may result in increased surface blood circulatory, and return to the standing position enabled convective heat transfer to the environment and thermal balance. Considering this observation, maintained by the cooled cow. Significantly low and almost stable, skin temperature highlights the significant role of conductive cooling with properly adopted chilled water temperature.

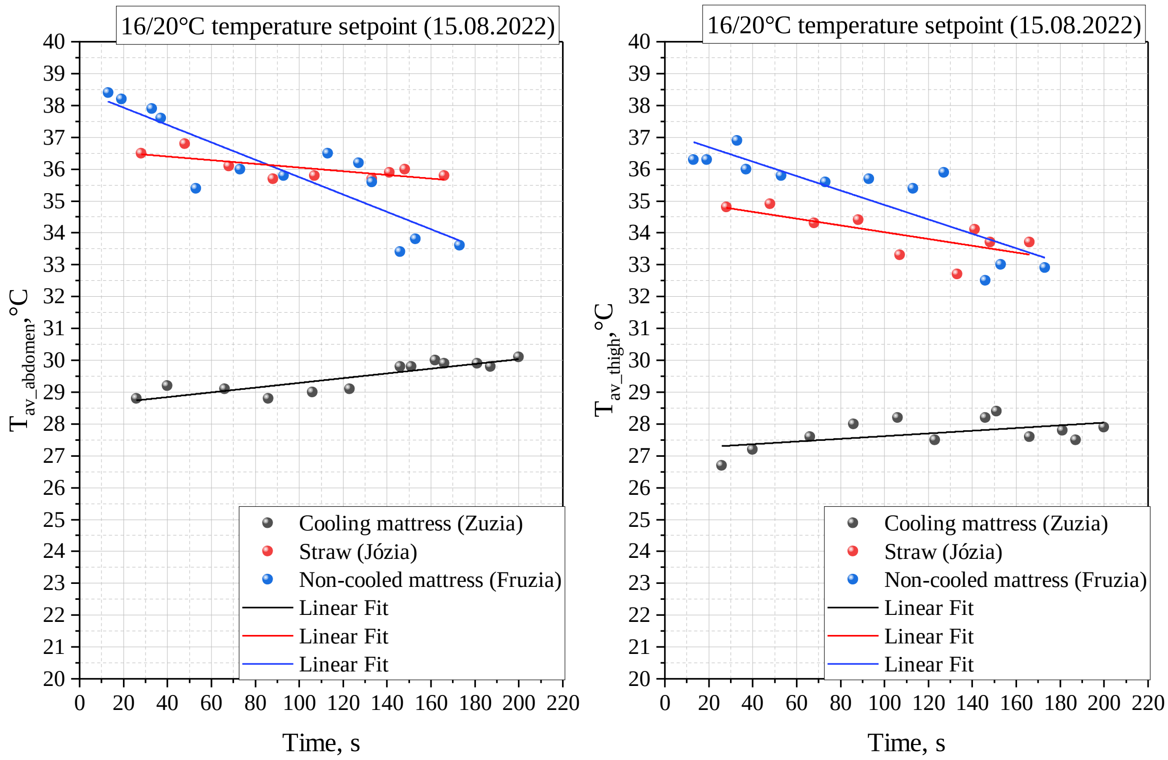

Figure 6.17. Skin temperature of the abdomen and thigh regions for the last day of the experimental series of 2022 with 16°C (diurnal) and 20°C (nocturnal) chilled water temperature setpoint presented for all examined cows.

Table 6.6. Fitting analysis for the results presented in Figure 6.17.

Graph	**Abdomen area**			**Thigh area**		
Fitting	y=a+b·x			y=a+b·x		
Bedding type:	a	b	R^2	a	b	R^2
Cooling mattress	28.5	-0.01	0.76	27.2	0.00	0.27
Straw	36.6	-0.01	0.53	35.1	-0.01	0.51
Non-cooled matress	38.5	-0.03	0.78	37.1	-0.02	0.72

6.3.2.Main conclusions from the experimental campaign of 2022

The experimental campaign conducted in the summer period of 2022 proved the cooling effectiveness of the developed water mattress working under real barn conditions. Its surface temperature achieved lower values than the reference non-cooled commercial water mattress for all chilled water temperature setpoints: 10°C, 13°C, 16°C, and 19°C. However, the insulative properties of the rubber resulted in a high-temperature difference between the surface and supplying chilled water. The observed thermal inertia of the developed water mattress suggests its predisposition for cyclical operation mode, which could be beneficial in terms of electricity consumption reduction, which was one of the subjects of further investigation in the 2023 experimental campaign. Although the stable level of temperature difference between the inlet and outlet indicates undisturbed water flow through the mattress, the specific information about water distribution inside the mattress channel's structure could be better interpreted from the thermocouple readings. However, due to technical problems mentioned in the methodology in Section 6.2 of this PhD thesis, this parameter was also further investigated in the second experimental campaign in 2023.

The cooling effect on the animal's body of the developed water mattress was proved within conducted IR thermography through recorded lower skin temperature than for the cows lying on the reference non-cooled beddings. However, it was observed that the cooling effect range depends on the proper chilled water temperature selection in terms of the animal thermoregulatory systems and environmental conditions. The chilled water temperature setpoint of 10°C was too low for the animal's body in heat stress conditions, causing a quick return of the cow's body to its normal temperature, within the activated surface blood circulation. Therefore, obtained results, indicated the chilled water temperature of 16°C the most optimal for animal's thermoregulatory systems in high ambient temperature conditions. However, the complexity of animals' thermoregulatory systems focuses further research on the physiological reactions of the cow to different chilled water temperature setpoints and their influence on the level of heat stress experienced by the cow. Investigation of these thermal mechanisms was therefore the main aim of the conducted in 2023 experimental campaign.

6.3.3. Experimental campaign 2023: investigated heat stress alleviation effect in relation to the chilled water temperature distribution inside the developed water mattress

The following subsection presents the main results obtained during the second experimental campaign conducted in the same barn. Contrary to the previous campaign's experiments the main goal was to assess the influence of the developed cooling water mattress on the animal's thermal balance and heat stress relief experience. Furthermore, the previously described cyclical operation of the developed water mattress was verified. The extended experimental set-up enabled the comparison of the collected data for two cooling water mattresses.

This section will be divided in the same as in the previously described experimental campaign in three areas of analysis: environmental data expanded by the cooling rate parameter, the cooling effect of water mattresses, and last but not least, the response from the animal's body, expanded by the newly measured physiological parameters, such as the rumen temperature, the skin temperature, the core temperature, and the heart rate.

Environmental conditions of conducted experiments

The second experimental campaign was conducted in a similar summer period to the previous year, between 12.08.2023 and 07.09.2023, characterized by high air temperature, with two significant heat waves. The first one was 8-day long, observed between 13th and 18th of August 2023, which was especially important due to its long duration, reducing animals' capabilities to recovery, including nights, due to high nocturnal air ambient temperature and THI level (c.f.

Figure 6.18). The second one was 5-day long, and occurred between 22nd and 26th of August 2023, followed by the weather breakdown from 28th of August to 1st of September. September days were characterized by the high even for Polish climate conditions outdoor temperature, however, the barn's indoor temperature was reduced thanks to the few colder days, which permitted cooling down the cowshed, influencing its thermal inertia. The instantaneous THI level crossed the threshold of 72 before the weather breakdown, reaching even a value of 76, varying between 68 and 72 in September (c.f. Figure 6.18).

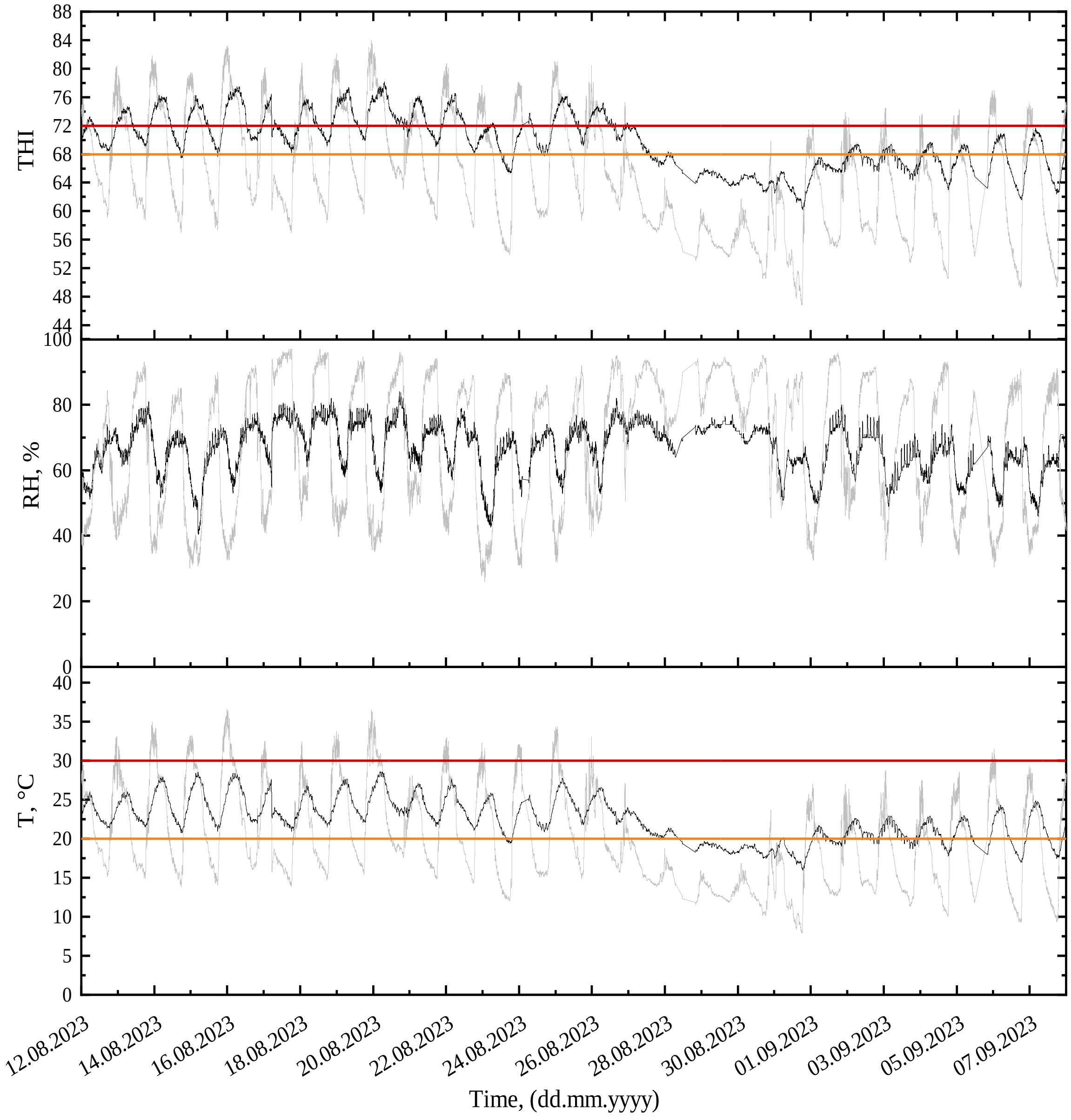

Figure 6.18. Indoor (black line) and outdoor (gray line) environmental conditions, such as instantaneous THI with a marked heat stress threshold of 72 (red line), and 68 (orange line), relative humidity, and air temperature, with a marked threshold level of 30°C considered for 3day long heat waves, and 20°C (orange line) as threshold of cattle's thermal comfort, during the second experimental campaign from 12.08.2023 to 07.09.2023.

Such thermal distribution within experimental days emphasizes the need for cooling, due to the prolongate time of heat stress conditions with reduced capabilities for the animal's natural return to its thermal balance.

Cooling rate

A new parameter, namely a cooling rate, was used for the investigation of animal comfort based on environmental conditions. It is an indicator used in the zootechnical sector to designate optimal conditions of breeding and is measured by the katathermometer. Dry measurement takes into consideration convective heat losses, wet one includes also evaporative heat losses. According to [75] its optimal value for milk cows housed in tethered barns should be within the range of 2.7 and 3.6. Figure 6.19 presents cooling rate values obtained for the entire experimental campaign.

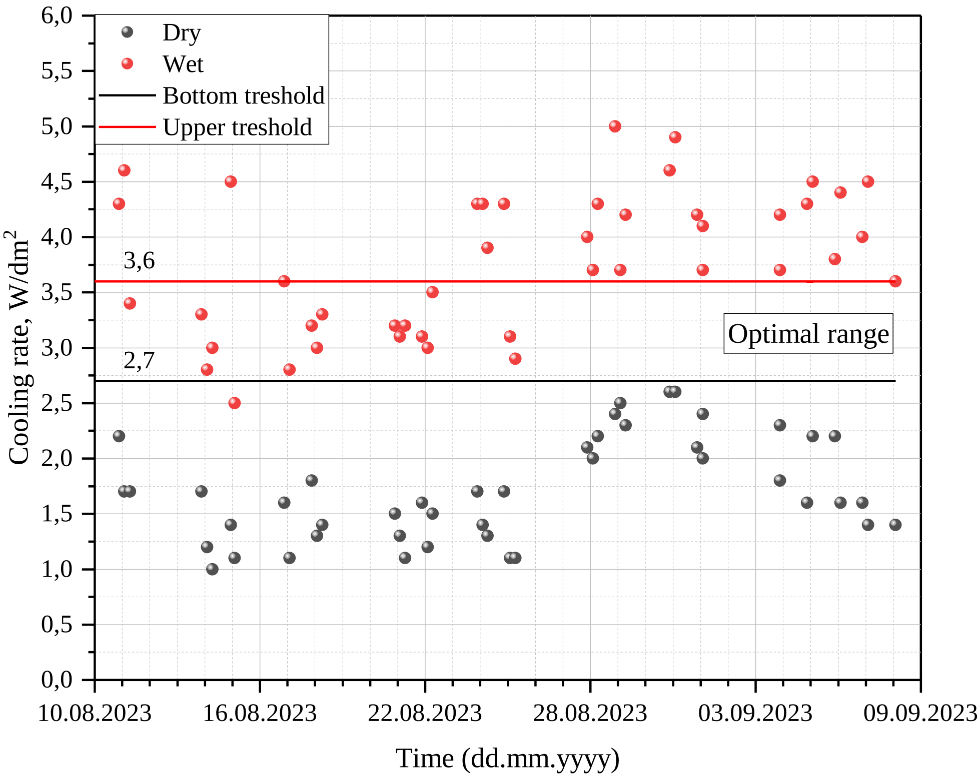

Figure 6.19. Cooling rate measured with wet and dry katathermometer within experimental campaign from 12.08.2023 to 07.09.2023 (plus two days before and after the considered experimental period) with marked optimal range.

If we consider only convective heat losses, the thermal load connected with the barn's environmental conditions was too high to cope with by the examined animals. On the other hand, adding evaporative heat losses changed significantly that relation exceeding the upper values, which suppose conditions of too intensive cooling. However, assessment of the evaporative heat losses mainly applies to the barns equipped with a system of sprinklers, which results in wetting the entire surface of the animal body. Such a state of wetting is not possible to occur as a result of the active sweating process only. Although, for the conducted study only dry measurement is applicable, results obtained with the wet method, illustrate limitations of the available systems based on the open water cycles such as sprinkles, which cannot adapt to animals' needs by fluent regulation of the transferred heat. In this perspective, the developed solution based on the cooling water mattress is highly perspective for precisive farming.

Water mattress cooling effect in real barn conditions

Likewise in a previous year, the cooling effect of the water mattress in the experimental campaign 2023 was evaluated using inlet and outlet temperature from the water mattresses and their surface temperature. However, in this campaign measurement of the chilled water temperature inside the water mattress provided essential information about the mattresses' water temperature distribution. Furthermore, the heat transfer conditions were assessed, especially when the cyclical operation mode of the mattress was applied. In this section of the presented PhD thesis, a complete study of those parameters will be presented.

The chilled water temperature at the inlet and outlet of both cooling water mattresses is presented in Figure 6.20. During continuous operation mode, mattresses worked simultaneously, which can be observed as the same trend in the aforementioned graphs. Its stable character within three chilled water temperature setpoints 16°C, 13°C, and 19°C proved proper operation of the extended experimental setup.

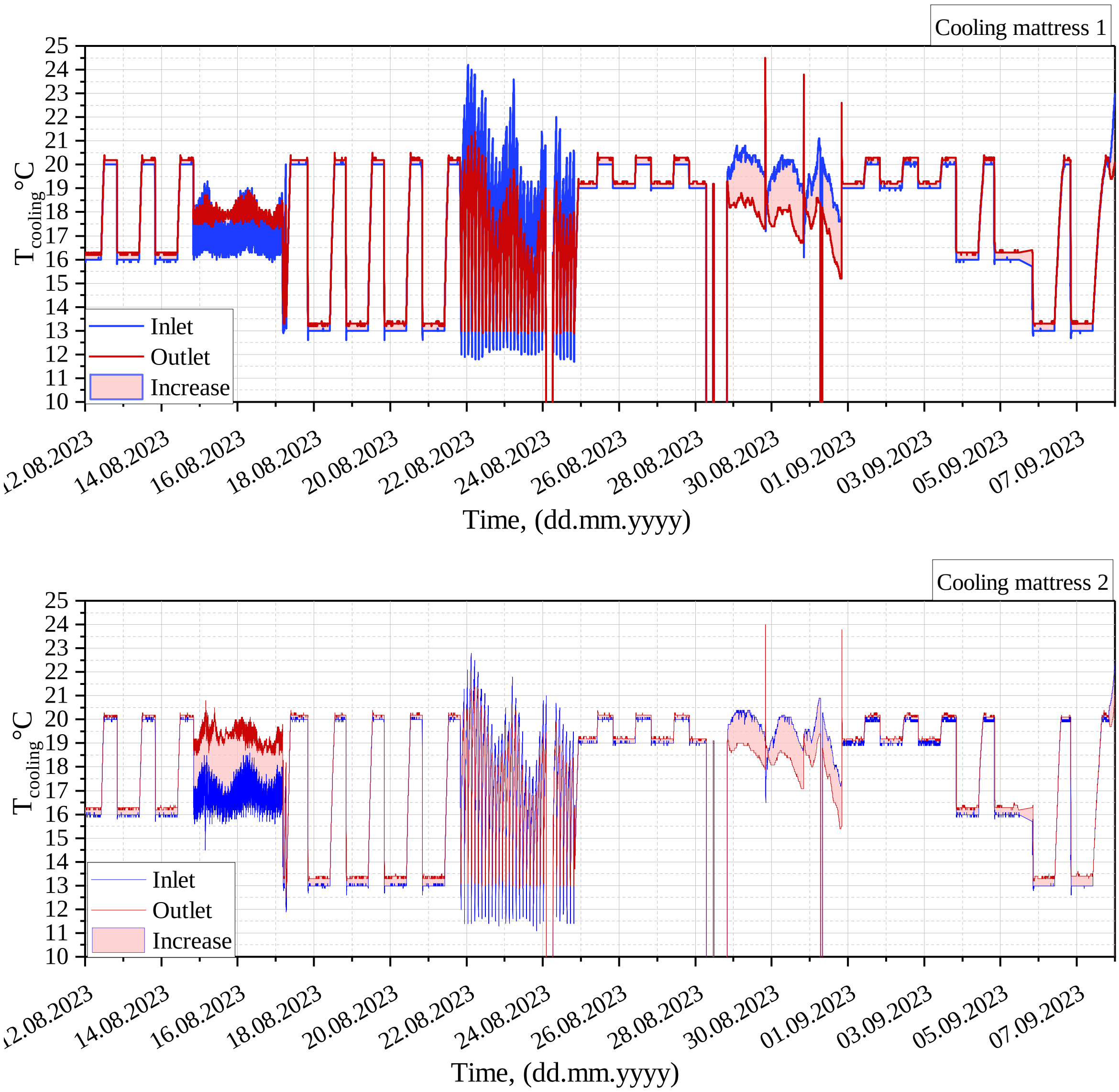

Figure 6.20. Inlet and outlet temperatures measured for both cooling water mattresses during the experimental campaign in 2023.

However, the cyclical operation mode indicates the independence of cooling water mattresses correlated with the applied algorithm based on the comparison of the mattress' outlet temperature with the chilled water temperature setpoint plus 1°C of the increase, deciding when to turn on the circulation pumps. That is why, the inlet temperature periodically dropped below the setpoint - when regulation was based on the outlet temperature. The inlet temperature was defined by the chilled water temperature supplied from the cold storage tank. It needs to be highlighted that due to hydraulical reasons the entering and leaving temperature sensors were located in the supply and return mattress pipes of the cooling system, respectively, and for that reason, their indication when the pumps were turned off, was highly influenced by the environmental conditions and small water volume within the pipe. To assess fully this operation mode, the average temperature inside the water mattress was also analyzed and presented in Figure 6.21. The cyclical operation applied for chilled water 16°C temperature setpoint was based on the first algorithm, in which pumps' deactivation period was only 10 min, and the decision-making process was based on the inlet temperature which was changed during the experiments. Applied further modifications, shifted operation to the outlet temperature continuous monitoring, and prolongate deactivation period, to be sure that the chilled water temperature setpoint among the entire mattress was achieved. For that reason, these data are presented in Figure 6.21 b for illustration purposes and not further analyzed.

Analysis of the results for the experimental series with a 13°C chilled water temperature setpoint provides exemplary data with the expected trend for the newly applied operation mode. It can be observed that within each 2h when pumps were turned off, the temperature inside the cooling water mattresses increased by 2-3°C for Zuzia's mattress and 3-4°C for Fruzia's mattress, maintaining properly their cooling effect on the animals (c.f. Figure 6.21 a). However, such a trend occurred both during the day and night. It needs to be considered that diurnal increase was more conditioned by high environmental conditions. Contrary to the nocturnal increase, occurring when animals rest in a lying position for a longer period.

In the experimental series with a 19°C cooling water temperature setpoint, the algorithm for the operation in this mode was not well adapted to the narrow difference between temperature setpoint and environmental conditions. Temperature measured at the outlet was used to activate the pumps. Furthermore, due to the bigger diameter at the outlet, which resulted in a greater volume of water, the temperature was naturally lower than at the inlet. As a result, pumps were activated only at 8:00, reacting to the temperature decrease, instead of an increase, visible in Figure 6.21 c, as the rapid peak of outlet temperature. However, such an operation provided interesting data, about the heat transfer between the animal and the water mattresss' surface and therefore for the chilled water, and the thermal inertia of the mattresses within 24h without water flow.

Due to the similar environmental conditions to the chilled water temperature setpoints, an influence of the air temperature in the water heating up process was limited to the ambient temperature highest value of 20°C (c.f. Figure 6.12). In Figure 6.21 c can be observed, that the temperature inside the water mattress first increased rapidly to the value of 20-21°C, which may be correlated with both factors, striving for balance with the environment, and animals lying down in the morning hours. Further temperature increase was correlated with the heat transfer from the animal, the visible peaks of temperature indicate the cow's resting periods. Between 2:00 and 8:00, when animals were lying down for the longest time, the temperature increased by around 2°C, achieving 24-25°C. Such observation indicates intensive heat transfer between the animal and chilled water.

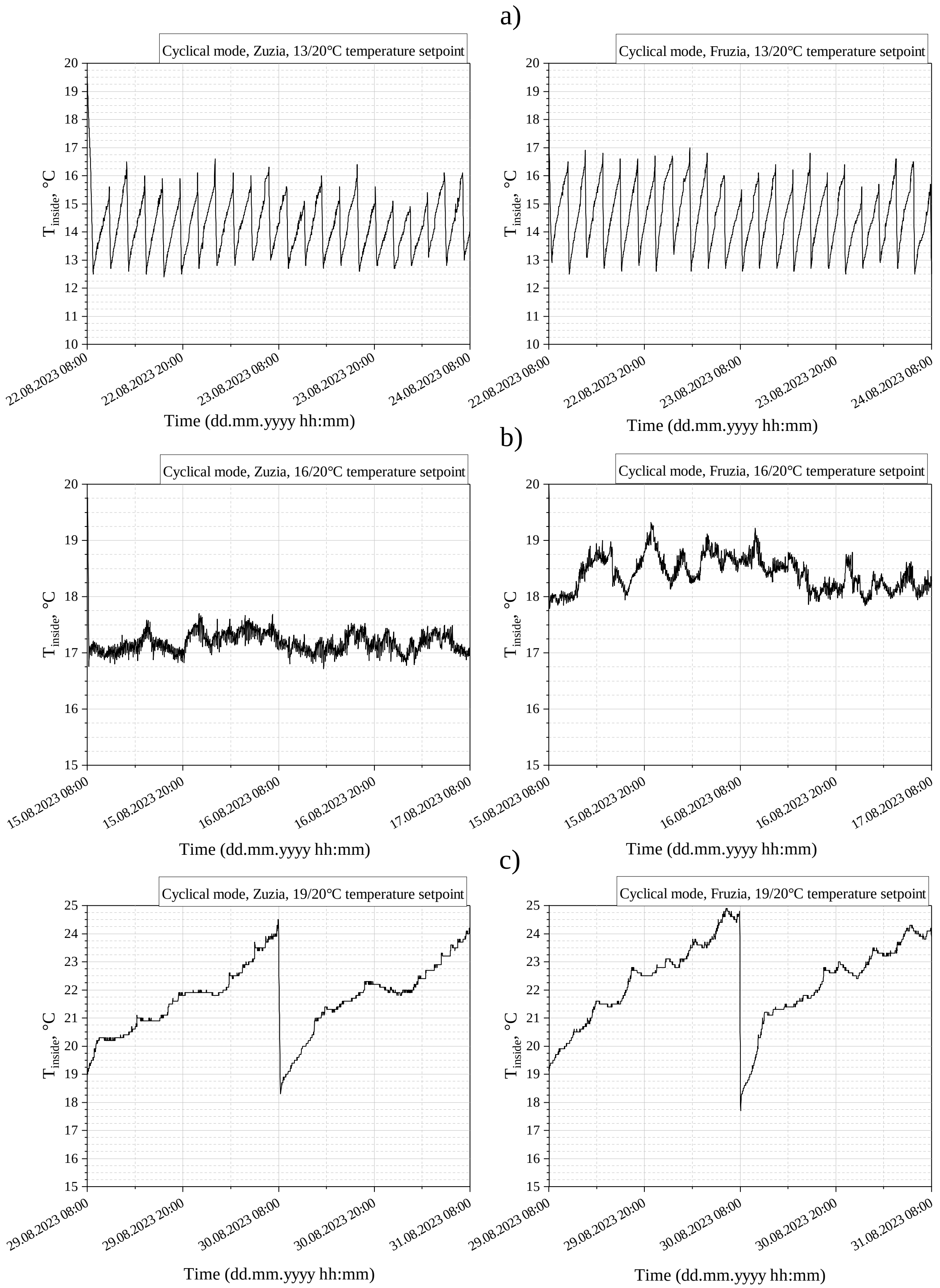

Figure 6.21. Average temperature of the chilled water inside both water mattresses within cyclical operation mode of for: a) 13°C, b) 16°C, c) 19°C chilled water temperature setpoints.

It leads to the conclusion that the cyclical operation mode could be a profitable solution in terms of the future analysis of electricity consumption. However, such a solution needs a universal algorithm properly adapted to environmental conditions. Furthermore, the pumps' deactivation period is highly important to maintain a proper cooling effect of the mattress, due to its fast heating up and thermal inertia in contact with the environment.

To observe the water distribution inside the water mattress data from the thermocouples located inside the water mattresses were grouped into three experimental series 13°C, 16°C, and 19°C mattress' chilled water supply temperature setpoints working in a continuous mode and presented in Figure 6.22 and Figure 6.23. Line graphs show that the temperature among both water mattresses varied within ±1°C. However, observations made in the steady state before the experiments indicated differences in thermocouples' readings within the same range, which is also consistent with sensor indication error. In comparison with the stacked graphs it can be observed that the main trend of all temperatures maintained the same among both mattresses. Only T2 and T4 for Zuzia's cooling water mattress and T13 for Fruzia's cooling water mattress responded to the temperature changes crossing that range, which could be connected with local heating up, due to the mattress deformation by animal's hoofs and reduced thickness of the water pillow in that area. To conclude, the water distribution inside the water mattress was proved to be uniform in both water mattresses during all experimental period.

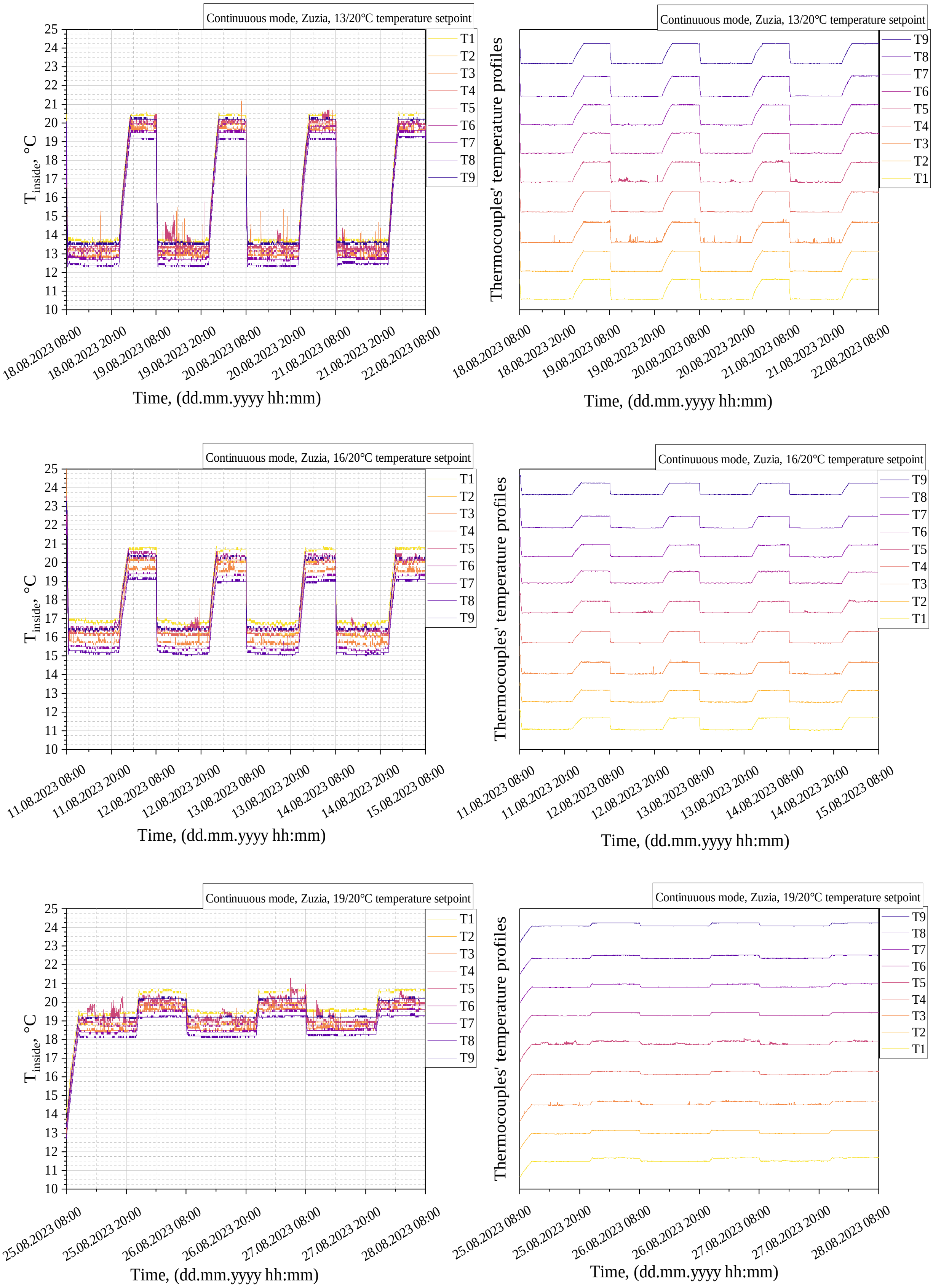

Figure 6.22. Temperature inside the first (Zuzia's) cooling water mattress during the experimental series with 13°*C*, 16°C, and 19°C chilled water temperature setpoints, on the right hand side as a stacked graph, on which each temperature profile is separately presented.

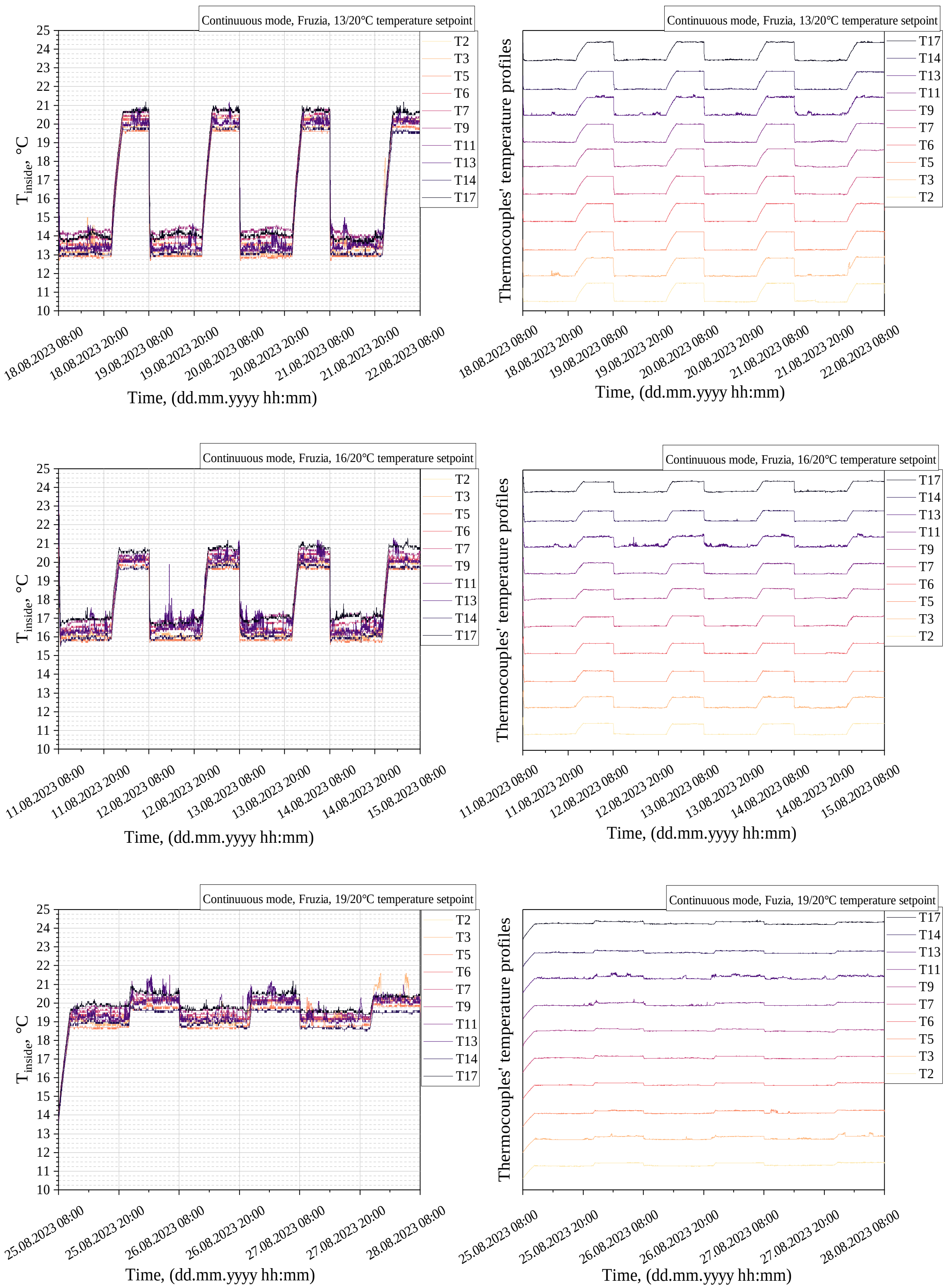

Figure 6.23. Temperature inside the second (Fruzia's) cooling water mattress during the experimental series with 13°C, 16°C, and 19°C chilled water temperature setpoints, on the right hand side as a stacked graph, on which each temperature profile is separately presented.

The last indicator of the mattresses' cooling properties was their surface temperature. The average surface temperature measured for both, the cooling water mattresses and non-cooled mattresses studied during all experimental series are presented in Figure 6.24. It can be observed that within all experimental series, the surface temperature of the cooling water mattress was significantly lower than the commercial non-cooled mattress, providing a cooling effect on the animals' bodies. The measured temperature of cooling water mattresses varied between 19°C and 22°C, achieving the highest temperature for the lowest setpoint, which was tested within the hottest days. On the other hand, for the series with 19°C temperature setpoint conducted during the weather breakdown was at the stable level of 21°C. Similar relations but for higher temperatures can be observed for commercial non-cooled mattresses. Nevertheless, it should be highlighted that the water temperature inside the cooling mattresses was close to the previously selected setpoints, based on the measurement from the thermocouples presented in Figure 6.22 and Figure 6.23. This particular situation could be justified by the influence of both, the insulative properties of the rubber and environmental conditions, which leads to the heating up of the surface by hot air high and the film of liquids such as urine on it.

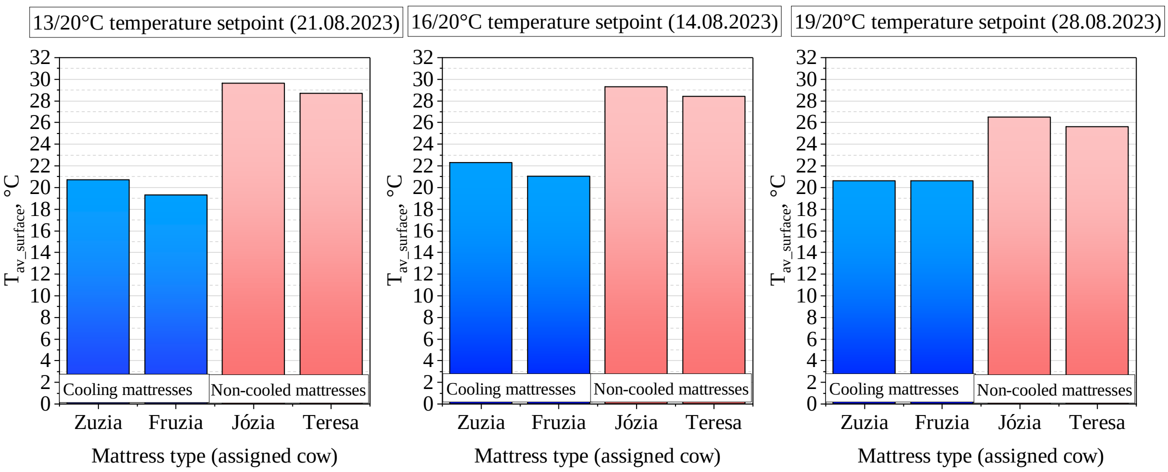

Figure 6.24. Average surface temperature of both, cooling and commercial mattresses, measured in the afternoon hours on the last day of the experimental series in 2023.

Thermal images taken for the same experimental days, presented in Figure 6.25 - Figure 6.28 indicate lower surface temperatures of all mattresses compared to the measurements taken with the thermometer. For the 13°C and 16°C chilled water temperature setpoints, the average developed water matress' surface temperatures were 2.4°C and 1.6/2.1°C (Fruzia/Zuzia) higher than the selected setpoints, respectively. Theoretically, such a relation indicates a less influencive effect of the insulative properties of the rubber and environmental conditions. However, the reverse relation was observed for the experimental series with a 19°C temperature setpoint, where the average temperature from thermal images was lower than the setpoint. Taking into account the mattress' interior temperature (c.f. Figure 6.27) such a result is rather unlikely. Considering the ambient temperature on that day, which was similar to the setpoint, such a result could be an effect of the narrow temperature difference between the environment and the object. To verify this theory, the analysis from the first day of the experimental series was also conducted, when the ambient temperature was higher. Results presented in Figure 6.28 indicate its validity. A similar challenge could occur for days with the higher ambient temperature and thermal images of the uncooled water mattresses. However, the influence of the liquid film and external particles on the mattress surface on both, measured temperature and mattress emissivity, which is difficult for precise estimation in a real barn environment, needs to be also taken into account. Nevertheless, both measurement methods highlight a significant difference between cooling and commercial (non-cooled) water mattresses.

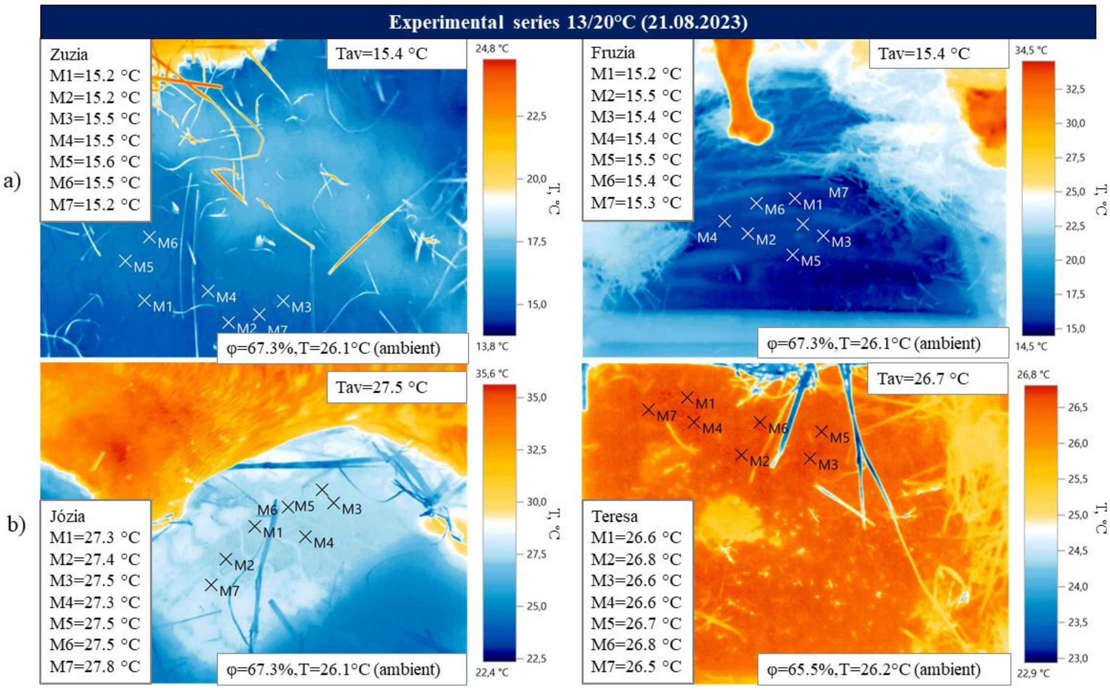

Figure 6.25. Thermal images of the water mattresses: a) cooling ones at upper images, b) reference ones (non cooled) on the bottom images, taken on the last day of the experimental series with 13°C chilled water temperature setpoint (21.08.2023).

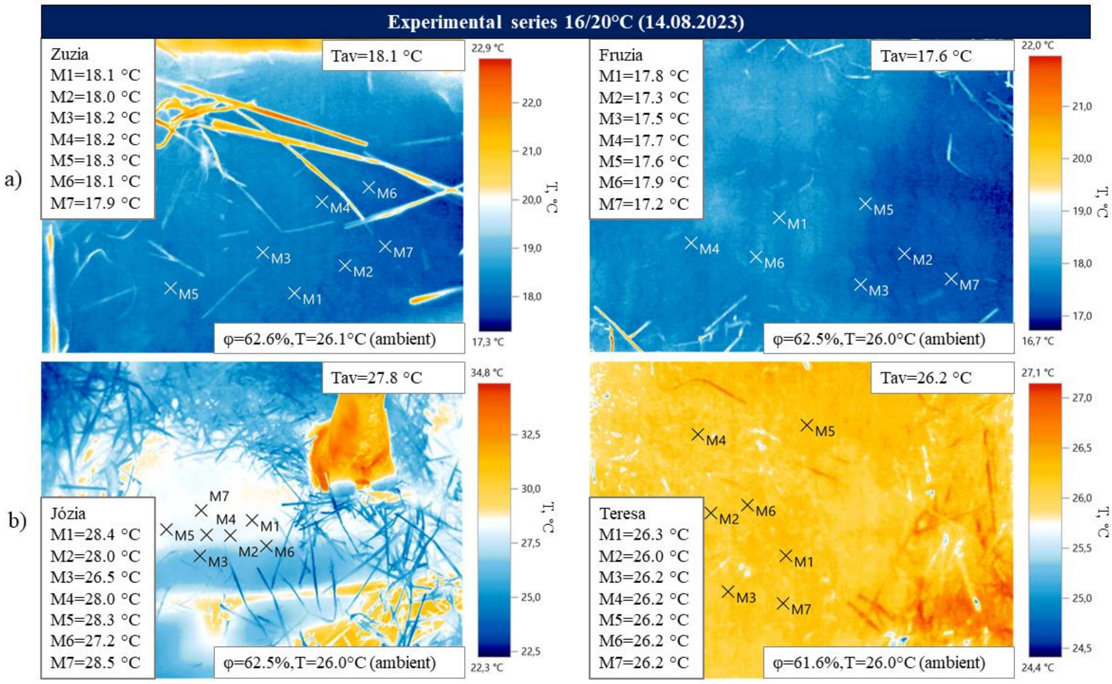

Figure 6.26. Thermal images of the water mattresses: a) cooling ones at upper images, b) reference ones (non cooled) on the bottom images, taken on the last day of the experimental series with 16°C chilled water temperature setpoint (14.08.2023).

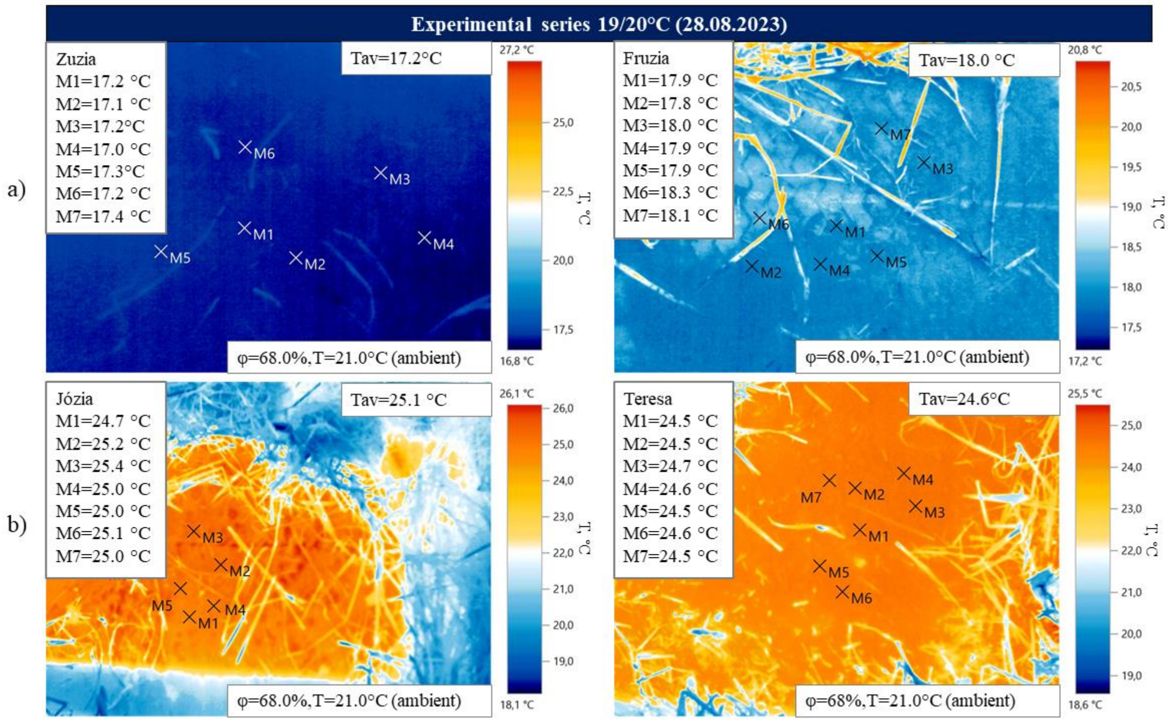

Figure 6.27. Thermal images of the water mattresses: a) cooling ones at upper images, b) reference ones (non cooled) on the bottom images, taken on the last day of the experimental series with a 19°C chilled water temperature setpoint (28.08.2023).

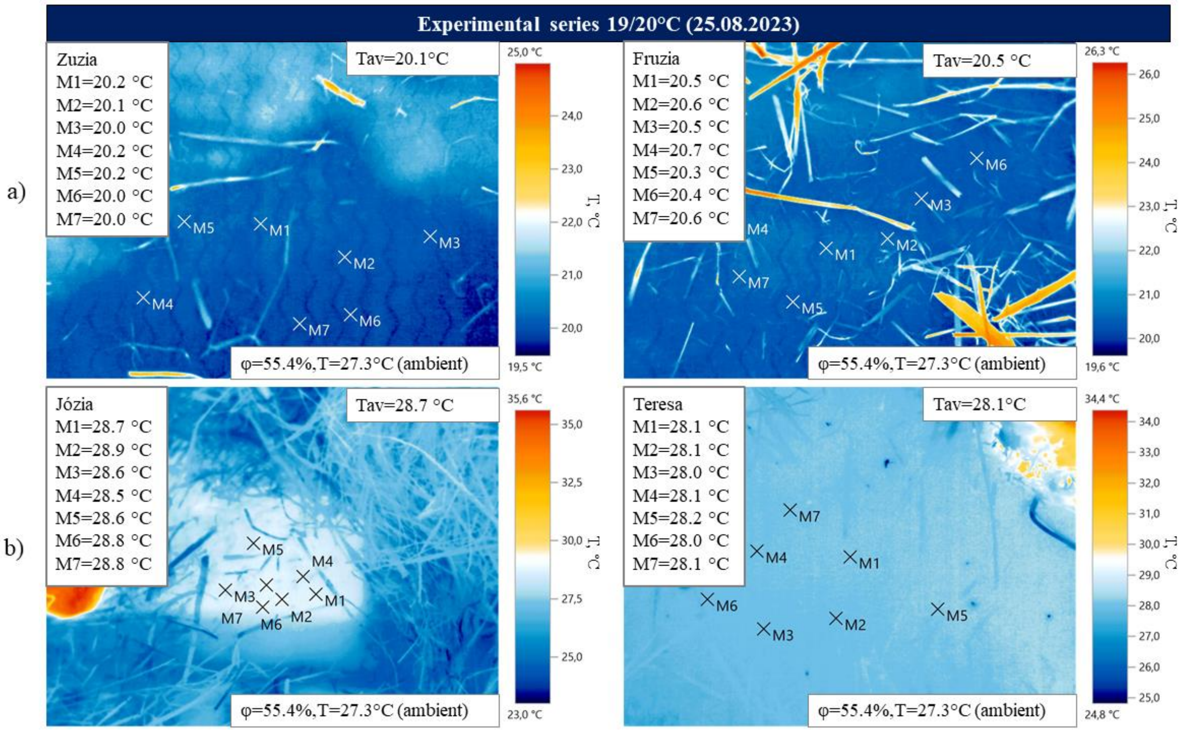

Figure 6.28. Thermal images of the water mattresses: a) cooling ones at upper images, b) reference ones (non-cooled) on the bottom images, taken on the first day of the experimental series with a 19°C chilled water temperature setpoint (25.08.2023).

Animal's response to conductive cooling – IR thermography

Similarly to the previous experimental campaign, the direct cooling effect of the developed mattresses on animals' bodies was investigated by IR thermography. The sequence of thermograms with 30 s sampling period was taken after animals got up from their beddings.

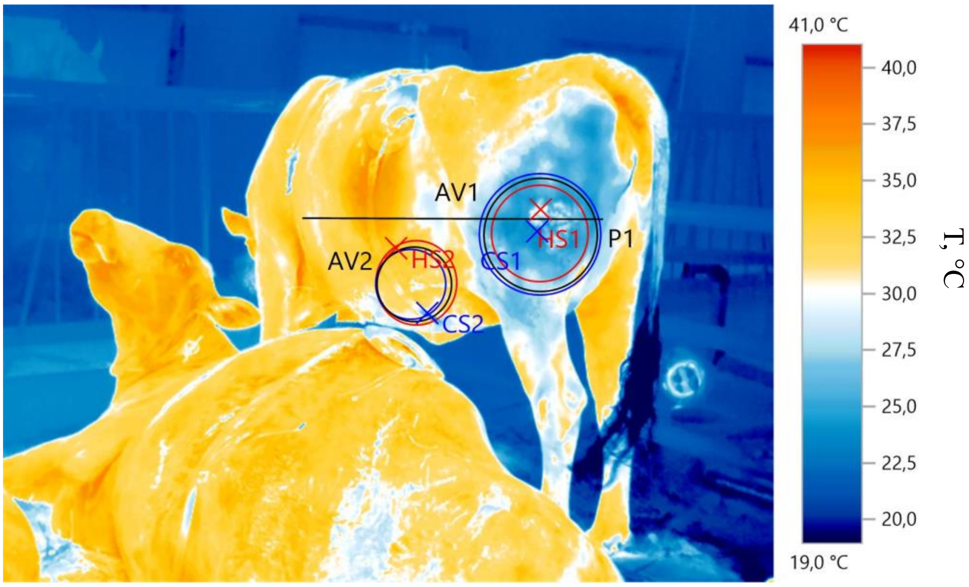

Figure 6.29. IR thermography for cooled cow (Zuzia) after getting from her bedding during the experimental series with 19°C chilled water temperature setpoint (28.08.2023).

The exemplary thermograms for the cooled cow (Zuzia) and non-cooled cow (Józia) with considered regions of analysis are presented in Figure 6.29 and Figure 6.30, respectively.

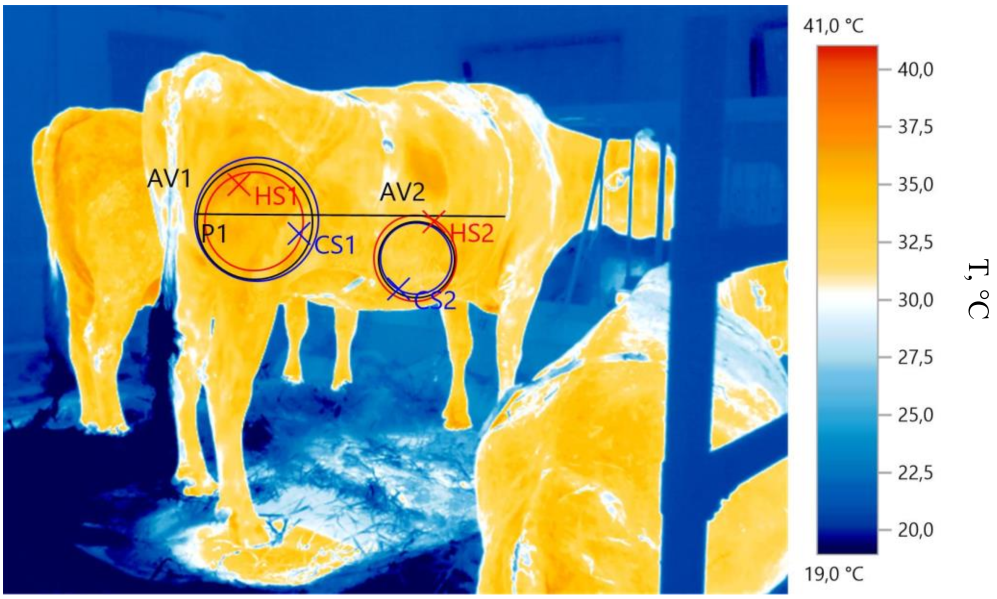

Figure 6.30. IR thermography for non-cooled cow (Józia) after getting from her bedding during the experimental series with 19°C chilled water temperature setpoint.

Furthermore, in Figure 6.31 the temperature distribution among animals' bodies from both thermograms (P1 line) is presented.

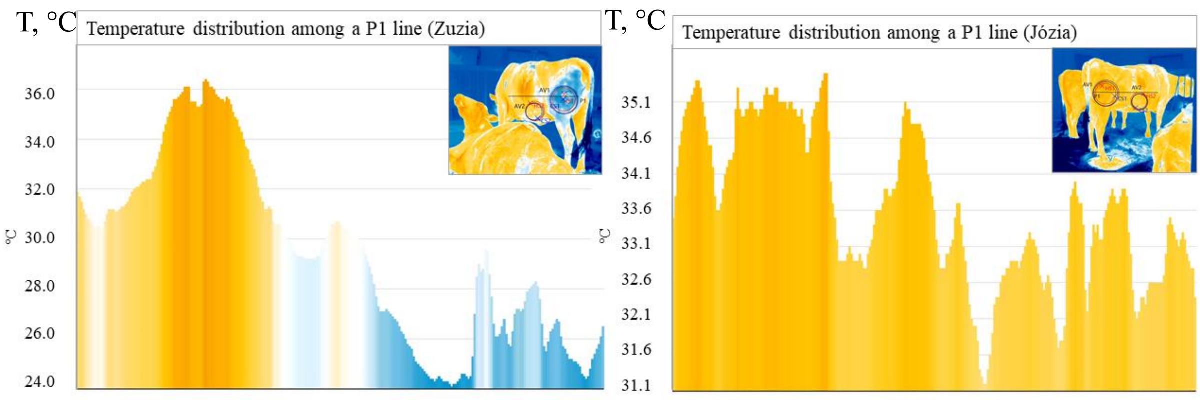

Figure 6.31. Temperature distribution among the P1 lines (from the front leg toward the thigh) from Figure 5.39 and Figure 5.40.

The results of average temperature in the thigh and abdomen regions for the 3rd day of the experimental series with 13°C, 16°C, and 19°C chilled water temperature setpoints working on continuous mode are presented in Figure 6.32 and Figure 6.33, with fitting analysis in Table 6.7 and Table 6.8, respectively. It can be observed that for the abdomen regions, the difference in skin temperature between animals is narrow, changing in the range of 2°C, with no direct recognition of the cooled cows. Such an effect could be caused by positions taken by animals. The abdomen region visible on the thermograms is taken from the side, which was only partially cooled down by the mattresses' surfaces. Furthermore, results for the experimental series with a 19°C temperature setpoint are characterized by lower skin temperatures, due to its realization during colder days, when convective heat losses are reduced by restricted surface blood circulation. Considering the results for the non-cooled cows, the influence of the location of all cows needs to be highlighted. Józia was lying in the middle of two cooled cows, which influenced the thermal conditions around her, by increasing the thermal load and reducing air movement. Teresa on the other hand was lying alone on the opposite side, giving her space for cooling within air movement, which was reflected in her lower skin temperature.

Analyzing results for the thigh region within the experimental series it can be observed that the cooling effect of the developed mattresses was the lowest for the 13°C water temperature setpoint. According to the results achieved in the experimental campaign of 2022, high skin temperature recorded by IR thermography could be caused by intensive blood circulation, and that delay in thermography recording, which was due to the simultaneous getting up of the animals could result in missing first minutes with the lowest temperature of the tissues. The most intensive cooling effect on the other hand can be observed for Zuzia's mattress and 16°C of the chilled water temperature setpoint, where temperature achieved 26°C at the beginning of the process, and increased within the next 10 min to 31°C, being below the skin temperature of non-cooled cows. Although a similar relation can be observed for the 19°C chilled water temperature setpoint, the ratio of that increase is lower in that case, and temperatures of both, cooled and non-cooled cows became the same at the end of the considered period. A similar tendency was observed in the experimental campaign of 2022, when the monitored skin temperature increased from 26 to 28°C within 5 min from animals getting up. However, a different characteristic is observed for the second cooled cow – Fruzia, for which skin temperature achieved values similar to the non-cooled cows. The reason for that difference could be in her enlarged space for lying down, which crossed the area of the cooling mattress, due to her location in the barn, as well as the irregular thickness of the straw layer on mattresses' surfaces.

Assuming the results obtained first cooled cow (Zuzia), being the reference one, and considering the cooling effect of the developed water mattresses, the observations are in alignment with the results obtained in the experimental campaign of 2022. They indicated that the chilled 13°C cooling water temperature setpoint is too low for high ambient temperatures, and the 16°C setpoint seems to be the most preferable in terms of animal thermal comfort for such an environment. However, the 19°C setpoint also resulted in a significant cooling effect, even during colder days. Theoretically, it could be beneficial in terms of both, cooling effectiveness and reduction of electricity consumption of the entire chilled water production and distribution system, during hot days, which could be a good direction for further research.

Table 6.7. Fitting analysis for the results presented in Figure 6.32.

Graph			**a) abdomen area**			**b) thigh area**		
Fitting			y=a+b·x			y=a+b·x		
Setpoint, mattres type and cow:			a	b	R^2	a	b	R^2
13/20°C	Cooling	Fruzia	33.9	0.13	0.84	33.1	0.24	0.83
	Non-cooled	Józia	34.8	0.02	0.02	36.1	-0.15	0.73
	Cooling	Zuzia	34.8	-0.05	0.29	34.1	0.10	0.46
	Non-cooled	Teresa	32.0	0.14	0.42	32.6	0.20	0.81
16/20°C	Cooling	Fruzia	35.6	-0.07	0.35	32.6	0.34	0.59
	Non-cooled	Józia	35.3	0.04	0.02	33.9	0.09	0.28
	Cooled	Zuzia	33.8	0.07	0.19	26.2	0.51	0.94
	Non-cooled	Teresa	34.2	0.10	0.58	33.9	0.06	0.16
19/20°C	Cooling	Fruzia	33.4	0.06	0.22	33.5	-0.10	0.45
	Non-cooled	Józia	32.8	-0.04	0.11	33.9	-0.20	0.59
	Cooling	Zuzia	32.2	-0.01	0.00	27.5	0.50	0.85
	Non-cooled	Teresa	32.3	-0.05	0.15	31.6	0.08	0.31

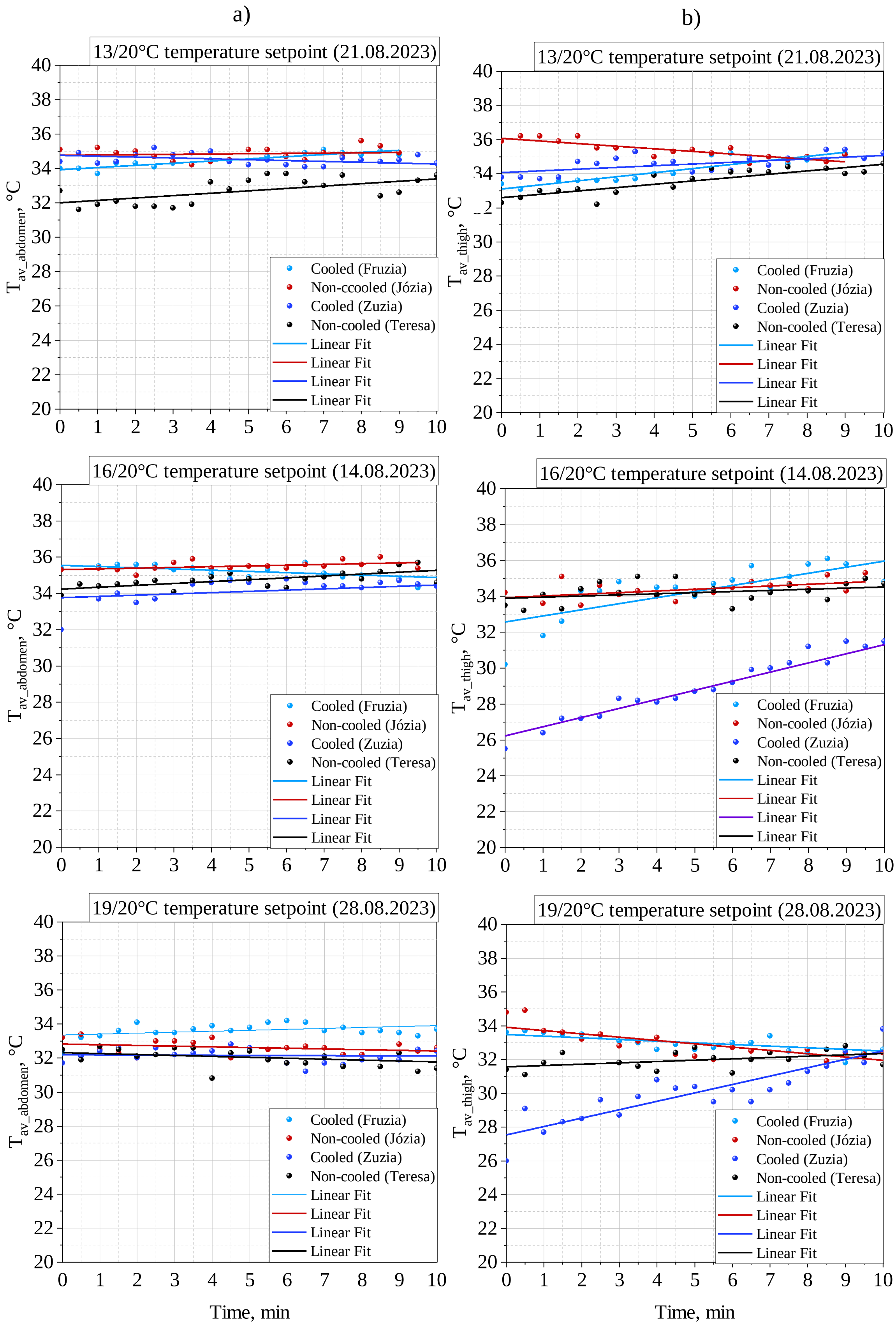

Figure 6.32. Skin temperature in the a) abdomen and b) thigh area of each examined cow within 10 min from their getting up recorded by IR thermography on the 3rd day of the experimental series conducted in 2023 with 13°C, 16°C, and 19°C chilled temperature setpoints.

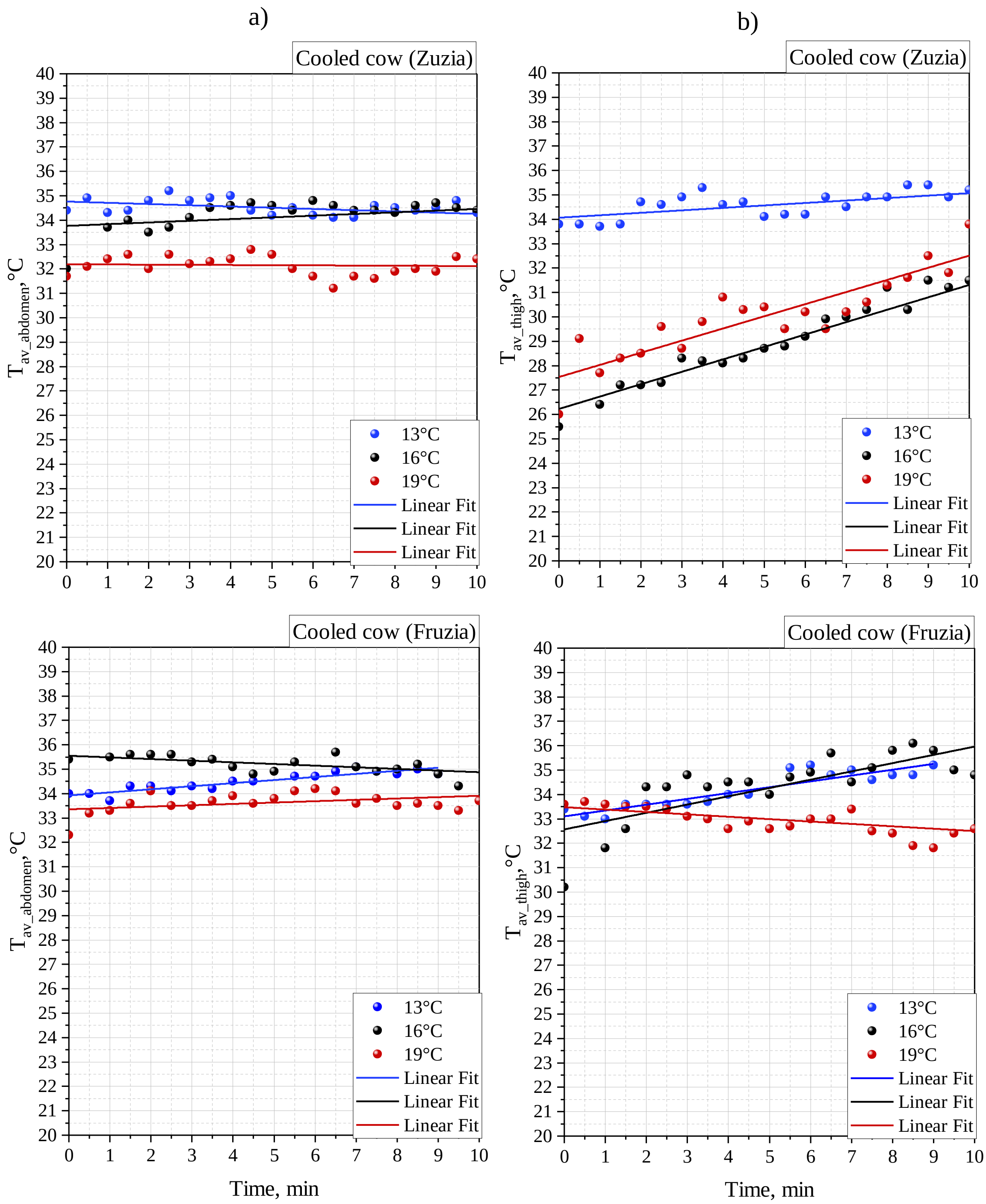

Figure 6.33. Results of the IR thermography for cooled cows (Zuzia and Fruzia) in the: a) abdomen and b) thigh area compared within chilled water temperature setpoints of 13°C, 16°C, and 19°C during experimental campaign of 2023.

Table 6.8. Fitting analysis for the results presented in Figure 6.33.

Graph		**a) abdomen area**			**b) thigh area**		
Fitting		y=a+b·x			y=a+b·x		
Cow	**Setpoint**	a	b	R^2	a	b	R^2
Zuzia	13°C	34.8	-0.05	0.29	34.1	0.10	0.46
	16°C	33.8	0.07	0.19	27.5	0.50	0.85
	19°C	32.2	-0.01	0.00	26.2	0.51	0.94
Fruzia	13°C	35.6	-0.07	0.39	33.1	0.24	0.83
	16°C	33.9	0.13	0.84	32.6	0.34	0.59
	19°C	33.4	0.06	0.22	33.5	-0.10	0.45

Animals physiological reaction – core body temperature

The experimental campaign of 2023 provided a new perspective for the applied cooling solution by the assessment of animals' thermal comfort within their physiological reactions. Main indicator of experienced by cattle heat stress is a core body temperature, which may vary in terms of the biological location being monitored and applied for this purpose instruments. In this study three different measurements were conducted, the rumen temperature, manual measurement of the rectal temperature, and the core body temperature, as the innovative, non-invasive approach, being an interesting perspective in terms of the future farming technology. In this section of the presented PhD thesis discussion of the gathered data will be presented.

Rumen temperature of three studied cows: Zuzia and Fruzia lying on the cooling water mattresses, and Józia lying on the non-cooled commercial water mattress, during experimental series with 13°C, 16°C and 19°C chilled water temperature setpoints for the continuous mode of mattresses' operation is presented in Figure 6.34. Due to the research activities of Wroclaw University of Environmental and Life Sciences, the rumen temperature sensors were already installed and working for three cows, when experiments started. The fourth cow – Tereska was not covered by this monitoring system, and therefore she is excluded from the presented results.

The location of the applied sensors in the rumen is the reason for its sensitivity to the changes in the temperature caused by the water intake. For that reason, the producer developed an algorithm, which recognizes the water intake periods and recalculates the temperature with that consideration. Such a temperature is presented in Figure 6.34. Line graphs present detailed temperature distribution in considered experimental series for each examined cow, and stacked graphs present each trend separately relative to the 39°C temperature threshold. Cattle can regulate its core body temperature from 38°C to 39°C with a mean value of 38.6±0.5°C [83] for that reason 39°C was selected as the threshold, informing when thermoregulation processes are not sufficient for cow's heat relief. However, rumen temperature can be also influenced by the digestive processes, increasing its value up to 0.5°C [77]. Comparing the obtained using rumen sensors data with the manually measured rectal temperature data (c.f. Figure 6.35), it could be observed that measured values are lower and more dispersed around the mean value indicated in [83] which proved the influence of the mentioned previously factors. For that reason rumen temperature of each cow oscillates close to 39°C, being more stable in the nocturnal hours when both, digestive processes and drinking behaviours become less active during the resting period.

Investigating the relation between animals' rumen temperature within the experimental series, can be observed that the temperature of the non-cooled cow (Józia) was higher than the cooled ones (Zuzia and Fruzia). For the experimental series with the 13°C and 19°C of the chilled water temperature setpoints, that difference was narrow and could be an effect of the natural characteristic of the animal, related to its metabolism. However, for a series with the 16°C of the chilled water temperature setpoint, that rumen temperature difference became significant. Furthermore, the rumen temperature of cooled cows (Zuzia and Fruzia) was maintained below the threshold of 39°C, contrary to the non-cooled cow (Józia). Such observations indicated the 16°C of chilled water temperature setpoint as the most appropriate for the animal in terms of its thermal needs and active heat transfer with the developed cooling water mattress. Such a conclusion is in alignment with the observations made in the experimental campaign of 2022, described in Subsection 6.3.1 of this PhD thesis.

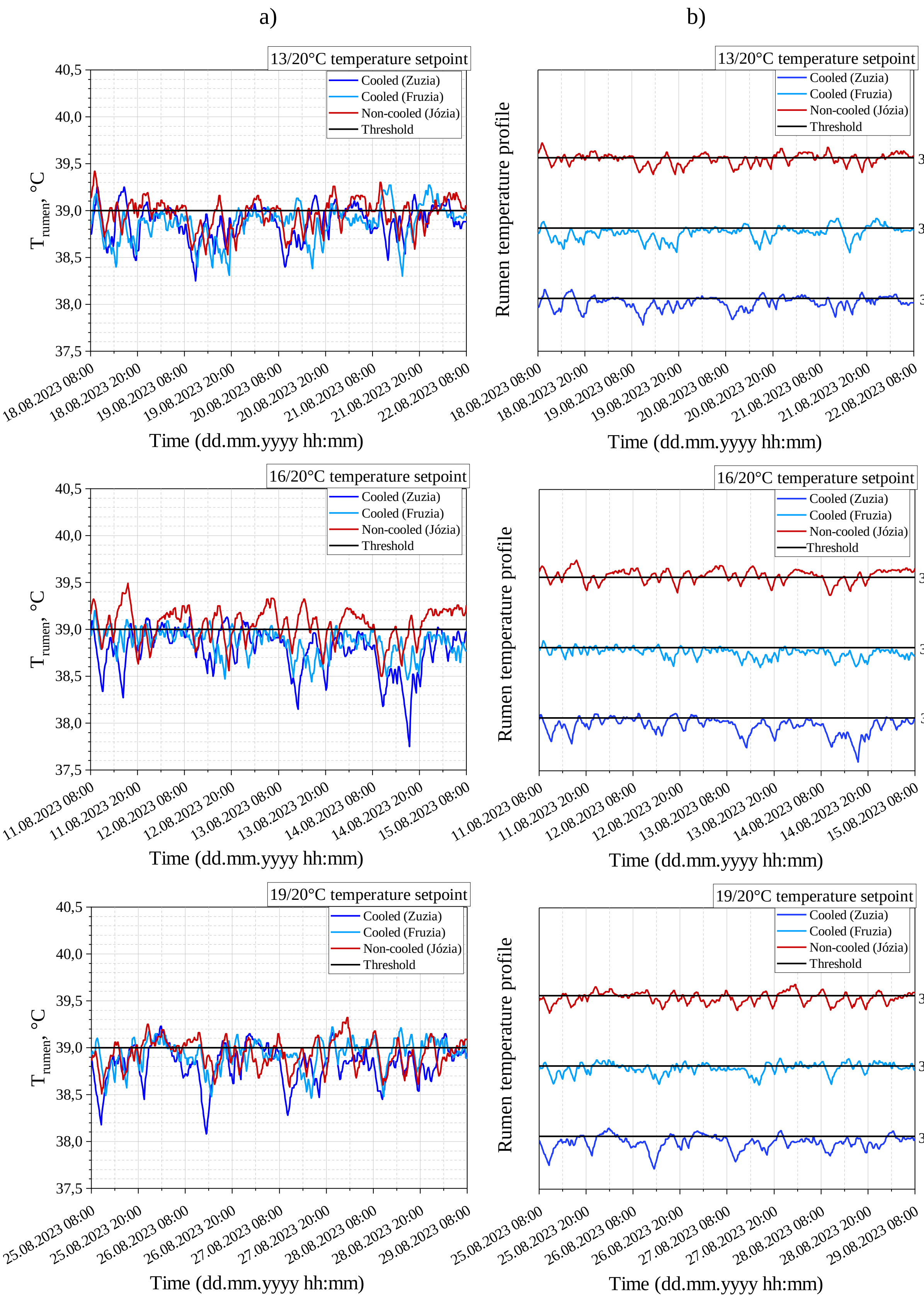

Figure 6.34. Rumen temperature recorded during experimental series with 13°C, 16°C, and 19°C chilled water temperature setpoints and the continuous mode of operation: a) line graph b) stacked graph with rumen temperature separately presented for each cow.

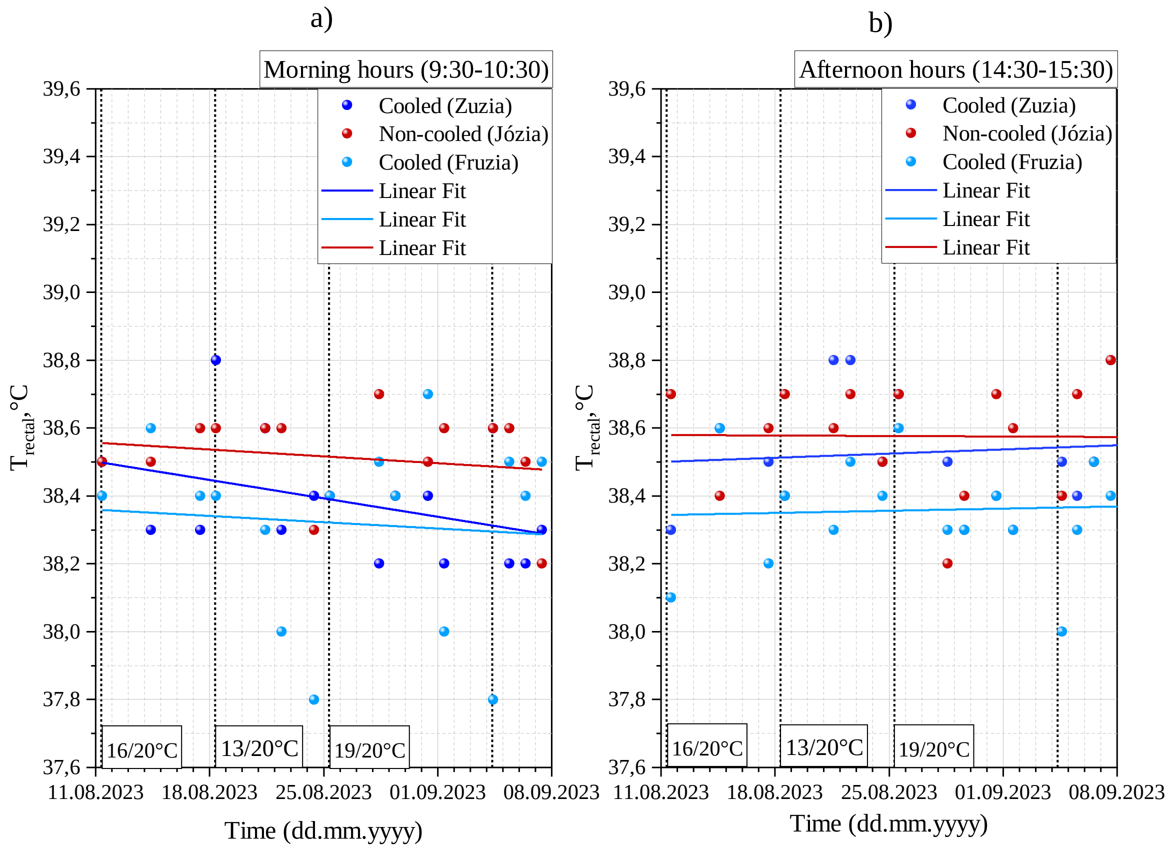

Figure 6.35. Rectal temperature during the entire experimental campaign of 2023 grouped to: a) morning and b) afternoon hours of measurement with marked (dot line) beginning of the experimental series with 13°C, 16°C, and 19°C chilled water temperature setpoints.

Table 6.9. Fitting analysis for the results presented in Figure 5.35.

Graph	**a) morning hours**			**b) afternoon hours**		
Fitting	y=a+b·x			y=a+b·x		
Cow:	a	b	R^2	a	b	R^2
Zuzia	19090.2	-7.7 E^{-3}	0.15	-4271.2	1.8 E^{-3}	0.01
Fruzia	6559.5	-2.7 E^{-3}	0.01	-2198.3	9.1 E^{-4}	0.00
Józia	7142.7	-2.9 E^{-3}	0.04	542.3	-2.1 E^{-5}	0.00

Rectal temperature was measured twice a day, in the morning and afternoon hours, for the first and last day of each experimental series. Data were grouped by time of the day, due to the influence of both, changes related to the natural daily cycle and differences in environmental conditions, and are presented in Figure 6.35. Linear fitting (with detailed parameters in Table 6.9) applied to the results from the entire experimental campaign, for both morning and afternoon hours, indicated higher rectal temperature for the non-cooled cow (Józia) than cooled ones (Zuzia and Fruzia) demonstrating the overall cooling effect of the developed cooling water mattress on animals body. A decreasing trend observed for all examined cows for the morning hours could be a result of decreasing nocturnal temperatures of the air and natural temperature changes in the menstrual cycle. On the other hand, an increasing trend for cooled cows for the afternoon hours could be an effect of changing diurnal chilled water temperature setpoints, which since 25.08.2023 til 04.09.2023 were maintained at 19°C. Furthermore, the experimental series with a 13°C chilled water temperature setpoint may affect the trend, due to the increased measured rectal temperature in those days, exceeding the current fitting. According to the observations from the IR thermography from both experimental campaigns, the 13°C chilled water temperature setpoint could be too low for the animal, resulting in changes in blood circulation, and limited convective heat losses to the environment. Simultaneously, the experimental series in 2023 with this setpoint was the period of a prolongate heat wave, which could exaggarated this effect.

Lastly, due to the constraints of the commercially available sensors for core body temperature continuous measurement, a new approach for its designation was applied. Measurement was based on the skin temperature measurement that will be described in the paragraph of this PhD thesis, and applied in the algorithm developed by the sensor's manufacturer, where the weight and activity of the user were the additional inputs. However, the target recipient of the sensor is a human being, which resulted in the limitation to 300 kg of body weight and selection of activities based on the sports categories. For that reason, all obtained results are characterized by the diminished temperature range. In Figure 6.36, the exemplary data for the experimental series with the 13°C chilled water temperature setpoint, are juxtaposed with the previously described rumen temperature. It can be observed that data recorded by CORE sensors are characterized by a higher range of variation, especially visible for the non-cooled cow (Józia). It is probably caused by a high susceptibility of the applied algorithm to the measured skin temperature changes, which will be presented in the next section in Figure 6.37.

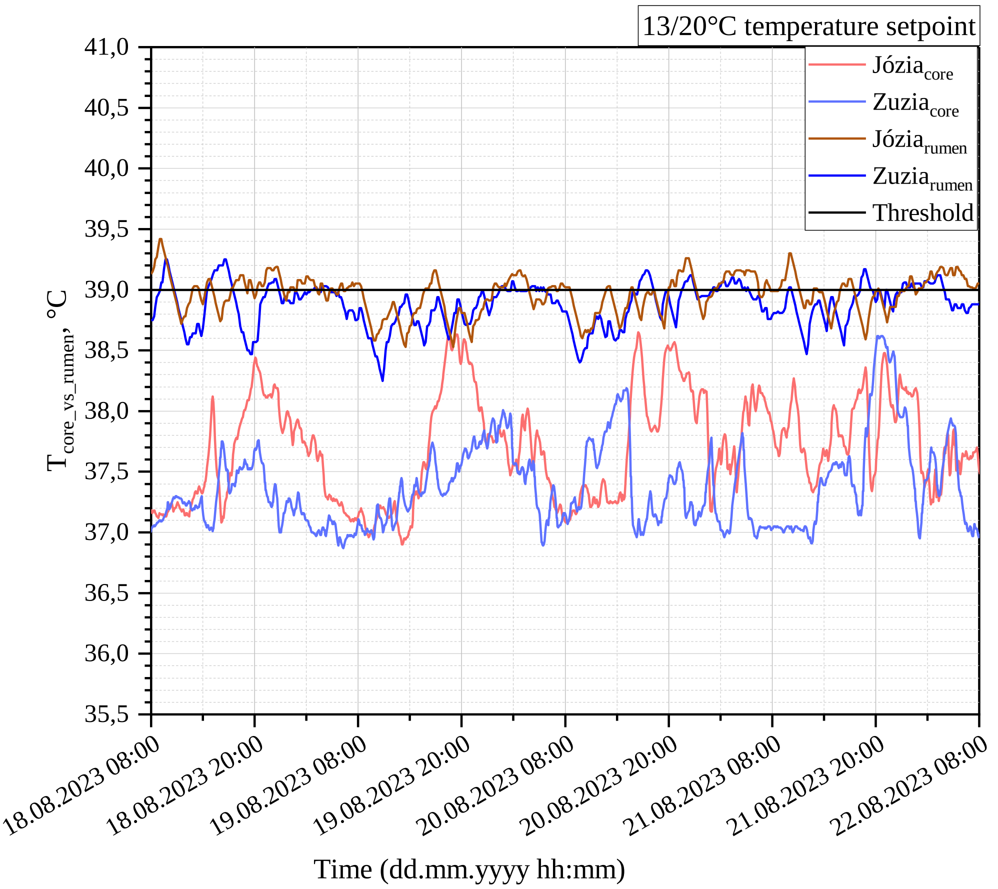

Figure 6.36. Core body temperature juxtaposed with rumen temperature for cooled (Zuzia) and non-cooled (Józia) cows, during experimental series 2023 with 13°C cooling water temperature setpoint and the developed water mattress' continuous operation mode.

Although obtained data are not directly used in the analysis, they highlighted the potential of that monitoring approach, especially in terms of the non-invasive character of that sensor, contrary to the commercially available solutions for the zootechnical sector. However, due to its innovative character for such an application, a separate study under the supervision of experts in the zootechnical field is required to fully asses the character of obtained data in terms of the temperature fluctuations and thermal balance of the animal. It may be a possible solution for future development in terms of its applicability in precisive breeding.

Animals physiological reaction – skin temperature

Another physiological reaction of the animal monitored during the experimental campaign of 2023 was its skin temperature. This parameter depends on the thermal regulation by the blood circulation system, and the density of the blood vessels in the considered region of the body, as well as environmental conditions. In the conducted experiments the previously described sensor was located on the left side of the body, over the front limb, close to the heart. Obtained data for experimental series with 13°C, 16°C, and 19°C chilled water temperature setpoints and continuous operation mode are presented in Figure 6.37. Due to the measurement disruptions, results for only one non-cooled cow (Józia), and one cooled cow (Zuzia) are compared. It can be observed that in diurnal hours skin temperature usually increased between 8:00 and 20:00, and decreased in nocturnal hours, achieving its drop around 8:00. A similar trend was observed for the barn's indoor air temperature. Such a relation indicates the correlation of the measured skin temperature with the ambient temperature, which influences the thermoregulatory mechanism.

For the 13°C chilled water temperature setpoint, the skin temperatures for both cows were very similar, and achieved their peaks around 35-36°C, which is the temperature range measured also in [84]. For a 16°C chilled water temperature setpoint, the trend for the cooled cow (Zuzia) became more irregular during the second day of the experiments, preceded by a large temperature drop for both cows, but achieving higher values than for the non-cooled cow (Józia). This tendency could suggest more active thermoregulatory processes connected with the heat transfer between the mattress and the animal. Diurnal temperatures achieved similar as in previous series values of 35-36°C. For the experimental series with 19°C chilled water temperature a decreasing tendency in skin temperature within experimental days can be observed, caused by changing environmental conditions before the weather breakdown. Its diurnal and nocturnal values became similar at the level of 33-34°C. It is an important observation in terms of the selection of chilled water temperature setpoint during colder days. Reduced skin temperature indicates lower cooling needs of the animal, and limited heat transfer between the cooling water mattress and animal body, due to the reduced temperature difference. Therefore, those days would be the most preferable for a cyclical operation of the cooling mattress. The local temperature peaks, outliing from the main trend for each considered experimental period could be connected with the rotation of the belt with the sensors in the way, that animal was lying on it, or being in contact with another cow, pressing sensor skin to skin. Nonetheless, in the general perspective the skin temperatures for cooled, as well as non-cooled cows were similar, and the influence of thermoregulatory processes connected with changes in blood circulation had rather local character, as the result of direct contact with the cooling water mattress.

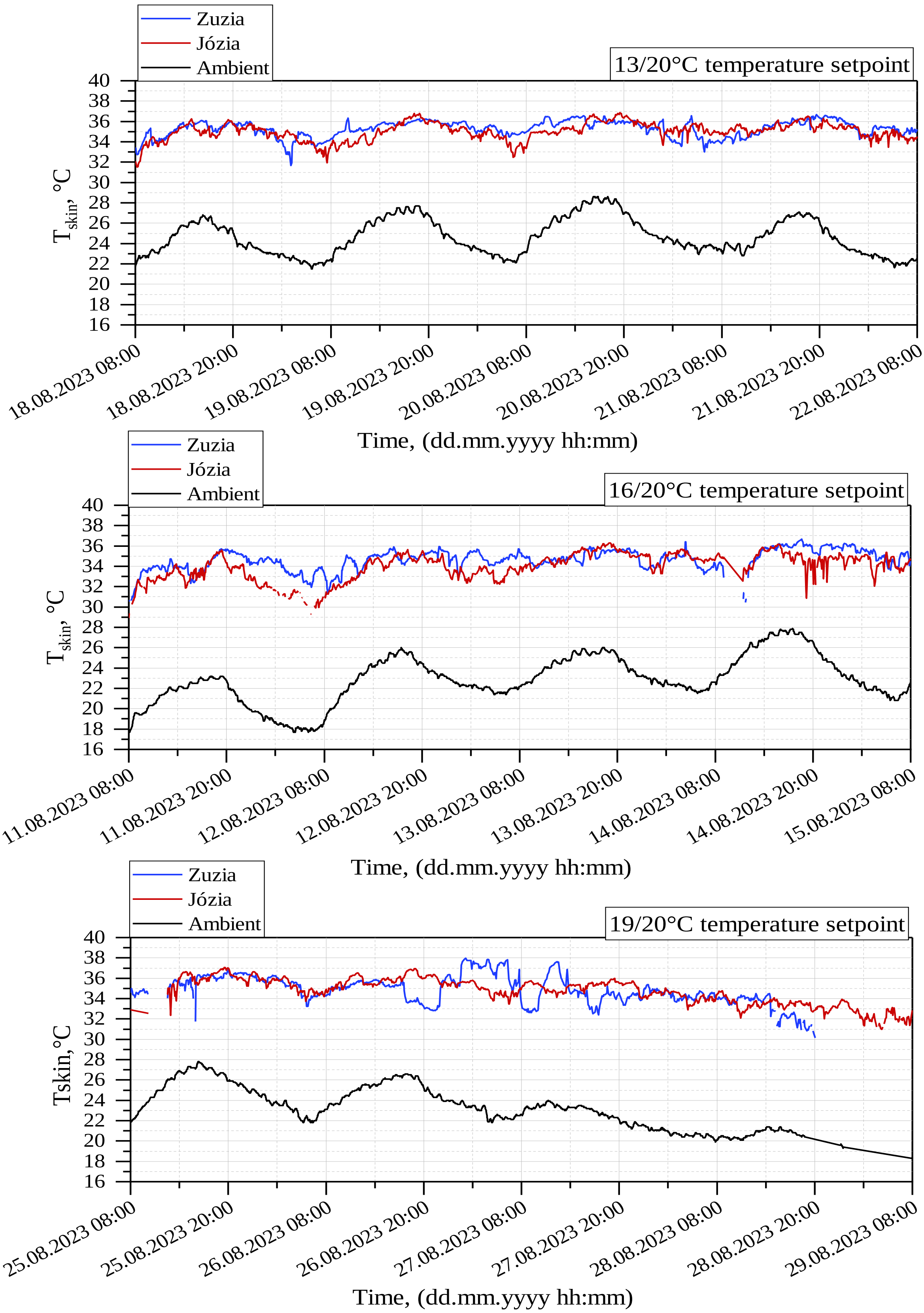

Figure 6.37. Skin temperature for cooled (Zuzia) and non-cooled (Józia) cows, as well as air ambient temperature, recorded during experimental series 2023 with 13°C, 16°C, and 19°C chilled water temperature setpoints, and the developed water mattress’ continuous operation mode.

The new approach for animals' skin temperature measurement applied within this PhD thesis indicated its potential for future development and application in precisive breeding. However, due to its novel character, more studies with improved measurement methodology are required to verify their accuracy. However, skin temperature regulation takes part in the first stages of animal thermoregulatory mechanisms, and for that reason, such a solution enabling ongoing monitoring could be especially useful in early heat stress detection.

Animals physiological reaction – heart rate

The stress reaction of the animal, including the heat stress can be also detected through the heart rate measurement. The usually applied method of assessing its value applies the stethoscope to listen and count the heart rate on the left-hand side of the cow's chest, behind the cow's elbow. However, this method enables only point measurement, which can be additionally disrupted by the presence of a humane. To measure the heart rate continuously, the heart rate sensor was applied and located in the mentioned previously area, which was described in Subsection 6.2.4. of this PhD thesis. Although each cow was monitored using a separate sensor, due to numerous technical obstacles, finally data from only one of them were saved (for the cooled cow Fruzia).

The heart rate value can vary depending on the animals' activity, and reaction to stress conditions, including the thermal regulation process activated under heat heat stress conditions. According to veterinary sources [85], for resting dairy cattle it can vary in the range of 48 and 84 beats per minute (bpm). Figure 6.38 presents data collected for the cooled cow (Fruzia) during the last day (14^{th} of August) of the experimental series of 2023 with a 16°C chilled water temperature setpoint. It can be observed that most of the recordings were within the indicated range. Although the afternoon hours were characterized by higher ambient temperature, especially that is was during the heat wave period, the measured heart rate was the most stable and within the natural range, during these hours. However, there are visible 20-40 min long intervals in the morning hours (marked with red frame in Figure 6.38), when the heart rate increased above 200 bpm. The recorded values are significantly too high for cattle, especially for the longer periods, which submit obtained data under careful consideration in terms of their usefulness. However, heart rate is a very susceptible parameter, which can be influenced by various elements from the environment, for that reason the careful study of the animal's behaviour and barn conditions, based on camera recordings would be advisable before determining the suitability of the data. For the presented in Figure 6.38 measurements, the behavioral recordings indicated that the increased above the threshold heart rate, ofently occurred when there was some interaction with the animal in their bedding areas, for example, due to the manual measurements, or correction of sensors' location. Furthermore, the social aspect between animals needs to be considered, as potentially influencing, due to their physical and emotional interactions. For the aforementioned two peaks above 200 bpm, the rectal temperature measurement and Inertia sensors' correction were observed, respectively to the order in which they appear.

Furthermore, due to signal disruptions, probably caused by drying out the sensor's surface, as well as moving it during cow's activity or loading with body weight, when the animal was lying, collected data are characterized by the measurement gaps observable in different time intervals. Major gaps for considered data are presented as the transparently red rectangles in Figure 6.38. Data gathered during other experimental days are characterized by even longer periods with no data acquisition, it varies among the days, especially when there was no possibility to monitor the measurement being present in the barn. The mentioned issues could also influence the quality of obtained data, especially during the nocturnal hours, when long periods with the heart rate measured above the mentioned threshold were also recorded. For that reason presented data are considered to be illustrative ones, in terms of the applied measurement method.

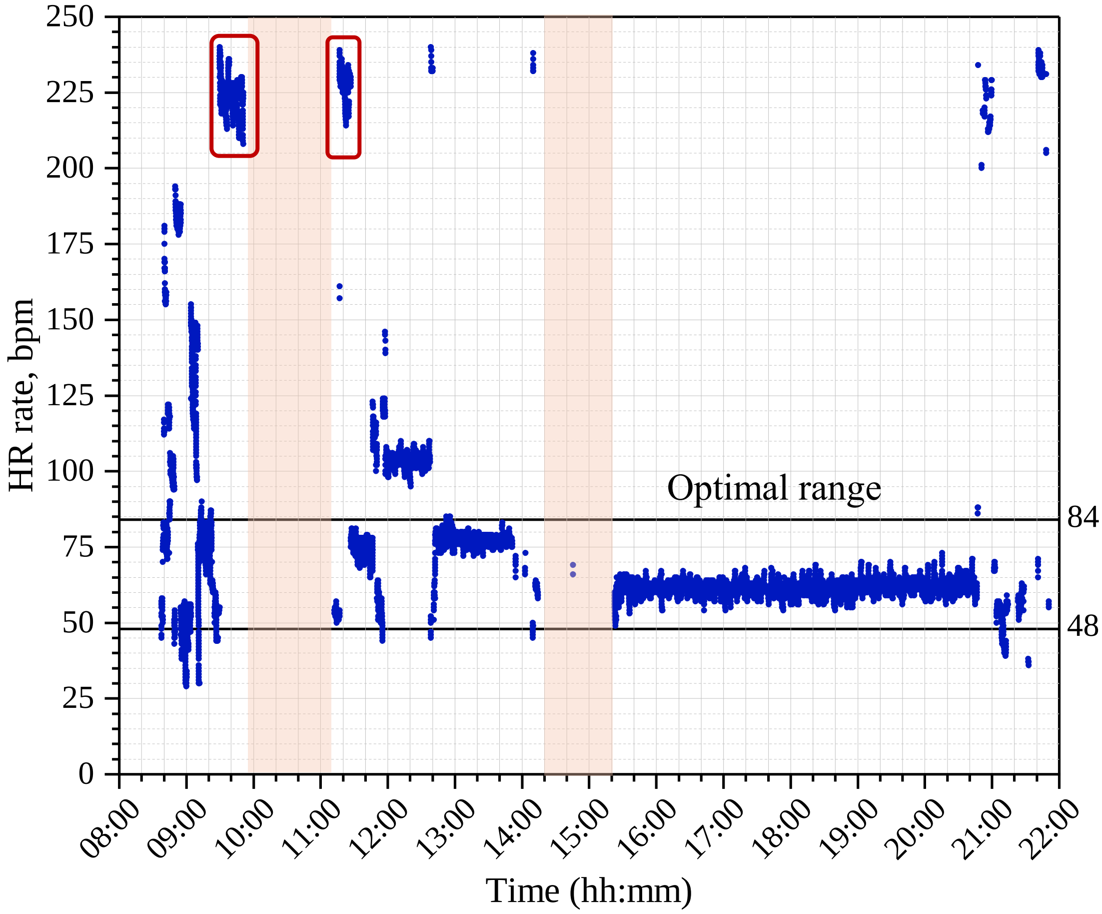

Figure 6.38. Heart rate measured for cooled cow (Fruzia), recorded during the last day (14th of August) of experimental series of 2023 with 16°C chilled water temperature setpoint, with two major measurement gaps marked with the transparently red rectangles.

It is worth mentioning that a similar application of the heart rate sensor was studied in [86], showing its potential in digitalized farming systems. However, this study considered a short-term measurement with a special focus on the method itself. Conducted in PhD this thesis study measurements, applied a similar approach in real barn conditions, revealing the challenges of its everyday use. Therefore, at this moment, its applicability is more adjusted to the research phase with a small number of examined cows, when the position of the sensor, and its wetting level can be monitored and corrected. Furthermore, the high susceptibility of this parameter indicates that such a study needs to consider a detailed behavioral analysis to assess the validity of obtained results, especially in the changing barn's conditions. Nevertheless, the proposed heart rate measurement is a promising approach that can be used for animals' ongoing observation, especially in terms of the early detection of the potential stressors, influencing their well-being including thermal stress.

6.3.4. Main conclusions from the experimental campaign of 2023

The main goal of the experimental campaign conducted in the summer period of 2023 was to investigate the operation of the water mattress in terms of the water distribution in its interior and its thermal inertia, as the continuity of the first campaign conducted in 2022. The network of the thermocouples in the mattress channel structure proved the uniform water distribution, achieving the chilled water temperature setpoint with ±1°C variation, during mattress operation in real barn conditions, which is a final confirmation of the developed water mattress design. Furthermore, the applied cyclical operational mode proved intensive heat transfer between the animal and the mattress' surface, and therefore the chilled water, increasing the water temperature between 2°C and 4°C during the 2h period of the pump's deactivation, still providing the cooling effect. Therefore, such a solution could be beneficial in terms of the entire chilled water production and distribution system's electricity consumption. However, the algorithm applied to such an operational mode needs to be properly adapted to the environmental conditions. Furthermore, the appropriately selected pump's deactivation sequence becomes crucial for water temperature control and cooling effect management.

The main focus of the conducted experimental campaign was oriented on the animal response to the cooling by monitoring the physiological reactions such as the core body temperature, the skin temperature, and the heart rate. Results of the conducted IR thermography indicated the 16°C, as the most preferable chilled water temperature setpoint in terms of animal thermal response, which was in alignment with results from the experimental campaign of 2022. Such a conclusion was also reflected by the results of rumen temperature, which reached the most significant difference relative to the non-cooled cow (Józia) for this setpoint. However, the 19°C setpoint could also have a profound effect, if applied during hot days, which is a potential direction of further research. The cooling effect of developed mattresses was also visible in measured rectal temperature, for which linear fitting was higher for the non-cooled cow (Józia). Although, the skin temperature was similar between both cows, due to the local cooling effect of the mattress, an important observation was the reduced skin temperature level achieved for colder days. Therefore, the cooling temperature setpoint needs to be selected considering the reduced need for heat dissipation via surface blood circulation, indicating a specific potential for the cyclical operational mode for such environmental conditions. Furthermore, the measured cooling rate highlighted the limitation of the commonly used sprinkler-based systems for such conditions, indicating the knowledge-gap, that the developed water mattress fulfills, due to its closed water cycle application.

Chapter 7

Thermal balance for cattle

This section will focus on the cows' response to changing environmental conditions in terms of their physiological reactions as the thermoregulatory mechanisms. Previously described experimental campaigns in the cowshed conditions indicated the influence of cows' thermoregulatory mechanisms on the cooling capability of the developed water mattress, highlighting the importance of properly selected, its supplying chilled water temperature setpoint in terms of cows' thermal response to environmental conditions. The main goal of the presented in this chapter analysis is to observe, which thermoregulatory mechanism is the most effective in thermal relief of the animal for selected thermal conditions in the barn, and how this influences the validity of using conductive cooling with selected chilled water temperature setpoint for those conditions. That is why, the thermoregulatory mechanisms will be described in detail within this chapter, with an emphasis on understanding their physical phenomenon in terms of the heat transfer for different environmental conditions. First, the introduction to animals' thermal physiology will be presented. Secondly, based on the experimental data, the thermal balance of the animal will be conducted, which will consider evaporation, radiation, conduction, and sweating as heat dissipation mechanisms. Simplified formulas for cattle thermal balance presented in this chapter are taken from the zootechnical literature of Wroclaw University of Environmental and Life Sciences [75]. To this end, such an approach will enable to assess the potential of the developed water mattress in terms of the thermoregulatory mechanisms of the animal for different environmental conditions.

7.1. Introduction to thermal physiology of cattle

In the following subsections both, heat production, and four mechanisms of heat dissipation: conduction, convection, radiation, and evaporation will be described in detail in terms of animal thermoregulatory systems.

7.1.1. Heat production

Heat produced by the organism can vary in a wide range depending on its natural metabolism, activity, and environmental, and physical conditions. Basic metabolic rate is defined by heat produced by the animal being in complete physical and mental peace, in a fasting state, and in thermally neutral conditions. Such heat production is necessary to maintain the vital functions of the organism Basic equation that describes heat production in this state is related to the weight of the animal. For the warm-blooded animals, it was observed that metabolic rate varies in proportion to 0.75 power of body mass, despite differences in geometric shape or body chemical composition. For dairy cattle, that equation needs to be modified by the milk production rate. There are different forms of that equation, depending on the approach. In this study, the feed intake and its composition were not monitored, and for the estimation of the heat production the simplified Equation 7.1, according to [87] was used, which is presented below:

$$\dot{Q}_{metabolic} = c_h \cdot BW^{0.75}/3.6 \tag{7.1}$$

where:

$\dot{Q}_{metabolic}$ – metabolic heat production, W
c_h - heat production coefficient (44.1 for high production cows (daily milk yield ≥ 30 kg), 37.8 for intermediate production cows (daily milk yield < 30 kg) and 29.7 for dry cows), -
BW – the body weight of the animal, kg

Each deviation from the basic state leads to the thermogenesis increase. The main focus of this thesis is on the analysis of the change in environmental conditions and their influence on heat production and thermal regulation by cattle. A more detailed description of the relation between heat production, ambient temperature, and body temperature will be discussed in Subsection 7.1.6 of this PhD thesis.

7.1.2. Conduction

Conductive heat transfer occurs between two environments that are in direct contact and characterized by the temperature difference between them, being the heat transfer engine. Particles with a higher temperature (and higher kinetic energy) transfer energy to the particles with a lower temperature. The heat transfer rate depends on the thermal conductivity coefficient and temperature difference between considered environments. The smaller the coefficient, the greater the insulating properties. The important aspect of the thermoregulation of the animal is its hair coating due to its high insulative properties, being the result of the large amount of stagnant air between hairs [88].

Considering animal thermal balance, conductive heat transfer occurs between animals' skin being in direct contact with the bedding, characterized by lower temperature, and can be described by Equation 7.2 [75], presented below:

$$\dot{Q}_{conduction} = \lambda \cdot S_{skin}(t_{skin} - t_{bedding}) \tag{7.2}$$

where:
$\dot{Q}_{conduction}$ – conductive heat losses, W
λ - thermal conductivity coefficient (for rubber 17.4÷26.6 [75]), W/m^2·°C
S_{skin} – skin surface, m^2
t_{skin} – skin temperature, °C
$t_{bedding}$ - bedding temperature, °C

Considering these aspects, thermal regulation by the animal is based on vasomotor and pilomotor reactions that regulate the temperature difference and insulative properties of the fur, respectively. The mammals' dermis is blood-supplied by the capillary network (being the heat exchanger with the environment). Blood circulation is regulated by the contraction of the precapillary arterioles: the stronger the contraction, the reduced number of capillaries, is supplied by the blood. When the precapillary valve (c.f.Figure 7.1) is entirely closed, then part of the capillary network is excluded from the circulation, and blood flows to the veins through the arteriovenous anastomosis (which could be compared to a bypass in a hydraulic network). As a result, the lower amount of animals' internal heat is transferred to the skin and dissipated to the environment. The main concept of that regulation system is presented in Figure 7.1. When the ambient temperature is high (or in the case of increased physical exertion), the blood circulation through the skin is intensified, and the temperature of the skin becomes similar to the core body temperature, increasing the animal's heat dissipation capabilities. On the contrary, when the ambient temperature is low, the skin blood circulation is reduced, resulting in lower skin temperature and decreased heat losses to the environment. In the case of large animals, such as a cow, this cooling mechanism can reach deep tissues because of the fat layer that becomes a thermal insulator.

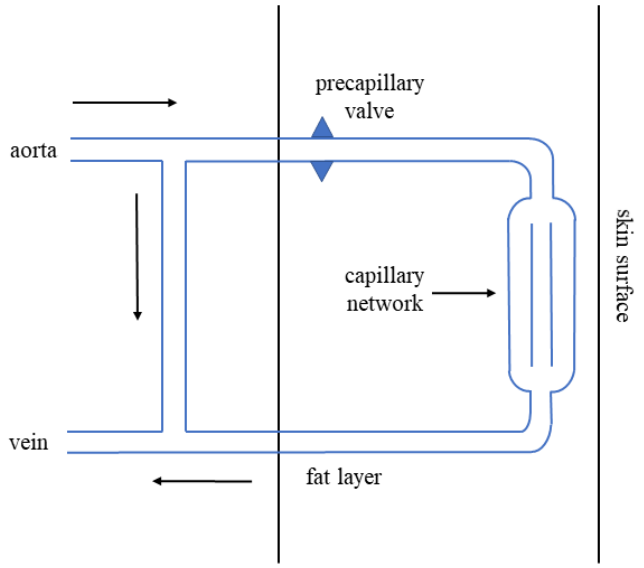

Figure 7.1. Scheme of skin vascularization lying on the layer of fat, arrows indicate a direction of blood flow, source: [88].

7.1.3. Convection

Convective heat transfer occurs when liquids (gas or fluid) flow around the materials that are characterized by the temperature difference relative to the liquid. Considering heat losses from the animal, it is the air that flows around its body. Due to the heat transfer, the air gets warmer, and its specific density becomes reduced, causing rising upward of that air portion. As a result, the colder air replaces that space around the animal's body, and the heating process starts again, causing air circulation, which occurs as long as the temperature difference is preserved. Heat dissipation can be intensified in the case of forced convection when the velocity of the air is a significant parameter of their regulation. Fan systems previously described in Chapter 1 of this PhD thesis, applied to the barn are based on this mechanism. According to zootechnical literature [75] it can be described by Equation 7.3, presented below:

$$\dot{Q}_{convection} = k \cdot 1.163 \cdot S_{skin}\sqrt{v} \cdot (t_{skin} - t_{air}) \tag{7.3}$$

where:

$\dot{Q}_{convection}$ – convective heat losses, W
k – convective heat losses coefficient (3.8÷4.2 [75])
S_{skin} – skin surface, m^2
v – air velocity, m/s
t_{skin} – skin temperature, °C
t_{air} - air temperature, °C

The total skin surface of the animal can be calculated based on cow body weigh following the formula proposed by Brody [89] for Bos taurus cattle, presented by Equation 7.4.

$$S_{skin,t} = 0.14 \cdot BW^{0,57} \tag{7.4}$$

where:
$S_{skin,t}$ – total skin surface of Bos taurus cattle, m^2
BW – body weight of the cow, kg

Animals' thermal regulation through the convective heat dissipation is based on the same vasomotor mechanism as it was described for the conduction. Changing the skin blood flow through the capillary network regulates the skin temperature and intensification of the heat transfer (c.f.Figure 7.2). However, this aspect needs to be extended by the role of the previously introduced layer of fat. Although for the colder environment, it protects animals thanks to the insulative properties, in extremely hot weather conditions, it becomes an additional barrier for heat dissipation. For that reason, the number of mammals is equipped with a natural countercurrent heat exchanger, presented in a simplified way in Figure 7.2 [88]*Figure 7.4*. It is also worth mentioning that convective heat losses are also influenced by the pilomotor mechanisms, which regulate the amount of stagnant air between hairs, and thus the insulative properties of the coating layer. Thanks to that, the skin temperature under the coating is maintained between 1°C up to 3°C lower than the rectal temperature [88]. In the case of cattle, the thermoregulation mechanism is still under study, where the horns' function is one the natural, but still untapped and yet not fully discovered animals' capabilities used in their thermal processes [90].

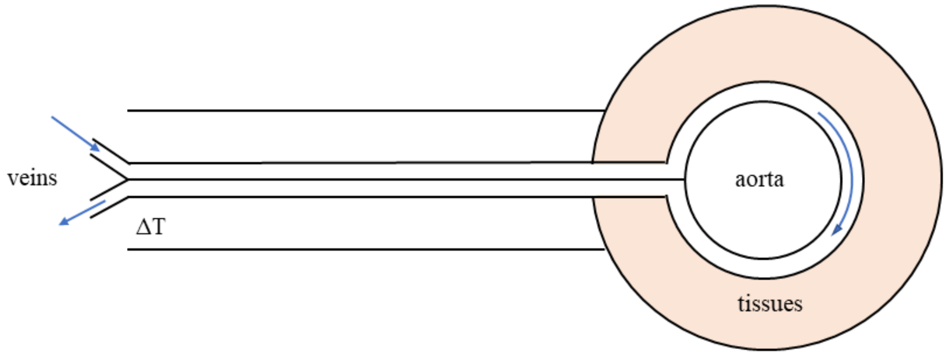

Figure 7.2. Simplified scheme of natural countercurrent heat exchangers occuring in the number of mammals' species, source [88].

7.1.4. Radiation

Radiation is the wave propagation with length depending on the temperature of the emitting body. For that reason, it does not require any molecular center to propagate. In that mechanism energy is transferred to the environement by each object with the temperature above absolute zero, with the velocity of the sun light. Sun emits the entire spectrum of light. However, objects at the temperature below 500°C that are considered in this study, emit mainly infrared radiation.

Human and animal bodies are known as perfectly black relative to the infrared radiation (thermal), and they partially reflect the visible radiation. The absorbed radiation, regardless of its type, converts into heat. Considering these aspects, heat dissipation through radiation depends on the temperature difference between animals and surroundings that absorb it, as well as the surface of the animal body. In some situations, for example, when animals are breeding in the direct sun, the amount of absorbed radiation can be higher than the one emitted to the environment, influencing their core body temperature and behavioral reactions connected to thermal regulation [88]. However, the experiments considered within this PhD thesis were conducted only inside the barn, and for that reason, the influence of solar radiation on animals' thermal balance was omitted.

The amount of heat emitted by the animal through radiation according to [75] can be described with Witty formula given by Equation 7.5, presented below:

$$\dot{Q}_{radiation} = \alpha \cdot S_{skin} \cdot (t_{skin} - t_{sur}) \tag{7.5}$$

where:
$\dot{Q}_{radiation}$ – radiative heat losses, W
α – emissivity coefficient (0.05 for -20°C and 0.08 for 30°C [75])
S_{skin} – skin surface, m^2
t_{skin} – skin temperature, °C
t_{sur} – temperature of the surroundings, °C

7.1.5. Evaporation

Heat dissipation by evaporation is based on a transfer to the liquid, such amount of heat that is necessary to change its phase to the gas. Evaporative heat depends on the liquid and its temperature. Considering the animals' bodies, the water, being the main component of sweat, saliva, and internal fluids lining a respiratory tract, by evaporation receives a significant amount of the heat. This mechanism of thermal regulation becomes especially important, when the ambient temperature is equal and higher than the skin temperature, limiting heat dissipation by convection, radiation, and conduction for conventional bedding type. In such a situation, it becomes the only mechanism that protects the animal against overheating. The heat of evaporation for sweat and saliva differs from each other, for sweat and skin temperature 35°C is assumed to be equal 2.42 kJ/g [88]. However, the amount of produced sweat is difficult to asses, and for that reason in thermal balance only evaporation through the respiratory tract is considered, which can be calculated with Equation 7.6 [75], presented below:

$$\dot{Q}_{evaporation} = 0.585 \cdot Q \cdot 1.163 \tag{7.6}$$

where:
$\dot{Q}_{evaporation}$ – evaporative heat losses, W
Q – production of the water vapor, g/h (c.f. Table 7.1)
0.585 – the heat of the evaporation of 1g of water

Table 7.1. Production of the water vapor (in g/h) by cattle with body weight between 300 and 600 kg for ambient temperatures in the range of 15 and 35°C [75].

Body weight, kg	**Ambient temperature*, °C**				
	15	**20**	**25**	**30**	**35**
300	250	320	390	470	550
400	295	370	460	570	675
500	330	420	540	660	780
600	360	470	590	730	880

There are four methods for heat dissipation by evaporation: sweating, panting, diffusion, and drooling, where the first two are the most effective for large animals, and that is why, those two will be further discussed. For cattle sweating process is similar to that in humans. However, the number of sweat glands responsible for sweat secretion per unit of skin surface area is much lower than for humans. For that reason, even if the ambient temperature is high, sweat is not observed on the hair coating. Whereas, panting can be understood as high-frequency breathing accompanied by an increase in the minute volume of air, being a thermoregulatory reaction aimed at increasing heat dissipation. In mammals, including cattle, increased respiratory rate is accompanied by the breaths shallowing. However, for prolongate exposition to air characterized by high temperature and humidity, breathing reaches the second phase, in which the respiration rate is reduced, and breaths are deepened. Both described mechanisms are important for brain homeothermy, based on maintaining its temperature at a stable level.

7.1.6. Influence of the ambient temperature on heat production

Considering the genesis of the heat production and thermal regulation mechanism that were presented previously, in this section the role of ambient temperature in their activation will be discussed in detail.

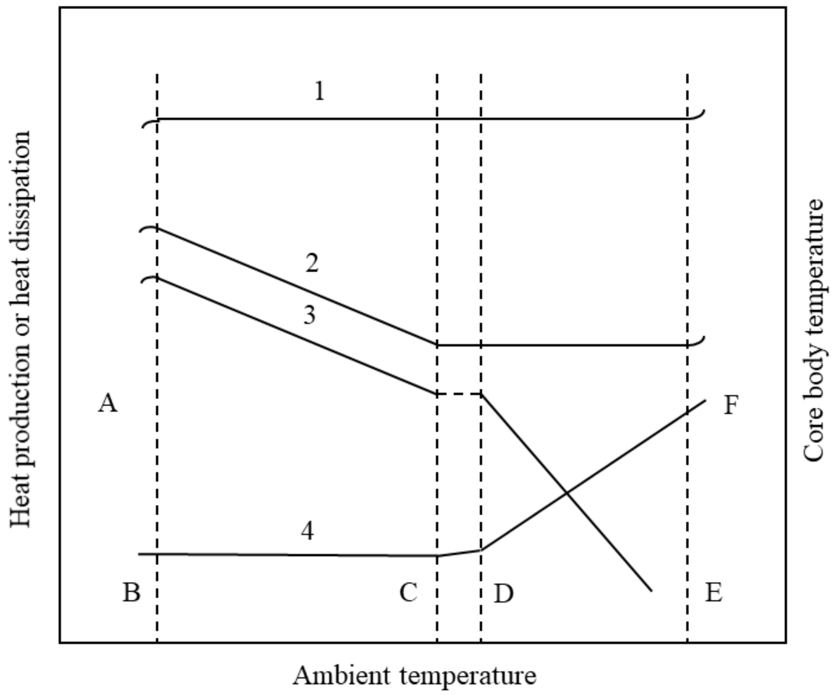

Figure 7.3. Scheme of the relation between ambient temperature, core body temperature, and heat production or heat dissipation for warm-blooded animals: A – hypothermia zone; B – temperature, for which top metabolism occurs, C – bottom critical temperature, D – temperature, when quick evaporative heat losses occur, E - top critical temperature, F- hyperthermia zone; 1 – body temperature, 2 - heat production, 3 – sensible heat losses, 4 – evaporative heat losses, source: [88].

In Subsection 7.1.1 of this PhD thesis, it was said, that basic heat production is defined for the neutral environmental conditions. However, the definition of those conditions can vary between the moment, when heat production is the lowest, and the one, when thermoregulatory efforts are the lowest. In Figure 7.3 further thermoregulatory zones are schematically presented.

Ambient temperatures, for which the animal maintains its core body temperature in a specific range by activating previously described thermoregulatory mechanisms, are presented by the line section between B and E. When the temperature drops below B, the state of hypothermia begins (A), in which the animal dissipates more heat, than can produce. Temperature marked by E in Figure 7.3 is the upper threshold, above which, the described mechanisms for thermal regulation (thermolysis) are not sufficient in heat dissipation, and more heat is produced than lost to the environment. Above that value, the state of hyperthermia (F) occurs. Both A and F zones are dangerous for animals' health and may cause their death. Line 2 represents the relationship between environmental conditions and heat production. It can be observed that with increasing ambient temperature, heat production and sensible heat losses (line 3) decrease until they reach their minimum in point C. Between points C and D, both heat production and the thermoregulatory effort are the lowest. That region is the most preferable for the animal. Section CE represents the state when heat production is the lowest. However, when the ambient temperature increases above a D value, the evaporative heat losses increase rapidly, due to sweating or panting mechanisms. They become crucial in thermal regulation, causing however, an additional effort for the animal organism.

Therefore, developed in this PhD thesis cooling solution is the response to the specific needs of the animal when the ambient temperature exceeds a D value. The maintained low temperature of the water mattress enables sensible heat losses through conduction and radiation, even when the ambient temperature is close to the temperature of the cows' skin. Furthermore, it influences the microclimate around the animals' bodies, lowering the local air temperature, and influencing the intensity of active thermoregulatory mechanisms. Such capabilities reduce the thermoregulatory effort of the animal, improving its well-being.

7.2. Thermal balance for cattle cooled by the developed cooling water mattress

In this section of the presented PhD thesis the described previously thermoregulatory mechanisms and potential heat losses to the environment through them will be presented, adopting measurements from the second experimental campaign conducted in 2023. The main goal is to designate the potential heat dissipation through each thermoregulatory mechanism for real barn conditions, including the influence of applying the developed in this PhD thesis innovative cooling water mattress.

For this purpose, several parameters were taken into account: cows' skin temperature from the flank region (T_{skin}), which was assumed as an average surface value designated within the IR thermography, the water mattress' surface temperature ($T_{surf,mat}$), as well as the velocity of the air (v_{air}) and ambient temperature (T_{air}). Values were taken for the last day of each experimental series with water temperature setpoints of 13°C, 16°C, and 19°C, respectively, the same as results of IR thermography previously presented in Chapter 6 of this PhD thesis. The last day of the experimental series was assumed to be more representative than the first one, due to additional time for animals adaptation to the new cooling parameters. Evaluated cows were unified in terms of body weight, assuming 500 kg, due to the lack of detailed information. According to Equation 7.1 and Equation 7.4, based on the body weight, the cows' heat production and skin surface were also unified. Calculations considered two situations, when cows are lying on their beddings, and standing, respectively. When standing, radiation was considered separately between animal and bedding, and environment. For that reason, the skin surface being in direct contact with the water mattress was assumed to be 20% of the total surface, according to the literature [58]. Heat production was calculated for dried cows using Equation 7.1. Calculated values are summarized in Table 7.2

Table 7.2. The unified characteristics of the considered cows.

$\boldsymbol{S_{skin,t}}$, m^2	$\boldsymbol{S_{skin,c}}$, m^2	$\boldsymbol{S_{skin,r}}$, m^2	BW, kg	$\boldsymbol{\dot{Q}_{metabolic}}$, W
4.84	0.97	3.87	500	872

Where:
$S_{skin,c}$ – skin surface being in direct contact with the bedding,
$S_{skin,r}$ – the difference between total surface and surface in direct contact with the bedding.

In heat dissipation calculations, values of the heat loss coefficients have been assumed as follows: for the radiation, the value of 0.08, for the convection the value of 4 W/m^2 K, being the one assumed previously in simulations, presented in Chapter 3 of this PhD thesis. For conduction the minimal value from a given range was considered, due to a specific characteristic of the reinforced rubber used for cattle. The production of the water vapor was calculated for specific values of ambient temperature using linear interpolation. All necessary data from the experiments, as well as the results of calculations, have been summarized in Table 7.3

Table 7.3. Summarized data for calculations of potential heat losses from the animals for experimental series with 13°C, 16°C, and 19°C chilled temperature setpoints, respectively, where: (S) is for standing position and (L) is for lying position of the cow.

						Experimental series with 13°C chilled water temperature setpoint							
Mattress	**Cow**	T_{skin}	$T_{surf,mat}$	T_{air}	v_{air}	Radiation		Convection		Conduction	Evaporation	Sum (L)	Sum (S)
		°C	°C	°C	m/s	W		W		W	W	W	W
						(S)	(L)	(S)	(L)				
Cooling	Zuzia	34.8	20.7	25.1	0.11	286	210	72	58	237	369	874	727
Non-cooled	Józia	35.7	29.6	24.7	0.11	271	238	82	66	103	362	768	715
Cooling	Fruzia	33.9	19.3	24.7	0.11	278	199	69	55	246	362	862	709
Non-cooled	Teresa	33.9	28.7	22.9	0.11	266	238	82	66	88	333	724	681
						Experimental series with 16°C chilled water temperature setpoint							
Mattress	**Cow**	T_{skin}	$T_{surf,mat}$	T_{air}	v_{air}	Radiation		Convection		Conduction	Evaporation	Sum (L)	Sum (S)
		°C	°C	°C	m/s	W		W		W	W	W	W
						(S)	(L)	(S)	(L)				
Cooling	Zuzia	34.6	26.1	22.2	0.08	251	184	54	43	209	385	821	690
Non-cooled	Józia	34.2	27.5	29.3	0.08	171	145	43	34	82	408	670	622
Cooling	Fruzia	35.9	26.7	21.0	0.08	279	199	59	47	251	395	891	733
Non-cooled	Teresa	34.1	25.8	28.4	0.08	210	179	53	42	96	380	698	643
						Experimental series with 19°C chilled water temperature setpoint							
Mattress	**Cow**	T_{skin}	$T_{surf,mat}$	T_{air}	v_{air}	Radiation		Convection		Conduction	Evaporation	Sum (L)	Sum (S)
		°C	°C	°C	m/s	W		W		W	W	W	W
						(S)	(L)	(S)	(L)				
Cooling	Zuzia	34.2	20.6	21.0	0.10	359	285	94	75	229	302	891	755
Non-cooled	Józia	33.7	26.5	20.8	0.10	318	279	92	73	121	299	772	708
Cooling	Fruzia	33.5	20.6	20.8	0.10	344	274	90	72	217	299	863	733
Non-cooled	Teresa	32.6	25.6	21.0	0.10	288	251	83	66	118	302	736	673

The obtained results indicated, that for the environmental conditions of conducted experiments, the highest potential of the heat dissipation was through evaporation, then radiation, conduction, and finally convection, being the least effective method. Although evaporation seems to bring the highest potential as the heat dissipation method, it also affects the animal's organism by the water and mineral loss (considering sweating), and in case of panting, flushing out the blood' alkaline reserves and physical effort of the respiratory muscles [88]. As the natural thermoregulatory mechanism, it becomes crucial, when the ambient temperature is similar or higher than the skin temperature, making other methods ineffective. Convection, on the other hand, for barns with natural ventilation only, and without the fan system, has very limited influence on heat dissipation, especially for higher ambient temperatures. Applying the innovative cooling water mattress developed in this PhD thesis increases not only conductive heat losses during a lying period, but also the radiative heat losses, when the cow is standing. To underline even more the influence of the cooling mattress within each experimental series, obtained for non-cooled and cooled cows heat values were averaged among obtained this way two groups, for both standing and lying positions, respectively. The difference between cooled and non-cooled cows in heat dissipation for both positions is presented as the bar graph in Figure 7.4. The highest influence of the cooling on the cow, understood as the aforementioned difference, for the barn's environmental conditions, was obtained for the experimental series with a 13°C chilled water temperature setpoint, reaching 172 W in lying and 79 W in standing position, respectively. Therefore, a comparison with traditional straw bedding, characterized by a higher temperature, would result in a larger difference and could be an interesting future direction of studies.

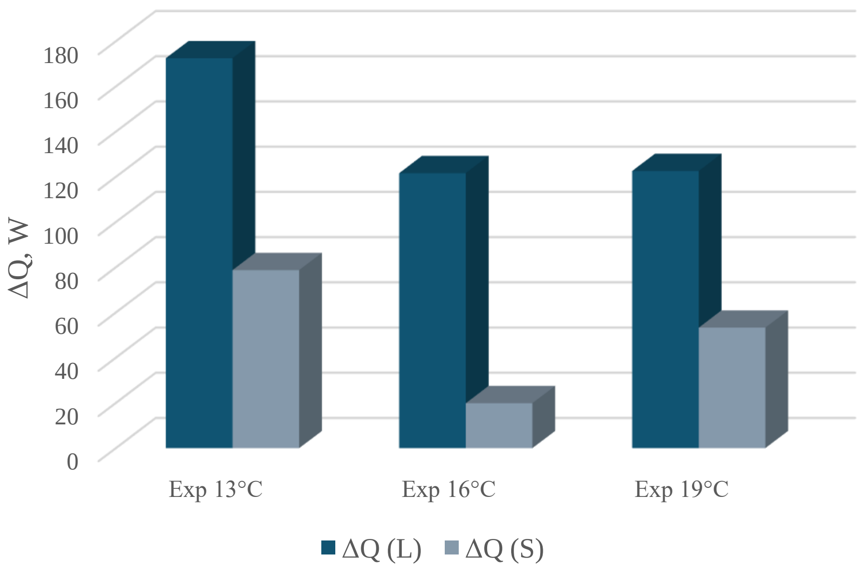

Figure 7.4. The average difference in the heat dissipation between cooled and non-cooled cows, divided between the lying (L) and standing (S) positions for each considered experimental series (Exp) in 2023.

To observe the theoretical influence of ambient temperature, air velocity, and the cooling water mattress' surface temperature on the relation between different thermal mechanisms of heat dissipation, additional calculations have been conducted. For this purpose, based on the previously described in this section of this PhD thesis values observed during the experiments, the output values of the following parameters were assumed: 25°C of ambient temperature, 0.10 m/s of air velocity, 35°C of cow's skin temperature, as well as 20°C of cooling mattress', and 28°C of non-cooled mattress' surface temperatures, respectively. The ambient temperature was analyzed on two additional levels: 30°C and 35°C, being equal to the assumed cow's skin temperature, limiting the convective and radiative heat losses. For each ambient temperature level, two more cooling mattress' surface temperatures were assumed: 4°C and 16°C, respectively. Additionally, the influence of the change in the air velocity to 0.30 m/s and 0.60 m/s on convective heat losses was analyzed. Results are presented in Table 7.4.

Table 7.4. Summarized data for calculations of potential heat losses from the animals using cooling and non-cooled water mattresses assuming three levels of ambient temperature and three levels of cooling water mattress surface temperature, in which 35°C was assumed skin temperature of the animal, and 0.1 m/s was assumed velocity of the air, in table (S) is for standing position and (L) is for lying position of the cow.

The ambient temperature of 25°C and the cooling mattress surface temperatures of 4°C, 16°C, and 20°C

Mattress	$T_{surf,mat}$	Radiation		Convection		Conduction	Evaporation	Sum (L)	Sum (S)
	°C	W		W		W	W	W	W
		(S)	(L)	(S)	(L)				
	20	297				252		893	736
Cooling	16	319	216	71	57	320	367	960	757
	4	383				522		1162	822
Non-cooled	28	254	216	71	57	118	367	758	692

The ambient temperature of 30°C and the cooling mattress surface temperatures of 4°C, 16°C, and 20°C

Mattress	$T_{surf,mat}$	Radiation		Convection		Conduction	Evaporation	Sum (L)	Sum (S)
	°C	W		W		W	W	W	W
		(S)	(L)	(S)	(L)				
	20	189				252		838	674
Cooling	16	211	108	36	28	320	449	905	695
	4	275				522		1107	760
Non-cooled	28	146	108	36	28	118	449	703	630

The ambient temperature of 35°C and the cooling mattress surface temperatures of 4°C, 16°C, and 20°C

Mattress	$T_{surf,mat}$	Radiation		Convection		Conduction	Evaporation	Sum (L)	Sum (S)
	°C	W		W		W	W	W	W
		(S)	(L)	(S)	(L)				
	20	81				252		783	612
Cooling	16	103	0	0	0	320	531	850	633
	4	167				522		1052	698
Non-cooled	28	38	0	0	0	118	531	648	568

Conducted calculations proved the increasing importance of evaporation as the heat dissipation mechanism, when the ambient temperature is growing, due to decreasing and becoming almost neglectable effect of convection and radiation. Applying the cooling water mattress developed within this PhD thesis, changes this relation, providing effective cooling, which for very low mattress temperatures reaches values close, or even higher, to the one obtained with evaporation. The heat dissipation through the conduction using cooling water mattress itself, in comparison to the non-cooled mattress with assumed constant surface temperature, is the same regardless of the ambient temperature. However, its importance is changing in terms of its relation to other heat dissipation mechanisms. Its values presented as the difference between the cooled and non-cooled cows are presented in Figure 7.5. The surface temperature of 4°C provides very high values of potential conductive heat dissipation. However, such a value would be too low in terms of the activated thermoregulatory mechanisms focused on the blood circulation system, which was observed through the results obtained in the experimental campaigns. Nevertheless, the limited possibility of heat dissipation, when the ambient temperature increases to values, being close to the skin temperature, underlines the importance of each cooling technique for those temperature levels. It also makes the obtained results satisfactory, especially considering their total values (c.f Table 7.4) , being close to the cow heat production.

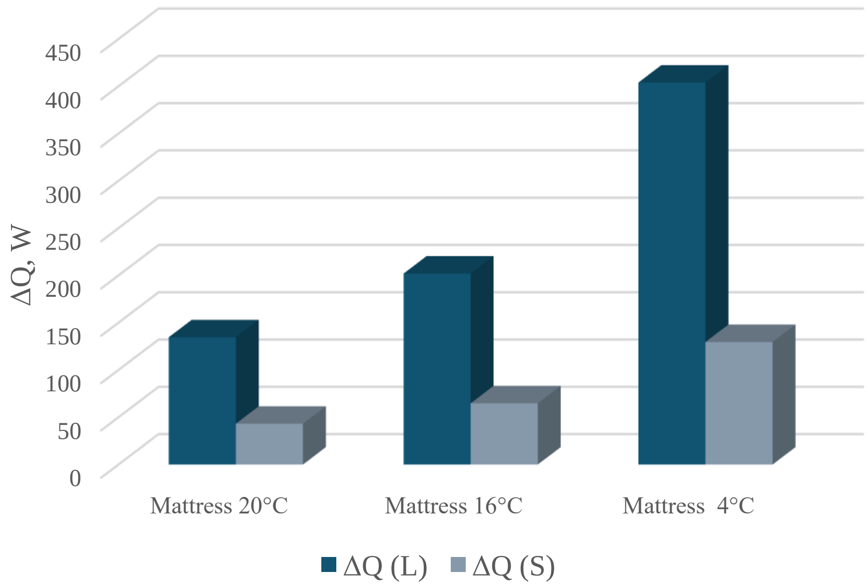

Figure 7.5. The difference in the heat dissipation between cooled and non-cooled cows, divided between the lying (L) and standing (S) positions for each considered temperature of the cooling water mattress surface, which is the same for each studied ambient temperature.

The influence of the air velocity was analyzed only for the ambient temperature of 25°C. Change from 0.10 m/s to the value of 0.30 m/s resulted in 123 W of heat dissipation for the standing cow and 99 W for the lying one. Whereas, for the air velocity of 0.60 m/s those values increased to 174 W and 139 W, respectively. Such results indicate an increase of only about 50 W relative to the lower values, highlighting the limited potential of the convective cooling methods.

7.3. Conclusions from the thermal balance for cattle

Conducted thermal balance for cattle indicated the potential of the developed wihtin this PhD thesis cooling water mattress as not only a conductive cooling method but also as a radiative one, working also when the animal is standing. The importance of that solution increases when the ambient temperature becomes similar to the temperature of the animal's skin, and convective or radiative heat losses become less effective or even ineffective for conventional beddings. Although, the potential cooling effect for the lowest cooling water temperature setpoint would be high, and close to the evaporative heat losses, the experimental observations indicated natural limitations of such heat transfer, due to the natural thermoregulatory mechanisms of the animal. However, more experiments with the lower mattress' supplying chilled water temperature setpoints are required to confirm it. Therefore, an attractive future work could consist of studying the developed solution working in tandem with other cooling technologies, adjusted by a control algorithm to the environmental conditions.

Chapter 8

Conclusions and future works

The main goal of this PhD thesis was to design and develop the cooling water mattress as a conductive cooling solution for cattle, presenting a novel approach to the cow's heat stress alleviation. The raised research topic addressed an important issue of an effective cooling strategy for cattle during thermally challenging events, becoming even more important in terms of climate change and its influence on ambient temperatures increase and prolongate heatwave periods. Simultaneously, the complexity of cooling cowsheds, due to great thermal losses through its structure creates a significant research area focused on animal thermal comfort, and the sustainable approach for cooling, traversing boundaries of different science disciplines, combining thermal science with technical and economic challenges. Since there was little research on conductive cooling methods, in this PhD the novel cooling water mattress was designed and developed, allowing for direct heat transfer from the animal to circulating in its interior chilled water.

To address the aforementioned goal several research stages were applied, including simulation and design of the cooling water mattress, its development, laboratory tests, and finally its application in real barn conditions. The conducted study applied a CFD modeling approach, during which four different geometries of the water mattress were analyzed in terms of the chilled water distribution and potential heat transfer on their surfaces, assumed to be in direct contact with cows' skin temperature of 35°C. At this stage of the study, the water mattress design was selected, for which both of the considered aspects were characterized by the highest potential in mattress future application, taking also into account the feasibility of the prototype and animal's welfare. Obtained results indicated a high potential for heat transfer between animal and chilled water, in comparison to the conductive cooling solutions, previously studied by the scientists. Hereby, the conducted analysis allowed for answering the first research question presented in Chapter 2 of this PhD thesis, namely: "What geometry of the cooling water mattress improves the heat transfer between chilled water and animal, compared to known conductive cooling solutions, while ensuring animal comfort?".

The selected design was then developed as a real-scale prototype, which was tested in both laboratory and real barn conditions, in which its cooling effectiveness was proved. Experimental campaigns in real barn conditions were conducted in two summer periods, in 2022 (30 days) and 2023 (29 days), during which 3 and 4 cows were involved, respectively. In order to answer the second research question, presented in Chapter 2 of this PhD thesis ("What setpoints of the water mattress' operating parameters ensure the appropriate level of animal cooling?") during those campaigns different operational settings of the water mattress were tested for changing environmental conditions to asses which one would be most appropriate for animal cooling. Thereby, four levels of the chilled water temperature were tested: 10°C, 13°C, 16°C, and 19°C. Observations that were made during those campaigns indicated that the cow's natural thermoregulatory mechanisms, within which the animal adapts to different environmental conditions, could influence the heat transfer with the developed water mattress, being also a new environment for the animal. It concerns mostly a cow's blood circulatory system, which reacts directly to the ambient conditions. The conducted experiments in mild and moderate heat stress conditions indicated the 16°C chilled water temperature as the most suitable in terms of animal thermal reaction observable by the IR thermography and reduced rumen temperature. However, the preferable operation of such a system would be based on adaptation of its operational parameters to the animal's individual thermal needs within changing environmental conditions, being a complex issue. The first experimental campaign already revealed that it is extremely difficult to predict or assess the thermal response of the individual animal in terms of the experienced heat stress. To gain more insight into this area and attempt to answer the research question, concerning how the developed water mattress influences the animal's physiological and behavioral reactions in terms of its thermal comfort, presented previously in Chapter 2 of this PhD thesis, the main interest of the second experimental campaign was to investigate the animal's heat stress indicators. For this purpose, the specially developed measurement strategy of cow's physiological reactions as thermal indicators was applied. The novel approach for the measurements of the skin temperature and heart rate of the animal was challenged by the real barn conditions, making the obtained results difficult for precise assessment. This highlighted the complexity of the animal's unambiguous response evaluation in terms of the heat stress intensity.

Following the presented results, the conducted study confirmed the research hypothesis, which was raised within this PhD thesis, namely: *The modified flow-based water mattress for cattle is an effective cooling method allowing the reduction of cow's heat stress.* It can be stated, that the developed cooling water mattress was proved to be an effective cooling method for cattle in mild and moderate heat stress environmental conditions, observed even for the Polish climate, which was also reflected in the physiological reactions of the animal. However, due to the frontier character of this study, in the knowledge from different disciplines, at this moment there is a lack of available sensors, apparatus, and methodology, to bring into light one specific parameter defining the threshold of the animal's heat stress level, to which obtained results could be addressed. The research community is still looking for that answer, putting in collaboration the specialists from different scientific fields. Therefore the potential in this research area is still undiscovered.

Furthermore, observations from the conducted experiments led also to further conclusions about the future application of the developed solution on the industrial level. The operation of the water mattress in the real barn conditions indicated a higher mattress' supplying chilled water temperature than the primary assumed, as more suitable for the animal, therefore reducing the matress' surface heat fluxes in comparison to the obtained in the simulation. According to the experimental observations, the animals' natural thermoregulatory mechanisms presumably could limit the cooling capability of the developed water mattress depending on the environmental conditions. Moreover, the thermal inertia of the water mattress indicated the possible shift to the so-called cyclical operation of the water mattress, studied during the second experimental campaign, during which circulation pumps would be cyclically turned off, after achieving the selected chilled water temperature setpoint. Such results are beneficial from the chilled water production and distribution point of view, due to the higher operational chilled water temperature and reduced electricity consumption of the entire system.

Furthermore, the novel cooling approach has special potential in terms of its application in the boundary weather conditions during the summer periods. For colder days, as well as for extremely hot days, the application of other cooling technologies is limited. The measured during the second experimental campaign cooling rate indicated that for the colder days, wetting animals' bodies using sprinklers could be a reason for exceeding the optimal conditions threshold, causing too cold environment for the animals. On the other hand, during extremely hot days, when the ambient temperature is close to the temperature of the skin if conventional beddings are used, the convective heat losses are limited, as well as the radiative heat losses. Therefore, one of the possible future applications for the developed within this PhD thesis water mattress could be its operation in the industrial scale barn with other cooling technologies, adjusted to environmental conditions by the specially developed control algorithm.

The conducted study considered a two-bedding system, powered by the conventional chiller. However, the developed solution can be easily scalable to the multi-bedding system applied in the industrial scale barns' conditions, working in a so-called close water circuit, representing a great potential for water savings, especially in regions characterized by high water scarcity. Particularly those regions are often characterized by challenging weather conditions, with the large number of cattle, making the developed water mattress-based cooling solution meet their needs. However, it would require a prolongate study in different environmental conditions to verify the efficiency, the electricity and the water savings compared to the other open water circuit-based cooling systems.

Furthermore, the developed water mattress-based cooling system applied in livestock buildings could be coupled with hybrid systems based on renewable energy sources, such as the photovoltaic system, geothermal system, or absorption chiller, providing a green cooling solution, with reduced CO_2 emissions, being especially important in terms of climate change mitigation and adaptation strategies. It becomes even more important considering the lower electrical energy requirement for higher chilled water temperature setpoints, which were established as preferable by the animals during the conducted experimental campaigns. As an example, the absorption-based cooling solution could play a particularly great role, due to the use of naturally available in such place resources. Manure generated by animals could be used for biogas production and then applying the biogas-fueled engine-generator the system would produce enough chilled water to supply the industrial scale, cooling mattress distribution system, simultaneously covering the electricity needs of the entire facility. As a result, cooling, electricity, and hot water needs would be covered by one system, allowing even to store or distribute the surpulus of thermal or electrical energy. Theoretically, such an approach provides an innovative and greener solution for the breeding sector, which contributes to sustainable production. Therefore, the feasibility, affordability, as well as life cycle assessment study of a conductive cooling water mattress supplied by the absorption chiller could be an interesting direction for future works.

Literature

[1] H. Ritchie, P. Rosado, V. Samborska. Our World in Data. 2024 [Online]. Available: https://ourworldindata.org/climate-change. [Date of access: 17 December 2024].

[2] J. Wibig. Hot Days and Heat Waves in Poland in the Period 1951–2019 and the Circulation Factors Favoring the Most Extreme of Them. *Atmosphere. 2021,* 12(3), 340 https://doi.org/10.3390/atmos12030340

[3] A. M. Tomczyk, E. Bednorz. Heat waves in Central Europe and tropospheric anomalies of temperature and geopotential heights. *International Journal of Climatology. 2019,* 9, 4189–4205. https://doi.org/10.1002/joc.6067

[4] D. Barriopedro, R. García-Herrera, C. Ordóñez, D.G. Miralles, S. Salcedo-Sanz. Heat Waves: Physical Understanding and Scientific Challenges. *Reviews of Geophysics. 2023,* 61(2). https://doi.org/10.1029/2022RG000780

[5] World Health Organization [Online]. Available: https://www.who.int/news-room/fact-sheets/detail/climate-change-heat-and-health. [Date of access: 17 December 2024].

[6] Q. Zhao, Y. Guo, T. Ye, A. Gasparrini, S. Tong, A. Overcenco et al. Global, regional, and national burden of mortality associated with non-optimal ambient temperatures from 2000 to 2019: a three-stage modelling study. *Lancet Planet Health. 2021,* 5, 415-425. https://doi.org/10.1016/S2542-5196(21)00081-4

[7] J. Ballester, M. Quijal-Zamorano, R. F. Méndez Turrubiates, F. Pegenaute, F. R. Herrmann, J. M. Robine et al. Heat-related mortality in Europe during the summer of 2022. *Nature Medicine. 2023, 29,* 1857–1866. https://doi.org/10.1038/s41591-023-02419-z

[8] P. Thornton, G. Nelson, D. Mayberry, M. Herrero. Increases in extreme heat stress in domesticated livestock species during the twenty-first century. *Global Change Biology.* 2021, 27(22), 5762 - 5772. https://doi.org/10.1111/gcb.15825

[9] T. L. Mader, L. J. Johnson, J. B. Gaughan. A comprehensive index for assessing environmental stress in animals. *Journal of Animal Science.* 2010, 88(6), 2153–2165. https://doi.org/10.2527/jas.2009-2586

[10] X. Wang, B. S. Bjerg, C. Y. Choi, C. Zong, G. Zhang. A review and quantitative assessment of cattle-related thermal indices. *Journal of Thermal Biology. 2018,* 77, 24-37. https://doi.org/10.1016/j.jtherbio.2018.08.005

[11] S. Asma-Sadeque. The Guardian. 16 June 2022 [Online]. Available: https://www.theguardian.com/us-news/2022/jun/16/cattle-deaths-kansas-heat-wave-climate. [Date of access: 17 December 2024].

[12] T. Polansek. Reuters. 7 August 2023 [Online]. Available: https://www.reuters.com/world/us/heat-humidity-kill-hundreds-us-cattle-during-worlds-hottest-month-2023-08-07/. [Date of access: 17 December 2024].

[13] Enerdata (World Energy & Climate Statistics – Yearbook 2024) [Online]. Available: https://yearbook.enerdata.net/total-energy/world-consumption-statistics.html. [Date of access: 17 December 2024].

[14] Our World in Data. 2024 [Online]. Available: https://ourworldindata.org/worlds-energy-problem. [Date of access: 17 December 2024].

[15] Food and Agriculture Organization of the United Nations. [Online]. Available: https://openknowledge.fao.org/server/api/core/bitstreams/bc8810ae-2a13-4cfe-b019-339158c7e608/content/src/html/chapter-1-3.html. [Date of access: 18 December 2024].

[16] World Resources Institute [Online]. Available: https://www.wri.org/freshwater. [Date of access: 18 December 2024].

[17] M. Armstrong. Statista. 22 March 2024 [Online]. Available: https://www.statista.com/chart/26140/water-stress-projections-global/. [Date of access: 18 December 2024].

[18] Food and Agriculture Organization of the United Nations [Online]. Available: https://www.fao.org/interactive/state-of-food-security-nutrition/en/. [Date of access: 18 December 2024].

[19] Food and Agriculture Organization of the United Nations (FAOSTAT) [Online]. Available: https://www.fao.org/faostat/en/#data. [Date of access:: 18 December 2024].

[20] J. D. Allen, S. D. Anderson, R. J. Collier, J. F. Smith. Managing Heat Stress and Its Impact on Cow Behavior. *Proceedings of the 11th Western Dairy Management Conference,* Reno, NV, 2013.

[21] X. Chen, C. Li, T. Fang, J. Yao, X. Gu. Effects of heat stress on endocrine, thermoregulatory, and lactation capacity in heat-tolerant and -sensitive dry cows. *Frontiers in Veterinary Science.* 2024, 11, 1405263.

[22] N. B. Cook, R. L. Mentink, T. B. Bennett, K. Burgi. The Effect of Heat Stress and Lameness on Time Budgets of Lactating Dairy Cows. *Journal of Dairy Science.* 2007, 90(4), 1674-1682. https://doi.org/10.3168/jds.2006-634

[23] P. Pragana, P. R. Archana, J. Aleena, V. Sejian, G. Krishnan, M. Bagath et. al. Heat stress and dairy cow: Impact on both milk yield and composition. *International Journal of Dairy Science. 2017,* 12(1), 1-11. https://doi.org/10.3923/ijds.2016

[24] D.Y. Liu, S. J. He, S. Q. Liu, Y. G. Tang, E. H. Jin, H. L. Chen, et al. Daidzein enhances immune function in late lactation cows under heat stress. *Animal Science Journal. 2014,* 85(1), 85-89. https://doi.org/10.1111/asj.12080

[25] J. W. West. Effects of heat-stress on production in dairy cattle. *Journal of Dairy Science,* 2003, 86(6), 2131-2144. https://doi.org/10.3168/jds.S0022-0302(03)73803-X

[26] J. M. C. Van Os. Considerations for Cooling Dairy Cows with Water. *Veterinary Clinics of North America: Food Animal Practice.* 2019, 35(1), 157-173. https://doi.org/10.1016/j.cvfa.2018.10.009

[27] C. J. C. Muller, J.A. Botha, W. Coetzer, W. Smith. Effect of shade on various parameters of Friesian cows in a Mediterranean climate in South Africa. 2. Physiological responses. *South African Journal of Animal Science. 1994,* 24(2), 56-60.

[28] T. M. Widowski. Shade-seeking behavior of rotationally-grazed cows and calves in a moderate climate. *Livestock Environment IV: Proceedings of the 6th International Symposium,* Louisville, KY, 2001.

[29] P. E. Kendall, P. P. Nielsen, J. R. Webster, G. A. Verkerk, R. P. Littlejohn, L. R. Matthews. The effects of providing shade to lactating dairy cows in a temperate climate. *Livestock Science.* 2006, 103, 148-157. https://doi.org/10.1016/j.livsci.2006.02.004

[30] D. Renaudeau, A. Collin, S. Yahav, V. de Basilio, J. L. Gourdine, R. J. Collier. Adaptation to hot climate strategies to alleviate heat stress in livestock production. *Animal.* 2012*,* 6(5), 707-728. https://doi.org/10.1017/S1751731111002448

[31] V. K. Firfiris, A. G.Martzopoulou, T. A. Kotsopoulos. Passive cooling systems in livestock buildings towards energy saving: A critical review. *Energy and Buildings.* 2019, 202, 109368. https://doi.org/10.1016/j.enbuild.2019.109368

[32] R. K. Tabase, G. Næss, Y. Larring. Ammonia and methane emissions from small herd cattle buildings in a cold climate. *Science of The Total Environment.* 2023, 903, 166046. https://doi.org/10.1016/j.scitotenv.2023.166046

[33] M. R. Mondaca. Ventilation Systems for Adult Dairy Cattle. *Veterinary Clinics of North America Food Animal Practice.* 2019, 35(1), 139-156. https://doi.org/10.1016/j.cvfa.2018.10.006

[34] Phason [Online]. Available: https://phasoncontrols.com/ventilation/dual-ventilation-systems/. [Date of access: 18 December 2024].

[35] B. Ji, T. Banhazi, K. Perano, A. Ghahramani, L. Bowtell, C. Wang et al. A review of measuring, assessing and mitigating heat stress in dairy cattle. *Biosystems Engineering.* 2020, 199(1), 4-26. https://doi.org/10.1016/j.biosystemseng.2020.07.009

[36] M. R. Mondaca, C.Y. Choi, N. B. Cook. Understanding microenvironments within tunnel-ventilated dairy cow freestall facilities: examination using computational fluid dynamics and experimental validation. *Biosystems Engineering. 2019*, 183(12),70-84. https://doi.org/10.1016/j.biosystemseng.2019.04.014

[37] L. Magrin, M. Brscic, I. Lora, C. Rumor, L. Tondello, G. Cozzi et al. Effect of a ceiling fan ventilation system on finishing young bulls' health, behaviour and growth performance. *Animal. 2017,* 11(6), 1084-1092. https://doi.org/10.1017/S1751731116002482

[38] X. Wang, G. Zhang, C. Y. Choi. Effect of airflow speed and direction on convective heat transfer of standing and reclining cows. *Biosystems Engineering.* 2018, 167, 87-98. https://doi.org/10.1016/j.biosystemseng.2017.12.011

[39] D. E. Spiers, J. N. Spain, M. R. Ellersieck, M. C. Lucy. Strategic application of convective cooling to maximize the thermal gradient and reduce heat stress response in dairy cows. *Journal of Dairy Science. 2018,* 101(9), 269-8283. https://doi.org/10.3168/jds.2017-14283

[40] Wentylatory [Online]. Available: https://wentylatory.pl/pl/c/Wentylatory-do-obor/93. [Date of access: 18 December 2024].

[41] X. Wang, G. Zhang, C. Y. Choi. Evaluation of a precision air-supply system in naturally ventilated freestall dairy barns. *Biosystems Engineering.* 2018*,* 175, 1-15. https://doi.org/10.1016/j.biosystemseng.2018.08.005

[42] M. Cao, L. Rong, C.Y. Choi, K. Wang, X. Wang. Computational evaluation of air jet cooling from a perforated air ducting system to mitigate heat stress of cows in free stalls. *Computers and Electronics in Agriculture.* 2022, 199, 107198. https://doi.org/10.1016/j.compag.2022.107198

[43] M. Cao, R. Yang, C. Y. Choi, L. Rong, G. Zhang, K. Wang et al. Effects of discharge angle of jet from a slot orifice on cooling performance for a perforated air ducting system in dairy cattle barn. *Computers and Electronics in Agriculture.* 2023, 210, 107890. https://doi.org/10.1016/j.compag.2023.107890

[44] M. R. Mondaca, C. Y. Choi. Experimental Validation of Computational Fluid Dynamics (CFD) Model of Perforated Polyethylene Tube Ventilation Systems in Dairy Operations. *Transactions of the ASAE*. 2014, 6(60), 4530-4536. https://doi.org/10.13031/trans.59.11909

[45] S. Jung, H. Chung, M. R. Mondaca, K. V. Nordlund, C. Y. Choi. Using computational fluid dynamics to develop positive-pressure precision ventilation systems for large-scale dairy houses. *Biosystems Engineering.* 2023*,* 227, pp. 182-194. https://doi.org/10.1016/j.biosystemseng.2023.02.003

[46] W. Zhang, R. Yang, C. Y. Choi, L. Rong, G. Zhang, K. Wang. Recent research and development of individual precision cooling systems for dairy cows – A review. *Computers and Electronics in Agriculture. 2024,* 225, 109248. https://doi.org/10.1016/j.compag.2024.109248

[47] Agriexpo [Online]. Available: https://www.agriexpo.online/prod/marko-hohler-sp/product-188820-142498.html. [Date of access: 18 December 2024].

[48] E. A. Almuhanna, G. R. Gamea, O. E. Osman, F. M. Almahdi. Performance of roof-mounted misting fans to regulate heat stress in dairy cows. *Journal of Thermal Biology.* 2021, 99, 102984. https://doi.org/10.1016/j.jtherbio.2021.102984

[49] J. M. Chen, K. E. Schütz, C. B. Tucker. Cooling cows efficiently with sprinklers: Physiological responses to water spray. *Journal of Dairy Science.* 2015*,* 98 (10), 6925-6938. https://doi.org/10.3168/jds.2015-9434

[50] D.V. Armstrong. Heat Stress Interaction with Shade and Cooling. *Journal of Dairy Science. 1994, 7*7(7), 2044-2050. https://doi.org/10.3168/jds.S0022-0302(94)77149-6

[51] C. L. Stull, L. L. McV. Messam, C. A. Collar, N.B. Peterson, A.R. Castillo, B. A. Reed, et al. Precipitation and Temperature Effects on Mortality and Lactation Parameters of Dairy Cattle in California. *Journal of Dairy Science.* 2008, 91(12), 4579-4591. https://doi.org/10.3168/jds.2008-1215

[52] A. M. Wilson, T. C. Wright, J. P. Cant, V. R. Osborne. Behavioral and physiological responses to an inspired-air supplemental cooling system for dairy cows in free-stall housing. *animal,* 2023, 17(8) 100887. https://doi.org/10.1016/j.animal.2023.100887

[53] E. Chen, V. Narayanan, T. Pistochini, E. Rasouli. Transient simultaneous heat and mass transfer model to estimate drying time in a wetted fur of a cow. *Biosystems Engineering, 2020,* 195(6), 116-135. https://doi.org/10.1016/j.biosystemseng.2020.04.011

[54] Avidity Science [Online]. Available: https://www.avidityscience.com/ag-pet/cattle-cooling/controllers-and-electric-valves. [Date of access: 20 December 2024].

[55] J. Harner, AGProud, 23 June 2011. [Online]. Available: https://www.agproud.com/articles/22124-sprinkler-systems-for-cooling-dairy-cows-at-a-feed-line. [Date of access: 20 December 2024].

[56] Skov-Secco United by Dairy [Online]. Available: https://www.skov-secco.com/products/cooling/pad-cooling/. [Date of access: 20 December 2024].

[57] R. Grant. Taking Advantage of Natural Behavior Improves Dairy Cow Performance. *Western Dairy Management Conference,* Reno, NV, 2007.

[58] K.R. Bastian, K. G. Gebremedhin, N. Scott. A finite difference model to determine conduction heat loss to a water-filled mattress for dairy cows. *Transactions of ASAE. 2003, 46(3), 773-780.* https://doi.org/10.13031/2013.13592

[59] J. Radoń, W. Bieda, J. Lendelová, Š. Pogran. Computational model of heat exchange between dairy cow and bedding. *Computers and Electronics in Agriculture. 2014,* 107, 29-37. https://doi.org/10.1016/j.compag.2014.06.006

[60] X. A. Ortiz, J. F. Smith, F. Rojano, C. Y. Choi, J. Bruer, T. Steele, et al. Evaluation of conductive cooling of lactating dairy cows under controlled environmental conditions. *Journal of Dairy Science,* 98(3), 1-13. https://doi.org/10.3168/jds.2014-8583

[61] W. Zhao. Evaluation of dairy freestall conductive cooling system. Masters thesis, University of Florida, 2017. https://ufdc.ufl.edu/ufe0050798/00001

[62] M. R. Mondaca, F. Rojano, K. Gebremedhin, C. Y. Choi. A conjugate heat and mass transfer model to evaluate the efficiency of conductive cooling for dairy cattle. *Transactions of ASABE.* 2013, 56(6), 1471-1482. https://doi.org/10.13031/trans.56.10178

[63] F. Rojano. Computational modeling to reduce impact of heat stress in lactating cows, PhD Thesis, The University of Arizona, 2013. http://hdl.handle.net/10150/272838

[64] K. M. Perano, J. G. Usack, L. T. Angenent, K. G. Gebremedhin. Production and physiological responses of heat-stressed lactating dairy cattle to conductive cooling. *Journal of Dairy Science. 2015,* 98(8), 5252-5261. https://doi.org/10.3168/jds.2014-8784

[65] K. Perano, T. Shelford, K. G. Gebremedhi. Experimental analysis of condensation rate in conductive cooling systems for dairy cattle. *Applied Engineering in Agriculture. 2018,* 34(2), 425-436. https://doi.org/ 10.13031/aea.12259

[66] K. G. Gebremedhin, B. Wu, K. Perano. Modeling conductive cooling for thermally stressed dairy cows. *Journal of Thermal Biology.* 2016, 56, 91-99. https://doi.org/10.1016/j.jtherbio.2016.01.004

[67] BioretAgri [Online]. Available: https://agri.bioret-corp.com/en/our-products/cow-mattresses/aquaclim-water-mattress-cow/. [Date of access: 20 December 2024].

[68] Water Energy Innovations [Online]. Available: https://droughtresilience.com/technology/technology-profiles/evaporative-conduction-cow-cooling/. [Date of access: 09 January 2025].

[69] ANSYS I., ANSYS Fluent Theory Guide (Release 15.0), 2013.

[70] Omega Engieenering. HFS Heat Flux Sensor Instruction Manual [Online]. Available: https://assets.omega.com/manuals/UHFS-09_manual.pdf. [Date of access: 29 January 2024].

[71] Y. Wang, B. Sua, J. Wua. Simulation and optimization of giant radial tire vulcanization, *Procedia Engineering.* 2012, 31, 723 – 726. https://doi.org/10.1016/j.proeng.2012.01.1092

[72] National Research Council Guide for the Care and Use of Laboratory Animals. Washington, DC, U.S.A.: The National Academies Press, 2011.

[73] National Research Guide to Environmental Research on Animals. Washington, DC, U.S.A.: The National Academies Press, 1971.

[74] Collective work edited by R. Kołacz, Z. Dobrzański. Higiena i dobrostan zwierząt gospodarskich. Wrocław: Uniwersytet Przyrodniczy we Wrocławiu, 2019.

[75] Z. Dobrzański, R. Kołacz. Przewodnik do ćwiczeń z zoohigieny. Wrocław: AWA, 1996.

[76] N. E. McGowan, D. M. Scantlebury, A. G. Maule, N. J. Marks. Measuring the emissivity of mammal pelage. *Quantitative InfraRed Thermography Journal.* 2018*,* 15(2), 214–222. https://doi.org/10.1080/17686733.2018.1437239

[77] J. M. Bewley, M. E. Einstein, M. W. Grott, M. M. Schutz. Comparison of Reticular and Rectal Core Body Temperatures in Lactating Dairy Cows. *Journal of Dairy Science. 2008,* 91(12), 4661-4672. https://doi.org/10.3168/jds.2007-0835

[78] R. W. Shephard, S. K. Maloney. A review of thermal stress in cattle. *Australian Veterinary Journal. 2023,* 101(11), 417-429. https://doi.org/10.1111/avj.13275

[79] J. Jędruszkiewicz, J. Wibig, P. Piotrowski. Heat waves in Poland: The relations to atmospheric circulation and Arctic warming. *International Journal of Climatology. 2024,* 44(7), 2189-2206. https://doi.org/10.1002/joc.8448

[80] S. Gupta, A. Sharma, A. Joy, F. R. Dunshea, S. S. Chauhan. The Impact of Heat Stress on Immune Status of Dairy Cattle and Strategies to Ameliorate the Negative Effects. *Animals.* 2023, 13(1), 107. https://doi.org/10.3390/ani13010107

[81] P. Herbut, S. Angrecka. Forming of temperature-humidity index (THI) and milk production of cows in the free-stall barn during the period of summer heat. *Animal Science Papers & Reports.* 2012*,* 30(4), 363–372.

[82] R. B. Zimbelman, R. P. Rhoads, M. Rhoads, G. Duff, L. Baumgard, R. J. Collier. A Re-Evaluation of the Impact of Temperature Humidity Index (THI) and Black Globe Humidity Index (BGHI) on Milk Production in High Producing Dairy Cows. *Proceedings of the Southwest Nutrition Conference,* Tucson. 2009.

[83] M. A. Islam, S. Lomax, A. K. Doughty, M. R. Islam, P. C. Thomson, C. E. F. Clark. Revealing the diversity of internal body temperature and panting response for feedlot cattle under environmental thermal stress. *Nature Scientific Reports.* 2023*,* 13, 4879. https://doi.org/10.1038/s41598-023-31801-7

[84] H. X. Kou, Y. Q. Zhao, K. Ren, X. Chen, Y. Q. Lu, D. Wang. Automated measurement of cattle surface temperature and its correlation with rectal temperature. *PLoS ONE,* 2017, 12(4), 0175377. https://doi.org/10.1371/journal.pone.0175377

[85] D. Detweiler, H. Erickson. Dukes' Physiology of Domestic Animals, Cornell University Press, 2004.

[86] M. Wierig, L. Mandtler, P. Rottmann, V. Stroh, U. Müller, W. Büscher et al. Recording Heart Rate Variability of Dairy Cows to the Cloud—Why Smartphones Provide Smart Solutions. *Sensors,* 2018, 18(8), 2541. https://doi.org/10.3390/s18082541

[87] J. Li, V. Narayanan, E. Kebreab, S. Dikmen, J.G. Fadel. A mechanistic thermal balance model of dairy cattle. *Biosystems Engineering. 2021,* 209, 256-270. https://doi.org/10.1016/j.biosystemseng.2021.06.009

[88] P. Poczopko. Ciepło a życie. Zarys termofizjologii zwierząt, Łódź: PWN, 1990.

[89] S. Brody. Bioenergetics and Growth with Special Reference to the Energetic Efficiency Complex in Domestic Animals. New York: Reinhold Publishing Corporation, 1945.

[90] M. Algra, L. de Keijzer, S. S. Arndt, F. J. C. M. van Eerdenburg, V. C. Goerlich. Evaluation of the Thermal Response of the Horns in Dairy Cattle. *Animals,* 2023, 13 (3), 500. https://doi.org/10.3390/ani13030500

List of Tables

List of Figures